MOLECULAR AND METABOLIC BASIS OF RIPENING AND POSTHARVEST PHYSIOLOGY IN BLUEBERRY

by

TEJ PRASAD ACHARYA

(Under the Direction of Savithri U. Nambeesan)

ABSTRACT

The southern highbush (*Vaccinium corymbosum*) and rabbiteye (*V. virgatum*) blueberries are commonly grown cultivars in the southeastern U.S. The objective of this study was to investigate mechanisms involved in ripening and factors affecting postharvest fruit quality in blueberry. The first study investigated the molecular and metabolic basis of regulating fruit development and ripening in rabbiteye blueberry, revealing continual sucrose uptake during fruit ripening, stimulated glycolysis, tri-carboxylic acid (TCA), and anthocyanin-related metabolism during ripening. Follow-up gene expression analyses revealed important genes associated with sugar, acid, and anthocyanin metabolism. The second study investigated the effect of ethylene releasing plant growth regulators (PGRs) on ripening, metabolite composition, and postharvest fruit quality attributes. Both ethephon and 1-amino cyclopropane 1-carboxylic acid (ACC) transiently stimulated sugar, acid, and anthocyanin metabolism, increasing the rate of ripening with minimal impact on fruit quality attributes. The increase in transcript abundance of *VACUOLAR INVERTASE* (*vINV*), *PHOSPHOENOLPYRUVATE CARBOXYKINASE* (*PEPCK*), and anthocyanin biosynthesis related genes, were associated with ethylene-induced ripening related changes. The third study characterized ripening related transcription factors (TFs) during

fruit development and ripening, and identified four important TFs, potentially involved in fruit ripening. Among them, the transcript abundance of *VvMADS7*, *VvNAC1*, and *VvNAC2* increased after the application of ethephon, suggesting that they are ethylene inducible. The transcript abundance of *VvNAC8* remained unaffected by ethylene application, suggesting that the expression of this gene during ripening is independent of ethylene-mediated signaling. The fourth study used the linear and LASSO regression models to identify physical traits and metabolite markers associated with fruit firmness during postharvest storage. This study identified titratable acidity (TA), specifically quinate and citrate, exhibited positive associations with fruit firmness. Conversely, sugars and amino acids displayed negative associations with fruit firmness. In summary, our research has shed light on both the applied aspect like utilization of PGRs as a ripening aid, and basic aspects of ripening and postharvest physiology mechanisms in blueberries, which can be utilized to improve ripening characteristics, fruit quality, and postharvest shelf-life.

INDEX WORDS: blueberry, ripening, postharvest physiology, sugar, acid, anthocyanin, plant growth regulators, transcription factors, fruit firmness

MOLECULAR AND METABOLIC BASIS OF RIPENING AND POSTHARVEST PHYSIOLOGY IN BLUEBERRY

by

TEJ PRASAD ACHARYA

BS., Tribhuvan University, Nepal, 2013

MS., Virginia Tech, 2018

A Dissertation Submitted to the Graduate Faculty of The University of Georgia in Partial Fulfillment of the Requirements for the Degree

DOCTOR OF PHILOSOPHY

ATHENS, GEORGIA

2023

MOLECULAR AND METABOLIC BASIS OF RIPENING AND POSTHARVEST PHYSIOLOGY IN BLUEBERRY

by

TEJ PRASAD ACHARYA

Major Professor:	Savithri U. Nambeesan
Committee:	Dayton Wilde
	Angelos Deltsidis
	Dennis Phillips
	Juan Carlos Melgar

Electronic Version Approved:

Ron Walcott
Vice Provost for Graduate Education and Dean of the Graduate School
The University of Georgia
December 2023

DEDICATION

This work is dedicated to my beloved parents (Devi Ram Acharya and Shanti Devi Acharya), my wife (Susmita Dahal), my brother (Num Acharya), and my sisters (Mamita Sharma and Uma Acharya).

ACKNOWLEDGEMENTS

I consider myself extremely fortunate to have Dr. Savithri Nambeesan as my advisor. Her unwavering motivation has consistently inspired me to strive for academic excellence. Dr. Nambeesan has given me the freedom to work on various projects, offered valuable suggestions, and assisted me in every aspect of my research. I would like to express my deep gratitude and appreciation to my committee members: Drs. Dayton Wilde, Angelos Deltsidis, Dennis Phillips, and Juan Carlos Melgar, for their invaluable guidance and constructive feedback throughout my studies at UGA.

I would also like to extend my thanks to Dr. Anish Malladi for his support and guidance in several projects, as well as for his valuable suggestions. My heartfelt appreciation goes out to my fellow lab members: John, Mark, Ranveer, Yi-Wen, Bayleigh, Yanyu, Krittika, Mary, Shane, Ashley, Priyanka, and all student workers, especially Micah, for their assistance during summer field research, lab work, and feedback in our lab meetings. I am also grateful to all the faculty members, staff, and graduate students in the Horticulture Department at UGA for their unwavering support, guidance, and friendships.

Finally, I would like to express my gratitude to my wife, parents, and family members for their unwavering support, love, and guidance throughout my academic journey.

TABLE OF CONTENTS

Page

LIST OF TABLES

Page

LIST OF FIGURES

Page

CHAPTER 1

INTRODUCTION AND LITERATURE REVIEW

Blueberries (*Vaccinium spp*.) are in-demand fruit worldwide due to their flavor and abundance in bioactive compounds, such as procyanidins, anthocyanins, flavonols, and chlorogenic acid (Koca and Karadeniz, 2009; Reque et al., 2016; Shi et al., 2017). These compounds have important health benefits because of their antioxidant, antimicrobial, antidiabetic, anticancer, and cardioprotective activities (Cappai et al., 2018). From 2000 to 2017, worldwide blueberries production has increased by 100% and 42% in terms of production area and yield per unit area, respectively (Fig. 1.1; FAO, 2019).

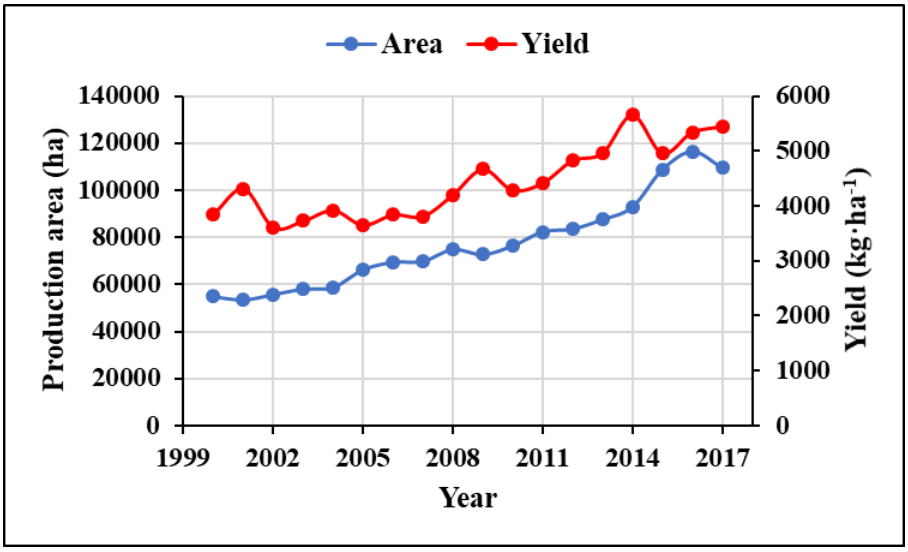

Figure 1.1: Status of blueberry production area and production yield worldwide. Data represent from 2000 to 2017 (FAO, 2019).

Blueberries are perennial flowering plants in the family Ericaceae. The size of blueberry shrubs can vary from 10 cm to 4 meters. The leaves can be ovate to lanceolate shape, and either deciduous or evergreen in nature. The flowers are bell-shaped with a red, white, pale pink or tinged greenish color. The United States (U.S.) is the leading producer of blueberries in the world (FAO, 2019). Five main types of blueberries are grown in the U.S.: lowbush, half-high, northern highbush, southern highbush, and rabbiteye (Strik et al., 2014). Lowbush and half-high bush blueberry are smaller shrubs and are found in the northern part of the U.S. and Canada. Half-highbush blueberry can tolerate temperatures as low as -35 ºF to -45 ºF (Strik et al., 2014). The northern highbush type is the most prevalent in the Pacific Northwest of the U.S. (Norvell, 1982). The southern highbush was developed by crossing northern highbush cultivars with *Vaccinium spp.* found in Florida and the southeastern U.S. (Williamson et al., 2019). These types of cultivars require low-chilling temperatures and is commonly produced in the southern part of the U.S. Rabbiteye blueberry originated and are native to the southeastern U. S. (Strik et al., 2014). These cultivars can be readily grown in areas with long and hot summers. Of these types, southern highbush and rabbiteye are the major cultivars grown in Georgia.

Blueberries for fresh market are generally hand harvested due to their fragile nature (Gallardo et al., 2018). Also, blueberries can be harvested mechanically, improving harvesting efficiency, and minimizing production cost (Brown et al., 1996; Malladi et al., 2013; Casamali et al., 2016). Generally, machine harvested blueberry fruit are used for processing to make juices, jams and jellies. However due to labor-related issues, the blueberry industry is moving towards machine harvesting fruit for fresh market. Some of the problems associated with mechanical harvesting include low harvest efficiency due to uneven ripening, high proportion of fruit being

damaged, and a decline in postharvest fruit quality (Takeda et al., 2008). The bottlenecks associated with harvesting and handling of fruit is further exacerbated with limited knowledge in the understanding of blueberry ripening and postharvest physiology. During ripening, all blueberry fruits within a plant do not ripen uniformly/at the same time and therefore, multiple harvests are needed throughout the growing season. Harvesting can be labor-intensive and adds significantly to production-related costs (Suzuki et al., 1997). After harvest, fruit quality in blueberry decreases due to dehydration, loss of firmness, loss of flavor, and pathogen susceptibility. The reduction in fruit quality can result in inferior fruit and consumer dissatisfaction. Further, there is limited basic information on mechanisms of ripening and loss of fruit quality during postharvest storage in blueberries. Investigating mechanisms that influence ripening and postharvest fruit quality will contribute to an improved fundamental understanding of these processes in blueberries. In the future, this information can be used to manipulate ripening to save production-related costs and to breed for fruit with good postharvest fruit quality to enhance consumer satisfaction.

Fruit ripening is a highly coordinated process involving physiological, biochemical, and molecular changes that collectively determine the development of the fruit's color, texture, sugar, acidity, and aroma volatiles (Quinet et al., 2019). In blueberry, an increase in sugar, volatiles, and anthocyanin concentration and a decrease in acid, flavonols, and hydrocinnamic acid concentration occurs during the ripening (Ayaz et al., 2001; Bouzayen et al., 2010; Silva et al., 2017). These changes are a result of transcriptional changes of ripening-related genes and enzymes involved in biochemical processes (Giovannoni, 2004). For example, fruit softening during ripening is partly due to the increase in the expression level of cell wall modifying

enzymes such as pectinesterase, pectate lyase, polygalacturonase, β-galactosidase, cellulose, and hemicellulose modifying enzymes (Chen et al., 2020; Li et al., 2021).

Climacteric and non-climacteric ripening physiology: Generally, fruits are classified as climacteric and non-climacteric based on their respiratory behavior and patterns of ethylene production during ripening. Climacteric fruits such as banana, tomato, and apple display an increase in respiration and ethylene production during ripening (Alexander and Grierson, 2002; Paul et al., 2012; Seymour et al., 2013). In these fruits, the regulation of ethylene production is autocatalytic, and ethylene positively regulates ripening-related changes (Yokotani et al., 2009; Liu et al., 2015). However, non-climacteric fruits such as citrus, strawberry, and grape do not display a rise in ethylene and respiration during ripening (Bouzayen et al., 2010). Despite this, there is some evidence from previous studies to suggest a rather small increase in ethylene production during ripening in grape and strawberry (Chervin et al., 2004; Iannetta et al., 2006). More recently the binary system of fruit ripening classification is losing traction with certain fruits such as kiwifruit and melon falling in-between the spectrum of climacteric and non-climacteric fruits (Périn et al., 2002; McAtee et al., 2015; Asiche et al., 2018; Pereira et al., 2020). Further other hormones such as abscisic acid (ABA) has shown to positively regulate ripening, with a larger role in non-climacteric fruit (Moya-León et al., 2019; Fenn and Giovannoni, 2021). Previous work indicated some contradictions in classifying the ripening behavior in blueberry. A few studies suggested a climacteric ripening behavior in blueberry due to an increase in respiration and ethylene production during the ripening (El Agamy et al., 1982; Suzuki et al., 1997). Also, application of ethylene releasing compound, ethephon accelerated

ripening in highbush (Eck, 1970) and rabbiteye (Dekazos, 1977; Wang et al., 2018) cultivars. However, Frenkel (1972) collected samples from various developmental and ripening stages which included, green, semi-red, pink, and blue stages, and did not find the climacteric rise in respiration or ethylene evolution. More recently blueberry fruit is classified as exhibiting atypical climacteric ripening physiology (Wang et al., 2022). Data from our laboratory indicated an increase in climacteric respiration and ethylene production during ripening in southern highbush and rabbiteye blueberry. However, an autocatalytic response to ethylene production was not evident, as the external application of ethylene-releasing plant growth regulators (PGRs) did not lead to an increase in 1-aminocyclopropane 1-carboxylic acid (ACC) concentration (ethylene precursor) and the transcript abundance of ethylene biosynthesis enzyme, 1-aminocyclopropane 1-carboxylic acid synthase (ACS) (Wang et al., 2022).

The effect of ethylene on ripening: The gaseous hormone ethylene plays a vital role in the ripening of climacteric fruit, and its role has been known for more than 50 years (Bapat et al., 2010). Two systems of ethylene production have been proposed in climacteric plants. System 1 occurs during the vegetative growth and during early fruit development, where ethylene inhibits its own production, thus being auto-inhibitory. In this case, the basal ethylene levels are maintained in both climacteric and non-climacteric plants (Alexander and Grierson, 2002). However, ethylene production by system 2 is an autocatalytic process that occurs during fruit ripening in climacteric fruits. Ethylene is produced from an amino acid precursor, methionine in a three-step process (Bleecker and Kende, 2000; Bapat et al., 2010). 1) S-ADENOSYL-L-METHIONINE (SAM) SYNTHETASE converts methionine into SAM. 2) Conversion of SAM to 1-aminocyclopropane-

1-carboxylic acid (ACC) by ACC SYNTHASE (ACS). 3) Conversion of ACC into ethylene by ACC OXIDASE (ACO). Once synthesized, ethylene is perceived by ethylene receptor proteins (ETR) located in the membrane of endoplasmic reticulum; these proteins are negative regulators of ethylene signaling (Liu et al., 2015; Chang, 2016). In the absence of ethylene, the ETR activates, CONSTITUTIVE TRIPLE RESPONSE1 (CTR1) which has a protein kinase domain that phosphorylates ETHYLENE INSENSTITIVE2 (EIN2) and inactivates it. Further downstream transcription factors (TFs) involved in ethylene signaling, such as EIN3 and ETHYLENE INSENSITIVE 3-LIKE1 (EIL1) are degraded by ETHYLENE INSENSITIVE3-BINDING F-BOX (EBF) proteins (Liu et al., 2015; Chang, 2016). When ethylene is present and bound to its receptor, it no longer activates the CTR1. Thus, the inhibition of EIN2 by CTR1 is no longer present. EIN2 gets cleaved and its C-terminal domain enters the nucleus and activates TFs EIN3 and EIL1. The activation of the TFs leads to an accumulation of another ethylene responsive TF called the ETHYLENE RESPONSE FACTOR (ERF). Finally, ERFs, activate ripening related genes involved in softening, color development, and formation of aroma (Liu et al., 2015; Chang, 2016). For example, ERF3 increased the expression of *MdMYB1* in apple (An et al., 2018), a gene responsible for positively regulating anthocyanin biosynthesis.

Ethylene-related plant growth regulators and their effect in ripening progression: The PGRs are natural or synthetic substances used to promote the growth/ alter the plant's several physiological activities. Ethephon (2-chloroethyl phosphonic acid), an ethylene releasing agent, has been extensively used to accelerate ripening and maintain postharvest fruit quality in climacteric fruits (Ampa et al., 2017; Li et al., 2017; Suehiro et al., 2019). In non-climacteric

fruit like lemon and grape, ethylene releasing compounds successfully enhance skin color (El-Kereamy et al., 2003; Zhang and Zhou, 2019). Application of ethephon increases internal ethylene concentration by 6-fold within 24 hours in grape (El-Kereamy et al., 2003). Ethephon is approved to promote early fruit color in northern highbush blueberries at the rate between ~500-1500 ppm (US-EPA, 2010); however, the higher rate (> 500ppm) may result in the fruit drop (abscission) (Dekazos, 1979; Malladi et al., 2012). Previous work from our laboratory indicated that a lower concentration of 250 ppm is sufficient to elicit a ripening response in blueberry without any adverse effect on fruit quality (Wang et al., 2018).

In comparison to ethephon, two other PGRs, aminoethoxyvinylglycine (AVG) and 1-methyl-cyclopropane (1-MCP) inhibit ethylene production and signaling respectively. 1-MCP binds to ethylene receptors and thus can block ethylene responses (Blankenship and Dole, 2003). The application of 1-MCP has the potential to delay ripening and hence to extend shelf-life in apple (Bai et al., 2005). However, it must be applied at the right dosage, at the proper ripening stage, and with the right postharvest handling operation. Postharvest application of 1-MCP in rabbiteye blueberry cultivar, Brightwell, increased ethylene production, decreased firmness, and had minimum effect on the total soluble solids content and titratable acidity (MacLean and NeSmith, 2011). The AVG is a chemical that inhibits ethylene production by inhibiting ACC synthase activity (Boller et al., 1979). AVG has shown to delay fruit ripening, reducing pre-harvest fruit drop, and ethylene production in apple (Rath et al., 2006).

Transcriptional regulation of fruit ripening: In climacteric and non-climacteric fruits, TFs play an important role in ripening, in addition to hormones. Among them, MADS

[MINICHROMOSOME MAINTENANCE FACTOR 1 (*Saccharomyces cerevisiae*), AGAMOUS (*Arabidopsis thaliana*), DEFICIENS (*Antirrhinum majus*) and SERUM RESPONSE FACTOR (*Homo sapiens*)] domain TFs are associated with floral development, fruit development, and ripening of fruits (Shore and Sharrocks, 1995; Ito et al., 2008; Díaz-Riquelme et al., 2009; Gramzow and Theissen, 2010; Ireland et al., 2013). In addition to MADS-box, TFs which belong to other families such as NAC [NO APICAL MERISTEM, (Petunia), *ARABIDOPSIS THALIANA* ACTIVATING FACTOR 1-2, and CUP-SHAPED COTYLEDON 2 (Arabidopsis)], HD-zip domain (HB-1), SQUAMOSA BINDING PROTEIN LIKE (SPL), APETALA (AP2a, ERF) also regulate tomato fruit ripening (Manning et al., 2006; Smaczniak et al., 2012; Shinozaki et al., 2018; Wang et al., 2019). Specifically, *RIPENING INHIBITOR* (*RIN*), *NON-RIPENING* (*NOR*), *APETALA2a*, *FRUITFULL* (*FUL1/TDR4* and *FUL2/MBP7*), *TAGL1*, and *NAC* are highly expressed during tomato fruit ripening (Carrasco-Orellana et al., 2018; Shinozaki et al., 2018). Similarly, in strawberry TFs such as *MYB-bHLH-WD40*, *NAC*, *FaTCP*, *FADOF2*, and *SEPALLATA (SEP) 1/2 -like* (*FaMADS9*) are expressed during ripening (Seymour et al., 2011; Schaart et al., 2013; Xu et al., 2013; Xie et al., 2020).

RIN belongs to the SEPALLATA subfamily of MADS TFs and is considered as the master regulator of fruit ripening. RIN plays a central role in the tomato fruit ripening and interacts with the promoter and other TFs like NOR, CNR, TDR4, and HB1, and can influence cell wall degradation, carotenoid accumulation, and ethylene production (Martel et al., 2011). The *rin* mutation results in impaired ripening, which cannot be rescued by exogenous ethylene application (Vrebalov et al., 2002; Manning et al., 2006). However, recently the role of *rin* mutants have been reconsidered after it was shown to be a negative gain of function mutation

(Ito et al., 2020). Further, the generation of RIN-CRISPR-Cas9 (RIN-CR-KO) lines indicated that RIN TFs may not be crucial for ripening initiation as discussed earlier, but it is important for ripening completion (Ito et al., 2017). In addition, other members of the MADS gene family, including TOMATO AGAMOUS-LIKE1 (TAGL1) as well as FRUITFUL homologs FUL1 and FUL2, have been demonstrated to positively regulate ripening by forming higher-order complexes with RIN (Itkin et al., 2009; Shima et al., 2013; Fujisawa et al., 2014). MADS TFs also regulate ripening in non-climacteric fruits like strawberry (Seymour et al., 2011; Lu et al., 2018). Silencing of the SEPALLATA *(SEP) 1/2-like* (*FaMADS9*) TF resulted in the inhibition of ripening-related attributes in strawberry (Seymour et al., 2011).

NAC is the largest family of TFs having a conserved N-terminal DNA binding and a variable C-terminal domain (Olsen et al., 2005). The members of the NAC TFs positively regulate fruit ripening and their cross talk with ethylene have been identified in banana, apple, and tomato (Shan et al., 2012; Wang and Xu, 2012; Gao et al., 2021). The NAC TF member, NOR positively influences fruit ripening. The silencing of *NOR-like1* through virus-induced gene silencing and *NAC-NOR* using CRISPR-Cas9 led to a reduction in fruit ripening initiation by lowering the accumulation of carotenoids, reducing chlorophyll metabolism, and decreasing the expression of genes involved in ethylene biosynthesis (Gao et al., 2018; Wang et al., 2019). Consistently, a transcriptomic analysis revealed that *NOR* had a positive regulatory effect on the expression of genes responsible for ethylene and carotenoid biosynthesis, as well as enzymes involved in cell wall modification (Gao et al., 2019). Furthermore, other members of the NAC gene family, including *SlNAC4*, were discovered to positively impact fruit ripening by reducing

chlorophyll breakdown and suppressing the expression of genes involved in ethylene and carotenoid biosynthesis when their expression was decreased via RNAi (Zhu et al., 2014). Nevertheless, it remains unclear whether NAC TFs form higher-order complexes to jointly regulate the ripening process (Gao et al., 2019). In strawberry, the NAC TF member, *FaNAC035* has been shown to induce ABA biosynthesis, and ABA, in turn, transcriptionally induces *FaNAC035,* hence positively influences ripening (Martín-Pizarro et al., 2021). Similarly, the cis-elements responsive to ABA and auxin were found in the promoter of *FcNAC1* in wild strawberry (Carrasco-Orellana et al., 2018). In addition, SPL-COLORLESS NON-RIPENING (CNR) is another TFs involved in fruit ripening. The *cnr* mutant in tomato resulted in the reduction of lycopene, total soluble solids content, ripening-related genes, and cell wall-degrading enzymes, leading to the formation of mature fruits with a colorless pericarp (Eriksson et al., 2004; Zhou et al., 2022). However, new studies with CNR-CR-KO lines indicates only a delayed ripening phenotype by 2 to 3 days, after which full coloration is obtained similar to the wild-type (Gao et al., 2019).

Carbohydrate and acid metabolism during the fruit development and ripening: The carbohydrate and acid metabolism during ripening plays an important role in fruit flavor formation. The perception of sweetness of fruits is determined by the balance between the sugar and acid content during ripening. Glucose, fructose, sucrose, and starch are the major carbohydrates, and malate and citrate are the major acids in fruits. Carbohydrate and acid metabolism are a series of dynamic reactions that involve synthesis and breakdown of intermediates directly connected to these pathways, or can serve as precursors for other pathways

of primary metabolism (e.g. starch synthesis) and secondary metabolism (e.g. synthesis of anthocyanin and flavonoid compounds).

During photosynthesis, carbon dioxide from the atmosphere is converted into triose phosphate through a series of chemical reactions. The triose phosphates are then utilized for the formation of sucrose in the cytosol of cells of the source tissue (leaf). Sucrose is then transported via phloem to sink tissues such as the root, stem, and fruits to provide the carbon and energy needed for their growth and development (Tauzin and Giardina, 2014). Excess of sugar molecules (ADP-glucose) formed during photosynthesis can be used for synthesis of starch. Starch is an insoluble polysaccharide composed of glucose and can be utilized for the long-term storage. The storage of starch molecules takes place in the chloroplast of leaf cells. The synthesis of starch also occurs in the sink organs described in the below section.

Starch metabolism: Two types of starch are found in the plants; transitory and storage starch. The formation of transitory starch occurs during the day in the source organ, and its breakdown occurs during the night when plants no longer synthesize carbon from photosynthesis (Pfister and Zeeman, 2016). This nocturnal breakdown of transitory starch maintains a continuous supply of carbon and energy for the plant, supporting metabolic activities and growth, especially during the night or in conditions of low photosynthesis. This process helps the plants to adapt to various environmental conditions and sustain growth and development. Plants prioritize the synthesis of transitory starch during periods of high photosynthesis, whereas they prefer sucrose synthesis during low photosynthetic activity (Weise et al., 2011). During the breakdown process, the transitory starch is enzymatically converted into glucose and maltose in chloroplast using

DEBRANCHING, GLUCAN WATER DIKINASE, PHOSPHOGLUCAN WATER DIKINASE, and β-AMYLASE enzymes (Kötting et al., 2005; Lu and Sharkey, 2006).

The synthesis of storage starch occurs in sink organs like roots, tubers, and fruits (Huang et al., 2021). This starch plays an important role in contributing to the total soluble sugars in the fruits during the ripening (Dinar and Stevens, 1981; Durán-Soria et al., 2020). During fruit development, ripening, and postharvest storage in fruits and vegetables, several enzymes regulate starch biosynthesis and degradation (Fig. 1.2). The ADP glucose phosphorylase (AGPase) is the rate-limiting step in starch biosynthesis, and an increase in its expression level results in higher accumulation of starch (Schaffer et al., 2000; Nakkanong et al., 2012). The concentration of starch also varies between climacteric and non-climacteric fruits, with generally more starch in climacteric fruits throughout fruit growth, development, and ripening (Chervin, 2020). Climacteric fruits like tomatoes, bananas, and apples, accumulate starch before the onset of ripening, and their degradation to soluble sugar occurs during the ripening period (Chervin, 2020). In non-climacteric fruits such as strawberries and grapes, starch concentration is higher in the mid developmental stages, specifically during véraison in grapes and immature stages in strawberries (Souleyre et al., 2004; Zhu et al., 2017). This suggests that starch accumulation in non-climacteric fruits primarily occurs during mid fruit growth and is followed by rapid degradation. Hence, during the later developmental stages, fruits no longer rely on starch degradation but depend on sugar translocation from the source tissues.

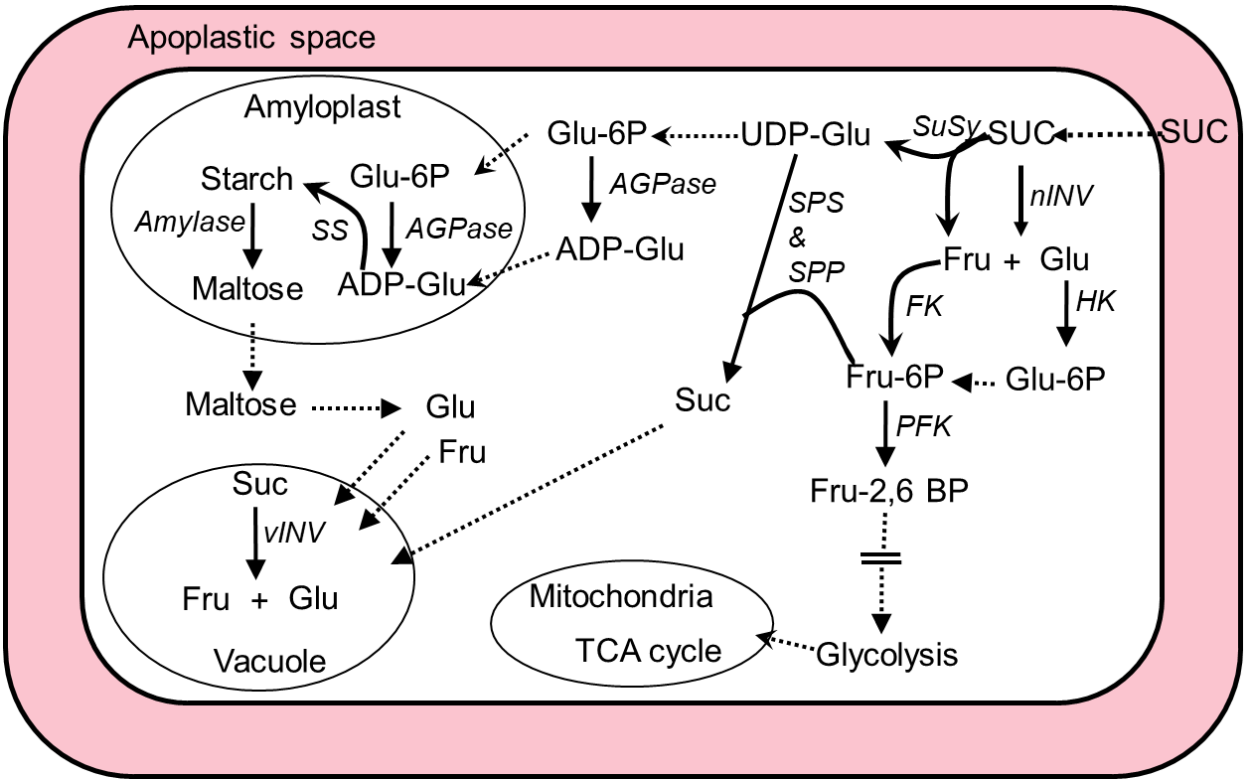

Figure 1.2: Sugar metabolism and biosynthesis in fruits.

Sugar metabolism: Glucose, fructose, and sucrose are the major sugars in fruits. The concentration of these compounds can vary among different fruits. In fruits like apple, guava, papaya, strawberry, and blueberry, glucose, and fructose are the major sugars (Batista-Silva et al., 2018). The catabolism of sucrose is carried out by the two major enzymes: INVERTASE (INV) and SUCROSE SYNTHASE (SuSy) (Fig. 1.2). There are three forms of INV that catabolizes sucrose into the glucose and fructose, and its activities occur in the extracellular space (CELL WALL INVERTASE: cwINV), cytosol (NEUTRAL INVERTASE: nINV), and vacuoles (VACUOLAR INVERTASE: vINV). During the initial growth phase of tomato, the increased activity of cwINV hydrolyzes sucrose into glucose and fructose, thereby establishing a

concentration gradient that enhances the export of sucrose into the companion cells and sieve elements of the phloem (Ruan, 2014). On the other hand, vINV is crucial for hexose accumulation and cell expansion in fruits throughout their development and ripening; nINV plays a significant role in maintaining sugar homeostasis in the cytoplasm, particularly when the activity of SuSy is diminished (Tang et al., 1999). The cytosolic enzyme SuSy catabolize sucrose into uridine diphosphate-glucose (UDP-glucose) and fructose, and plays an important role in the biosynthesis of starch, cellulose, lipids, and proteins. Its activity is generally higher in developing seeds and fruits than in the leaves (Ruan, 2014).

Sucrose can be resynthesized in fruit and this reaction is catalyzed by two enzymes, SUCROSE PHOSPHATE SYNTHASE (SPS) and SUCROSE PHOSPHATE PHOSPHATASE (SPP) (Fig. 1.2). The SPS converts UDP-glucose and fructose into Sucrose 6-phosphate, which is subsequently converted into sucrose by SPP, and the activity of these enzymes determines the sucrose concentration in the fruit. For example, the higher SPS activity is associated with greater sucrose/hexose ratio in pineapple fruit (Zhang et al., 2012). Despite its energetic cost, the resynthesize of sucrose is essential for efficiently distributing carbon compounds throughout the plant, as sucrose's metabolic stability, compared to hexoses, facilitates precise carbon molecule transportation to regions required for growth, development, and stress response (Ruan, 2014). The hexoses (glucose and fructose) formed as a breakdown of sucrose are phosphorylated by the HEXOKINASE (HK) and FRUCTOKINASE (FK), which are the key precursors for the fruit metabolic process like glycolysis and tricarboxylic acid (TCA) cycle (Stein and Granot, 2018). In addition, the excess amount of glucose, fructose, and sucrose are also stored in the vacuoles and utilized in the metabolic process during the ripening and postharvest storage. The sugar

alcohol like sorbitol also present in the fruits, and is primary translocating sugar in rosaceous family (Bieleski, 1969).

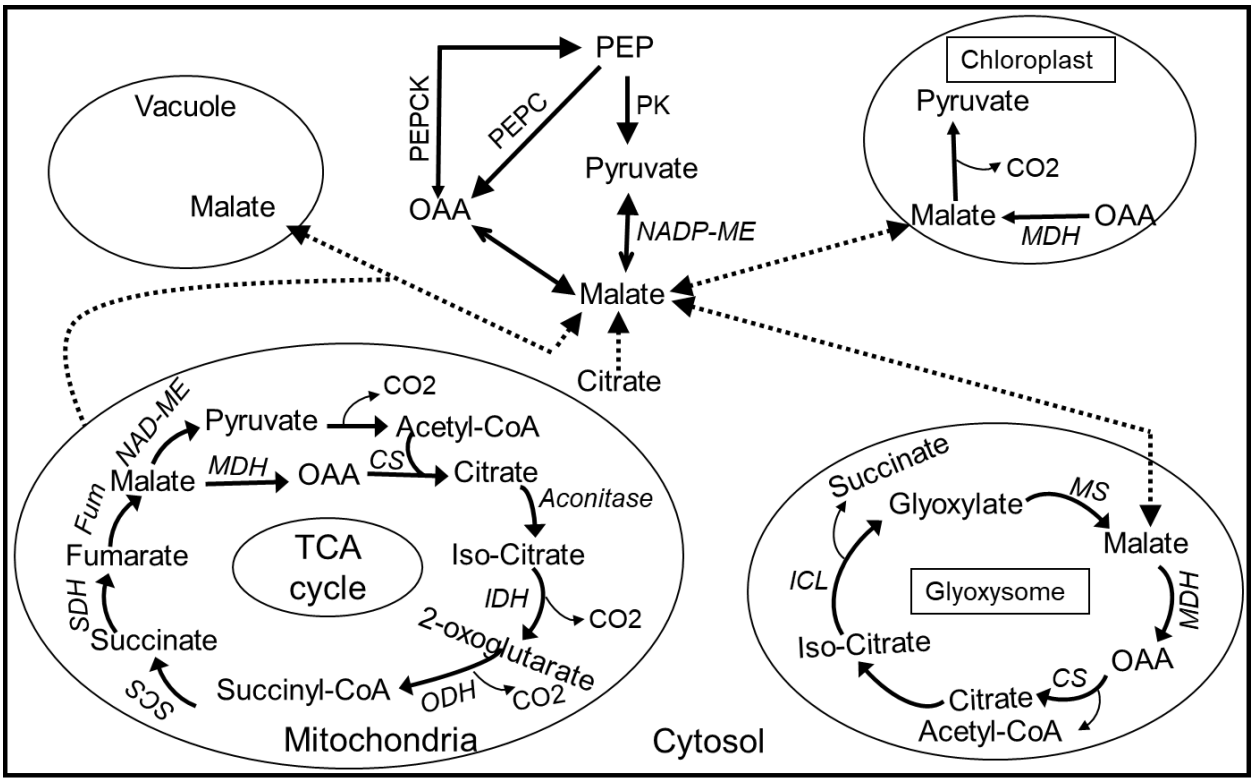

Figure 1.3: Acid metabolism and biosynthesis in fruits. Adapted from: (Sweetman et al., 2009).

Organic acid metabolism: Malate and citrate are the major primary acids that accumulate during fruit development and ripening. Malate is predominant acid in fruits like apple, banana, and grape, whereas citrate is the predominant acid in guava, citrus, and strawberry (Batista-Silva et al., 2018). Organic acid accumulation occurs earlier during fruit development, and is an important substrate needed for the respiratory burst during the onset of ripening in fruits

(Seymour et al., 2013). The synthesis of organic acids takes place in situ through the process of glycolysis from hexoses, and via starch and cell wall degradation intermediates.

Malate serves as the starting point for the synthesis of various organic acids. Malate is synthesized using the two pathways: 1. PHOSPHOENOLPYRUVATE CARBOXYLASE (PEPC)- NAD-MALATE DEHYDROGENASE (MDH) pathway and 2. NADP-MALIC ENZYME (NADP-ME) pathway in the cytoplasm. In the first pathway, the phosphoenolpyruvate synthesized from the glycolysis is first converted into oxaloacetate using PEPC, which is later converted into malate using NAD-MDH enzyme (Fig. 1.3). The oxaloacetate can also be converted back into the phosphoenolpyruvate using the PHOSPHOENOLPYRUVATE CARBOXYKINASE (PEPCK) enzyme. In the second pathway, pyruvate (end product of glycolysis) can be converted into the malate using the NADP-ME (Fig. 1.3). The higher activity of PEPC, NAD-MDH, and NADP-MEs during earlier developmental stages increased malate concentration in loquat fruits (Chen et al., 2009). The excess malate can also be stored in the vacuoles, and transported to the cytosol using a vacuolar transporter to be utilized for various metabolic processes later during fruit development and ripening (Sweetman et al., 2009).

PYRUVATE DEHYDROGENASE and PYRUVATE CARBOXYLASE are important enzymes involved in energy metabolism and carboxylation reactions, leading to the formation of acetyl-CoA and oxaloacetate, respectively, an important precursor for the tricarboxylic acid (TCA) cycle. During the TCA cycle, the formation of intermediate organic acids like citrate, isocitrate, α-ketoglutarate, fumarate, and succinate occurs (Fig. 1.3). Several intermediate

enzymes, including CITRATE SYNTHASE (CS), ACONITASE, ISOCITRATE DEHYDROGENASE (IDH), OXOGLUTARATEDEHYDROGENASE (ODH), SUCCINYL–COA SYNTHETASE (SCS), FUMARASE, and MALATE DEHYDROGENASE (MDH), are a part of the TCA cycle. The TCA cycle is crucial biochemical process where the majority of ATP synthesis occurs through the oxidation of NADH and $FADH_2$, accompanied by the release of CO_2. Citrate is the major primary acid accumulated during the TCA cycle, and excess amounts can be stored in the vacuoles (Hussain et al., 2017). The CS enzyme is involved in the conversion of oxaloacetate to citrate, but its role in citrate accumulation remains poorly understood. An increase in citrate levels in citrus fruits has been associated with higher transcript abundance of CS (Liu et al., 2007*)*. However, another study found no correlation between CS activity and citrate accumulation in fruits, suggesting that CS activity may not directly determine citrate concentration in fruits (Delhaize et al., 2003; Guo et al., 2016). Therefore, it is essential to understand the roles of all TCA intermediates in citrate accumulation.

Anthocyanin metabolism: The carbon metabolism also leads to the formation of secondary acids like quinate and shikimate. These acids are the precursors for the formation of anthocyanins in the fruits. Anthocyanins are polyphenolic compounds and previous studies have demonstrated the health benefits of these compounds as they have high antioxidant activity, preventing chronic diseases, cancer, and heart problems (Hou, 2003; Prior, 2004). The enzymes: PHENYLALANINE AMMONIA-LYASE (PAL), CHALCONE SYNTHASE (CHS), CHALCONE ISOMERASE (CHI), FLAVONOID 3’-HYDROXYLASE (F3'H), FLAVONOID 3',5’-HYDROXYLASE (F3'5'H), DIHYDROFLAVONAL 4-REDUCTASE (DFR),

ANTHOCYANIDIN 3-O-GLUCOSYLTRANSFERASE (UFGT), FLAVONOL SYNTHASE (FLS), and ANTHOCYANIDIN REDUCTASE (ANR) are involved in the biosynthesis of anthocyanin (Fig. 1.4).

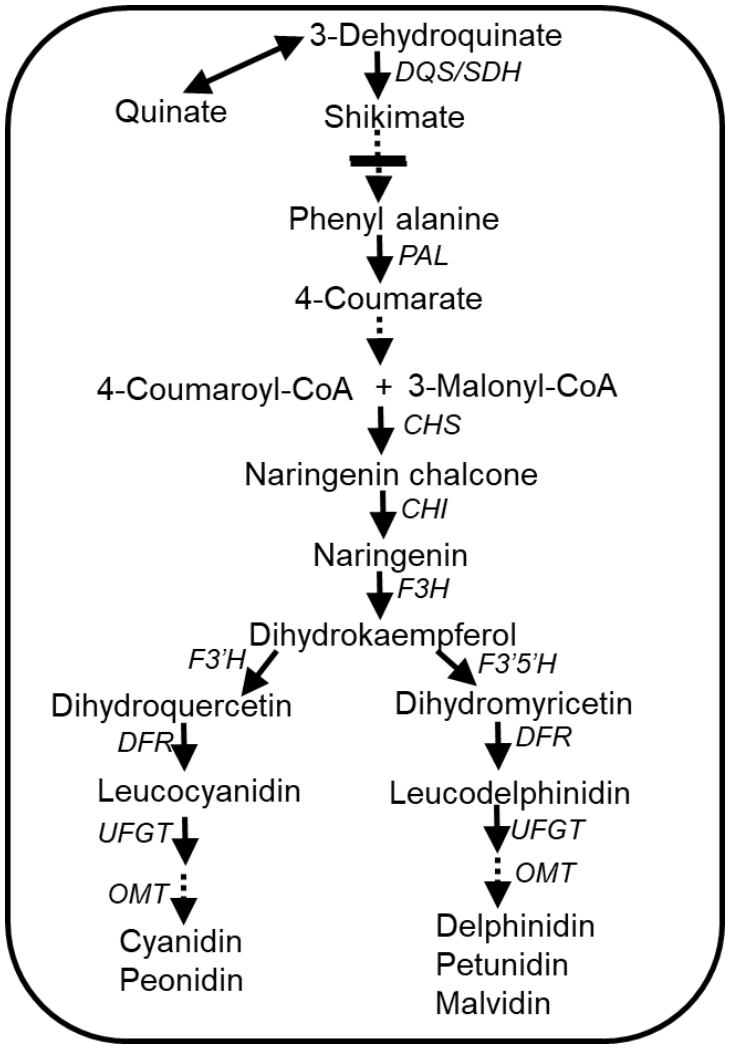

Figure 1.4: Anthocyanin metabolism and biosynthesis in fruits. Adapted from: (Ma et al., 2021).

Blueberry peel tissue contain various groups of anthocyanins such as delphinidin, cyanidin, petunidin, peonidin, and malvidin, that form derivatives with galactoside, glucoside,

and arabinoside; notably, malvidin 3-galactoside is present in substantial amounts (Wang et al., 2012). The anthocyanin accumulation increases during ripening and becomes maximum in blue fruit. This process is carried out by increased transcript abundance of anthocyanin biosynthesis-related genes during the ripening (Jaakola et al., 2002; Lin et al., 2018).

The goal of this study was to determine molecular and metabolic basis of ripening and postharvest physiology in blueberry. The specific objective are as follows:

- To determine sugar, acid, and anthocyanin metabolism during fruit development and ripening
- To determine effect of ethylene releasing PGRs on ripening, fruit metabolism, and postharvest fruit quality
- To characterize ripening related TFs during fruit development and ripening, and after application of ethylene releasing PGRs
- To predict fruit firmness using fruit physical and metabolic traits during postharvest storage

References

Alexander L, Grierson D (2002) Ethylene biosynthesis and action in tomato: a model for climacteric fruit ripening. Journal of experimental botany **53:** 2039-2055.

Ampa K, Saito T, Okawa K, Ohara H, Kondo S (2017) Effects of ethephon and abscisic acid application on ripening-related genes in 'Kohi'kiwifruit (Actinidia chinensis) on the vine. Horticultural Plant Journal **3:** 29-33.

An J-P, Wang X-F, Li Y-Y, Song L-Q, Zhao L-L, You C-X, Hao Y-J (2018) EIN3-LIKE1, MYB1, and ETHYLENE RESPONSE FACTOR3 act in a regulatory loop that synergistically modulates ethylene biosynthesis and anthocyanin accumulation. Plant Physiology **178:** 808-823.

Asiche WO, Mitalo OW, Kasahara Y, Tosa Y, Mworia EG, Owino WO, Ushijima K, Nakano R, Yano K, Kubo Y (2018) Comparative transcriptome analysis reveals distinct ethylene–independent regulation of ripening in response to low temperature in kiwifruit. BMC plant biology **18:** 1-18.

Ayaz F, Kadioglu A, Bertoft E, Acar C, Turna I (2001) Effect of fruit maturation on sugar and organic acid composition in two blueberries (Vaccinium arctostaphylos and V. myrtillus) native to Turkey.

Bai J, Baldwin EA, Goodner KL, Mattheis JP, Brecht JK (2005) Response of four apple cultivars to 1-methylcyclopropene treatment and controlled atmosphere storage. HortScience **40:** 1534-1538.

Bapat VA, Trivedi PK, Ghosh A, Sane VA, Ganapathi TR, Nath P (2010) Ripening of fleshy fruit: molecular insight and the role of ethylene. Biotechnology advances **28:** 94-107.

Batista-Silva W, Nascimento VL, Medeiros DB, Nunes-Nesi A, Ribeiro DM, Zsögön A, Araújo WL (2018) Modifications in organic acid profiles during fruit development and ripening: correlation or causation? Frontiers in Plant Science **9:** 1689.

Blankenship SM, Dole JM (2003) 1-Methylcyclopropene: a review. Postharvest biology and technology **28:** 1-25.

Bleecker AB, Kende H (2000) Ethylene: a gaseous signal molecule in plants. Annual review of cell and developmental biology **16:** 1-18.

Boller T, Herner RC, Kende H (1979) Assay for and enzymatic formation of an ethylene precursor, 1-aminocyclopropane-1-carboxylic acid. Planta **145:** 293-303.

Bouzayen M, Latché A, Nath P, Pech J-C (2010) Mechanism of fruit ripening. *In* Plant developmental biology-Biotechnological perspectives. Springer, pp 319-339.

Brown G, Schulte N, Timm E, Beaudry R, Peterson D, Hancock J, Takeda F (1996) Estimates of mechanization effects on fresh blueberry quality. Applied engineering in agriculture **12:** 21-26.

Cappai F, Benevenuto J, Ferrão LFV, Munoz P (2018) Molecular and genetic bases of fruit firmness variation in blueberry—A review. Agronomy **8:** 174.

Carrasco-Orellana C, Stappung Y, Mendez-Yañez A, Allan A, Espley R, Plunkett B, Moya-Leon M, Herrera R (2018) Characterization of a ripening-related transcription factor FcNAC1 from Fragaria chiloensis fruit. Scientific reports **8:** 10524.

Carrasco-Orellana C, Stappung Y, Mendez-Yañez A, Allan A, Espley R, Plunkett B, Moya-Leon M, Herrera R (2018) Characterization of a ripening-related transcription factor FcNAC1 from Fragaria chiloensis fruit. Scientific reports **8:** 1-12.

Casamali B, Williamson JG, Kovaleski AP, Sargent SA, Darnell RL (2016) Mechanical harvesting and postharvest storage of two southern highbush blueberry cultivars grafted onto Vaccinium Arboreum rootstocks. HortScience **51:** 1503-1510.

Chang C (2016) Q&A: How do plants respond to ethylene and what is its importance? BMC biology **14:** 7.

Chen F-X, Liu X-H, Chen L-S (2009) Developmental changes in pulp organic acid concentration and activities of acid-metabolising enzymes during the fruit development of two loquat (Eriobotrya japonica Lindl.) cultivars differing in fruit acidity. Food Chemistry **114:** 657-664.

Chen T, Qin G, Tian S (2020) Regulatory network of fruit ripening: current understanding and future challenges. New Phytologist **228:** 1219-1226.

Chervin C (2020) Should starch metabolism be a key point of the climacteric vs. non-climacteric fruit definition? Frontiers in Plant Science **11:** 609189.

Chervin C, El-Kereamy A, Roustan J-P, Latché A, Lamon J, Bouzayen M (2004) Ethylene seems required for the berry development and ripening in grape, a non-climacteric fruit. Plant Science **167:** 1301-1305.

Dekazos E (1979) Maturity and quality responses of'Tifblue'rabbiteye blueberries to SADH and ethephon [Growth regulators]. *In* Proceedings of the Florida State Horticultural Society.

Dekazos ED (1977) Effects of preharvest applictions of ethephon and SADH on ripening, firmness and storage quality of rabbiteye blueberries (cv.'T 19'). *In* Proceedings of the... annual meeting.

Delhaize E, Ryan PR, Hocking PJ, Richardson AE (2003) Effects of altered citrate synthase and isocitrate dehydrogenase expression on internal citrate concentrations and citrate efflux from tobacco (Nicotiana tabacum L.) roots. Plant and Soil **248:** 137-144.

Díaz-Riquelme J, Lijavetzky D, Martínez-Zapater JM, Carmona MJ (2009) Genome-wide analysis of MIKCC-type MADS box genes in grapevine. Plant physiology **149:** 354-369.

Dinar M, Stevens M (1981) The Relationship between Starch Accumulation and Soluble Solids Content of Tomato Fruits1. Journal of the American Society for Horticultural Science **106:** 415-418.

Durán-Soria S, Pott DM, Osorio S, Vallarino JG (2020) Sugar signaling during fruit ripening. Frontiers in Plant Science **11:** 564917.

Eck P (1970) Influence of Ethrel upon highbush blueberry fruit ripening. Horticultural Science **5:** 23-25.

El-Kereamy A, Chervin C, Roustan JP, Cheynier V, Souquet JM, Moutounet M, Raynal J, Ford C, Latché A, Pech JC (2003) Exogenous ethylene stimulates the long-term expression of genes related to anthocyanin biosynthesis in grape berries. Physiologia plantarum **119:** 175-182.

El Agamy S, Aly M, Biggs R (1982) Fruit maturity as related to ethylene in'Delite'blueberry. *In* Proceedings of the... annual meeting Florida State Horticultural Society.

Eriksson EM, Bovy A, Manning K, Harrison L, Andrews J, De Silva J, Tucker GA, Seymour GB (2004) Effect of the Colorless non-ripening mutation on cell wall biochemistry and gene expression during tomato fruit development and ripening. Plant Physiology **136:** 4184-4197.

FAO (2019) Food and Agriculture Organization of the United Nations. FAOSTAT. Crops. http://www.fao.org/faostat/en/#data/QC. Access 22 Jan. 2020.

Fenn MA, Giovannoni JJ (2021) Phytohormones in fruit development and maturation. The Plant Journal **105:** 446-458.

Frenkel C (1972) Involvement of peroxidase and indole-3-acetic acid oxidase isozymes from pear, tomato, and blueberry fruit in ripening. Plant Physiology **49:** 757-763.

Fujisawa M, Shima Y, Nakagawa H, Kitagawa M, Kimbara J, Nakano T, Kasumi T, Ito Y (2014) Transcriptional regulation of fruit ripening by tomato FRUITFULL homologs and associated MADS box proteins. The Plant Cell **26:** 89-101.

Gallardo RK, Stafne ET, DeVetter LW, Zhang Q, Li C, Takeda F, Williamson J, Yang WQ, Cline WO, Beaudry R (2018) Blueberry producers' attitudes toward harvest mechanization for fresh market. Horttechnology **28:** 10-16.

Gao Y, Fan ZQ, Zhang Q, Li HL, Liu GS, Jing Y, Zhang YP, Zhu BZ, Zhu HL, Chen JY (2021) A tomato NAC transcription factor, SlNAM1, positively regulates ethylene biosynthesis and the onset of tomato fruit ripening. The Plant Journal **108:** 1317-1331.

Gao Y, Wei W, Zhao X, Tan X, Fan Z, Zhang Y, Jing Y, Meng L, Zhu B, Zhu H (2018) A NAC transcription factor, NOR-like1, is a new positive regulator of tomato fruit ripening. Horticulture research **5.**

Gao Y, Zhu N, Zhu X, Wu M, Jiang C-Z, Grierson D, Luo Y, Shen W, Zhong S, Fu D-Q (2019) Diversity and redundancy of the ripening regulatory networks revealed by the fruitENCODE and the new CRISPR/Cas9 CNR and NOR mutants. Horticulture Research **6.**

Giovannoni JJ (2004) Genetic regulation of fruit development and ripening. The plant cell **16:** S170-S180.

Gramzow L, Theissen G (2010) A hitchhiker's guide to the MADS world of plants. Genome biology **11:** 214.

Guo L-X, Shi C-Y, Liu X, Ning D-Y, Jing L-F, Yang H, Liu Y-Z (2016) Citrate accumulation-related gene expression and/or enzyme activity analysis combined with metabolomics provide a novel insight for an orange mutant. Scientific Reports **6:** 29343.

Hou D-X (2003) Potential mechanisms of cancer chemoprevention by anthocyanins. Current molecular medicine **3:** 149-159.

Huang L, Tan H, Zhang C, Li Q, Liu Q (2021) Starch biosynthesis in cereal endosperms: An updated review over the last decade. Plant communications **2.**

Hussain SB, Shi C-Y, Guo L-X, Kamran HM, Sadka A, Liu Y-Z (2017) Recent advances in the regulation of citric acid metabolism in citrus fruit. Critical reviews in plant sciences **36:** 241-256.

Iannetta PP, Laarhoven LJ, Medina-Escobar N, James EK, McManus MT, Davies HV, Harren FJ (2006) Ethylene and carbon dioxide production by developing strawberries show a correlative pattern that is indicative of ripening climacteric fruit. Physiologia Plantarum **127:** 247-259.

Ireland HS, Yao JL, Tomes S, Sutherland PW, Nieuwenhuizen N, Gunaseelan K, Winz RA, David KM, Schaffer RJ (2013) Apple SEPALLATA1/2-like genes control fruit flesh development and ripening. The Plant Journal **73:** 1044-1056.

Itkin M, Seybold H, Breitel D, Rogachev I, Meir S, Aharoni A (2009) TOMATO AGAMOUS-LIKE 1 is a component of the fruit ripening regulatory network. The Plant Journal **60:** 1081-1095.

Ito Y, Kitagawa M, Ihashi N, Yabe K, Kimbara J, Yasuda J, Ito H, Inakuma T, Hiroi S, Kasumi T (2008) DNA-binding specificity, transcriptional activation potential, and the rin mutation effect for the tomato fruit-ripening regulator RIN. The Plant Journal **55:** 212-223.

Ito Y, Nishizawa-Yokoi A, Endo M, Mikami M, Shima Y, Nakamura N, Kotake-Nara E, Kawasaki S, Toki S (2017) Re-evaluation of the rin mutation and the role of RIN in the induction of tomato ripening. Nature plants **3:** 866-874.

Ito Y, Sekiyama Y, Nakayama H, Nishizawa-Yokoi A, Endo M, Shima Y, Nakamura N, Kotake-Nara E, Kawasaki S, Hirose S (2020) Allelic mutations in the ripening-inhibitor locus generate extensive variation in tomato ripening. Plant physiology **183:** 80-95.

Jaakola L, Määttä K, Pirttilä AM, Törrönen R, Kärenlampi S, Hohtola A (2002) Expression of genes involved in anthocyanin biosynthesis in relation to anthocyanin, proanthocyanidin, and flavonol levels during bilberry fruit development. Plant physiology **130:** 729-739.

Koca I, Karadeniz B (2009) Antioxidant properties of blackberry and blueberry fruits grown in the Black Sea Region of Turkey. Scientia Horticulturae **121:** 447-450.

Kötting O, Pusch K, Tiessen A, Geigenberger P, Steup M, Ritte G (2005) Identification of a novel enzyme required for starch metabolism in Arabidopsis leaves. The phosphoglucan, water dikinase. Plant physiology **137:** 242-252.

Li L, Guo M, Wang X, Zhang X, Liu T (2017) Effects and Mechanism of 1-Methylcyclopropene and Ethephon on Softening in Ailsa Craig Tomato Fruit. Journal of Food Processing and Preservation **41:** e12883.

Li S, Chen K, Grierson D (2021) Molecular and hormonal mechanisms regulating fleshy fruit ripening. Cells **10:** 1136.

Lin Y, Wang Y, Li B, Tan H, Li D, Li L, Liu X, Han J, Meng X (2018) Comparative transcriptome analysis of genes involved in anthocyanin synthesis in blueberry. Plant Physiology and Biochemistry **127:** 561-572.

Liu M, Pirrello J, Chervin C, Roustan J-P, Bouzayen M (2015) Ethylene control of fruit ripening: revisiting the complex network of transcriptional regulation. Plant physiology **169:** 2380-2390.

Liu Y, Liu Q, Xiong J, Deng X (2007) Difference of a citrus late-ripening mutant (Citrus sinensis) from its parental line in sugar and acid metabolism at the fruit ripening stage. Science in China Series C: Life Sciences **50:** 511-517.

Lu W, Chen J, Ren X, Yuan J, Han X, Mao L, Ying T, Luo Z (2018) One novel strawberry MADS-box transcription factor FaMADS1a acts as a negative regulator in fruit ripening. Scientia Horticulturae **227:** 124-131.

Lu Y, Sharkey TD (2006) The importance of maltose in transitory starch breakdown. Plant, cell & environment **29:** 353-366.

Ma Y, Ma X, Gao X, Wu W, Zhou B (2021) Light induced regulation pathway of anthocyanin biosynthesis in plants. International journal of molecular sciences **22:** 11116.

MacLean DD, NeSmith DS (2011) Rabbiteye blueberry postharvest fruit quality and stimulation of ethylene production by 1-methylcyclopropene. HortScience **46:** 1278-1281.

Malladi A, Vashisth T, Johnson LK (2012) Ethephon and methyl jasmonate affect fruit detachment in rabbiteye and southern highbush blueberry. HortScience **47:** 1745-1749.

Malladi A, Vashisth T, NeSmith S (2013) Development and evaluation of a portable, handheld mechanical shaker to study fruit detachment in blueberry. HortScience **48:** 394-397.

Manning K, Tör M, Poole M, Hong Y, Thompson AJ, King GJ, Giovannoni JJ, Seymour GB (2006) A naturally occurring epigenetic mutation in a gene encoding an SBP-box transcription factor inhibits tomato fruit ripening. Nature genetics **38:** 948-952.

Martel C, Vrebalov J, Tafelmeyer P, Giovannoni JJ (2011) The tomato MADS-box transcription factor RIPENING INHIBITOR interacts with promoters involved in numerous ripening processes in a COLORLESS NONRIPENING-dependent manner. Plant physiology **157:** 1568-1579.

Martín-Pizarro C, Vallarino JG, Osorio S, Meco V, Urrutia M, Pillet J, Casanal A, Merchante C, Amaya I, Willmitzer L (2021) The NAC transcription factor FaRIF controls fruit ripening in strawberry. The Plant Cell **33:** 1574-1593.

McAtee PA, Richardson AC, Nieuwenhuizen NJ, Gunaseelan K, Hoong L, Chen X, Atkinson RG, Burdon JN, David KM, Schaffer RJ (2015) The hybrid non-ethylene

and ethylene ripening response in kiwifruit (Actinidia chinensis) is associated with differential regulation of MADS-box transcription factors. BMC plant biology **15:** 1-16.

Moya-León MA, Mattus-Araya E, Herrera R (2019) Molecular events occurring during softening of strawberry fruit. Frontiers in plant science **10:** 615.

Nakkanong K, Yang JH, Zhang MF (2012) Starch accumulation and starch related genes expression in novel inter-specific inbred squash line and their parents during fruit development. Scientia horticulturae **136:** 1-8.

Norvell DJ (1982) An evaluation of chilling models for estimating rest requirements of highbush blueberries (Vaccinium corymbosum L.).

Olsen AN, Ernst HA, Leggio LL, Skriver K (2005) NAC transcription factors: structurally distinct, functionally diverse. Trends in plant science **10:** 79-87.

Paul V, Pandey R, Srivastava GC (2012) The fading distinctions between classical patterns of ripening in climacteric and non-climacteric fruit and the ubiquity of ethylene—an overview. Journal of food science and technology **49:** 1-21.

Pereira L, Santo Domingo M, Ruggieri V, Argyris J, Phillips MA, Zhao G, Lian Q, Xu Y, He Y, Huang S (2020) Genetic dissection of climacteric fruit ripening in a melon population segregating for ripening behavior. Horticulture research **7.**

Périn C, Gomez-Jimenez M, Hagen L, Dogimont C, Pech J-C, Latché A, Pitrat M, Lelièvre J-M (2002) Molecular and genetic characterization of a non-climacteric phenotype in melon reveals two loci conferring altered ethylene response in fruit. Plant Physiology **129:** 300-309.

Pfister B, Zeeman SC (2016) Formation of starch in plant cells. Cellular and Molecular Life Sciences **73:** 2781-2807.

Prior R (2004) Absorption and metabolism of anthocyanins: potential health effects. Phytochemicals: Mechanisms of action**:** 1-19.

Quinet M, Angosto T, Yuste-Lisbona FJ, Blanchard-Gros R, Bigot S, Martinez J-P, Lutts S (2019) Tomato fruit development and metabolism. Frontiers in plant science**:** 1554.

Rath AC, Kang I-K, Park C-H, Yoo W-J, Byun J-K (2006) Foliar application of aminoethoxyvinylglycine (AVG) delays fruit ripening and reduces pre-harvest fruit drop and ethylene production of bagged "Kogetsu" apples. Plant Growth Regulation **50:** 91.

Reque PM, Steckert EV, dos Santos FT, Danelli D, Jablonski A, Flôres SH, Rech R, de O. Rios A, de Jong EV (2016) Heat processing of blueberries and its effect on their physicochemical and bioactive properties. Journal of Food Process Engineering **39:** 564-572.

Ruan Y-L (2014) Sucrose metabolism: gateway to diverse carbon use and sugar signaling. Annual review of plant biology **65:** 33-67.

Schaart JG, Dubos C, Romero De La Fuente I, van Houwelingen AM, de Vos RC, Jonker HH, Xu W, Routaboul JM, Lepiniec L, Bovy AG (2013) Identification and characterization of MYB-b HLH-WD 40 regulatory complexes controlling proanthocyanidin biosynthesis in strawberry (F ragaria× ananassa) fruits. New phytologist **197:** 454-467.

Schaffer AA, Levin I, Oguz I, Petreikov M, Cincarevsky F, Yeselson Y, Shen S, Gilboa N, Bar M (2000) ADPglucose pyrophosphorylase activity and starch accumulation in

immature tomato fruit: the effect of a Lycopersicon hirsutum-derived introgression encoding for the large subunit. Plant Science **152:** 135-144.

Seymour GB, Østergaard L, Chapman NH, Knapp S, Martin C (2013) Fruit development and ripening. Annual review of plant biology **64:** 219-241.

Seymour GB, Ryder CD, Cevik V, Hammond JP, Popovich A, King GJ, Vrebalov J, Giovannoni JJ, Manning K (2011) A SEPALLATA gene is involved in the development and ripening of strawberry (Fragaria× ananassa Duch.) fruit, a non-climacteric tissue. Journal of experimental botany **62:** 1179-1188.

Shan W, Kuang J-f, Chen L, Xie H, Peng H-h, Xiao Y-y, Li X-p, Chen W-x, He Q-g, Chen J-y (2012) Molecular characterization of banana NAC transcription factors and their interactions with ethylene signalling component EIL during fruit ripening. Journal of Experimental Botany **63:** 5171-5187.

Shi M, Loftus H, McAinch AJ, Su XQ (2017) Blueberry as a source of bioactive compounds for the treatment of obesity, type 2 diabetes and chronic inflammation. Journal of Functional Foods **30:** 16-29.

Shima Y, Kitagawa M, Fujisawa M, Nakano T, Kato H, Kimbara J, Kasumi T, Ito Y (2013) Tomato FRUITFULL homologues act in fruit ripening via forming MADS-box transcription factor complexes with RIN. Plant Molecular Biology **82:** 427-438.

Shinozaki Y, Nicolas P, Fernandez-Pozo N, Ma Q, Evanich DJ, Shi Y, Xu Y, Zheng Y, Snyder SI, Martin LB (2018) High-resolution spatiotemporal transcriptome mapping of tomato fruit development and ripening. Nature communications **9:** 1-13.

Shore P, Sharrocks AD (1995) The MADS-box family of transcription factors. European Journal of Biochemistry **229:** 1-13.

Silva S, Costa EM, Coelho MC, Morais RM, Pintado ME (2017) Variation of anthocyanins and other major phenolic compounds throughout the ripening of four Portuguese blueberry (Vaccinium corymbosum L) cultivars. Natural product research **31:** 93-98.

Smaczniak C, Immink RG, Angenent GC, Kaufmann K (2012) Developmental and evolutionary diversity of plant MADS-domain factors: insights from recent studies. Development **139:** 3081-3098.

Souleyre EJ, Iannetta PP, Ross HA, Hancock RD, Shepherd LV, Viola R, Taylor MA, Davies HV (2004) Starch metabolism in developing strawberry (Fragaria× ananassa) fruits. Physiologia Plantarum **121:** 369-376.

Stein O, Granot D (2018) Plant fructokinases: evolutionary, developmental, and metabolic aspects in sink tissues. Frontiers in Plant Science **9:** 339.

Strik BC, Finn CE, Moore PP (2014) Blueberry Cultivars for the Pacific Northwest. A Pacific Northwest Extension Publication. Oregon State University-University of Idaho-Washington State University. Access 23 Jan. 2020. https://catalog.extension.oregonstate.edu/.

Suehiro Y, Mochida K, Tsuma M, Yasuda Y, Itamura H, Esumi T (2019) Effects of abscisic acid/ethephon treatments on berry development and maturation in the yellow-green skinned ‘Shine Muscat’grape. The Horticulture Journal **88:** 189-201.

Suzuki A, Kikuchi T, Aoba K (1997) Changes of ethylene evolution, ACC content, ethylene forming enzyme activity and respiration in fruits of highbush blueberry. Journal of the Japanese Society for Horticultural Science **66:** 23-27.

Sweetman C, Deluc LG, Cramer GR, Ford CM, Soole KL (2009) Regulation of malate metabolism in grape berry and other developing fruits. Phytochemistry **70:** 1329-1344.

Takeda F, Krewer G, Andrews EL, Mullinix B, Peterson DL (2008) Assessment of the V45 blueberry harvester on rabbiteye blueberry and southern highbush blueberry pruned to V-shaped canopy. HortTechnology **18:** 130-138.

Tang G-Q, Lüscher M, Sturm A (1999) Antisense repression of vacuolar and cell wall invertase in transgenic carrot alters early plant development and sucrose partitioning. The Plant Cell **11:** 177-189.

Tauzin AS, Giardina T (2014) Sucrose and invertases, a part of the plant defense response to the biotic stresses. Frontiers in plant science **5:** 293.

Vrebalov J, Ruezinsky D, Padmanabhan V, White R, Medrano D, Drake R, Schuch W, Giovannoni J (2002) A MADS-box gene necessary for fruit ripening at the tomato ripening-inhibitor (rin) locus. Science **296:** 343-346.

Wang A, Xu K (2012) Characterization of two orthologs of REVERSION-TO-ETHYLENE SENSITIVITY1 in apple. Journal of Molecular Biology Research **2:** 24.

Wang R, da Rocha Tavano EC, Lammers M, Martinelli AP, Angenent GC, de Maagd RA (2019) Re-evaluation of transcription factor function in tomato fruit development and ripening with CRISPR/Cas9-mutagenesis. Scientific reports **9:** 1-10.

Wang SY, Chen H, Camp MJ, Ehlenfeldt MK (2012) Flavonoid constituents and their contribution to antioxidant activity in cultivars and hybrids of rabbiteye blueberry (Vaccinium ashei Reade). Food Chemistry **132:** 855-864.

Wang Y-W, Acharya TP, Malladi A, Tsai H-J, NeSmith DS, Doyle JW, Nambeesan SU (2022) Atypical climacteric and functional ethylene metabolism and signaling during fruit ripening in blueberry (Vaccinium sp.). Frontiers in Plant Science **13:** 932642.

Wang Y-W, Malladi A, Doyle JW, Scherm H, Nambeesan SU (2018) The Effect of Ethephon, Abscisic Acid, and Methyl Jasmonate on Fruit Ripening in Rabbiteye Blueberry (Vaccinium virgatum). Horticulturae **4:** 24.

Weise SE, van Wijk KJ, Sharkey TD (2011) The role of transitory starch in C3, CAM, and C4 metabolism and opportunities for engineering leaf starch accumulation. Journal of experimental botany **62:** 3109-3118.

Williamson JG, Phillips DA, Lyrene P, Munoz PR (2019) Southern Highbush Blueberry Cultivars from the University of Florida: HS1245, rev. 2/2019. Edis **2019.**

Xie Y-G, Ma Y-Y, Bi P-P, Wei W, Liu J, Hu Y, Gou Y-J, Zhu D, Wen Y-Q, Feng J-Y (2020) Transcription factor FvTCP9 promotes strawberry fruit ripening by regulating the biosynthesis of abscisic acid and anthocyanins. Plant Physiology and Biochemistry **146:** 374-383.

Xu X, Yin L, Ying Q, Song H, Xue D, Lai T, Xu M, Shen B, Wang H, Shi X (2013) High-throughput sequencing and degradome analysis identify miRNAs and their targets involved in fruit senescence of Fragaria ananassa. PLoS One **8.**

Yokotani N, Nakano R, Imanishi S, Nagata M, Inaba A, Kubo Y (2009) Ripening-associated ethylene biosynthesis in tomato fruit is autocatalytically and developmentally regulated. Journal of experimental botany **60:** 3433-3442.

Zhang P, Zhou Z (2019) Postharvest ethephon degreening improves fruit color, flavor quality and increases antioxidant capacity in 'Eureka'lemon (Citrus limon (L.) Burm. f.). Scientia Horticulturae **248:** 70-80.

Zhang X-M, Wang W, Du L-Q, Xie J-H, Yao Y-L, Sun G-M (2012) Expression patterns, activities and carbohydrate-metabolizing regulation of sucrose phosphate synthase, sucrose synthase and neutral invertase in pineapple fruit during development and ripening. International journal of molecular sciences **13:** 9460-9477.

Zhou T, Li R, Yu Q, Wang J, Pan J, Lai T (2022) Proteomic Changes in Response to Colorless nonripening Mutation during Tomato Fruit Ripening. Plants **11:** 3570.

Zhu M, Chen G, Zhou S, Tu Y, Wang Y, Dong T, Hu Z (2014) A new tomato NAC (N AM/A TAF1/2/C UC2) transcription factor, SlNAC4, functions as a positive regulator of fruit ripening and carotenoid accumulation. Plant and Cell Physiology **55:** 119-135.

Zhu X, Zhang C, Wu W, Li X, Zhang C, Fang J (2017) Enzyme activities and gene expression of starch metabolism provide insights into grape berry development. Horticulture research **4.**

CHAPTER 2

MOLECULAR AND METABOLIC BASIS OF RIPENING IN RABBITEYE BLUEBERRY

[1] Tej P. Acharya and Savithri U. Nambeesan. To be submitted to Horticulture Research.

Abstract

The rabbiteye blueberry (*V. virgatum* Ait.) is a commonly grown cultivar in the southeastern U.S. Sugar, acid, and anthocyanin accumulation during ripening is responsible for fruit flavor and color. However, the molecular and metabolic regulation of blueberry fruit ripening has still not been thoroughly investigated. This study aimed to determine sugar, acid, and anthocyanin metabolism during fruit development and ripening. Fruits were collected from two cultivars, Premier and Powderblue at multiple developmental stages, which included green, immature fruit up until fully blue to capture various phases of ripening initiation and progression. Sugars, acids, and amino acids were measured using gas chromatography, and anthocyanins compounds using high-performance liquid chromatography. In both cultivars, the major sugars, glucose, fructose, and sucrose increased during ripening initiation and progression until the fully ripe stage. The major acids, malate and quinate decreased during ripening in both cultivars, whereas citrate transiently increased during ripening initiation only in 'Powderblue'. The concentration of starch was very low in all stages of fruit development used in this study. We identified 15 different anthocyanins, that increased during ripening with a maximum concentration at the fully ripe stage. In addition, differentially expressed genes from a 'Powderblue' fruit transcriptome was used to perform weighted gene co-expression network analysis (WGCNA) to identify key gene modules that correlate with metabolites. We identified a module consisting of 2,131 transcripts, which are positively correlated with sugars and anthocyanins, and negatively correlated with acids (malate, quinate). The GO enrichment analysis of this module identified transcripts related to sugar, acid, and phenylpropanoid biosynthesis pathway. Some of these transcripts including

several other sugar and acid metabolism-related genes were validated using qRT-PCR analysis. The transcript abundance of *VACUOLAR INVERTASE*, *SUCROSE SYNTHASE*, *SUCROSE PHOSPHATE SYNTHASE*, *HEXOKINASE*, and *PHOSPHOFRUCTOKINASE*, increased during ripening suggesting active sucrose catabolism and re-synthesis, and glycolysis during fruit ripening. *PHOSPHOENOL PYRUVATE CARBOXYKINASE* increased during fruit ripening and was negatively correlated with malate concentrations, suggesting synthesis of phosphoenol pyuruvate may be directed towards anthocyanin production during ripening. In addition, the expression of several anthocyanin biosynthesis-related genes was positively correlated with accumulation of anthocyanins during ripening. Overall, this study provided insights into sugar and acid metabolism during fruit ripening in rabbiteye blueberry.

Keywords: sugar, organic acid, metabolites, anthocyanin, fruit development, ripening

Introduction

Fruit ripening is a highly coordinated process involving physiological, biochemical, and molecular changes that collectively determine the development of the fruit's color, texture, sugar, acidity, and aroma volatiles (White, 2002). Blueberry (*Vaccinium sp.*) fruit exhibit a double sigmoidal growth curve and can be divided broadly into three stages (Retamales and Hancock, 2018). Stage I is the rapid cell division stage, lasting for 25-35 days of fruit development, depending on the cultivar and environmental conditions (Birkhold et al., 1992; Cano-Medrano and Darnell, 1997). At this stage, fruit have a higher concentration of organic acids, such as citrate, malate, and quinate, and lower concentration of sugars. Stage II lasts for 30-40 days, where cell division slows down and seed development occurs (Edwards et al., 1972; Retamales and Hancock, 2018). During stage III, growth is resumed mainly due to cell enlargement, and lasts about 30-60 days until fruit maturity (Birkhold et al., 1992; Cano-Medrano and Darnell, 1997; Retamales and Hancock, 2018). During fruit maturity and ripening, as fruit change color from green to pink to blue, the concentration of organic acids starts to decline and that of sugars and anthocyanins increase.

During the course of plant growth and development, mainly sugars like sucrose, sorbitol, and occasionally trehalose, raffinose, mannitol, and stachyose are translocated from maturing leaf (source organs) to young leaf, fruit, root, shoot, and other developing organs such as tubers (sink organs) (Zimmermann and Ziegler, 1975; Rennie and Turgeon, 2009). Among them, sucrose is the primary translocating sugar in fruits like citrus, persimmon, tomato, grape, strawberry, and banana (Yamaki, 2010; Lemoine et al., 2013). However, in fruits belonging to

the Rosaceae family like apple, sorbitol (sugar alcohol) is the major translocating sugar (Bieleski, 1969). Sink tissues are dependent on these translocated sugars as a means of providing energy, and to be used for the synthesis of nucleotides, amino acids and structural carbohydrates such as cellulose and starch (Stein and Granot, 2019). Sucrose that is unloaded from the phloem can enter the sink tissue symplastically via plasmodesmata (Lemoine et al., 2013; Braun et al., 2014). Another route of sucrose entry is via the apoplastic space, where it can be translocated via sucrose transporters into sink cells or broken down into glucose and fructose via cell wall invertases (cwINV), and then be transported into sink cells via hexose transporters (Braun et al., 2014; Stein and Granot, 2019). Once sucrose has entered sink cells, it can have multiple fates. Sucrose can be transported into the vacuoles for storage, or broken down via vacuolar invertase (vINV) and stored as hexose sugars and/or fructans, which is catalyzed by fructosyltransferases (FTs). In the cytosol, sucrose can be hydrolyzed irreversibly by cytosolic INV into glucose and fructose, or by sucrose synthase (SuSy) that reversibly cleaves sucrose to fructose and UDP-glucose.

The direction of catalysis of SuSy depends on pH with sucrose synthesis predominantly occurring at a more alkaline pH of 7.5-9.5 and catabolism at pH 5.5-7.5 (Bungaruang et al., 2013; Schmölzer et al., 2016). There is some evidence to suggest that SuSy may also catalyze sucrose into ADP glucose and fructose, thus playing a direct role in starch synthesis (Baroja-Fernández et al., 2003; Stein and Granot, 2019). This phenomenon may be more pronounced in sink tissues, where reduced SuSy activity leads to a decrease in starch levels in maize endosperm, potato tubers, and carrot taproots (Chourey and Nelson, 1976; Zrenner et al., 1995; Tang and Sturm, 1999; Stein and Granot, 2019). Thus SuSy activity may be directly contributing

to sink strength by increasing sink organ size (Stein and Granot, 2019). This hypothesis is supported by studies showing that a reduction in SuSy activity in sink tissues decreased seed weight in pea and tuber weight in potato (Zrenner et al., 1995; Craig et al., 1999). In tomato fruit, there has been some controversy regarding the role of SuSy, with transgenic antisense SuSy lines demonstrating reduced sucrose import into fruit only at 7 days after anthesis (DAA) without affecting later stages of fruit development, including starch accumulation (D'Aoust et al., 1999). However, strawberry fruits with virus induced gene silencing of *FaSuSy1* exhibited a retardation in ripening (Zhao et al., 2017).

The cwINV and vINV exhibit their highest activity within the pH range of 4.5-5.0, while nINV reaches its peak at a neutral or slightly alkaline pH (7-7.8) (Sturm, 1999). Sink tissues, such as tomato fruit, exhibit a preference for SuSy over INV during early developmental stages, but as ripening progresses, acid INV activity increases (Wang et al., 1994). SuSy plays a more significant role in sucrose unloading during the rapid growth phase, whereas the regulation of hexose concentration in leaves and fruit primarily depends on vINV activity (Nguyen-Quoc and Foyer, 2001). Sucrose hydrolysis also occurs within the fruit apoplastic space by cwINV, albeit at a slower rate than SuSy-mediated hydrolysis (Nguyen-Quoc and Foyer, 2001). The increased activity of cwINV hydrolyzes sucrose into glucose and fructose, thereby establishing a concentration gradient that enhances the export of sucrose from source to sink (Ruan, 2014). On the other hand, vINV is crucial for hexose accumulation and cell expansion in fruits throughout their development and ripening; nINV plays a significant role in maintaining sugar homeostasis in the cytoplasm, particularly when the activity of SuSy is diminished (Tang et al., 1999). Reducing INV activities leads to a decreased hexose-to-sucrose ratio without altering the total

amount of soluble sugars in potato tubers and sugarcane culm (Zrenner et al., 1996; Rossouw et al., 2010). In muskmelon, the suppression of acid INV via an antisense approach results in smaller leaves and thinner stems, ultimately causing a 60% reduction in fruit size (Yu et al., 2008).

In addition to sucrose import to the fruit, re-synthesis of sucrose occurs in the cytosol by the action of two enzymes, sucrose phosphate synthase (SPS) and sucrose 6-phosphatase (SPP). The higher SPS activity is associated with the greater sucrose/hexose ratio in pineapple fruit (Zhang et al., 2012). The transcript level and activity of SPS increased later during ripening and is associated with the increase in sucrose level in apple (Li et al., 2012). The overexpression of *SPS* in tomato leaves (maize *SPS* in tomato) and *Arabidopsis* resulted in the accumulation of more sucrose with less starch in the leaves (Worrell et al., 1991; Galtier et al., 1993; Signora et al., 1998). In addition, overexpression of *SPS* affected carbon partitioning, as more carbon is allocated in the shoots and less in roots (Galtier et al., 1993). Despite its energetic cost, the re-synthesis of sucrose is essential for efficiently distributing carbon compounds throughout the plant, as sucrose's metabolic stability, compared to hexoses, facilitates precise transport of carbon to support regions of growth and development (Ruan, 2014). In addition, the excess amount of glucose, fructose, and sucrose are stored in the vacuoles and utilized in the metabolic process during the ripening and postharvest stages.

Two types of starch are found in plants: transitory and storage starch. The formation of transitory starch occurs during the day in the source organ, and its breakdown occurs during the night when plants no longer synthesize carbon from photosynthesis (Pfister and Zeeman, 2016). During the breakdown process, the transitory starch is enzymatically converted into glucose and

maltose in chloroplast using DEBRANCHING, GLUCAN WATER DIKINASE, PHOSPHOGLUCAN WATER DIKINASE, and β-AMYLASE enzymes (Kötting et al., 2005; Lu and Sharkey, 2006). The synthesis of storage starch occurs in the sink organs like roots, tubers, and fruits (Huang et al., 2021). Multiple enzymes are involved in starch synthesis. Among them, ADP glucose phosphorylase (AGPase) is the rate-limiting step in starch biosynthesis, and an increase in its expression level resulted in the higher accumulation of starch in squash and tomato (Schaffer et al., 2000; Nakkanong et al., 2012). Similarly, starch accumulation during the early developmental stages is associated with the higher AGPase activity in tomato (Robinson et al., 1988). The overexpression of AGPase cytosolic large subunit genes using *Agrobacterium* mediated transformation increased the activity of AGPase and starch content in wheat (Kang et al., 2013). In strawberry, AGPase protein was detected, however displayed no association with starch accumulation during fruit development and ripening (Souleyre et al., 2004). In addition, other studies found that together with AGPase, other enzymes like SuSy, FRUCTOKINASE (FK), and STARCH SYNTHASE (SS) are the rate limiting enzymes in starch synthesis and their decreased activities are associated with the reduction in starch accumulation (Schaffer and Petreikov, 1997, 1997). Finally, the breakdown of starch occurs by amylase into maltose, then maltose enters the cytosol, where it can be converted into glucose. The reduction in starch concentration is associated with increased α-amylase activity and reduced sugar concentration in tomato (Dinar and Stevens, 1981).

The hexoses (glucose and fructose) formed as a breakdown of sucrose are phosphorylated by hexokinase (HK) and FK, which are the key precursors for the fruit metabolic process during respiration (Stein and Granot, 2018). Two major metabolic cycles occur for the fruit respiration:

glycolysis and tricarboxylic acid (TCA) cycle. Organic acid accumulation occurs earlier during fruit development, and is an important substrate needed for the respiratory burst during the onset of ripening in fruits (Seymour et al., 2013). The metabolism of organic acids such as malate and citrate are mainly responsible for the variation in the acidity of the fruits (Sweetman et al., 2009). The higher activity of PHOSPHOENOLPYRUVATE CARBOXYLASE (PEPC), NAD-MALATE DEHYDROGENASE (NAD-MDH), and NADP-MALIC ENZYME (NADP-ME) during earlier developmental stages increased malate concentration in the loquat fruits (Chen et al., 2009). The increase in activity of PEPCK is related to the decrease in concentration of malate and citrate in the fruits (Famiani et al., 2005). The excess malate can also be stored in the vacuoles and utilized in the metabolic process later during fruit development and ripening. During its utilization, malate can be transported from the vacuoles to the cytosol using the vacuolar transporter (Sweetman et al., 2009). Malate can enter the mitochondria to be consumed in the tricarboxylic acid (TCA) cycle leading to the synthesis and metabolism of citrate. The TCA cycle is the crucial biochemical process where the majority of ATP synthesis occurs through the oxidation of NADH and $FADH_2$, accompanied by the release of CO_2. Citrate is the major primary acid to accumulate during the TCA cycle, and excess amounts can be stored in vacuoles (Hussain et al., 2017). Citrate synthase (CS) is involved in the conversion of oxaloacetate to citrate, but its role in citrate accumulation is not clearly understood.

The carbon metabolism also leads to the formation of secondary acids like quinate and shikimate from phosphoenolpyruvate (PEP). These acids are the precursors for the formation of anthocyanins in the fruits. Anthocyanin are polyphenolic compounds and previous studies have demonstrated the health benefits of these compounds as they have high antioxidant activities,

preventing chronic diseases, cancer, and heart problems (Hou, 2003; Prior, 2004). Accumulation of anthocyanin during ripening is a result of increased transcript abundance of anthocyanin biosynthesis-related genes (Jaakola et al., 2002; Lin et al., 2018). The over expression of *CHALCONE SYNTHASE* (*CHS*) by *Agrobacterium* mediated transformation increases flavonoid content (Hu et al., 2020; Yin et al., 2020). The CRISPR/Case9 knockout of *FLAVONOID 3'-HYDROXYLASE* (*F3'H*) produced a distinct reddish orange phenotype in place of red by increasing the ratio of pelarogonidin to cyanidin (Nitarska et al., 2021). The increase in transcript abundance of *PHENYLALANINE AMMONIA LYASE* (*PAL), CHS, F3'H, FLAVONOL SYNTHASE* (*FLS*), *CHS, ANTHOCYANIDIN 3-O-GLUCOSYLTRANSFERASE* (*UFGT*), and *ANTHOCYANIDIN SYNTHASE* (*ANS*) during bilberry and northern highbush blueberry during ripening indicates an important role for these enzymes in anthocyanin accumulation (Jaakola et al., 2002; Lin et al., 2018).

The rabbiteye blueberry (*V. virgatum* Ait.) is an important, commonly grown blueberry in the southeastern U.S. A previous study observed increased concentrations of glucose, fructose, and sucrose in ripe fruits compared to unripe fruits, as well as a decrease in major acids like malate, citrate, and quinate during ripening, although these comparisons were limited to highbush and native Turkish blueberries using few developmental stages (Ayaz et al., 2001; Hwang et al., 2020). Therefore, there is a need for a comprehensive study to investigate sugar, acid, and anthocyanin metabolism, along with the role of their biosynthesis genes in blueberry. Hence, the primary objectives of this study were to elucidate the molecular and metabolic basis of sugar, starch, acid, and anthocyanin metabolism throughout various developmental stages and ripening in rabbiteye blueberry.

Materials and Methods

Plant material

Fruits samples were collected from two rabbiteye cultivars (Premier and Powderblue) in 2020 from the Durham Horticulture Farm, Athens, Georgia. Fruits were collected from five developmental stages and categorized as stages S4, S5, S6, S7, and S8 based on Zifkin et al. (2014). Stages S4 and S5 were collected based on fruit size (S4 < 9 mm, and S5 >9-<13 mm in diameter), and stages S6, S7, and S8 were based on the fruit color (S6: 25-50% light pink skin, S7: predominately light to dark pink skin with some blue, and S8: blue skin) (Fig. 2.1A). Fruit diameter and weight were measured using the Vernier caliper and precision weighing balance, respectively. Ethylene evolution and respiration rate were measured as described by Wang et al., (2022). All samples were collected in four replicates and frozen in liquid nitrogen at -80°C until further analysis. The experimental design was completely randomized with four replications.

Metabolite analysis using gas chromatography: Sugars, acids, and amino acids were extracted according to (Beshir et al., 2017), with some modifications. Frozen fruit tissues were ground into a fine powder using a mortar and pestle in liquid nitrogen. Then, 125-150 mg of fruit powder was extracted into 1.5 ml methanol containing 0. l25 mg/ml of phenyl-β-D-glucoside as an internal standard. Next, methanol extracted samples were centrifuged at 22,000 g for 30 min at 4 ℃. Following this, 100 µl of supernatant was transferred into a 300 µl glass insert (Insert glass flat, Thomas scientific, Swedesboro, NJ, USA) in a 2 ml gas chromatography (GC) vial (SureSTART vial, Thermo Fisher Scientific, Rockwood, TN, USA). The solvent was placed in a dry bath set at 45 ℃ and evaporated using nitrogen gas. Subsequently, samples were derivatized

by methoxymation followed by silylation. First, 50 µl of methoxamine (20 mg methoxamine in 1 ml pyridine) was added to each sample and heated at 50 ℃ for 30 minutes. Then, 100 µl of N-Methyl-N-(trimethylsilyl) trifluoroacetamide (MSTFA) + 1% trimethylchlorosilane (TMCS) was added to each sample and heated at 50 °C for 30 minutes. Finally, the derivatized samples were used to quantify the metabolites.

Initially, metabolites were identified using GC-Mass Spectrometry equipped with a quadrupole mass spectrometer (GCMS), using a small subset of samples. Next, all samples were run on a GC-Flame Ionization Detector (GC-FID) (GC-2014; Shimadzu, Japan) with HP-5 fused capillary column (J&W Scientific, Fulsom, CA, USA; length=25m x 0.2 mm x 0.33 µm, ID=4293415) using the same method as the GCMS. Helium was used as a carrier gas. Samples were injected using a 20:1 split ratio. The initial temperature of the oven was set up at 120 ℃ for 1 minute. Then, at the rate of 4 °C per minute ramped to 180 ℃, 0.5 min at 180 °C, 0.5 ℃ per minute ramped to 185 ℃, 0.5 min at 185 ℃, 1 ℃ per minute ramped to 210 ℃, 0.5 minutes at 210 ℃, 10 °C per minute ramped to 260 °C, and finally held for 12 minutes at 260 °C. For sample quantification, a separate standard solution was prepared for each of the identified metabolites. The standards were extracted and derivatized as described for the fruit samples and run on GC-FID. Standard curves generated individually for every metabolite was used for quantification, and presented as the concentration in fresh weight basis. The amount of metabolites per fruit was calculated by multiplying the average fruit weight by the concentration at that stage.

Starch quantification: Leaf and fruit samples from S4, S5, and S6 stages from 'Premier' and 'Powderblue' were collected at 9 am, 2 pm, and 7 pm in 2021. All samples were stored and ground in liquid N_2, similar to that described for metabolite analysis. Starch quantification was performed following the protocol in Smith and Zeeman (2006) with some modifications.

First, 80-100 mg of finely ground samples were extracted with 1.5 ml of 80% ethanol in a 2 ml tube with a snap lock, then incubated at 80 ℃ for 10 minutes, followed by centrifugation for 5 minutes at 12,500 *g*. The resulting supernatant was discarded and the above steps were repeated twice to ensure removal of all soluble sugars. After that, 500 µl of autoclaved water was added to the pellet and samples were incubated at 100 ℃ for 10 minutes. Next, 500 µl equaling 35 units of amyloglucosidase was added, and samples were mixed using a shaker (HL-2000 HybriLinker, Upland, CA, USA) at 150 *g* for 24 hours at 55 ℃. Finally, 25 µl of supernatant was mixed with 975 µl of buffer (0.1 M HEPES, 0.5 mM ATP, 1 mM NAD, 4 mM $MgCl_2$). The development of NADH during the conversion of glucose to 6-phosphogluconate was measured at 340 nm using spectrophotometer (GENESYS 10S UV-VIS, Thermon Scientific, China). Finally, a glucose standard curve was prepared for starch quantification in glucose equivalents.

Anthocyanin analysis using high-performance liquid chromatography: For anthocyanin quantification, the protocol was based on (Downey and Rochfort, 2008), with some modifications. Around 100 to 125 mg of sample was extracted using 1 mL of 50% (v/v) methanol. Next, the samples were left undisturbed in the dark for one hour, followed by sonication using a water bath sonication (Bransonic 220, Parrot Drive, Conn, USA.) for 20 minutes. Finally, samples were centrifuged at 22,000 *g* for 10 minutes at room temperature. Then

the supernatant was filtered through a 0.45 µm filter and transferred into the 2 ml GC vial. For analysis, a 30 µl injection volume was used.

Anthocyanins were first determined by liquid chromatography-mass spectrometry-mass spectrometry (LCMS-MS) in the Proteomics and Mass Spectrometry Facility, University of Georgia using a subset of samples. The elution time, m/z ratio, and fragmentation of anthocyanin molecule are in Table 2. S1 and compound identification was determined by comparing the m/z ratio and their fragmentation to previously published articles (Prior et al., 2001; Wu and Prior, 2005). Anthocyanins start to accumulate during ripening initiation at S6 stage. We used a subset of samples (2 replications) from S4 and S5 stages from both cultivars. Since no anthocyanins were detected, further quantification was performed on S6-S8 stages of fruit development.

Next all samples were run on high-performance liquid chromatography (HLPC) coupled with a photodiode array detector (PAD) (Waters, Milford, MA, USA), which was used to monitor chromatogram wavelength at 520 nm. For both LCMS-MS and HPLC, the same conditions were used.

The Discovery C-18 column (15cm x 4.6 mm, 5µm, Sigma-Aldrich Inc, ST. Louis, MO, USA) was used with solvent A being water with 10% formic acid and B being methanol with 10% formic acid. The LC gradient started at 10% B and ramped to 12% B in 14 minutes then to 16% B by t=24 min, 25% B by t=28 min, 50% B by t=32 min, and then back 10% B by t=35-38 min. The flow rate was 1 ml/min. The standard curve of malvidin-3-O galactoside was used for quantification of all anthocyanins. Total anthocyanin content was expressed as the summation of all anthocyanins identified in this study.

Weighted gene co-expression network and gene ontology analysis: The weighted gene co-expression network analysis (WGCNA) was performed between differentially expressed genes (DEGs) obtained from the previous publication (Wang & Nambeesan, in submission), and selected metabolites (sucrose, glucose, fructose, starch, malate, citrate, quinate, shikimate, and total anthocyanin) from this study. Fruit samples from the 'Powderblue' at the S4/S5, S6, S7, and S8 stages were subjected to RNA sequencing. Differential expression analysis was conducted between each pair of ripening stages, employing a false discovery rate (FDR) threshold of <0.01 and a fold change criterion of >= 2. Additionally, metabolites such as sugars and acids were selected based on their higher concentrations during ripening. Starch was chosen due to its significance in the carbohydrate metabolism pathway and fruit ripening. As all anthocyanin compounds exhibited similar concentration patterns during fruit development and ripening, only the total anthocyanin data was included in the WGCNA. The stepwise network construction method was used for module detection. The soft threshold power of 20 was selected. Then, the merge dynamic method was used for the final module construction by cutting the height of 0.25 from the dynamic tree cut as described in the method (Langfelder and Horvath, 2008). After that, the correlation between the modules and metabolites was performed using function corAndPvalue from the 'WGCNA' package (Langfelder and Horvath, 2008). The correlation > 0.80 (positive correlation) or < –0.80 (negative correlation) and *P*-value <0.05 were considered as significantly different. Gene ontology (GO) enrichment analysis was performed with the WGCNA modules that were highly correlated with metabolites using the AriGO v2.0 tools (Tian et al., 2017). The *P*-values were corrected using the false discovery rate (FDR), and the GO term

<0.05 FDR was considered significantly enriched. The visualization of GO enrichment was done using the R-studio.

Quantitative RT-PCR: Transcript abundance of sugar and acid-related genes were measured by quantitative real-time polymerase chain reaction (qRT-PCR) as described below. Total RNA was extracted using the modified cetyltrimethylammonium bromide (CTAB) method described previously (Vashisth et al., 2011). After treatments with DNase enzymes, complementary DNA (cDNA) was prepared using reverse transcriptase from 1 µg of total RNA. Afterward, qRT-PCR was performed using the PowerUP SYBR green master mix in a MX3005P quantitative real-time PCR (qRTPCR) instrument (Agilent Technologies, United States). All the genes for this study was identified from a fruit transcriptome generated previously in our laboratory with the cultivar Powderblue (Wang and Nambeesan, 2022). The list of genes and primers used for this study is presented in the Table 2. S2. Three reference genes were used for the normalization of target genes, which are: *UBIQUITIN-CONJUGATING ENZYME* (*UBC28*), *RNA HELICASE-LIKE* (*RH8*), and *CLATHRIN ADAPTER COMPLEXES MEDIUM SUBUNIT FAMILY PROTEIN* (*CACSa*). The mean PCR efficiency of each primer was calculated using LinReg PCR (Ruijter et al., 2009). Relative quantity (RQ) values were calculated after PCR efficiency correction. To calculate normalized RQ values (NRQ) for a specific sample, the RQ values of that sample were normalized using the geometric mean of the RQ values from reference genes associated with that sample. The standard error was determined as described previously (Rieu and Powers, 2009). The NRQs values after $\log_2$ transformation were used for the statistical data analysis. Finally,

expression of all genes were presented as fold change with reference to the transcript abundance of ‘Powderblue’ at S4 developmental stages.

Statistical analysis: Data were analyzed and visualized using the R-studio 2023 (R core 2023, Vienna, Austria). Analysis of variance (ANOVA) was performed to evaluate the significance of the treatment effect. Multiple comparison tests were performed using Fisher's least significant difference (LSD) at the 0.05 significance level. Principal components analysis (PCA) was performed using the FactoMiner and factoextra software in R. The first two principal component contributions, loading and scree plots, are presented in this study.

Results

Physiological parameters of developing blueberry fruits: Fruit weight and diameter increased from the S4 to S5 stages by 2.3- and 1.4-fold in ‘Premier’, and 1.5- and 1.2-fold in ‘Powderblue’, respectively (Fig. 2.1B, C). Then, fruit weight and diameter remained similar during S5 to S7 stages, except for ‘Premier’, where S6 had a slightly higher weight and diameter than S5. The fruit weight and diameter of fruit transitioning from S7-S8 stage increased by 1.5- and 1.1-fold in ‘Premier’ and 1.7- and 1.2-fold in ‘Powderblue’, respectively. Comparing the cultivars, Premier had greater fruit weight and diameter than Powderblue.

Overall respiration and ethylene production were similar in S4 to S5 developmental stages (Fig. 2.1D, E). From S6 to S7, respiration production increased by 1.6- and 1.5-fold in ‘Premier’ and ‘Powderblue’, respectively (Fig. 2.1D). Similarly, ethylene production increased from S6 to S8, by 2.1- and 1.8-fold in ‘Premier’ and ‘Powderblue’, respectively (Fig. 2.1E). The

respiration rate was similar between ‘Premier’ and ‘Powderblue’; however, ethylene production was more significant in ‘Premier’ compared to ‘Powderblue’.

Association between metabolite composition during the fruit development and ripening: To determine the variation among metabolites during fruit development and ripening in both cultivars, a PCA was conducted (Fig. 2.2, Fig. 2. S1). Overall, 74.9% of the variation in data was explained by the first two dimensions (Fig. 2.2A). The first dimension captured the variation among the developmental stages, where S4 to S8 separated on the X-axis. Malate and quinate were mainly associated with S4 and S5 stages. In contrast, the major sugars and total anthocyanins were associated with the S8 stages. Dimension 2 depicted the variation among the cultivars, where Powderblu’ and Premier separated on the Y-axis (Fig. 2.2A). Analysis of the loading plot explained the contribution of each metabolite in the first two PCs (Fig. 2.2B). Most of the metabolites accounted for over 5% of the variance in the first two PC, with the exception of malate, glutamate, citrate, fumarate, succinate, sorbitol, and starch, which contributed less than 5%.

The relationship among all metabolites was performed using Pearson's correlation for ‘Premier’ and ‘Powderblue’. Among them, major sugars were highly positively correlated with each other in both cultivars with correlation ranging from r=0.98-1.0. The sugars were negatively correlated with major acids, malate and quinate. Malate and quinate were positively correlated in both cultivars. We did not find a strong correlation (r>0.80) between starch and the major sugars (glucose, fructose, and sucrose) in ‘Premier’ and ‘Powderblue’. Citrate was not correlated with the major sugars (sucrose, fructose, glucose) and acids (malate, quinate).

Metabolites analysis: The patterns in sugar concentration during fruit development were similar in both Premier and Powderblue (Fig. 2.3A-C). The three major sugars, sucrose, fructose, and glucose, increased from S4 to S8 stages by 7.2-, 32.0-, and 34.4-fold respectively. The concentration of the three sugars increased steadily during the early and mid-fruit development stages (S4-S7), then increased rapidly at later developmental stages (S7-S8). The sucrose, fructose, and glucose concentration from S7 to S8 increased by 1.8-, 1.9-, and 1.8-fold in 'Premier' and 2.3-, 3.0-, and 2.9-fold in 'Powderblue' (Fig. 2.3A-C). The amounts of sucrose, fructose, and glucose in each fruit, followed a pattern similar to the concentration, with all three sugars increasing during fruit development and ripening (Fig. 2. S2A-C). Myo-inositol (sugar alcohol) was similar until the S7 stage in 'Premier'; then, it increased by 1.2-fold from S7 to S8 (Fig. 2.S4A). In 'Powderblue', myo-inositol was lowest at the S5 stage, increased by 1.2-fold from S5 to S6, and remained similar during later developmental stages. The other sugars detected included xylose, sorbitol, and maltose, however their concentration was very low in both cultivars (Fig. 2. S4B-D).

Overall, the concentration of starch was very low in 'Premier' (0.035 mg/g FW) and 'Powderblue' (0.044 mg/g F.W.) in the S8 stage (Fig. 2.3D). The amount of starch per fruit was low and increased during ripening in both cultivars (Fig. 2. S2D). When starch measurements were repeated to account for diurnal variations, fruit at S4, S5, and S6 stages still displayed very low starch concentrations at all three time points (9 am, 2 pm and 7 pm) in both cultivars (Fig. 2.S3A-C). In the leaf, the concentration of starch steadily increased reaching a maximum value at 2 pm and 7 pm in 'Premier' and 7 pm in 'Powderblue' (Fig. 2.S3D). In comparison to 9 am,

the leaf starch concentrations increased by 2.0 and 2.1-fold in ‘Premier’ and by 10.1 and 17.3-fold in ‘Powderblue’ at 2 pm and 7 pm, respectively. The starch concentration in ‘Premier’ leaf was higher than in the ‘Powderblue’ leaf.

Malate, citrate, quinate, and shikimate were the major acids in blueberries (Fig. 2.3E-H). Among them, quinate was the predominant acid during fruit development, including in ripe fruit. Malate concentration was greater at early fruit development stages than citrate, whereas the concentration of both acids were similar in ripe fruit (Fig. 2.3E, F). The patterns in organic acid concentration during fruit development were similar in both cultivars. The concentrations of malate increased from S4 to S5 stages by 1.3- and 1.5-fold in ‘Premier’ and ‘Powderblue’, respectively, and subsequently continued to decline during later stages of fruit development in both cultivars (Fig. 2.3E). In ‘Premier’, malate concentration decreased by 1.2-, 1.2-, and 3.1-fold between S5 to S6, S6 to S7, and S7 to S8 stages, respectively. Similarly, in ‘Powderblue’, malate decreased by 1.3- and 4.3-fold between S6 to S7, and S7 to S8 stages, respectively. The concentration of citrate was similar in ‘Premier’ during all stages of fruit development analyzed in this study. In ‘Powderblue’, citrate concentration was maximum at the S6 stage, increased by 1.6-fold from S5 to S6, then declined by 1.3-fold between the S6 and S7, and remained similar in S7 and S8 stages (Fig.2.3F). The concentration of quinate continuously decreased, whereas shikimate concentration increased during fruit development and ripening (Fig.2.3G, H). Quinate decreased by 1.2-, 1.3-, and 1.6-fold between S4 to S5, S5 to S6, and S7 to S8 stages in ‘Premier’. Similarly, it decreased by 1.2 -, 1.2- and 2.6-fold between S4 to S6, S6 to S7 and S7 to S8 stages, respectively, in ‘Powderblue’. On the other hand, shikimate increased by 2.0- and 1.4-fold between S7 to S8 stages in ‘Premier’ and ‘Powderblue’, respectively.

We also determined the amount of malate, citrate, quinate, and shikimate per fruit (Fig. 2. S2E-H). The amount of malate per fruit increased by 3.0-fold from S4 to S5, then remained similar till S7 stage, after that decreased by 2.1-fold from S7 to S8 in 'Premier' (Fig. 2. S2E). In 'Powderblue', it increased by 2.2-fold from S4 to S5, remained similar till S6, and again decreased by 1.2- and 2.5-fold between S6 to S7 and S7 to S8, respectively. The amount of citrate per fruit increased during the ripening with 1.4- and 1.7-fold greater in S8 compared to S7 in 'Premier' and 'Powderblue', respectively (Fig. 2. S2F). In case of quinate, amount increased by 1.9- and 1.4-fold between S4 to S5 in 'Premier' and 'Powderblue', respectively (Fig. 2. S2G). It remained similar in 'Premier' from S5 to S8. In 'Powderblue' it was similar from S5 to S7, after that it decreased by 1.5-fold between S7 and S8 stages. The amount of shikimate per fruit increased during the fruit development and ripening, and pattern was similar to the concentration (Fig. 2. S2H). In addition, we also detected other organic acids such as succinate, fumarate (only in 'Powderblue'), and glycerate in both cultivars; however, their concentration was very low (Fig.2. S4E-G).

Glutamate and aspartate were the major amino acids detected during fruit development and ripening. The concentration of glutamate remained similar at S4, S5, and S6 stages, then it increased by 1.2- and 1.4-fold from S6 to S7 and S7 to S8 stages, respectively, in 'Premier' (Fig.2. S4H). In 'Powderblue', glutamate concentration was similar at S4 and S5 stages, increased by 1.3-fold from S5 to S6, and then remained similar during later stages of fruit development. The concentration of aspartate was not different during fruit development and ripening in both cultivars (Fig.2. S4I). Overall, alanine, serine, and threonine concentrations at

S8 stages were very low being, 0.023, 0.04, and 0.015 in ‘Premier’, and 0.009, 0.029, and 0.014 mg/g F.W. in ‘Powderblue’, respectively (Fig.2. S4J-L).

We determined 15 different anthocyanin in S8 stage in both cultivars (Table 2.1). In the S6 developmental stage, only one anthocyanin (Cya 3-gal) was detected in ‘Premier’ and three different anthocyanins (Cya 3-gal, Pet 3-gal/Cya 3-ara) in ‘Powderblue. In S7 stage, seven different anthocyanin compounds (Cya 3-gal, Pet 3-gal/Cya 3-ara, Peo 3-gal, Mal 3-gal, Peo 3-ara, Mal 3-ara) were detected in ‘Premier’, whereas in ‘Powderblue’ 10 different anthocyanin compounds (seven of them was same as ‘Premier’ with three additional ones: Cya 3-glu, Peo-3-glu, Mal 3-glu) were detected (Table 2.1). All anthocyanin compounds in the S8 stage were significantly higher than each anthocyanin at S6 and S7 developmental stages. Mal 3-gal was the most abundant anthocyanin compound present in both cultivars. The total anthocyanin concentration in ‘Premier’ and ‘Powderblue’ increased between S7 to S8 by 24.1-fold in ‘Premier’, and 25.9-fold in ‘Powderblue’, respectively (Table 2.1).

Weighted gene co-expression network and gene ontology enrichment analysis: WGCNA analysis using the ‘Powderblue’ fruit transcriptome (Wang & Nambeesan, 2023), identified 9 modules (Fig. 2.4A). The majority of genes (40.8%) were assigned to the purple module, followed by the darkturquoise module (37.9) whereas the grey (0.05%) and paleturquoise modules (0.89%) contained fewer genes (Figure 2. S5). Correlation analysis among all modules and major metabolites revealed that, the darkturquoise model was positively correlated with the sucrose (r=0.95, *P*=<0.0001), fructose (r=0.97, *P*=<0.0001), glucose (r=0.97, *P*=<0.0001), shikimate (r=0.89, *P*=0.001), and total anthocyanin (r=0.88, *P*=0.002) (Fig. 2.4B). In contrast,

the darkturquoise model was negatively correlated with the malate (r=-0.91, *P*=<0.0001) and quinate (r=-0.95, *P*=<0.0001) (Fig. 2.4B).

Further, we performed a GO enrichment analysis of genes using the darktourquoise module. Some of the top 10 GO enrichment terms according to the number of genes present included single organism metabolic process, oxidation-reduction process, small molecule metabolic process, organic acid metabolic process, and carbohydrate metabolic process (Fig. 2.4C). When ranked according to significance (lowest *q*- value), some of the top 10 GO enrichment terms included genes related to the oxidation-reduction process, aromatic amino acid metabolic and catabolic process (tyrosine metabolic and catabolic process, phenylalanine metabolic process) and organic acid catabolic process (Fig. 2.4D). The carbohydrate and organic acid metabolic process included genes involved in glycolysis, starch biosynthesis, and TCA cycle like *HK, FK, PFK, PYRUVATE KINASE (PK), AGPase, PEPCK, CS, GLYCERALDEHYDE-3-PHOSPHATE DEHYDROGENASE* (Fig. 2.5). The single-organism metabolic, oxidation-reduction, and aromatic amino acids metabolic process included the genes involved in the phenylpropanoid pathway, and the former two GO categories also included genes related to sugar, starch, and organic acid biosynthesis.

Expression analyses of genes involved in sugar, starch, acid, and anthocyanin metabolism: In the 'Powderblue' transcriptome (Wang & Nambeesan, submitted), we identified differentially expressed genes associated with various metabolic pathways, including sucrose degradation and synthesis, glycolysis, sugar transport, starch degradation and synthesis, malate metabolism, glyoxylate and the TCA cycle, as well as anthocyanin biosynthesis (Fig. 2.5).

The transcript per million (TPM) values of enzymes involved in sucrose degradation and synthesis, such as *SuSy2*, *vINV*, *nINV*, *SPS2*, and *SPP*, were higher in the S8 stage compared to the S4/S5 stage (Fig. 2.5). Meanwhile, enzymes related to the rate-limiting steps in glycolysis and sugar transport, generally increased during ripening, with the exception of PK, where one transcript (PB.10586) increased, while another (PB.10586) decreased (Fig. 2.5). Among all sugar metabolism-related genes, *vINV* exhibited the highest transcript abundance. Additionally, the *SUGAR TRANSPORT* gene (e.g., PB.6921) showed abundant expression. Mainly, genes involved in sucrose synthesis, and transport, and glycolysis were primarily found in the darkturquoise module, which displayed a positive correlation with sugar levels. Compared to S4/S5 stage, the gene expression of *SuSy*, *nINV*, *vINV*, *SPS*, *SPP* increased during the ripening (S7/S8) stage (Fig. 2.7A).

The TPM values of starch degradation enzymes were relatively low, except for *1,4-α-GLUCAN BRANCHING ENZYME* (*GBE*) and *β-AMYLASE*, which showed higher transcript abundance in S6 to S8 stages (Fig. 2.5). Other enzymes like *SS4*, *α-AMYLASE 2*, and *3* were more abundant in the S8 developmental stage than in the S4/S5 stages. However, *SS1* was more abundant in the earlier developmental stages (S4/S5) than in the later stages (S8). Among these, *AGPase* and *α-AMYLASE* were found in the darkturquoise module (Fig. 2.5). Compared to S4/S5 stage, the gene expression of *AGPase* and *AMYLASE* increased, and *SS* decreased during the ripening (S7/S8) stage (Fig. 2.7A).

The TPM values of cytosolic *NADP-ME*, mitochondrial *NAD-ME*, *ISOCITRATE DEHYDROGENASE* (*IDH*), glyoxysomal *MDH*, and *ISOCITRATE LYASE* (*ICL*) were higher in the S4/S5 compared to S8 stage (Fig. 2.5, Fig. 2.7 B). Conversely, the TPM values of *PEPCK*, *2-*

OXOGLUTARATE DH (ODH), glyoxysomal *CS*, and *BIFUNCTIONAL 3-DEHYDROQUINATE DEHYDRATASE/SHIKIMATE DH* (*DD/SDH*) were greater in the S8 than in the S4/S5 stage (Fig. 2.7B). In case of *PEPC*, it exhibited an increase until the S7 stage, followed by a decrease at the S8 stage (Fig. 2.5). Among them, *PEPCK* displayed higher transcript abundance and was found in the darkturquoise module.

Furthermore, we identified major anthocyanin biosynthesis-related genes with TPM values that were higher in the S7 and S8 developmental stages compared to S4/S5 or S6 developmental stages (Fig. 2.5, Fig. 2.7C). Additionally, all anthocyanin biosynthesis genes, except *ANTHOCYANIDIN REDUCTASE* (*ANR*), were detected in the darkturquoise module (Fig. 2.4B, Fig. 2.5).

Validation of genes with qRTPCR analysis: Selected genes related to sugar, acid and anthocyanin metabolism were validated using qRT-PCR analysis (Fig. 2.6). In general, patterns with qRTPCR results were similar to that observed with the 'Powderblue' transcriptome. The *SuSy2* transcript abundance increased from S4 to S5, then remained similar until S7 stage, and increased from S7 to S8 by 2.1-fold in 'Powderblue', however in 'Premier', the transcript abundance remained similar during fruit development (Fig. 2.6A). The relative expression of *vINV* increased by 4.1- and 15.8-fold in 'Premier' and 'Powderblue', respectively, from S4 to S5 stages, then thereafter remained similar in 'Premier' and 'Powderblue' during the remaining stages (Fig. 2.6B). The *AGPase* transcript abundance slightly increased from S4 to S5 then remained similar in 'Premier' and with no difference in 'Powderblue' (Fig. 2.6C). The rate-limiting enzyme in the glycolysis pathway, *PFK* increased during later stages of ripening (S7 and

S8), compared to earlier developmental stage (S4) by 1.7- and 3.2-fold in ‘Premier’ and ‘Powderblue’ respectively (Fig. 2.6D). The transcript abundance of cytosolic *PK* was similar during fruit development in ‘Premier’. However, it increased from S4 to S5 stages by 11.1-fold, then remained similar in ‘Powderblue’ (Fig.2.6E).

Similarly, transcript abundance *PEPC* was similar during fruit development in ‘Premier’, but in ‘Powderblue’ *PEPC* increased from S4 to S5 by 4.3-fold, then remained similar (Fig. 2.6F). The transcript abundance of *PEPCK* increased steadily and being maximal at S8 stage (2.3-fold greater in S8 than S6) in ‘Powderblue’. In contrast, in ‘Premier’, it increased by 3.0-fold from S4 to S6, and thereafter remained similar through the remainder of fruit development (Fig. 2.6G). The pattern of gene expression of mitochondrial *CS* was similar during fruit development in ‘Premier’. However, in ‘Powderblue’, it increased from S4 to S5 by 1.8-fold, and then remained similar during later fruit developmental stages (Fig. 2.6H).

We determined the gene expression of anthocyanin biosynthesis-related genes: *CHS1*, *2* and *UFGT1, 2*. In ‘Premier’, the transcript abundance of *CHS1* decreased from S4 to S5, and then increased from S5 to S6 by 15.4-fold and thereafter remained similar during fruit ripening (Fig. 2.6I). The transcript abundance of *CHS2* and *UFGT1* were not significantly different in ‘Premier’ (Fig. 2.6J, K). The expression of *UFGT2* decreased by 7.0-fold from S4 to S5 stage, then increased by 7.0-fold from S5 to S6 in ‘Premier’, and thereafter remained similar at S6, S7, and S8 stages (Fig. 2.6L). In ‘Powderblue’, the expression of *CHS1*, *CHS2*, *UFGT1*, and *UFGT2* increased by 42.7-, 7.7-, 4.6-, and 13.7-fold, respectively, from S5 to S8 stage (Fig. 2.6I-L).

Discussion

We collected fruit samples from stages S4 to S8 to observe changes that occur during ripening. Stages S4 and S5 represent mid-developmental stages, while ripening initiation occurs at S6, with ripening progression continuing into the S7 and S8 stages. In this study, the concentration of all three sugars, sucrose, fructose and glucose increased steadily during fruit ripening from S4 to S7 stage. Interestingly, at the final stage of ripening between the S7 and S8 stage there was a greater dramatic increase in the concentration of these sugars. Sucrose being the main translocating sugar, these results suggest that blueberry fruits continue to uptake sucrose from the source organs during ripening. Further, in our study, the concentration of glucose and fructose also continuously increased during the ripening suggesting that breakdown of imported sucrose occurs by sucrose catabolic enzymes. This was supported by high transcript abundance of the *BIDIRECTIONAL SUGAR TRANSPORTER N3-LIKE GENE* throughout all stages of fruit development and ripening. The positive correlation between sucrose and sugar transporter, further suggests a relationship between sugar import and distribution within the fruit throughout ripening. Such patterns of sugar accumulation seem to be unique in fruits. For example, similar to our study, continuous accumulation of sucrose, glucose and fructose was found in strawberry (Liu et al., 2020), and grape (Zhu et al., 2017). In apples, sucrose concentrations increased during ripening (Li et al., 2012). However, glucose concentration first decreased from 40 to 74 days after bloom (DAB), then increased during maturity, and fructose concentration increased steadily and slightly decreased during maturity in apples (Li et al., 2012). In tomato, the sucrose concentration was similar till the mature green/breaker stage, then it decreased during ripening, while the concentration of glucose and fructose remains similar

from green to ripe in tomato (Oms-Oliu et al., 2011), suggesting that starch catabolism contributed to the majority of carbon during ripening in tomato. In cherry tomato that specifically accumulates sucrose, the concentration of glucose and fructose increased from immature green to mature green stage, then it decreased during the breaker stage, and remained similar thereafter during ripening (Sun et al., 2022). However, in the hexose accumulating cherry tomato their concentration increased in pink and ripe fruit compared to earlier developmental stages, corresponding with a decrease in sucrose concentration (Sun et al., 2022), suggesting that catabolism of sucrose contributed to hexose accumulation. In bilberry, which is related to blueberry, sucrose content increased between the small unripe and purple fruit, after that it decreased in full ripe fruit (Samkumar et al., 2022). However, glucose and fructose content increased during fruit ripening similar to blueberry (Samkumar et al., 2022).

The two enzymes, *SuSy* and *INV* are involved in the catabolism of sucrose. Of all the sucrose metabolism-related enzymes, *vINV* showed the greatest TPM values suggesting its importance in sucrose catabolism. In this study, from S4/S5 to S6 stage, during ripening initiation, the transcript abundance of *vINV* goes up dramatically suggesting that during these developmental stages, sucrose is broken down and its products are accumulating in the vacuole. The higher expression of *vINV* suggests higher INV activity in the sink tissue, which is important for the maintaining the cellular hexose concentration (Nguyen-Quoc and Foyer, 2001). In this study, we did not detect *cwINV* during ripening. It is possible that its transcript abundance was too low to be detected. Nevertheless, these results suggest that sucrose catabolism in the apoplastic space may be absent or a minor component. Similar to our study, in tomato, only a small amount of sucrose is hydrolyzed by cwINV (N'tchobo, 1998; Nguyen-Quoc and Foyer,

2001). In this study, in the cytosol, the transcript abundance of *SuSy* is higher than *nINV*, suggesting that *SuSy* is mainly responsible for the catabolism of sucrose in the cytosol.

During later stages of fruit ripening from S6 to S8 stages, there was still a high transcript abundance of *vINV*, which suggest continued breakdown of sucrose in vacuoles to glucose and fructose. This is also supported by the approximately equal concentrations of glucose and fructose during the ripening, and their concentration being greater than that of sucrose. Higher hexose pools in sink tissues increase the concentration gradient that enhances the export of sucrose into the companion cells and sieve elements of the phloem in source tissues (Ruan, 2014). Increasing sucrose import into the fruit is accompanied by increased water transport leading to increase in fruit size and weight (Chen et al., 2020), that was evident in this study throughout ripening, including between the S7 and S8 stage. Also, *SuSy2* and *nINV* exhibits an increased trend between pink (S7) and ripe (S8) stages, suggesting an increased flux of sucrose into the cell, which leads to breakdown of sucrose into its hexose sugars. Similar to S4/S5 stage, *SuSy2* had a higher transcript abundance compared to *nINV* during late ripening stages, suggesting this may be the main route of sucrose catabolism in the cytosol during ripening progression as well.

Another route for sucrose synthesis is the re-synthesis of sucrose from UDP-glucose and fructose-6-phosphate using *SPS* and *SPP*, that can lead to sucrose accumulation in fruits. In this study although the transcript abundance of *SPS2* and *SPP* increased during ripening, the transcript abundance of *SPS2* was very low (TPM < 15), while the *SPP* transcript abundance was relatively higher during ripening (TPM <75), but less than *SuSY* and *vINV*. This suggests a

presence of sucrose-sucrose futile cycle being a minor component contributing to sucrose synthesis in blueberry fruit.

The sucrose in fruits can be converted into starch for storage which can be broken down to generate sugars later during fruit ripening. This starch plays an important role in contributing to the total soluble sugars in the fruits during the ripening (Dinar and Stevens, 1981; Durán-Soria et al., 2020). In climacteric fruits like tomato, banana, apple, and mango, the starch concentration increases till 60 days after anthesis, then decreased during the ripening (Chervin, 2020). However, in non-climacteric fruits like strawberries and grapes, the starch concentration is reduced to less than 1 mg/g F.W. within 20 days after anthesis (Chervin, 2020). In non-climacteric fruits like strawberries, starch accumulation during the early developmental stages contributed to only ~3% of the final sugar amount in ripe fruit (Souleyre et al., 2004). In this study, the concentration of starch was low in blueberry fruit (0.028-0.038 mg/g F.W. in S4 and S8 stage) starting from S4 developmental stage. In the case of blueberry, the concentration of starch was around 52-fold less than tomato (Petreikov et al., 2009), 15.7-fold less than non-climacteric fruit like strawberry and similar to the concentration of grape at the ripe stage (Souleyre et al., 2004; Zhu et al., 2017). Measurement of starch concentrations in the fruit and leaf at various times during the day supported that blueberry leaf accumulates transitory starch with limited fruit starch accumulation.

Despite lower concentration of starch during fruit development and ripening, all starch biosynthesis and degradation genes were present in blueberry fruit. Overall, the transcript abundance of starch synthesis enzymes was very low in blueberry, except for *SS1* and *GBEs.* The transcript abundance of *SS1* was higher during S4/S5 stage (TPM 72), and declined subsequently

during ripening (<14 TPM value). The *GBEs* transcript abundance was relatively high throughout the developmental stages. The expression of *AGPase*, a rate-limiting enzyme in the starch biosynthesis pathway increased during the ripening, but its transcript abundance was very low. Of the genes for starch degradation enzymes, *β-amylase* displayed higher transcript abundance in all developmental stages and its expression level increased during the ripening. Additionally, the transcript abundance of *β-amylase* was higher than the *GBEs*. Based on expression levels, it is possible that starch is degraded at a higher rate compared to its synthesis, however transcript abundance may not be reflective of enzyme activity. Further if starch synthesis is limited by fruit anatomical considerations requires further studies.

The *FK* and *HK* are the central enzymes for sugar homeostasis and are involved in the phosphorylation of fructose and glucose respectively. These enzymes play an important role in glycolysis and sucrose re-synthesis. In this study, *FK* and *HK* increased during ripening and are highly correlated with sugar concentration (present in darktourquoise module). In addition, the transcript abundance of other rate-limiting enzymes involved in the glycolysis (*PFK2, PFK3, PFK6*) also increased during ripening. The upregulation of these transcripts during ripening indicated an increase in glycolysis to support fruit respiration. This is supported by blueberry fruit that display a peak in respiration at the S7 stage.

The reverse process where the byproduct of glycolysis, pyruvate is converted back into glucose is termed as gluconeogenesis. In this study, we detected gluconeogenesis-related enzymes, *FRUCTOSE-1,6-BISPHOSPHATASE* and *PYRUVATE CARBOXYLASE* during fruit ripening stages, but their transcript abundance was very low suggesting no or minimal gluconeogenesis. The lack of active gluconeogenesis in blueberry fruit is also supported by the

equal concentration of glucose and fructose. If gluconeogenesis was active, it would have resulted in higher glucose concentration compared to fructose. Similarly, in grapes, which have similar concentrations of glucose and fructose, it was found that gluconeogenesis contributes to only 0.1-0.6% of the total amount of sugars (Famiani et al., 2016).

The primary acids that accumulate during the ripening in blueberry fruit are malate and citrate. At mid-developmental to ripening initiation stages (S4-S6), the concentration of malate was greater than that of citrate in rabbiteye blueberry. These amounts are different from southern highbush cultivars, where the concentration of citrate was substantially higher than the malate (Zhang et al., 2020). In our study, the malate concentration decreased as respiration increased. Similar to our study, plum fruits exhibited decrease in malate concentration, as they utilized malate as a substrate for respiration during ripening (Singh and Singh, 2008). In spite of decrease in concentration of malate during ripening the amount of malate per fruit remained similar from S5 to till S7 (pink) stages suggesting that fruit is still accumulating the malate. Thus the reduction in malate concentration may have occurred due to the dilution. From pink (S7) to ripe (S8) stage, degradation of malate occurs. Similar to our study, the content of malate decreased during the ripening in apricot, plumcot and plum (Bae et al., 2014).

Pyruvate from glycolysis can be converted to oxaloacetate (OAA) using PEPC and to malate using cytosolic MDH. During the S5 to S6 stage, the transcript abundance of *PEPC* was high suggesting the formation of OAA. In addition, the transcript abundance of *MDH* was high (TPM around 200) throughout the developmental stages. Although the reaction catalyzed by MDH is reversible, it is possible that during mid fruit development leading to ripening initiation, PEPC and MDH play a role in malate accumulation. Similar to our study, increase in gene

expression of *PEPC* during earlier fruit developmental stages is associated with increase in accumulation of malate in tomato and grape (Or et al., 2000; Guillet et al., 2002). Malate can be stored in the vacuoles and transported to cytosol or mitochondria depending on the metabolic status of the cell. The reaction catalyzed by PEPC also releases CO_2, and if it contributes to the respiratory surge during ripening is not clear. However, during the later stages ripening during S7 to S8, the concentration and amount of malate decreased suggesting malate utilization. During S6-S8 stage, *MDH* may catalyze conversion of malate into the OAA. This is supported in grape, where MDH is involved in the synthesis and degradation of malate during the pre-veraison and post-veraison stage, respectively (Sweetman et al., 2009). During later stages of ripening, OAA can be used towards synthesis of PEP, precursor for shikimate and secondary metabolites (discussed below). The synthesis and degradation of malate also occur using cytosolic NADP-MEs, that converts pyruvate to malate or vice-versa. In this study, the abundance of all transcripts coding for this enzyme is very high, and have similar levels during all developmental stages, except for PB.7196 transcripts, suggesting their active role in malate metabolism. The transcript abundance of PB. 7196 was higher during the mid-developmental stages suggesting the importance of this transcript in malate accumulation before ripening initiation. Citrate accumulates continuously during blueberry ripening with maximum amount in ripe fruits. It is possible that malate is being stored in the vacuole with some of it being distributed into the mitochondria for conversion to citrate. This may be reflected in overall lower citrate concentrations. The low concentration in citrate may also suggest continuous flux to the TCA cycle, supported by the increased in transcript abundance of *ODH*.

The continuous increase in *PEPCK* transcript abundance suggests conversion of OAA to PEP. A previous study found that greater activity of *PEPCK* corresponded with malate degradation (Famiani et al., 2005). Our data also supports the idea that in blueberry, the flux of malate stored in the vacuole is utilized towards generation of OAA via MDH and then PEP via PEPCK. PEP is not only a precursor that feeds into to the TCA cycle, but also the shikimate pathway, that leads to the formation of aromatic amino acids involved in the synthesis of anthocyanin and secondary metabolites. During this process, PEP forms both quinate and shikimate. In our study, the concentration of quinate was greater than malate and citrate. Later during the ripening, quinate concentration decreased, but content increased from S4 to S5 stage, then remained same during the ripening in 'Premier' and slightly decreased from S7 to S8 stages in 'Powderblue'. The decreased in quinate concentration in this study is possibly due to the dilution effect. However, stored quinate can also be used towards production of shikimate. In fact, shikimate concentration and content increased continuously during the ripening. This is also supported by the increased in transcript abundance of *DD/SDH*, an enzyme involved in the synthesis of shikimate from 3-dehydroquinate, which is a product of quinate catabolism.

During ripening, we also observed the involvement of glyoxylate cycle's involvement in which *CS* transcript abundance increased. In contrast, transcript abundance of *ICL* and *MDH* decreased during the ripening. In the glyoxylate cycle, malate is utilized as a carbon source in the metabolic process. Glyoxylate cycles were also found in other fruits like banana (Surendranathan and Nair, 1976). However, a previous study did not detect ICL protein in blueberry (Famiani et al., 2005). Hence, the enzyme activity of CS, ICL, and MS is necessary to investigate further for their potential role in glyoxylate cycle in rabbiteye blueberry.

In this study, we identified 15 different anthocyanins in ripe fruits. Among them, mal-3-gal concentration was greater in both 'Premier' and 'Powderblue', which is consistent with the previous study where they found a higher concentration of mal-3-gal (Wang et al., 2012). The

anthocyanin accumulation started at the onset of ripening (S6 stage) and became maximum at the ripe (S8 stage) fruit. The concentration of anthocyanin in this study was consistent with the anthocyanin determined in a previous publication in ‘Powderblue’ and less in ‘Premier’, respectively (Wang et al., 2012). The increased concentration of all anthocyanins in ripe fruits was due to the increase in the transcript abundance of the anthocyanin biosynthesis gene during ripening. Similar to our study, increase in transcript abundance of *PAL, CHS, F3'H, FLS, CHS, UFGT,* and *ANS* during bilberry and northern highbush blueberry during ripening led to an increase in anthocyanin accumulation (Jaakola et al., 2002; Lin et al., 2018).

Conclusion: Glucose, fructose, and sucrose are the major sugars, and they increased during the ripening. The continued increase in sucrose during ripening suggest import into fruit from leaf throughout ripening. Further, *vINV* plays an important role in breakdown of sucrose into glucose and fructose during blueberry fruit ripening. Increase in transcript abundance of glycolytic enzymes and decrease in malate is correlated with fruit respiration. Also, carbon during ripening is diverted towards the formation of anthocyanin compounds, as evidenced by the higher transcript abundance of *PEPCK* and anthocyanins concentration. The increased transcript abundance of the anthocyanin biosynthesis genes supports an increase in anthocyanin concentration. Overall, this study provides a deeper understanding of the molecular and metabolic basis of sugar, acid, and anthocyanin metabolism during fruit development and ripening in rabbiteye blueberry.

References

Ayaz F, Kadioglu A, Bertoft E, Acar C, Turna I (2001) Effect of fruit maturation on sugar and organic acid composition in two blueberries (Vaccinium arctostaphylos and V. myrtillus) native to Turkey.

Bae H, Yun SK, Yoon IK, Nam EY, Kwon JH, Jun JH (2014) Assessment of organic acid and sugar composition in apricot, plumcot, plum, and peach during fruit development. Journal of Applied Botany and Food Quality **87.**

Baroja-Fernández E, Muñoz FJ, Saikusa T, Rodríguez-López M, Akazawa T, Pozueta-Romero J (2003) Sucrose synthase catalyzes the de novo production of ADPglucose linked to starch biosynthesis in heterotrophic tissues of plants. Plant and cell physiology **44:** 500-509.

Beshir WF, Mbong V, Hertog ML, Geeraerd AH, Van den Ende W, Nicolaï BM (2017) Dynamic labeling reveals temporal changes in carbon re-allocation within the central metabolism of developing apple fruit. Frontiers in plant science **8:** 1785.

Bieleski R (1969) Accumulation and translocation of sorbitol in apple phloem. Australian Journal of Biological Sciences **22:** 611-620.

Birkhold KT, Koch KE, Darnell RL (1992) Carbon and nitrogen economy of developing rabbiteye blueberry fruit. Journal of the American Society for Horticultural Science **117:** 139-145.

Braun DM, Wang L, Ruan Y-L (2014) Understanding and manipulating sucrose phloem loading, unloading, metabolism, and signalling to enhance crop yield and food security. Journal of Experimental Botany **65:** 1713-1735.

Bungaruang L, Gutmann A, Nidetzky B (2013) Leloir glycosyltransferases and natural product glycosylation: Biocatalytic synthesis of the C-glucoside nothofagin, a major antioxidant of redbush herbal tea. Advanced Synthesis & Catalysis **355:** 2757-2763.

Cano-Medrano R, Darnell RL (1997) Cell number and cell size in parthenocarpicvs. Pollinated blueberry (vaccinium ashei) fruits. Annals of Botany **80:** 419-425.

Chen F-X, Liu X-H, Chen L-S (2009) Developmental changes in pulp organic acid concentration and activities of acid-metabolising enzymes during the fruit development of two loquat (Eriobotrya japonica Lindl.) cultivars differing in fruit acidity. Food Chemistry **114:** 657-664.

Chen J, Vercambre G, Kang S, Bertin N, Gautier H, Génard M (2020) Fruit water content as an indication of sugar metabolism improves simulation of carbohydrate accumulation in tomato fruit. Journal of Experimental Botany **71:** 5010-5026.

Chervin C (2020) Should starch metabolism be a key point of the climacteric vs. non-climacteric fruit definition? Frontiers in Plant Science **11:** 1931.

Chourey PS, Nelson OE (1976) The enzymatic deficiency conditioned by the shrunken-1 mutations in maize. Biochemical genetics **14:** 1041-1055.

Craig J, Barratt P, Tatge H, Déjardin A, Handley L, Gardner CD, Barber L, Wang T, Hedley C, Martin C (1999) Mutations at the rug4 locus alter the carbon and nitrogen metabolism of pea plants through an effect on sucrose synthase. The Plant Journal **17:** 353-362.

D'Aoust M-A, Yelle S, Nguyen-Quoc B (1999) Antisense inhibition of tomato fruit sucrose synthase decreases fruit setting and the sucrose unloading capacity of young fruit. The Plant Cell **11:** 2407-2418.

Dinar M, Stevens M (1981) The Relationship between Starch Accumulation and Soluble Solids Content of Tomato Fruits1. Journal of the American Society for Horticultural Science **106:** 415-418.

Downey MO, Rochfort S (2008) Simultaneous separation by reversed-phase high-performance liquid chromatography and mass spectral identification of anthocyanins and flavonols in Shiraz grape skin. Journal of Chromatography A **1201:** 43-47.

Durán-Soria S, Pott DM, Osorio S, Vallarino JG (2020) Sugar signaling during fruit ripening. Frontiers in Plant Science **11:** 564917.

Edwards T, Sherman W, Sharpe R (1972) Seed Development in Certain Florida Tetraploid and Hexaploid Blueberries1. HortScience **7:** 127-128.

Famiani F, Cultrera NG, Battistelli A, Casulli V, Proietti P, Standardi A, Chen Z-H, Leegood RC, Walker RP (2005) Phosphoenolpyruvate carboxykinase and its potential role in the catabolism of organic acids in the flesh of soft fruit during ripening. Journal of Experimental Botany **56:** 2959-2969.

Famiani F, Farinelli D, Frioni T, Palliotti A, Battistelli A, Moscatello S, Walker R (2016) Malate as substrate for catabolism and gluconeogenesis during ripening in the pericarp of different grape cultivars. Biologia plantarum **60:** 155-162.

Galtier N, Foyer CH, Huber J, Voelker TA, Huber SC (1993) Effects of elevated sucrose-phosphate synthase activity on photosynthesis, assimilate partitioning, and growth in tomato (Lycopersicon esculentum var UC82B). Plant Physiology **101:** 535-543.

Guillet C, Just D, Bénard N, Destrac-Irvine A, Baldet P, Hernould M, Causse M, Raymond P, Rothan C (2002) A fruit-specific phospho enol pyruvate carboxylase is related to rapid growth of tomato fruit. Planta **214:** 717-726.

Hu B, Yao H, Gao Y, Wang R, Li F, Guo J, Li K, Zhao M (2020) Overexpression of chalcone synthase gene improves flavonoid accumulation and drought tolerance in tobacco.

Huang L, Tan H, Zhang C, Li Q, Liu Q (2021) Starch biosynthesis in cereal endosperms: An updated review over the last decade. Plant communications **2.**

Hussain SB, Shi C-Y, Guo L-X, Kamran HM, Sadka A, Liu Y-Z (2017) Recent advances in the regulation of citric acid metabolism in citrus fruit. Critical reviews in plant sciences **36:** 241-256.

Hwang H, Kim Y-J, Shin Y (2020) Assessment of physicochemical quality, antioxidant content and activity, and inhibition of cholinesterase between unripe and ripe blueberry fruit. Foods **9:** 690.

Jaakola L, Määttä K, Pirttilä AM, Törrönen R, Kärenlampi S, Hohtola A (2002) Expression of genes involved in anthocyanin biosynthesis in relation to anthocyanin, proanthocyanidin, and flavonol levels during bilberry fruit development. Plant physiology **130:** 729-739.

Kang G, Liu G, Peng X, Wei L, Wang C, Zhu Y, Ma Y, Jiang Y, Guo T (2013) Increasing the starch content and grain weight of common wheat by overexpression of the cytosolic AGPase large subunit gene. Plant Physiology and Biochemistry **73:** 93-98.

Kötting O, Pusch K, Tiessen A, Geigenberger P, Steup M, Ritte G (2005) Identification of a novel enzyme required for starch metabolism in Arabidopsis leaves. The phosphoglucan, water dikinase. Plant physiology **137:** 242-252.

Langfelder P, Horvath S (2008) WGCNA: an R package for weighted correlation network analysis. BMC bioinformatics **9:** 1-13.

Lemoine R, Camera SL, Atanassova R, Dédaldéchamp F, Allario T, Pourtau N, Bonnemain J-L, Laloi M, Coutos-Thévenot P, Maurousset L (2013) Source-to-sink transport of sugar and regulation by environmental factors. Frontiers in plant science **4:** 272.

Li M, Feng F, Cheng L (2012) Expression patterns of genes involved in sugar metabolism and accumulation during apple fruit development. PloS one **7:** e33055.

Lin Y, Wang Y, Li B, Tan H, Li D, Li L, Liu X, Han J, Meng X (2018) Comparative transcriptome analysis of genes involved in anthocyanin synthesis in blueberry. Plant Physiology and Biochemistry **127:** 561-572.

Liu H-T, Ji Y, Liu Y, Tian S-H, Gao Q-H, Zou X-H, Yang J, Dong C, Tan J-H, Ni D-A (2020) The sugar transporter system of strawberry: genome-wide identification and expression correlation with fruit soluble sugar-related traits in a Fragaria× ananassa germplasm collection. Horticulture research **7.**

Lu Y, Sharkey TD (2006) The importance of maltose in transitory starch breakdown. Plant, cell & environment **29:** 353-366.

N'tchobo H (1998) Sucrose unloading in tomato fruits. II. Subcellular distribution of acid invertase and possible roles in sucrose turnover and hexose storage in tomato fruit. PhD thesis, Laval University.

Nakkanong K, Yang JH, Zhang MF (2012) Starch accumulation and starch related genes expression in novel inter-specific inbred squash line and their parents during fruit development. Scientia horticulturae **136:** 1-8.

Nguyen-Quoc B, Foyer CH (2001) A role for 'futile cycles' involving invertase and sucrose synthase in sucrose metabolism of tomato fruit. Journal of Experimental Botany **52:** 881-889.

Nitarska D, Boehm R, Debener T, Lucaciu RC, Halbwirth H (2021) First genome edited poinsettias: targeted mutagenesis of flavonoid 3′-hydroxylase using CRISPR/Cas9 results in a colour shift. Plant Cell, Tissue and Organ Culture (PCTOC) **147:** 49-60.

Oms-Oliu G, Hertog M, Van de Poel B, Ampofo-Asiama J, Geeraerd A, Nicolai B (2011) Metabolic characterization of tomato fruit during preharvest development, ripening, and postharvest shelf-life. Postharvest Biology and Technology **62:** 7-16.

Or E, Baybik J, Sadka A, Saks Y (2000) Isolation of mitochondrial malate dehydrogenase and phosphoenolpyruvate carboxylase cDNA clones from grape berries and analysis of their expression pattern throughout berry development. Journal of plant physiology **157:** 527-534.

Petreikov M, Yeselson L, Shen S, Levin I, Schaffer AA, Efrati A, Bar M (2009) Carbohydrate balance and accumulation during development of near-isogenic tomato lines differing in the AGPase-L1 allele. Journal of the American Society for Horticultural Science **134:** 134-140.

Pfister B, Zeeman SC (2016) Formation of starch in plant cells. Cellular and Molecular Life Sciences **73:** 2781-2807.

Prior R (2004) Absorption and metabolism of anthocyanins: potential health effects. Phytochemicals: Mechanisms of action**:** 1-19.

Prior RL, Lazarus SA, Cao G, Muccitelli H, Hammerstone JF (2001) Identification of procyanidins and anthocyanins in blueberries and cranberries (Vaccinium spp.) using high-performance liquid chromatography/mass spectrometry. Journal of agricultural and food chemistry **49:** 1270-1276.

Rennie EA, Turgeon R (2009) A comprehensive picture of phloem loading strategies. Proceedings of the National Academy of Sciences **106:** 14162-14167.

Retamales JB, Hancock JF (2018) Blueberries, Vol 27. Cabi.

Rieu I, Powers SJ (2009) Real-time quantitative RT-PCR: design, calculations, and statistics. The Plant Cell **21:** 1031-1033.

Robinson NL, Hewitt JD, Bennett AB (1988) Sink metabolism in tomato fruit: I. Developmental changes in carbohydrate metabolizing enzymes. Plant Physiology **87:** 727-730.

Rossouw D, Kossmann J, Botha FC, Groenewald J-H (2010) Reduced neutral invertase activity in the culm tissues of transgenic sugarcane plants results in a decrease in

respiration and sucrose cycling and an increase in the sucrose to hexose ratio. Functional Plant Biology **37:** 22-31.

Ruan Y-L (2014) Sucrose metabolism: gateway to diverse carbon use and sugar signaling. Annual review of plant biology **65:** 33-67.

Ruijter J, Ramakers C, Hoogaars W, Karlen Y, Bakker O, Van den Hoff M, Moorman A (2009) Amplification efficiency: linking baseline and bias in the analysis of quantitative PCR data. Nucleic acids research **37:** e45-e45.

Samkumar A, Karppinen K, Dhakal B, Martinussen I, Jaakola L (2022) Insights into sugar metabolism during bilberry (Vaccinium myrtillus L.) fruit development. Physiologia Plantarum **174:** e13657.

Schaffer AA, Levin I, Oguz I, Petreikov M, Cincarevsky F, Yeselson Y, Shen S, Gilboa N, Bar M (2000) ADPglucose pyrophosphorylase activity and starch accumulation in immature tomato fruit: the effect of a Lycopersicon hirsutum-derived introgression encoding for the large subunit. Plant Science **152:** 135-144.

Schaffer AA, Petreikov M (1997) Inhibition of fructokinase and sucrose synthase by cytosolic levels of fructose in young tomato fruit undergoing transient starch synthesis. Physiologia Plantarum **101:** 800-806.

Schaffer AA, Petreikov M (1997) Sucrose-to-starch metabolism in tomato fruit undergoing transient starch accumulation. Plant Physiology **113:** 739-746.

Schmölzer K, Gutmann A, Diricks M, Desmet T, Nidetzky B (2016) Sucrose synthase: A unique glycosyltransferase for biocatalytic glycosylation process development. Biotechnology advances **34:** 88-111.

Seymour GB, Østergaard L, Chapman NH, Knapp S, Martin C (2013) Fruit development and ripening. Annual review of plant biology **64:** 219-241.

Signora L, Galtier N, Skøt L, Lucas H, Foyer CH (1998) Over-expression of sucrose phosphate synthase in Arabidopsis thaliana results in increased foliar sucrose/starch ratios and favours decreased foliar carbohydrate accumulation in plants after prolonged growth with CO2 enrichment. Journal of Experimental Botany **49:** 669-680.

Singh S, Singh Z (2008) UP Hedrick Student Paper Award 2008 major flavor components in some commercial cultivars of Japanese plum. Journal of the American Pomological Society **62:** 185.

Smith AM, Zeeman SC (2006) Quantification of starch in plant tissues. Nature protocols **1:** 1342-1345.

Souleyre EJ, Iannetta PP, Ross HA, Hancock RD, Shepherd LV, Viola R, Taylor MA, Davies HV (2004) Starch metabolism in developing strawberry (Fragaria× ananassa) fruits. Physiologia Plantarum **121:** 369-376.

Stein O, Granot D (2018) Plant fructokinases: evolutionary, developmental, and metabolic aspects in sink tissues. Frontiers in Plant Science **9:** 339.

Stein O, Granot D (2019) An overview of sucrose synthases in plants. Frontiers in plant science **10:** 95.

Sturm A (1999) Invertases. Primary structures, functions, and roles in plant development and sucrose partitioning. Plant physiology **121:** 1-8.

Sun L, Wang J, Lian L, Song J, Du X, Liu W, Zhao W, Yang L, Li C, Qin Y (2022) Systematic analysis of the sugar accumulation mechanism in sucrose-and hexose-accumulating cherry tomato fruits. BMC Plant Biology **22:** 303.

Surendranathan K, Nair PM (1976) Stimulation of the glyoxylate shunt in gamma-irradiated banana. Phytochemistry **15:** 371-373.

Sweetman C, Deluc LG, Cramer GR, Ford CM, Soole KL (2009) Regulation of malate metabolism in grape berry and other developing fruits. Phytochemistry **70:** 1329-1344.

Tang G-Q, Lüscher M, Sturm A (1999) Antisense repression of vacuolar and cell wall invertase in transgenic carrot alters early plant development and sucrose partitioning. The Plant Cell **11:** 177-189.

Tang G-Q, Sturm A (1999) Antisense repression of sucrose synthase in carrot (Daucus carota L.) affects growth rather than sucrose partitioning. Plant molecular biology **41:** 465-479.

Tian T, Liu Y, Yan H, You Q, Yi X, Du Z, Xu W, Su Z (2017) agriGO v2. 0: a GO analysis toolkit for the agricultural community, 2017 update. Nucleic acids research **45:** W122-W129.

Vashisth T, Johnson LK, Malladi A (2011) An efficient RNA isolation procedure and identification of reference genes for normalization of gene expression in blueberry. Plant cell reports **30:** 2167-2176.

Wang F, Smith AG, Brenner ML (1994) Temporal and spatial expression pattern of sucrose synthase during tomato fruit development. Plant physiology **104:** 535-540.

Wang SY, Chen H, Camp MJ, Ehlenfeldt MK (2012) Flavonoid constituents and their contribution to antioxidant activity in cultivars and hybrids of rabbiteye blueberry (Vaccinium ashei Reade). Food Chemistry **132:** 855-864.

Wang Y-W, Acharya TP, Malladi A, Tsai H-J, NeSmith DS, Doyle JW, Nambeesan SU (2022) Atypical climacteric and functional ethylene metabolism and signaling during fruit ripening in blueberry (Vaccinium sp.). Frontiers in plant science **13.**

Wang Y-W, Nambeesan SU (2022) Full-length fruit transcriptomes of southern highbush (Vaccinium sp.) and rabbiteye (V. virgatum Ait.) blueberry. BMC genomics **23:** 1-15

White PJ (2002) Recent advances in fruit development and ripening: an overview. Journal of Experimental Botany **53:** 1995-2000.

Worrell AC, Bruneau J-M, Summerfelt K, Boersig M, Voelker TA (1991) Expression of a maize sucrose phosphate synthase in tomato alters leaf carbohydrate partitioning. The Plant Cell **3:** 1121-1130.

Wu X, Prior RL (2005) Systematic identification and characterization of anthocyanins by HPLC-ESI-MS/MS in common foods in the United States: fruits and berries. Journal of agricultural and food chemistry **53:** 2589-2599.

Yamaki S (2010) Metabolism and accumulation of sugars translocated to fruit and their regulation. Journal of the Japanese Society for Horticultural Science **79:** 1-15.

Yin Y-C, Hou J-M, Tian S-K, Yang L, Zhang Z-X, Li W-D, Liu Y (2020) Overexpressing chalcone synthase (CHS) gene enhanced flavonoids accumulation in Glycyrrhiza uralensis hairy roots. Botany Letters **167:** 219-231.

Yu X, Wang X, Zhang W, Qian T, Tang G, Guo Y, Zheng C (2008) Antisense suppression of an acid invertase gene (MAI1) in muskmelon alters plant growth and fruit development. Journal of Experimental Botany **59:** 2969-2977.

Zhang J, Nie J-y, Jing L, Zhang H, Ye L, Farooq S, Bacha SAS, Jie W (2020) Evaluation of sugar and organic acid composition and their levels in highbush blueberries from two regions of China. Journal of Integrative Agriculture **19:** 2352-2361.

Zhang X-M, Wang W, Du L-Q, Xie J-H, Yao Y-L, Sun G-M (2012) Expression patterns, activities and carbohydrate-metabolizing regulation of sucrose phosphate synthase, sucrose synthase and neutral invertase in pineapple fruit during development and ripening. International journal of molecular sciences **13:** 9460-9477.

Zhao C, Hua L-N, Liu X-F, Li Y-Z, Shen Y-Y, Guo J-X (2017) Sucrose synthase FaSS1 plays an important role in the regulation of strawberry fruit ripening. Plant Growth Regulation **81:** 175-181.

Zhu X, Zhang C, Wu W, Li X, Zhang C, Fang J (2017) Enzyme activities and gene expression of starch metabolism provide insights into grape berry development. Horticulture research **4.**

Zimmermann MH, Ziegler H (1975) List of sugars and sugar alcohols in sieve-tube exudates. In: M. H. Zimmermann and J. A. Milburn (eds.). Transport in plants I. Phloem transport. Springer-Verlag, Berlin.**:** 480–503.

Zrenner R, Salanoubat M, Willmitzer L, Sonnewald U (1995) Evidence of the crucial role of sucrose synthase for sink strength using transgenic potato plants (Solanum tuberosum L.). The Plant Journal **7:** 97-107.

Zrenner R, Schüler K, Sonnewald U (1996) Soluble acid invertase determines the hexose-to-sucrose ratio in cold-stored potato tubers. Planta **198:** 246-252.

Figures and Table

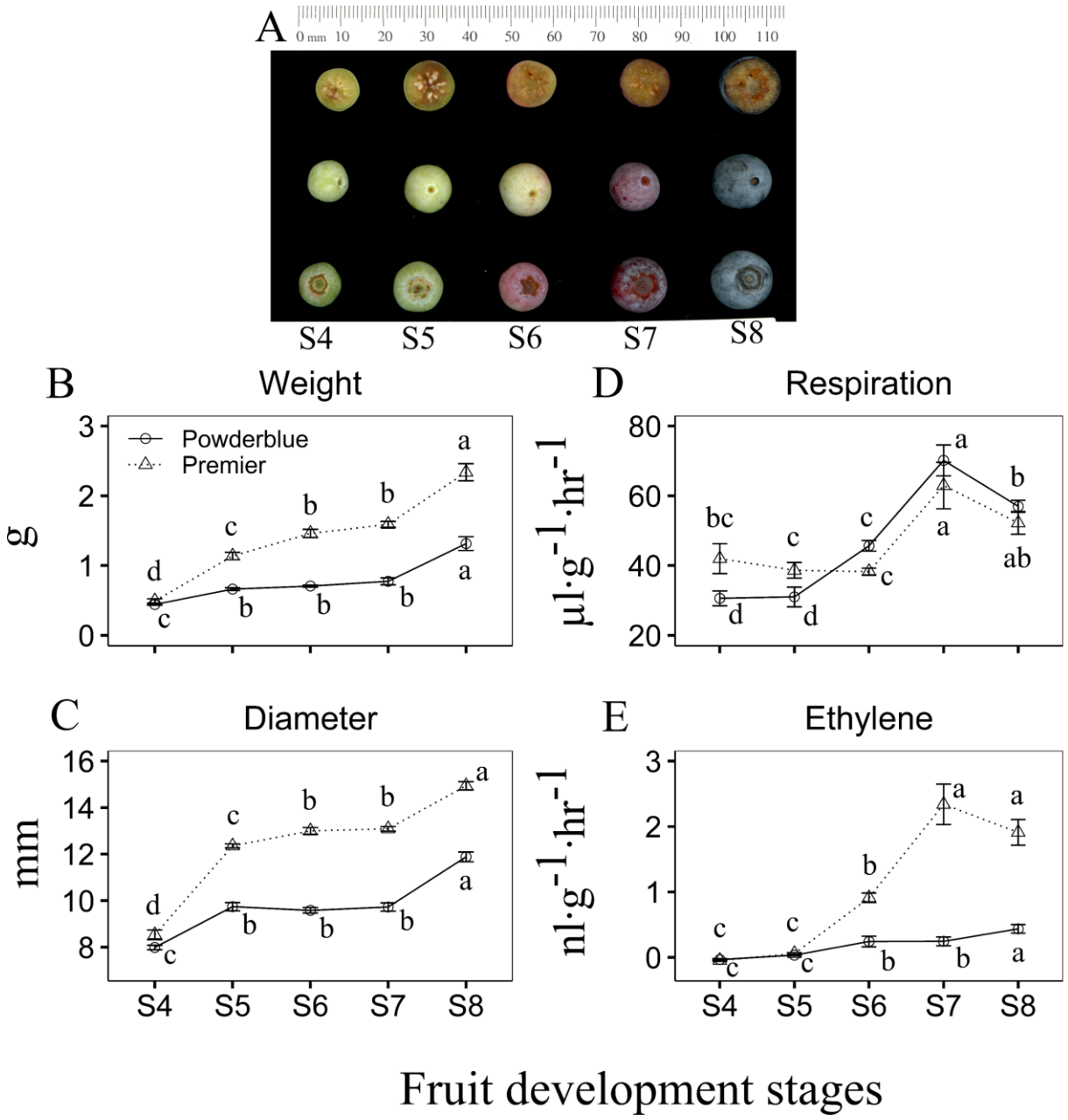

Figure 2.1: Fruit developmental stages (A), fruit weight (B), fruit diameter (C), respiration (D), and ethylene (E) production during fruit development and ripening. Values are mean ± S.E. (n=4). Different letter indicates significant differences in fruit development stages within given cultivars according to Fischer's LSD (α=0.05).

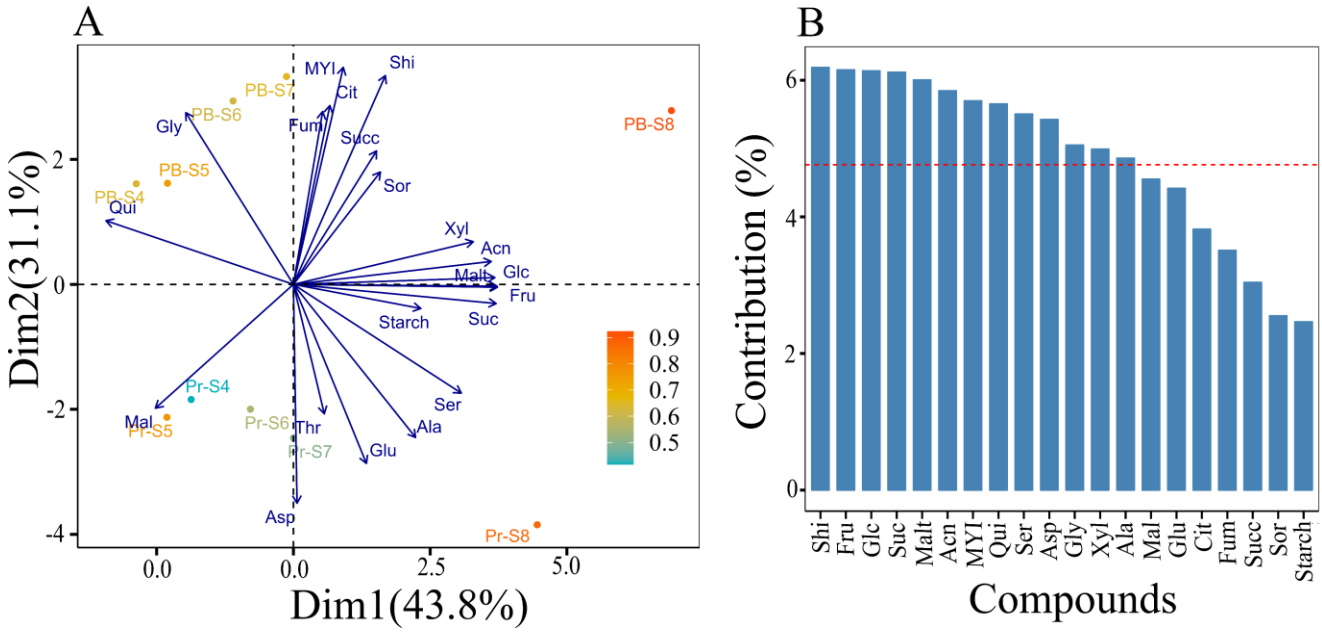

Figure 2.2: Principal component analysis (PCA) during the fruit development and ripening. A: PCA biplot showing variation of metabolites developmental stages and cultivars in first two components. B: Contribution of each metabolite in first two principal components (PC.). Glc: glucose, Fru: fructose, Suc: sucrose, Mal: malate, Asp: aspartate, Glu: glutamate, Cit: citrate, Qui: quinate, MYI: myo-inisitol, Ala: alanine, Succ: succinate, Gly: glycerate, Fum: fumarate, Ser: serine, Thr: threonine, Xyl: xylose, Sor: sorbitol, Malt: maltose, Shi: shikimate, Acn: Total anthocyanin.

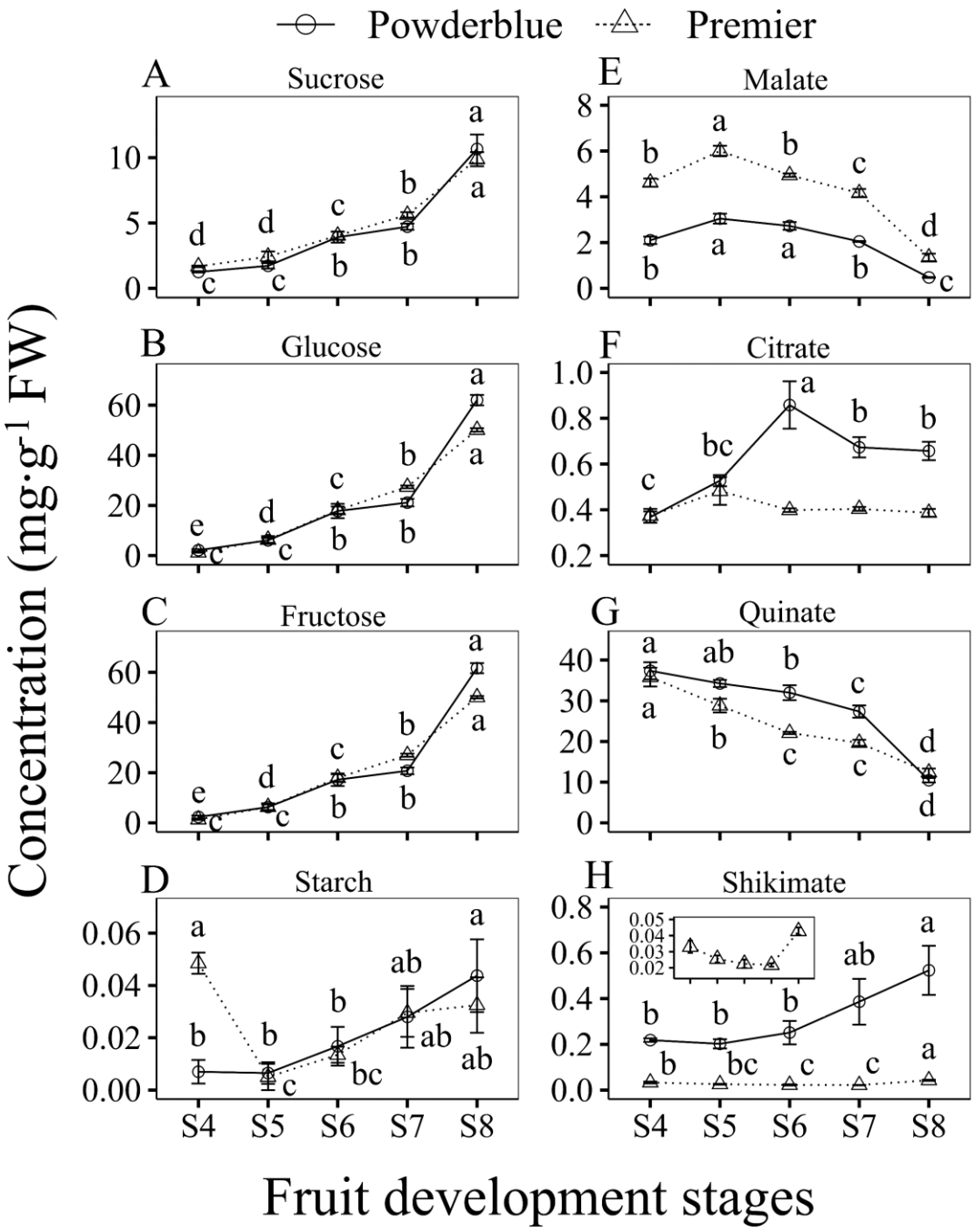

Figure 2.3: Sucrose (A), Glucose (B), Fructose (C). Starch (D), Malate (E), Citrate (F), Quinate (G), and Shikimate (H) concentration in blueberry during fruit development and ripening. Values are mean ± S.E. (n=4). Different letter indicates significant differences in fruit development stages within given cultivars according to Fischer's LSD (α=0.05).

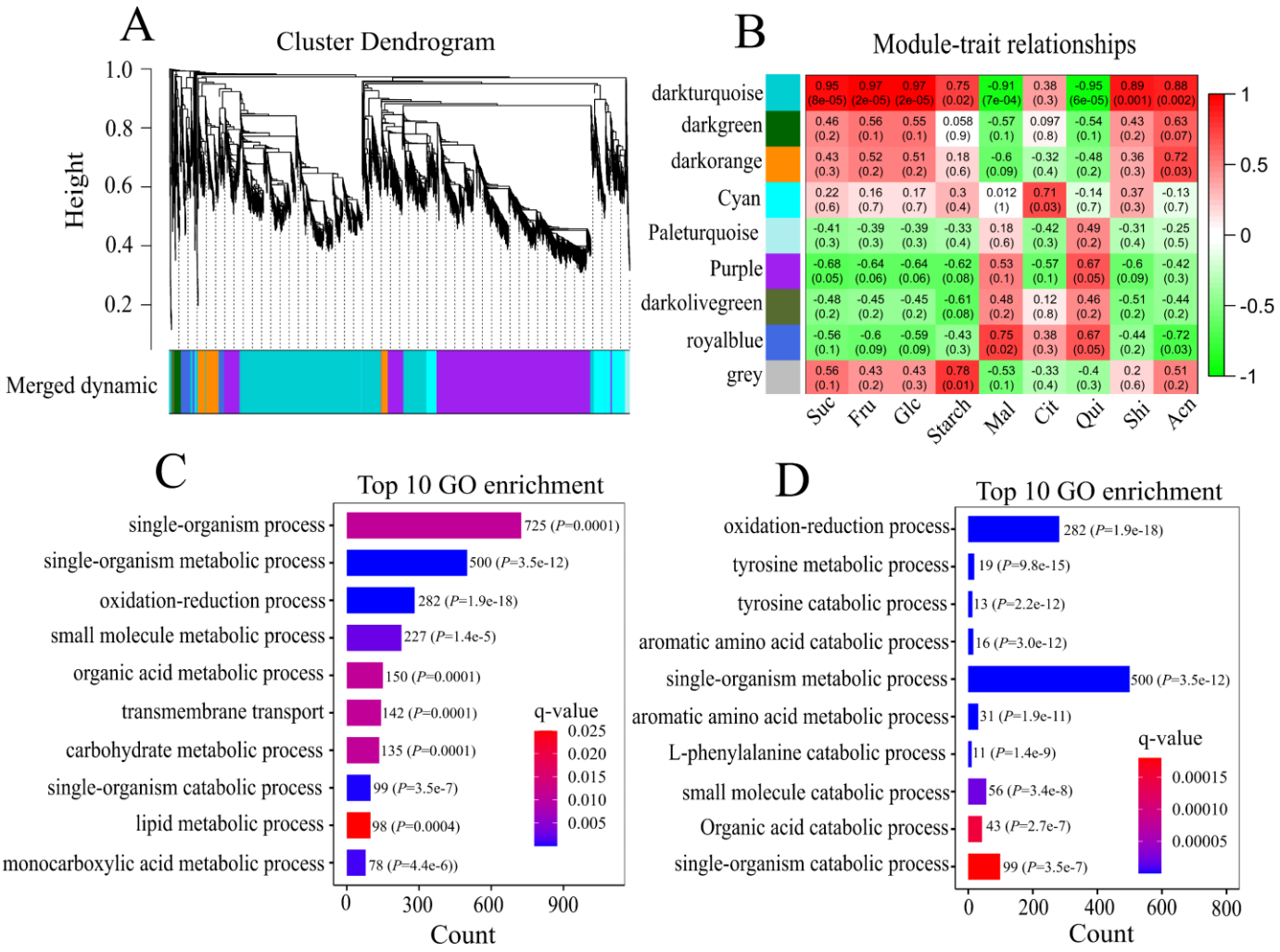

Figure 2.4: Weighted gene co-expression network analysis (WGCNA) of differentially expressed gene from ''Powderblue'' transcriptome during the fruit development and ripening. A: Hierarchical cluster presenting the 9 modules of differentially expressed gene. B: Module-metabolite association according to the Pearson's correlation. C, D: The top 10 biological process Gene ontology (GO) enrichment analysis of darkturquoise modules from WGCNA according to the highest number of gene present (C) and smallest q-value (D).

Gene id	S4/S5	S6	S7	S8	module	Role	Gene name
Sugar							
PB.12940	177	109	99	276	darkorange	Sucrose degredation	Sucrose synthase 2*
PB.14249	444	1300	1392	1026	cyan	Sucrose degredation	Vacuolar invertase*
PB.9014	16	14	10	28	darkorange	Sucrose degredation	Neutral invertase
PB.4305	5	11	13	14	darkturquoise	Sucrose synthesis	Sucrose-phosphate synthase 2
PB.6238	32	51	58	73	darkturquoise	Sucrose synthesis	Sucrose phosphate phosphatase
PB.15718	41	61	64	89	darkturquoise	Glycolysis	Hexokinase-1
PB.6242	8	16	28	34	darkturquoise	Glycolysis	Fructokinase-4
PB.8075	17	27	33	72	darkturquoise	Glycolysis	Phosphofructokinase 2
PB.2844	10	11	11	45	darkturquoise	Glycolysis	Phosphofructokinase 3
PB.7197	35	59	63	136	darkturquoise	Glycolysis	Phosphofructokinase 6*
PB.6063	48	31	21	34	purple	Glycolysis	Pyruvate kinase, cytosolic
PB.10586	7	8	30	22	darkturquoise	Glycolysis	Pyruvate kinase 2, cytosolic*
PB.6921	169	1172	2760	3601	darkturquoise	Sugar Transport	Sugar transporter N3-like
Starch							
PB.13245	12	20	26	34	darkturquoise	Starch synthesis	ADP-glucose phosphorylase*
PB.5877	72	14	4	4	purple	Starch synthesis	Starch synthase 1
PB.7224	6	4	5	14	darkorange	Starch synthesis	Starch synthase 4
PB.13234	114	196	231	197	cyan	Starch synthesis	1,4-alpha-glucan branching enzyme GlgB
PB.4473	29	21	13	23	purple	Starch synthesis	Isoamylase 1, chloroplastic
PB.5644	27	18	13	34	darkorange	Starch degradation	Phosphoglucan, water dikinase, chloroplastic
PB.1539	4	4	3	11	darkturquoise	Starch degradation	α-amylase 2
PB.8177	29	43	42	63	darkturquoise	Starch degradation	α-amylase 3
PB.6257	156	367	446	363	cyan	Starch degradation	β-amylase 1
Acid							
PB.7196	41	41	30	16	royalblue	Malate metabolism	NADP-malic enzyme
PB.2156	60	35	18	19	purple	Malate metabolism	NAD-malic enzyme, mitochondrial
PB.10260	63	32	19	36	purple	Malate metabolism	Malate DH, chloroplastic
PB.6758	41	20	16	20	purple	Glyoxylate cycle	Malate DH, glyoxysomal
PB.356	8	22	7	3	darkolivegreen	Glyoxylate cycle	Malate synthase, glyoxysomal
PB.14025	193	740	1158	1867	darkturquoise	Malate metabolism	Phosphoenolpyruvate carboxykinase*
PB.5134	59	121	75	29	royalblue	Malate metabolism	Phosphoenolpyruvate carboxylase*
PB.12152	87	118	143	203	darkturquoise	Glyoxylate cycle	Citrate synthase, glyoxysomal
PB.1371	36	22	14	18	purple	TCA cycle	Isocitrate dehydrogenase
PB.11775	50	63	61	107	darkturquoise	TCA cycle	2-oxoglutarate DH, mitochondrial
PB.12227	15	18	6	4	darkolivegreen	TCA cycle	Isocitrate lyase
PB.7468	162	629	844	596	purple	TCA cycle	Bifunctional 3-dehydroquinate dehydratase/shikimate DH
Anthocyanin							
PB.4323	30	52	190	128	darkturquoise	Anthocyanin biosynthesis	Phenylalanine ammonia-lyase
PB.103	20	155	897	673	darkturquoise	Anthocyanin biosynthesis	Chalcone synthase1*
PB.6264	139	120	370	345	darkturquoise	Anthocyanin biosynthesis	Chalcone synthase2*
PB.10264	75	76	153	111	darkturquoise	Anthocyanin biosynthesis	Chalcone isomerase1
PB.5959	114	141	508	355	darkturquoise	Anthocyanin biosynthesis	Chalcone isomerase2
PB.8864	24	32	153	158	darkturquoise	Anthocyanin biosynthesis	Flavonoid 3'-hydroxylase
PB.7103	95	332	767	729	darkturquoise	Anthocyanin biosynthesis	Flavanone 3'-hydroxylase
PB.13551	139	471	824	1207	darkturquoise	Anthocyanin biosynthesis	Flavonoid 3',5'-hydroxylase
PB.7103	95	332	767	729	darkturquoise	Anthocyanin biosynthesis	Flavanone 3-hydroxylase
PB.8840	114	110	349	281	darkturquoise	Anthocyanin biosynthesis	Dihydroflavonol 4-reductase
PB.4659	10	7	11	47	darkturquoise	Anthocyanin biosynthesis	Anthocyanidin 3-O-glucosyltransferase*
PB.3506	2	2	3	9	darkturquoise	Anthocyanin biosynthesis	Anthocyanidin 3-O-glucosyltransferase*
PB.4053	4	7	39	54	darkturquoise	Anthocyanin biosynthesis	Flavonol synthase
PB.4960	16	66	101	81	cyan	Anthocyanin biosynthesis	Anthocyanidin reductase

Figure 2.5: Heat map showing average value of transcript abundacne of sugar, starch, acid, and anthocyanin metabolism related gene from the 'Powederblue' transcriptomic data. The module represents the respective modules of those gene in weighted gene co-expression network analysis (WGCNA). Asterick sign in each gene ID indicate that those genes were validated using the RTPCR study.

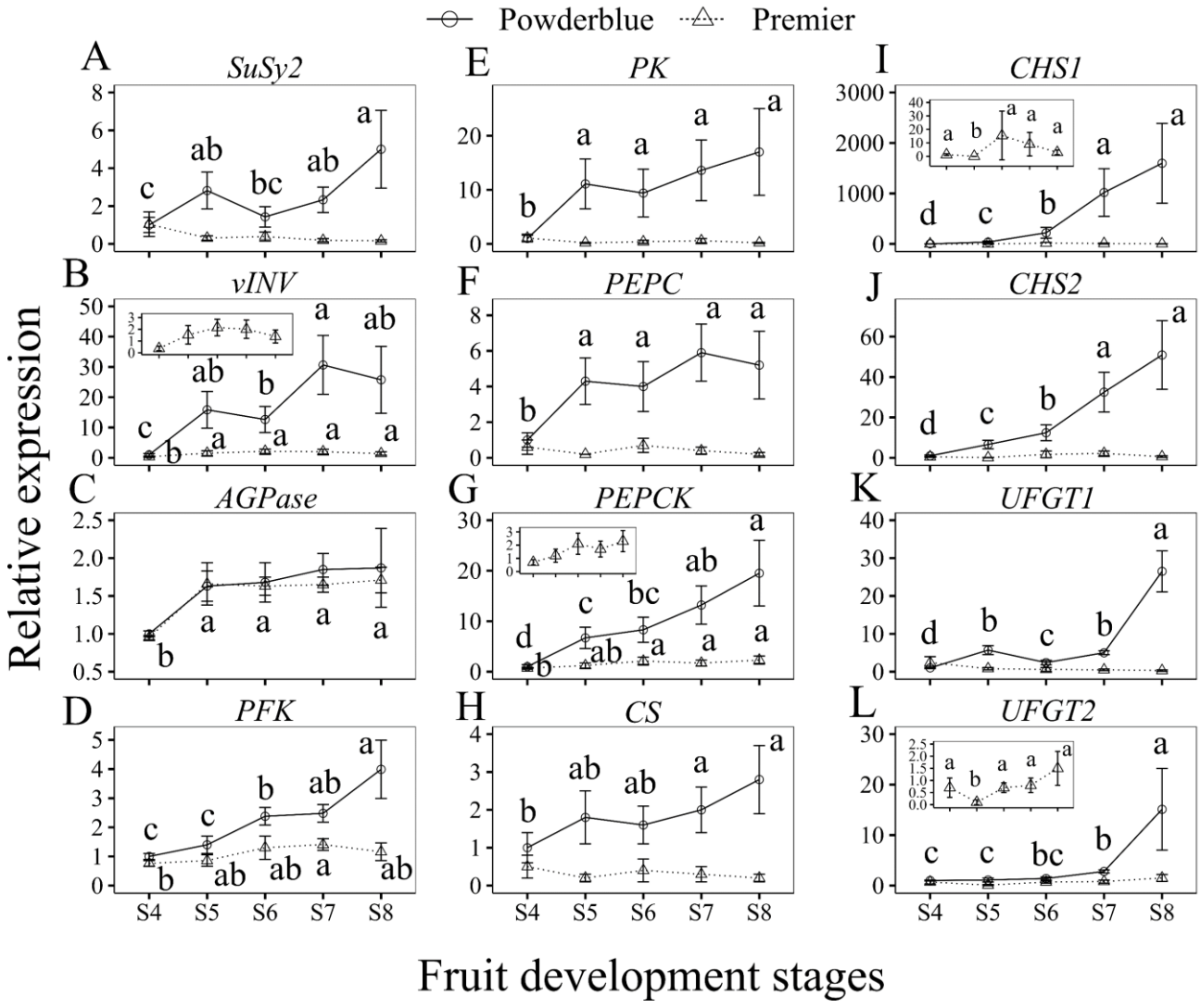

Figure 2.6: Relative abundance of transcripts involved in sugar, acid, starch, and anthocyanin biosynthesis related genes during fruit development and ripening. A: *SUCROSE SYNTHASE 2* (*SuSy2*), B: *VACUOLAR INVERTASE (vINV)*, C: *ADP-GLUCOSE PHOSPHORYLASE* (AGPase) D*: PHOSPHOFRUCTOKINASE* (*PFK*), E: *PYRUVATE KINASE* (*PK*), F: *PHOSPHOENOLPYRUVATE CARBOXYLASE (PEPC)*, G: *PHOSPHOENOLPYRUVATE CARBOXYKINASE (PEPCK)*, H: *CITRATE SYNTHASE (CS)*, I, J: *CHALCONE SYNTHASE1, 2* (*CHS1, 2*), K, L: *ANTHOCYANIDIN 3-O-GLUCOSYLTRANSFERASE1, 2* (*UFGT1, 2*). Values are mean ± S.E. (n=4). Different letters above symbols indicate that the means are significantly different across fruit developmental stages (within a cultivar) according to ANOVA and Fischer's LSD ($\alpha = 0.05$).

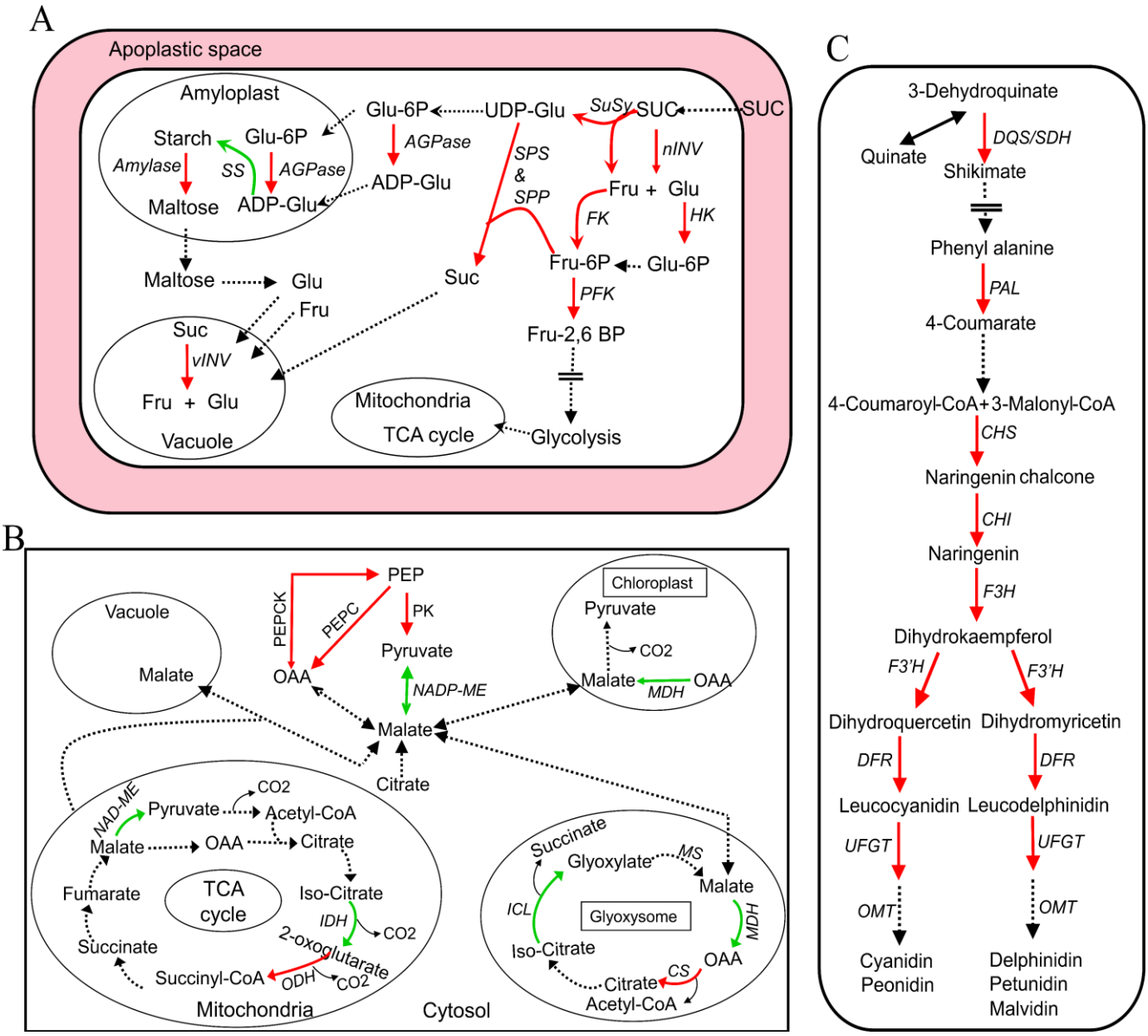

Figure 2.7: Sugar (A), organic acid (B), and anthocyanin (C) biosynthesis pathway during the fruit development and ripening in blueberry. Transcript abundance of mid development (S4/S5) and late development (S7/S8) were used for making the biochemical pathway. Red and green arrow indicate the increased and decreased in transcript abundance of enzymes from the 'Powderblue' transcriptome.

Table 2.1: Concentrations of anthocyanin at different developmental stages in blueberry.

	'Premier' (mg/100 g FW)				'Powderblue' (mg/100 g FW)			
Anthocyanin	**S6**	**S7**	**S8**	***P*-value**	**S6**	**S7**	**S8**	***P*-value**
Del 3-gal	0.00 ± 0. 00 b	0.00 ± 0. 00 b	16.60 ± 3.39 a	0.0014	0.00 ± 0. 00 b	0.00 ± 0. 00 b	18.58 ± 1.88 a	<0.0001
Del 3-glu	0.00 ± 0. 00 b	0.00 ± 0. 00 b	0.28 ± 0.12 a	0.0453	0.00 ± 0. 00 b	0.00 ± 0. 00 b	9.75 ± 0.92 a	<0.0001
Cya 3-gal	0.40 ± 0.08 c	1.93 ± 0.19 b	14.85 ± 0.67 a	<0.0001	0.53 ± 0.14 b	3.10 ± 0.92 b	25.95 ± 2.87 a	0.0001
Del 3-ara	0.00 ± 0. 00 b	0.00 ± 0. 00 b	6.48 ± 1.34 a	0.0015	0.00 ± 0. 00 b	0.00 ± 0. 00 b	11.35 ± 0.85 a	<0.0001
Cya 3-glu	0.00 ± 0. 00 b	0.00 ± 0. 00 b	0.55 ± 0.06 a	<0.0001	0.00 ± 0. 00 b	1.03 ± 0.37 b	14.15 ± 1.59 a	<0.0001
Pet 3-gal + Cya 3-ara	0.00 ± 0. 00 b	1.00 ± 0.12 b	21.03 ± 1.61 a	<0.0001	0.25 ± 0.05 b	1.53 ± 0.46 b	28.15 ± 2.05 a	<0.0001
Pet 3-glu	0.00 ± 0. 00 b	0.00 ± 0. 00 b	0.38 ± 0.06 a	0.0005	0.00 ± 0. 00 b	0.00 ± 0. 00 b	13.05 ± 0.87 a	<0.0001
Peo 3-gal	0.00 ± 0. 00 b	0.50 ± 0.04 b	6.63 ± 0.60 a	<0.0001	0.00 ± 0. 00 b	0.38 ± 0.14 b	8.05 ± 0.39 a	<0.0001
Pet 3-ara	0.00 ± 0. 00 b	0.00 ± 0. 00 b	5.5 ± 0.49 a	<0.0001	0.00 ± 0. 00 b	0.00 ± 0. 00 b	7.60 ± 0.38 a	<0.0001
Peo 3-glu	0.00 ± 0. 00 b	0.00 ± 0. 00 b	1.10 ± 0.11 a	<0.0001	0.00 ± 0. 00 b	0.65 ± 0.19 b	13.28 ± 0.70 a	<0.0001
Mal 3-gal	0.00 ± 0. 00 b	1.15 ± 0.12 b	34.15 ± 3.44 a	<0.0001	0.00 ± 0. 00 b	0.83 ± 0.24 b	30.95 ± 0.80 a	<0.0001
Peo 3-ara	0.00 ± 0. 00 b	0.18 ± 0.03 b	1.68 ± 0.22 a	0.0001	0.00 ± 0. 00 b	0.20 ± 0.04 b	2.80 ± 0.11 a	<0.0001
Mal 3-glu	0.00 ± 0. 00 b	0.00 ± 0. 00 b	1.60 ± 0.15 a	<0.0001	0.00 ± 0. 00 b	0.58 ± 0.18 b	28.63 ± 0.77 a	<0.0001
Mal 3-ara	0.00 ± 0. 00 b	0.40 ± 0.04 b	11.85 ± 1.13 a	<0.0001	0.00 ± 0. 00 b	0.45 ± 0.12 b	16.13 ± 0.42 a	<0.0001
Total anthocyanin	0.40 ± 0.08 b	5.08 ± 0.49 b	122.65 ± 10.33 a	<0.0001	0.75 ± 0.17 b	8.83 ± 2.59 b	228.40 ± 13.43 a	<0.0001

The data expressed as mean ± S.E. Different letters in each row per cultivars are significantly different according to Fischer's LSD (α=0.05).

Appendix A: Supplementary figures

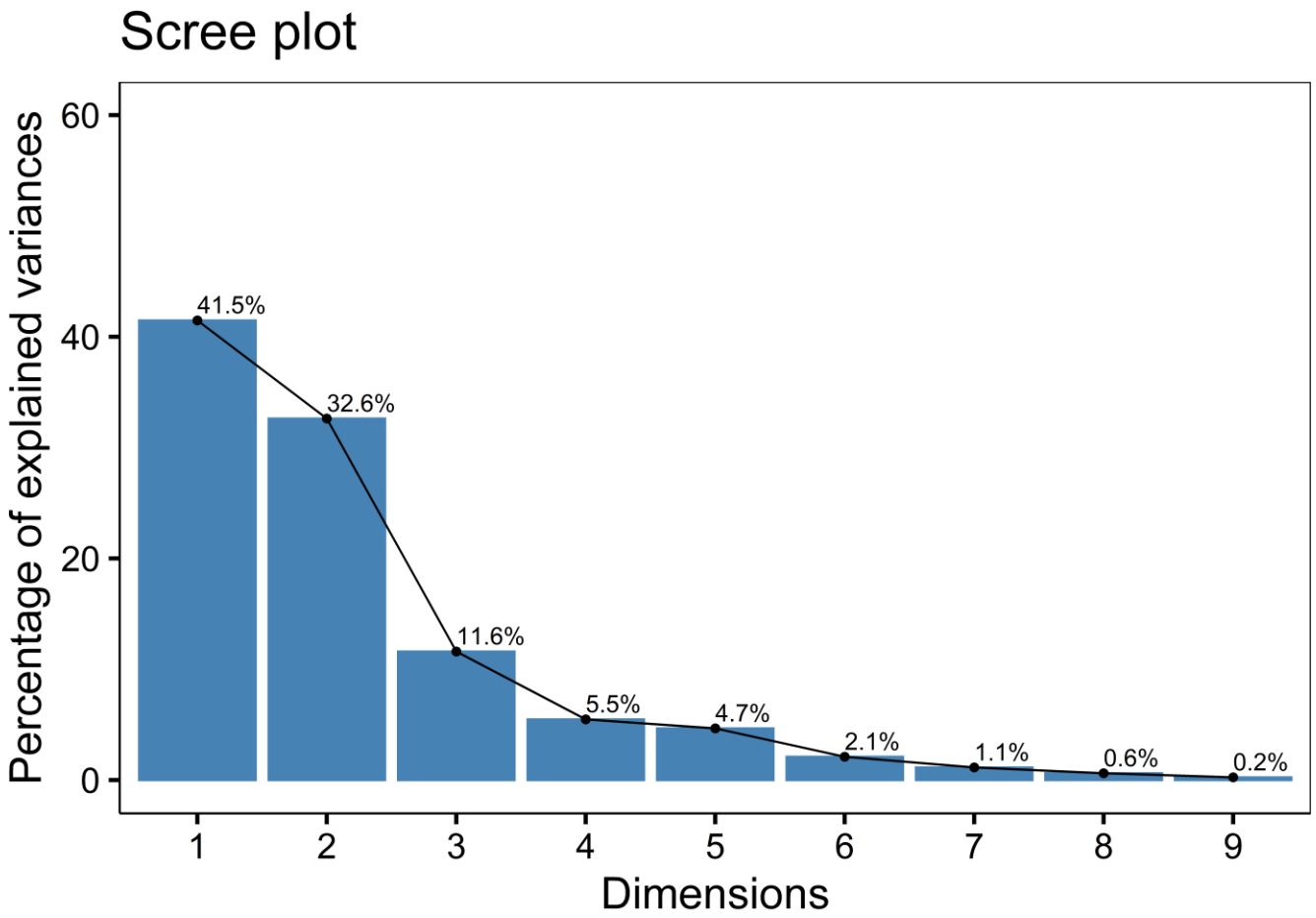

Figure 2. S1: Scree plots showing dimensions and percentage of variability explained by each dimension in principal component analysis.

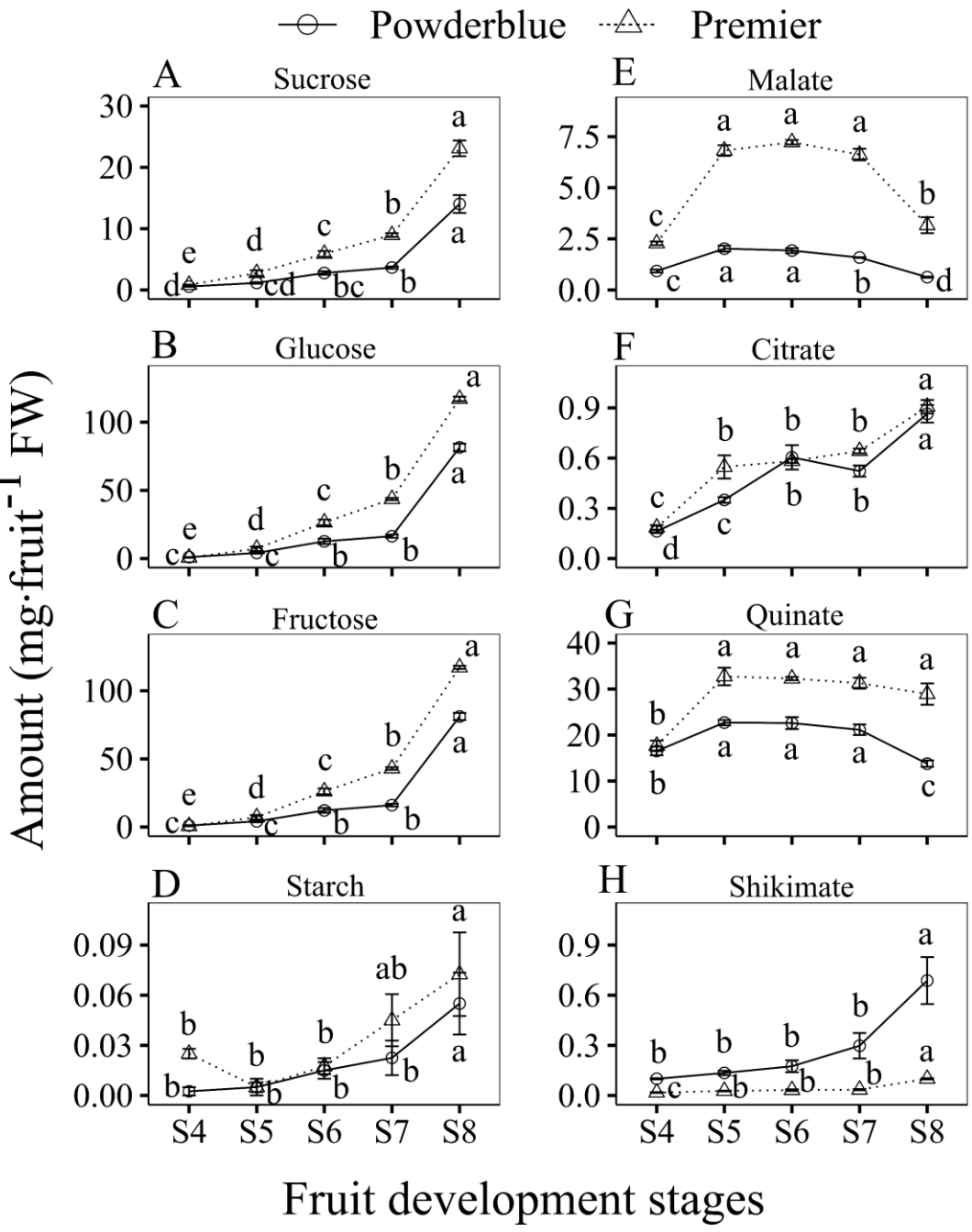

Figure 2. S2: Sucrose (A), Glucose (B), Fructose (C). Starch (D), Malate (E), Citrate (F), Quinate (G), and Shikimate (H) amount per fruit in blueberry during fruit development and ripening. Values are mean ± S.E. (n=4). Different letter indicates significant differences in fruit development stages within given cultivars according to Fischer's LSD (α=0.05).

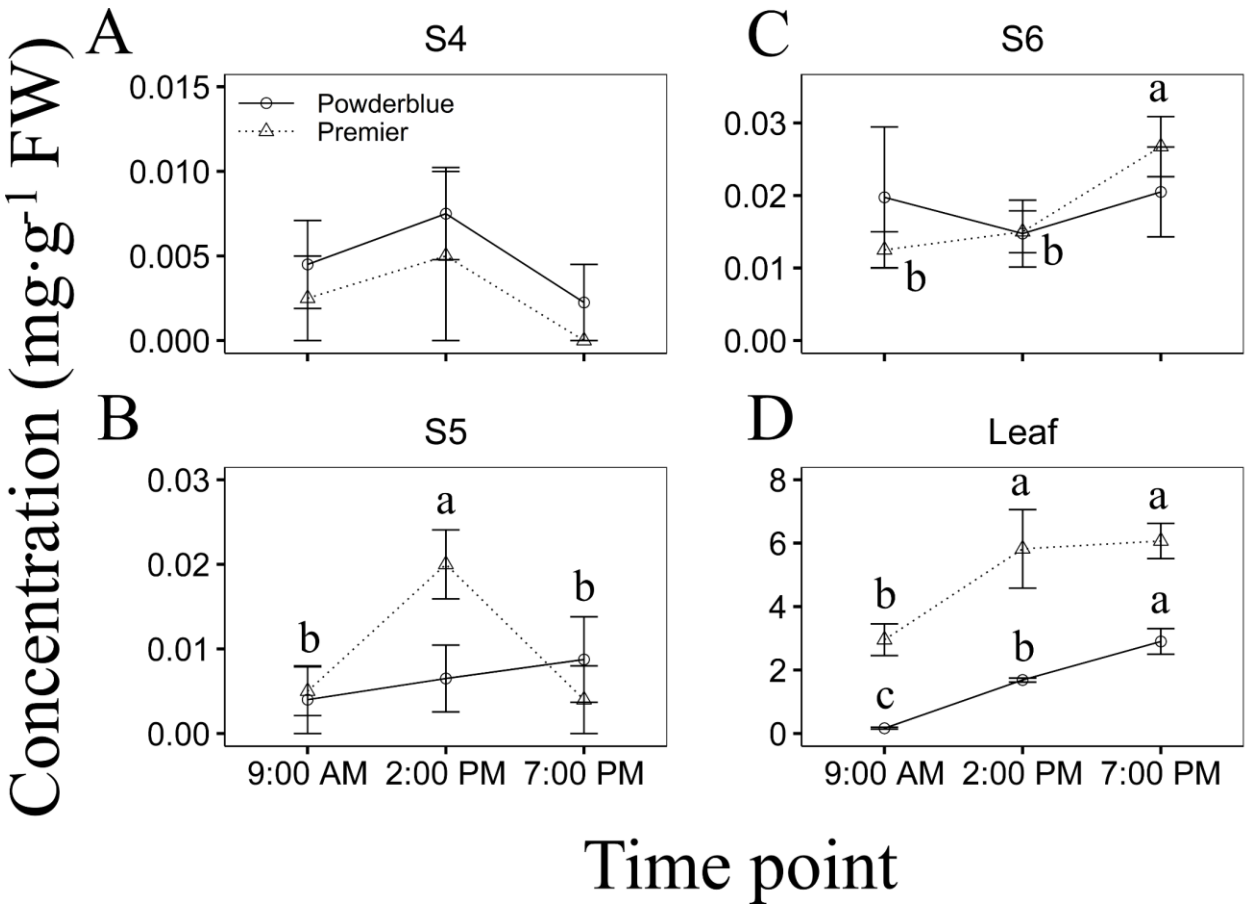

Figure 2. S3: Concentration of starch at different time of day. A: S4, B: S5, C: S6, D: S8 developmental stages. Values are mean ± SE (n=4). Different letter indicates significant differences in fruit development stages within given cultivars according to Fischer's LSD.

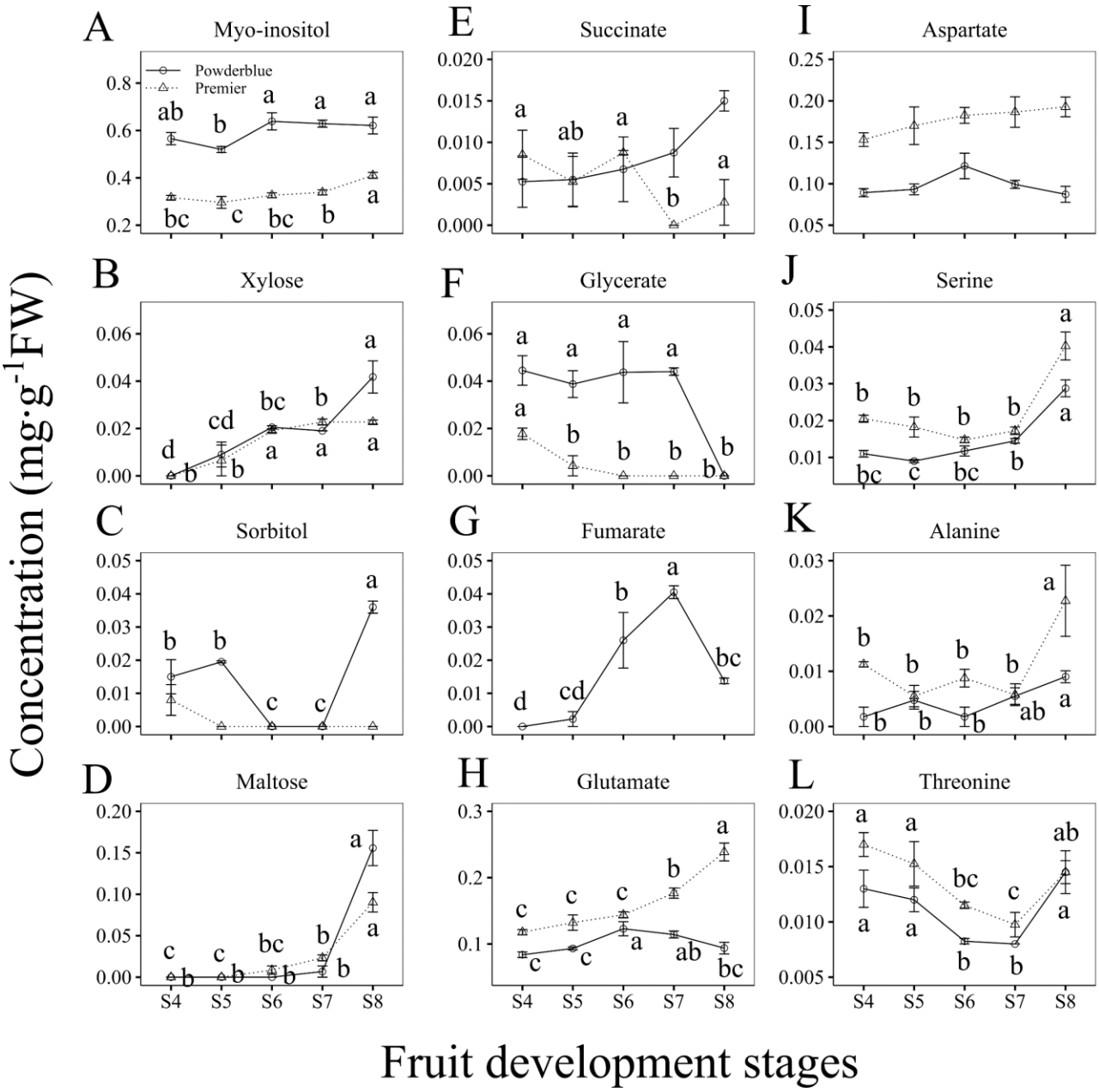

Figure 2. S4: Minor metabolites in blueberry during fruit development and ripening. A: myo-inositol, B: xylose, C: sorbitol, and D: maltose, E: succinate, F: glycerate, G: fumarate, H: glutamate, I: aspartate, J: serine, K: alanine, L: threonine. Values are mean ± S.E. (n=4). Different letter indicates significant differences in fruit development stages within given cultivars according to Fischer's LSD (α=0.05).

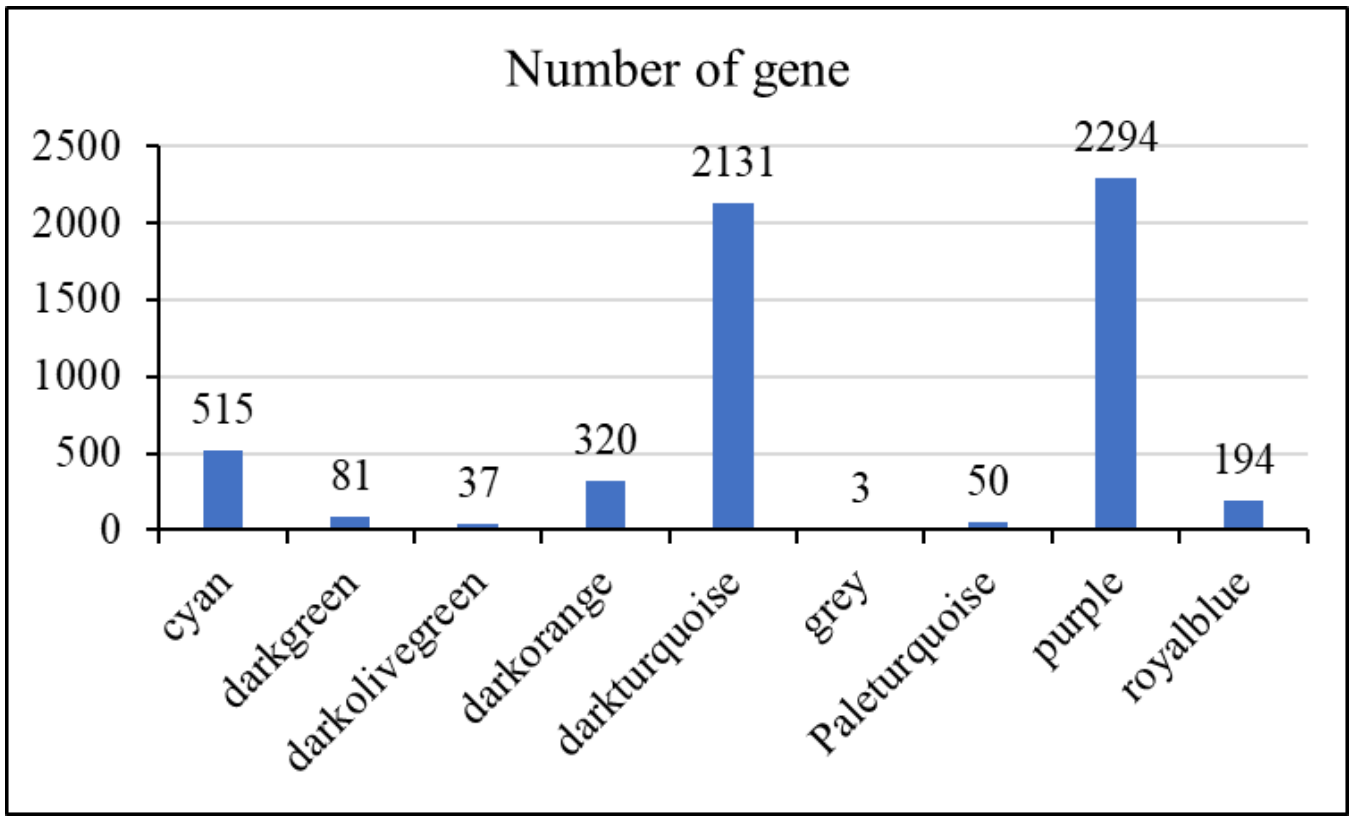

Figure 2. S5: Number of genes in weighted gene co-expression network analysis (WGCNA) modules.

Appendix B: Supplementary table

Table 2. S1: Retention times, mass spectral data, and anthocyanin compounds from 'Premier' and 'Powderblue'

Peak	Elution time (min)	$[M]^+$ (m/z)	MS/MS (m/z)	Anthocyanin Compound
1	8.86	465.1	303.05	delphinidin 3-galactoside
2	10.96	465.1	303.05	delphinidin 3-glucoside
3	12.35	449.1	287.06	cyanidin 3-galactoside
4	13.62	435.1	303.05	delphinidin 3-arabinoside
5	15.76	449.1	287.06	cyanidin 3-glucoside
6	18.29	479.1	317.07	petunidin 3-galactoside
7	18.29	419.1	287.06	cyanidin 3-arabinoside
8	21.99	479.1	317.07	petunidin 3-glucoside
9	23.18	463.1	301.07	peonidin 3-galactoside
10	25.2	449.1	317.07	petunidin 3-arabinoside
11	27.5	463.1	301.07	peonidin 3-glucoside
12	28.73	493.1	331.08	malvidin 3-galactoside
13	29.56	433.1	301.07	peonidin 3-arabinoside
14	30.5	493.1	331.08	malvidin 3-glucoside
15	31.45	463.1	331.08	malvidin 3-arabinoside

Table 2. S2: List of blueberry genes and primer sequences used for the quantitative PCR analyses

Gene	Accession number	Primer orientation	Primer sequences (5' to 3')
SuSY2	PB.576/2567/12940	Forward	5'- TCA GCG ATG GTC CCT TTG GC -3'
		Reverse	5'- ACA CCA GGC CTT GGA CGA AC -3'
vINV	PB.10450/10199/14249/5938	Forward	5'- TGC TAT GTT GGC TTG GCA GAG G -3'
		Reverse	5'- GGT GGT ACC ACC CCA AGT GAT AC -3'
AGPase	PB.13245/14754/3497/4667	Forward	5'- CTC CCC TTA AGG ACA CTA GTC CTG C -3'
		Reverse	5'- GAA CTT TGG CAG CAT CCT CAG GG -3'
PFK	PB.7197/968	Forward	5'- GGA GGG GAT GGA ACT CAA AAA GGA G -3'
		Reverse	5'- AGC AAC TAC AAC TTT GAG GCC ACG -3'
PEPC	PB.4955/5134	Forward	5'- CAC ACC GAC GTG ATG GAT GCT -3'
		Reverse	5'- GGC GTT CTT CAG ACC ATT CTC GAT -3'
PEPCK	PB.14025/14026/12415/5724/1624	Forward	5'- GCA CTG CTG GAG TGA GAA TGG C -3'
		Reverse	5'- TCA GGC TCT TTC TCG CCA GAC AA -3'
PK	PB.11411/12220	Forward	5'- GTG GGA ATC TTG AAG GAA CTG CCC -3'
		Reverse	5'- CAA GCA TTG GCA CGC TTC GG -3'
CS	PB.14402/2236	Forward	5'- AGG TGT TTC GGC GCT TTC CAA -3'
		Reverse	5'- GCG CTC CTG TTG TTC GGG AA -3'
CHS1	PB.103	Forward	5'-TTG GGC AAA GAG GCT GCT GTG-3'
		Reverse	5'-CGG CAT GTC GAC TCC CGA-3'
CHS2	PB.6264	Forward	5'-TCA CTT GGT CTT CTG CAC CAC CAG-3'
		Reverse	5'-CCC GCG GAA AGT GAC AGC A-3'
UFGT1	PB.4659	Forward	5'-CCT AAT AAT GAAA AGG CCA AGG CCA-3'
		Reverse	5'-TTG GAT CTC CGC CGC TGC A-3'
UFGT2	PB.3506	Forward	5'-CAG CTA AGG TGT TGC CTT CTA GGG TAC-3'
		Reverse	5'-GTA GAT CGG CGG GAC CTT ATC GTC AC-3'
CACS	Vashisth et al., 2011	Forward	5'-TTG GAT GGC GAA GAG AGG GTC TT-3'
		Reverse	5'-CCC AAC TTC AAA TCA GGC ATT CCA G-3'
UCE	Vashisth et al., 2011	Forward	5'-CCA TCC ACT TCC CTC CAG ATT ATC CAT-3'
		Reverse	5'-ACA GAT TGA GAG CAG CAC CTT GGA-3'
RHL	Vashisth et al., 2011	Forward	5'-GGT GAA TCG AGT AGA ACT GCT GGC-3'
		Reverse	5'-AGA TTC CTG CATG CAC CAT TCC GA-3'

CACS (*CLATHRIN ADAPTOR COMPLEXES SUBUNIT FAMILY Protein_25*), *UCE* (*UBIQUITIN-CONJUGATING ENZYME 28_27*), *RHL* (*RNA HELICASE-LIKE 8_28*)

CHAPTER 3

ETHEPHON AND ACC EFFECTS ON RIPENING, METABOLISM, AND POSTHARVEST FRUIT QUALITY IN BLUEBERRY

[2] Tej P. Acharya and Savithri U. Nambeesan. To be submitted to Frontier in Plant Science

Abstract

The plant hormone ethylene regulates fruit ripening and quality in climacteric fruits and can improve fruit color in non-climacteric fruits. Ethephon releases ethylene non-enzymatically upon absorption by plant cells. 1-Aminocyclopropane 1-carboxylic acid (ACC) is converted into ethylene through the enzymatic activity of ACC oxidase, which is not rate-limiting in blueberry fruit. This study tested the effect of ethylene-related plant growth regulators (PGRs), ethephon, and ACC on ripening, metabolite composition, and postharvest fruit quality attributes. Studies were performed in one southern highbush cultivar Miss Lilly in 2019 and two rabbiteye cultivars Premier and Powderblue in 2019 and 2020. Ethephon and ACC were applied at the rate of 250 ppm with 0.15% Latron B-1956, a nonionic surfactant. Over two years, both PGRs increased the rate of ripening as it allowed 20-35% more fruit to be harvested at 7-10 days after treatment (DAT) compared to the control. They also increased ethylene evolution at 1-3 DAT compared to the control. Ethylene-induced metabolite changes (sugar, acid, anthocyanins) were quantified using gas chromatography and high-performance liquid chromatography. Metabolite analysis indicated transient alteration of metabolites after application of ethephon and ACC. In this study, transient changes of sugars in 'Premier', malate and anthocyanins in both 'Premier' and 'Powderblue' were found. Changes in transcript abundance of *VACUOLAR INVERTASE*, *PHOSPHOENOLPYRUVATE CARBOXYKINASE*, and anthocyanin biosynthesis related genes, mediate these changes. The changes were transient as consistent effects of ethylene on sugar, acid, and anthocyanin metabolism could not be noted at 10 DAT. Postharvest fruit quality attributes, such as firmness (compression, puncture), total soluble solids, titratable acidity, and

visual quality, were not significantly affected by the PGR applications compared to control treatments, except that fruit weight decreased following ethephon treatment. This study demonstrated that ethylene-related PGRs can accelerate fruit ripening by increasing ethylene production and causing transient alterations in metabolites during ripening, while inducing minimal changes in postharvest fruit quality attributes.

Key words: ethephon, ACC, sugar, acid, anthocyanin, fruit quality

Introduction

Blueberry (*Vaccinium spp*.) is a 'super fruit' rich in flavor and health-promoting substances like phenolics, flavonoids, and anthocyanin compounds (Howard et al., 2003; Naczk et al., 2006). Due to their flavor, and consumer awareness of their health benefits, worldwide production of blueberries has increased by more than two-fold between 2013 and 2019 (Protzman, 2021). The mainly cultivated blueberry species are northern highbush (*V. corymbosum*), southern highbush (hybridization of *V. corymbosum* with *V. ashei*, *V. darrowii*, and *V. tenellum*), lowbush (*V. angustifolium*, *V. myrtilloides*, *V. boreale*), and rabbiteye (*V. virgatum*) (Strik, 2004). These species are grown across a wide range of climates based on their chilling requirements for floral development and cold hardiness. The northern highbush and lowbush species thrive in colder climates and require over 800 chilling hours, while the southern highbush and rabbiteye species perform well under warmer temperatures and need fewer than 600 chilling hours (Retamales and Hancock, 2018).

Fruit ripening is a highly coordinated process involving physiological, biochemical, and molecular changes that collectively determine development of the fruit's color, texture, sugar, acidity, and aroma volatiles (Quinet et al., 2019). Ripening initiation and progression is orchestrated by multiple transcription factors and phytohormones (ethylene, auxin, abscisic acid) and their interactions (Osorio et al., 2013). Similar to other fruits, an increase in sugars, volatiles, and anthocyanin concentrations and a decrease in acids, flavonols, and hydrocinnamic acid concentration occurs during blueberry ripening (Ayaz et al., 2001; Bouzayen et al., 2010; Silva et al., 2017). These processes are facilitated by changes in the expression levels of

ripening-related genes and enzymes (Giovannoni, 2004). For example, fruit softening during the ripening is partly due to the increase in the expression of cell wall-modifying enzymes, including pectinesterase, pectate lyase, polygalacturonase, β-galactosidase, as well as enzymes involved in cellulose and hemicellulose modification, such as 1,4-β-glucanase, xyloglucan transglycosylase/hydrolase, and expansin (Tucker et al., 2017; Li et al., 2021). Blueberry fruit are harvested after they are fully ripe and there is no subsequent improvement in their fruit quality during postharvest (PH) storage. They are also highly perishable, and their quality can deteriorate rapidly due to internal respiration, mechanical damage during handling and harvest, decay due to pathogens, and moisture loss (Hancock et al., 2008; Zhou et al., 2014). Therefore, maintaining quality after harvest is essential to extend shelf life of blueberry fruit.

The plant hormone ethylene plays an important role in positively regulating ripening. Ethylene is produced from an amino acid precursor, methionine, in a three-step process (Bleecker and Kende, 2000; Bapat et al., 2010). 1) S-adenosyl-L-methionine (SAM) synthetase converts methionine into SAM. 2) SAM is converted to 1-aminocyclopropane-1-carboxylic acid (ACC) by ACC synthase (ACS). 3) ACC is metabolized into ethylene by ACC oxidase (ACO). Fruits can be classified as climacteric and non-climacteric based on ethylene and carbon dioxide production during ripening. Climacteric fruits such as banana, tomato, and apple display increase in respiration and ethylene production during ripening (Alexander and Grierson, 2002; Paul et al., 2012; Seymour et al., 2013). In these fruits, regulation of ethylene is autocatalytic and ethylene is important for triggering ripening-related physiological changes (Yokotani et al., 2009; Liu et al., 2015). In contrast, non-climacteric fruits such as citrus, strawberry, and grape do not display a rise in ethylene and a respiratory peak during ripening (Bouzayen et al., 2010). In

these fruits, abscisic acid (ABA) plays a predominant role in facilitating ripening-related changes (Kumar et al., 2014; Chen et al., 2016; Pilati et al., 2017). Blueberry fruit display an increase in respiration and ethylene production during the ripening and PH stages (Wang et al., 2022). Further, the amount of ethylene production varies among cultivars. For example, ethylene production is higher in 'Miss Lilly' (southern highbush) and 'Premier' (rabbiteye) compared to Miss Jackie (southern highbush) and 'Powderblue' (rabbiteye), respectively (Wang et al., 2022). Peak values of respiration and ethylene production in blueberry are comparable to that in climacteric fruits such as apple and tomato (Andrews, 1995; Rudell et al., 2000). However, Wang et al. (2022) did not find an autocatalytic response after the application of an ethylene-releasing plant growth regulator (PGR), as evidenced by no effect in 1-amino cyclopropane-1 carboxylic acid (ACC) concentration and ACC synthase (ACS) transcript abundance. This study also indicated that blueberry fruit display functional ethylene signaling and subsequently classified blueberry as exhibiting atypical climacteric ripening physiology (Wang et al., 2022).

PGRs are natural or synthetic substances that promote plant growth and developmental processes (Basra, 2000). Among various PGRs, ethephon (2-chloroethyl phosphonic acid), which releases ethylene, has been extensively used to accelerate ripening and maintain PH fruit quality in climacteric fruits (Ampa et al., 2017; Li et al., 2017; Suehiro et al., 2019). In non-climacteric fruits like lemon and grape, ethephon is successfully used to enhance skin color (El-Kereamy et al., 2003; Zhang and Zhou, 2019). Previous studies found an increase in the ripening rate after preharvest ethephon application in rabbiteye blueberry (Ban et al., 2007; Wang et al., 2018). More recently it was shown that ethephon accelerates ripening by downregulation of photosynthesis-related genes (Wang and Nambeesan, *submitted*). However, the role of ethylene

in regulating fruit quality attributes such as sugars, acids and anthocyanins is not fully understood.

In this study, the effect of ethephon and the ethylene precursor, ACC, on ripening, fruit metabolism, and PH fruit quality were studied. The hypothesis was that both PGRs increase the rate of ripening by influencing sugar, acid, and anthocyanin metabolism without adversely affecting PH fruit quality. To address the hypothesis, the rate of ripening, ethylene production, respiration, and sugar, acid, and anthocyanin concentrations were analyzed following PGR application. In addition, fruit quality attributes were determined at multiple PH stages.

Material and Methods

Plant material: This study was performed with two rabbiteye cultivars (Premier and Powderblue) in 2019, 2020 and one southern highbush cultivar (Miss Lilly) in 2019. The cultivars, Premier and Powderblue were grown at the Durham Horticulture Farm, Athens, Georgia, whereas Miss Lilly was grown at the Alapaha Blueberry Research Farm, Alapaha, Georgia. The experimental design was completely randomized with four replications (one plant per treatment in each replicate).

Plant growth regulator treatments: Ethephon and ACC (Valent Bioscience LLC, Long Grove, IL) were applied at 250 $mg \cdot L^{-1}$ with 0.15% Latron-1956 (Southern Agricultural Insecticides, Inc. Hendersonville, NC) as a surfactant. Control treatments included only 0.15% Latron-1956 applications. These PGRs were sprayed on the whole plant until runoff using a hand pump sprayer in the morning (before 10 am). Approximately 30-40% of fruit were ripe at the time of

PGR application, with an exception in 2019 in ‘Premier’, where 55-60% of fruit were ripe. Before applying PGRs, all blue fruit were removed from the plants. Then, in each plant, shoots containing 50-150 fruits were tagged to determine the rate of ripening (3 shoots), ethylene evolution (2-3 shoots), carbon dioxide measurement (2 shoots), and metabolite analysis (3 shoots). Fruits from S1, S2, and S3 stages (Zifkin et al., 2012) of early fruit development were removed from the tagged branches. The treatment application and data collection details are summarized in Table 3. S1 and described below.

Rate of ripening: Green, pink, and ripe fruits were counted from the tagged branches. Fruits were categorized as "green" when they displayed full green coloration up to less than 50% pink; "pink" when exhibiting 50 to 100% pink coloration; and "ripe" when they had turned entirely blue. Finally, the percentages of fruit categorized into green, pink, and ripe were calculated to determine the ripening rate among treatment and control groups. An exception was made in the case of ‘Premier’ in 2019; since fruit were at an advanced growth stage before treatment application. In this case, green and pink fruits were counted together. The rate of ripening was determined at regular intervals. In 2019, fruits were counted at 0, 3, 5, and 7 days after treatment (DAT) in ‘Premier’; 0, 3, 5, and 10 DAT in ‘Powderblue’; and 0, 2, 5, and 9 DAT in ‘Miss Lilly’. In 2020, fruits were counted at 0, 3, 5, 7, and 10 DAT in both ‘Premier’ and ‘Powderblue’.

Ethylene and carbon dioxide measurement: Fruit were sampled randomly from the tagged branches. These represented a mixture of different developmental stages from the same branches.

Then, ethylene and carbon dioxide measurements were performed. Ethylene measurements were taken in both years (2019 and 2020), while carbon dioxide measurements were made in 2020. In 2019, fruit were collected at 2 and 4 DAT for ‘Premier’ and ‘Powderblue’, and 3 and 5 DAT for ‘Miss Lilly’. In 2020, fruits were collected at 3 and 5 DAT from both ‘Premier’ and ‘Powderblue’. Ethylene and CO_2 measurements were conducted on the same day for 'Premier' and 'Powderblue'. Fruit for 'Miss Lilly' were collected in clamshells and transported to Athens, GA where fruit were stored in a walk-in cooler set to 4 °C and 90 – 95% relative humidity. On the next day, these fruit were equilibrated to room temperature for several hours after which ethylene measurements were performed.

For ethylene measurements, approximately 25 g of fruit were placed into a 135 mL glass jar and tightly capped with a lid fitted with the septum. Fruits were incubated for four hours at room temperature, after which 1 mL of the headspace gas was taken from the jar using the syringe with a needle and injected into the Gas Chromatograph (GC) (GC-17A, Shimadzu, MD) equipped with a Hayesep-N micro packed column and a flame ionization detector. The injector and detector temperatures were set at 200 °C. The column's temperature was set at 60 °C for 4 min, ramped at 20 °C per min to 150 °C, and held for 1 min. Helium was used as the carrier gas. The sample chromatogram's peak area was quantified using a standard curve from the ethylene standards. Finally, the ethylene production rate was measured in $nL \cdot g^{-1} \cdot h^{-1}$ units.

For carbon dioxide determination, approximately 10 g of fruit were placed into a 495 mL glass jar and tightly capped with a lid fitted with the septum. Fruits were incubated for 1 hour at room temperature. Then, 60 mL of the headspace gas was taken from the jar using the syringe

with a needle and injected into the CO_2 analyzer (Quantek, MA, United States, Model 902P). Finally, the carbon dioxide production rate was measured and calculated as µL. $g^{-1}.h^{-1}$ unit.

Metabolites analysis: Fruits were collected randomly and consisted of different developmental stages fruit at 0, 3 and 5 DAT, from the tagged branches. In addition, fully ripe fruit were also collected at 10 DAT. After that, fruit were immediately frozen in liquid nitrogen and stored at -80°C until analysis. These studies were performed from fruit collected in 2020 from 'Premier' and 'Powderblue'. Metabolites were quantified using GC and high-performance liquid chromatography (HPLC).

Quantification of compounds using gas chromatography: Sugars, acids, and amino acids were extracted according to Beshir et al., (2017), with some modifications. Frozen fruit tissues were ground into a fine powder using a mortar and pestle in liquid nitrogen. Then, 125-150 mg of fruit powder was extracted into 1.5 mL methanol containing 0. l25 mg/mL of phenyl-β-D-glucoside as an internal standard. Next, methanol extracted samples were centrifuged at 22,000 *g* for 30 min at 4 ℃. Following this, 100 µL of supernatant was transferred into a 300 µL glass insert (Insert glass flat, Thomas scientific, Swedesboro, NJ, USA) in a 2 mL gas chromatography (GC) vial (SureSTART vial, Thermo Fisher Scientific, Rockwood, TN, USA). The solvent was placed in a dry bath set at 45 ℃ and evaporated using nitrogen gas. Subsequently, samples were derivatized by methoxymation followed by silylation. First, 50 µL of methoxamine (20 mg methoxamine in 1 mL pyridine) was added to each sample and heated at 50 ℃ for 30 min. Then, 100 µL of N-Methyl-N-(trimethylsilyl) trifluoroacetamide (MSTFA) +

1% trimethylchlorosilane (TMCS) was added to each sample and heated at 50 °C for 30 minutes. Finally, the derivatized samples were used to quantify the metabolites.

Samples were run on a Gas Chromatograph-Flame Ionization Detector (GC-FID) (GC-2014; Shimadzu, Japan) with HP-5 fused capillary column (J&W Scientific, Fulsom, CA, USA). Helium was used as a carrier gas. Samples were injected using a 20:1 split ratio. The initial temperature of the oven was set up at 120 °C for 1 min. Then, at the rate of 4 °C per min, it was ramped up to 180 °C, held for 0.5 min at 180 °C, ramped at 0.5 °C per minute to 185 °C, held at 0.5 min at 185 °C, ramped at 1 °C per minute to 210 °C, held for 0.5 minutes at 210 °C, ramped at 10 °C per minute to 260 °C, and finally held for 12 minutes at 260 °C. For sample quantification, a separate standard solution was prepared for each of the identified metabolites. The standards were extracted and derivatized as described for the fruit samples and run on the GC-FID. Standard curves generated individually for every metabolite were used for quantification.

Quantification of anthocyanin using high-performance liquid chromatography: The anthocyanin determination protocol was based on Downey and Rochfort (2008), with some modifications. Overall, 100 to 125 mg sample was extracted in 1 mL of 50% (v/v) methanol. Next, the samples were left undisturbed in the dark for one hour, followed by sonication (Bransonic 220, Parrot Drive, Conn.) for 20 min. Finally, samples were centrifuged at 22,000 *g* for 10 min at room temperature. Then the supernatant was purified through a 0.45 µm filter and transferred into the 2 mL GC vial. The injection volume for each analysis was 30 µL.

The quantifications were performed using HLPC coupled with a photodiode array detector (PAD) (Waters, Milford, MA, USA). A Discovery C-18 column (15cm x 4.6 mm, 5µm, Sigma-Aldrich Inc, ST. Louis, MO) was used for this study. Two mobile phases were used: first 10% formic acid in water (Solvent A) and the second 10% formic acid in methanol (solvent B), with a 1 mL/min flow rate. The following gradient flow rate was maintained: 0 min, 10% B; 14 min, 12% B; 25 min, 16% B; 28 min, 25% B; 32 min 50% B; 35-38 min, 10% B. The chromatogram was recorded at 520 nm. The standard curve of malvidin-3-O galactoside was prepared, and all anthocyanins were quantified using malvidin-3-O galactoside as a standard.

Quantitative RT-PCR: Gene expression analyses were performed using ethephon and control treated fruit from 2020. Fruit samples from 'Premier' and 'Powderblue' were obtained randomly at 0, 1, 2, and 3 DAT. Fruit samples at 0 and 3 DAT were the same as those used to determine metabolites. Fruit samples were collected, stored at -80 °C, and finely ground as explained for metabolite analyses. Transcript abundance of sugar, acid, and anthocyanin metabolism-related genes were determined by quantitative real-time polymerase chain reaction (qRT-PCR) as described below.

Total RNA was extracted using the modified cetyltrimethylammonium bromide (CTAB) method described previously (Vashisth et al., 2011). After DNAse treatment, complementary DNA (cDNA) was prepared using reverse transcriptase from 1 µg total RNA. qRT-PCR was performed using the PowerUP SYBR green master mix on a MX3005P quantitative real-time PCR instrument (Agilent Technologies, United States). All genes used in this study were identified from the 'Powderblue' transcriptome generated previously in our lab (Wang and

Nambeesan, 2022). The list of genes and primers used for this study is presented in the Table 3. S2. Three reference genes were used for the normalization of target genes, which are: *UBIQUITIN-CONJUGATING ENZYME* **(***UBC28*), *RNA HELICASE-LIKE* (*RH8*), and *CLATHRIN ADAPTER COMPLEXES MEDIUM SUBUNIT FAMILY PROTEIN* (*CACSa*). The mean PCR efficiency was calculated using LinReg PCR (Ruijter et al., 2009). Relative quantity (RQ) values were calculated after PCR efficiency correction. The normalized RQ (NRQ) values were calculated using the RQ values of the gene divided by the normalization factors (geometric mean of the RQ values of the reference genes). The standard error was determined as described previously (Rieu and Powers, 2009). The NRQ values after $\log_2$ transformation were used for statistical data analysis. Finally, the expression of all genes was presented as fold change with reference to the transcript abundance of a given gene in the control at 0 DAT.

Postharvest measurement: Fully ripe fruit were harvested at 9, 7, and 10 DAT in 'Miss Lilly', 'Premier', and 'Powderblue', respectively, in 2019, and at 10 DAT in 'Premier' and 'Powderblue' in 2020 (Table 3. S1). Fruit were stored in clamshells in a cooler set at 4 °C and relative humidity ranging from 90-95%. PH measurements were performed at three stages, i.e., PH + 3 days (PH3), PH10, and PH21.

The percentage of healthy fruit, firmness, weight, total soluble solid contents (TSS), and titratable acidity (TA) were evaluated at the PH stages. A total of 30 fruit from each replicate were used to determine the percentage of healthy fruit and fruit weight. Fruit not displaying shriveling, cracking, bruising, or mold symptoms were considered as healthy fruit. For fruit firmness, compression and skin puncture measurements were performed using a Fruit Texture

Analyzer [Model GS-15, Güss Manufacturing (Pty) Ltd., Strand, South Africa]. Twelve fruit from one replicate were used for textural analysis. To determine TSS and TA, fruit juice was extracted by crushing 40 g of fruit using a grinder, and fruit juice was extracted after filtering through a cheesecloth. The TSS and TA were determined using a digital handheld refractometer (Atago, USA) and automatic mini titrator (Hanna instruments, USA). The TA was measured as citric acid equivalents.

Statistical analysis: Data were analyzed and visualized using the R-studio 2023 (R core 2023, Vienna, Austria). Analysis of variance (ANOVA) was performed to evaluate the significance of the treatment effect. In addition, multiple comparison test was performed by Fisher's least significant difference (LSD) at the 0.05 significance level.

Results

Effect of ethylene releasing PGRs on rate of ripening: Overall, all cultivars displayed an increased rate of ripening in response to exogenous application of ethylene releasing PGRs: ethephon and ACC, compared to the control in both years (Fig. 3.1). In 2019, ethephon increased ripe fruit percentage by 75.3%, 60.9%, and 56.2% compared to the control at 2, 5, and 9 DAT, respectively, in 'Miss Lilly' (Fig. 3.1A). Similarly, ACC increased ripe fruit percentage by 46.4% and 53.1% at 5 and 9 DAT, respectively in 'Miss Lilly'. In addition, ethephon increased ripe fruit percentage by 25.4% and 25.7% compared to the control at 5 and 7 DAT, respectively, in 'Premier' 2019 (Fig. 3.1B), and 68.8%, 72.4% and 53.4% compared to control at 5, 7, and 10 DAT, respectively in 2020 (Fig. 3.1C). ACC also increased the percentage of ripe fruits by

33.1%, 47.2%, and 38.0% compared to the control at 5, 7, and 10 DAT, respectively, in ‘Premier’ 2020 (Fig. 3.1C). These results were consistent for ‘Powderblue’. In 2019, at 10 DAT, ethephon and ACC increased the percentage of ripe fruits compared to the control by 85.5% and 82.6%, respectively, in ‘Powderblue’ (Fig. 3. 1D), and by 111.6% and 67.8%, respectively in 2020 (Fig. 3.1E).

The increase in ripe fruit resulted in decreased green fruit in both ethephon and ACC treated fruits (Fig. 3. S1). In 2019, ethephon decreased the percentage of unripe (green and pink fruit pooled together) fruit compared to control at 5 and 7 DAT in ‘Premier’ (Fig. 3.S1A). Similarly, in 2020, ethephon decreased the percentage of green fruit at 5, 7, and 10 DAT, whereas ACC decreased the percentage of green fruit at 7 DAT, compared to the control, in ‘Premier’ (Fig. 3. S1B). These results were consistent with those of ‘Powderblue’ and ‘Miss Lilly’ (Fig. 3. S1C-E). Ethephon increased the proportion of pink fruit compared to the control at 3 and 5 DAT in ‘Powderblue’ in 2019, 2020, and 5 DAT in ‘Miss Lilly’ in 2019 (Fig. 3. S1G-I). Similarly, ACC increased the proportion of pink fruit compared to the control at 7 DAT in ‘Premier’ in 2020 and at 5 DAT in ‘Powderblue’ in 2020 and ‘Miss Lilly’ in 2019, respectively (Fig. 3. S1F-I).

Effect of ethylene releasing PGRs on ethylene and CO_2 production: Over the two years of study, in general both ethephon and ACC increased ethylene production compared with the control (Fig. 3.2). Ethephon and ACC, compared to the control increased ethylene evolution by 2.9- and 5.7-fold at 2 DAT in ‘Miss Lilly’ in 2019 and by 1.7- and 3.6-fold at 3 DAT in ‘Premier’ in 2020, respectively (Fig. 3.2A, C). There was no effect of ethephon and ACC on

ethylene production in ‘Premier’ in 2019 (Fig. 3.2B). Ethephon also increased ethylene production compared to the control by 4-fold at 2 DAT in ‘Powderblue’ in 2019 and by 5.8-, 4.2-, and 2.5-fold at 1, 3, and 5 DAT, respectively, in ‘Powderblue’ in 2020. In addition, ACC increased ethylene production compared to the control by 7.9- and 7.6-fold at 2 and 4 DAT in ‘Powderblue’ in 2019 and by 3.7-, 7.5-, and 2.9–fold in ‘Powderblue’ in 2020, respectively (Fig. 3. 2D, E). Compared to the control, both ethephon and ACC increased CO_2 production by 1.3- and 1.2-fold at 3 DAT in ‘Premier’ 2020 (Figure 3. 3A), but not in ‘Powderblue’ in 2020 (Fig. 3. 3B).

Effect of ethylene releasing PGRs on sugar metabolism: Compared to the control, ethephon increased the concentration of sucrose, glucose, and fructose at 3 DAT by 1.6-, 1.7-, and 1.7-fold, respectively, in ‘Premier’ (Fig. 3.4A-C). Similarly, ACC compared to the control increased the concentration of glucose and fructose by 1.6-fold in ‘Premier’ at 3 DAT. However, no treatment effects on these metabolites were noted at 10 DAT. However, the sugar-alcohol, myo-inositol, slightly increased at 10 DAT in ‘Premier’ following ethephon treatment (Fig. 3. S2A). In ‘Powderblue’, ethephon and ACC treatments did not affect sugars and myo-inositol concentrations at 3 and 5 DAT; however, at 10 DAT, control fruit displayed slightly increased concentrations of sucrose, glucose, and fructose than ethephon-treated fruit (Fig. 3.4D-F, Fig. 3. SF).

The gene expression of three sugar metabolism-related genes: *SUCROSE SYNTHASE 2* (*SuSY2*), *VACUOLAR INVERTASE* (*vINV*), and *NEUTRAL INV* (*nINV*), and one glycolysis-related gene: *PHOSPHOFRUCTOKINASE* (*PFK*) was determined. Ethephon did not influence the transcript abundance of *SuSY2* in ‘Premier’; however, in ‘Powderblue’, it increased it by 1.7-

fold at 1 DAT compared to the control (Fig. 3.4G, K). The transcript abundance of *vINV* increased by 1.7-fold at 2 DAT in 'Premier', and by 2.7- and 2.2-fold at 1 and 3 DAT in 'Powderblue', respectively in ethephon treated fruit compared to the control (Fig. 3.4I, M). In contrast, ethephon did not influence the transcript abundance of *nINV* and *PFK* in either cultivar (Fig. 3.4H, J, L, N).

Effect of ethylene releasing PGRs on acid metabolism: Ethephon treatment decreased malate concentration compared to the control at 3 and 5 DAT by 1.4- and 1.3-fold in 'Premier', and by 1.9-fold at 5 DAT in 'Powderblue' (Fig. 3.5A, C). Similarly, ACC decreased malate concentration compared to the control at 3 DAT by 1.4-fold in 'Premier'. However, ethephon and ACC treatment did not affect malate concentration at 10 DAT in either cultivar. In general, no effects of ethephon and ACC were noted on citrate concentration in either cultivar (Fig. 3. 5B, D). Similarly, the concentration of quinate was not affected by ethephon and ACC treatments in either cultivar, compared to the control (Fig. 3. S2B, G). Ethephon-treated fruit displayed increased concentration of shikimate compared to the control at 3 and 5 DAT by 1.5- and 1.8-fold, respectively, in 'Premier (Fig. 3. S2C). However, this effect was not observed with ACC treatment. In 'Powderblue', the concentration of shikimate was not different after treatments at any of the time-points evaluated, with the exception of 10 DAT where ethephon treatment resulted in slightly decreased concentration compared to the control (Fig. 3. S2H).

We also determined the gene expression of *PYRUVATE KINASE* (*PK*), *PHOSPHOENOLPYRUVATE CARBOXYLASE* (*PEPC*), *PHOSPHOENOLPYRUVATE CARBOXYKINASE* (*PEPCK*), and *CITRATE SYNTHASE* (*CS*) between the ethephon and

control-treated fruit at 0, 1, 2, and 3 DAT (Fig. 3. 5E-L). Ethephon increased the transcript abundance of *PK* at 3 DAT compared to the control by 1.2-fold in 'Premier', and by 1.4- and 1.7-fold at 1 and 3 DAT in 'Powderblue', respectively (Fig. 3. 5E, I). In contrast, ethephon decreased the transcript abundance of *PEPC* compared to the control by 1.7 fold at 2 DAT in 'Premier; but not in 'Powderblue' (Fig. 3. 5F, J). The effect of ethephon on *PEPCK*, was inconsistent. At 3 DAT, ethephon increased transcript abundance of *PEPCK* compared to the control by 1.6-fold in 'Premier'; whereas in 'Powderblue' it decreased expression by 1.2-fold (Fig. 3. 5G, K). The transcript abundance of *CS* did not change in response to ethephon treatment in both cultivars (Fig. 3. 5H, L).

Effect of ethylene releasing PGRs on amino acids: Ethephon and ACC did not affect aspartate concentration at any sampling time points in either cultivar (Fig. 3. S2D, I). Ethephon increased glutamate concentration by 2.4-fold at 5 DAT in 'Premier' but not in 'Powderblue' (Fig. 3. S2E, J). Similarly, ACC increased glutamate concentration at 5 DAT by 2.2-fold in 'Premier; but not in 'Powderblue'.

Effect of ethylene releasing PGRs on anthocyanin metabolism: In 'Premier', ethephon treatment increased the concentration of delphinidin 3-galctoside (del 3-gal), Cyanidin 3-galactoside (Cya 3-gal), cyanidin 3-glucoside (Cya 3-glu), petunidin 3-galactoside + cyanidin 3-arabinoside (Pet 3-gal + Cya 3-ara), peonidin 3-galactoside (Peo 3-gal), petunidin 3-arabinoside (Pet 3-ara), peonidin 3-glucoside (Peo 3-glu), malvidin 3-galactoside (Mal 3-gal), peonidin 3-arabinoside (Peo 3-ara), malvidin 3-glucoside (Mal 3-glu), and malvidn 3-arabinoside (Mal 3-

ara) at 3 DAT (Table 3. S3). Similarly, ACC cincreased the concentration of Cya 3-gal, Cya 3-glu, Pet 3-gal + Cya 3-ara, Peo 3-gal, Pet 3-ara, Mal 3-gal, Peo 3-ara, Mal 3-glu, and Mal 3-ara in 'Premier' at 3 DAT. Additionally, in 'Premier', ethephon increased the concentration of Cya 3-glu and Mal 3-ara; whereas ACC increased the concentration only of Mal 3-ara at 5 DAT (Table 3. S3).

In 'Powderblue', ethephon increased the concentration of Del 3-gal, delphinidin 3-glucoside (Del 3-glu), Cya 3-glu, Pet 3-gal + Cya 3-ara, Pet 3-ara, Peo 3-glu, Peo 3-ara, Mal 3-glu, and Mal 3-ara at 3 DAT (Table 3. S4). Similarly, ACC increased the concentration of Del 3-gal, Del 3-glu, and Pet 3-ara in 'Powderblue' at 3 DAT. Additionally, in 'Powderblue' ethephon increased the concentration of Cya 3-gal, Cya 3-glu, Pet 3-gal + Cya 3-ara, Peo 3-glu, Mal 3-gal, Peo 3-ara, Mal 3-glu, and Mal 3-ara at 5 DAT. At 5 DAT, ACC also increased the concentration of Cya 3-gal and Cya 3-glu in 'Powderblue' (Table 3. S4). The details of the effects of ethephon and ACC on anthocyanin concentrations are presented in the Table 3. S3, S4. Effects of these PGRs on three major anthocyanins are presented in Fig. 3.6A-F.

Ethephon increased the concentration of Del 3-gal, Cya 3-gal, and Mal 3-gal by 6.8-, 2.7-, and 2.5-fold at 3 DAT, respectively, in 'Premier' (Fig. 3. 6A-C). Similarly, ACC increased the concentration of Cya 3-gal and Mal 3-gal by 2.3-, and 3.1-fold, respectively in 'Premier' at 3-DAT. Additionally, ethephon increased the concentration of Del-3-gal by 1.9-fold at 3 DAT**,** and Cya 3-gal and Mal 3-gal by 1.9- and 2.2-fold at 5 DAT in 'Powderblue (Fig. 3. 6D-F). ACC also increased the concentration of Del-3-gal by 1.7-fold at 3 DAT, and Cya 3-gal by 1.5-fold at 5 DAT in 'Powderblue**'**.

Gene expression of key anthocyanin biosynthesis genes was determined (Fig. 3. 6G-N). Ethephon treatment increased the transcript abundance of *CHALCONE SYNTHASE1* (*CHS1*) at 3 DAT by 1.8-fold in 'Premier', and by 1.5- and 2.1-fold at 1 and 3 DAT in 'Powderblue' (Fig. 3. 6G, K). In addition, ethephon increased the transcript abundance of *CHS2* at 3 DAT by 2-fold in 'Premier', but not in 'Powderblue' (Fig. 3. 6H, L). Ethephon treatment increased the transcript abundance of *UFGT1* by 2.3-fold at 1 DAT in 'Powderblue' and that of *UFGT2* by 1.3-fold at 3 DAT in 'Premier' (Fig. 3. 6J, M). The transcript abundance of *UFGT1* in 'Premier; and *UFGT2* in 'Powderblue' were not affected by ethephon (Fig. 3.6I, N).

Effect of ethylene releasing PGRs on postharvest fruit quality attributes: Ripe fruit were harvested 7-10 DAT to determine their effects on fruit quality during storage (Tables 3. 1 & 3. 2). In general, the treatments did not significantly differ in their effects on fruit firmness, as assessed through compression and puncture tests (Table 3.1). However, there were a few exceptions: in 'Powderblue' 2019, puncture force at PH21 was increased by both ethephon and ACC, while in 'Powderblue' 2020, ethephon led to higher compression at PH21 compared to the control. Additionally, at PH3 in 'Powderblue' 2020, both ethephon and ACC resulted in higher puncture force than the control (Table 3.1).

Fruit weight was not different in 'Miss Lilly' and 'Premier' during the 2019 trial (Table 3.1). However, in 'Powderblue', ethephon decreased fruit weight compared to the control by 1.2-fold, 1.1-fold, and 1.2-fold at PH3, PH10, and PH21, respectively (Table 3. 1). Similarly, ACC decreased fruit weight compared to the control by 1.2-fold, 1.3-fold, and 1.2-fold at PH3, PH10, and PH21, respectively. During the 2020 trial, ethephon-treated fruit exhibited decreased fruit

weight at all sampling dates in 'Premier' and at PH3 in 'Powderblue'; however, no differences in fruit weight was observed between ACC and control treatments (Table 3. 1).

Additionally, inconsistent effects of ethephon and ACC on titratable acidity (TA) and total soluble solids (TSS) content were observed in both years (Table 3. 2). In 'Miss Lilly' 2019, no treatment effects on TA and TSS content were noted. In 'Premier 2019, the control treatment had higher TSS and TA content at PH10. In 'Powderblue' 2019, both ethephon and ACC treatments had lower TSS, and higher TA content at PH3 and PH10, respectively, compared to the control (Table 3. 2). These results were inconsistent with the 2020 trial, where no significant differences in TA and TSS content were observed, except at PH3 in 'Powderblue' (TSS was higher in control fruit). The percentage of defective fruit was not affected by ethephon and ACC treatments, except at PH21 in 'Powderblue' 2020, where ethephon, compared to the control, reduced the number of defective fruit (Table 3. 2).

Discussion

In this study, both ethephon and ACC increased the rate of ripening by enhancing the percentage of blue and pink fruits while reducing the number of green fruits. Previous studies have indicated accelerated ripening in response to ethephon applied at a rate between 500-1500 ppm (US-EPA, 2010). However, at these concentrations, ethephon can also cause fruit drop by inducing abscission (Dekazos, 1979; Malladi et al., 2012; Malladi et al., 2013). More recent work has demonstrated that 250 ppm of ethephon is sufficient to promote ripening by increasing the percentage of blue fruit (Wang et al., 2018). Further, transcriptome analyses, indicated that application of ethephon-derived ethylene promotes ripening initiation by downregulation of

photosynthesis related genes and by fine tuning the action of other hormones (Wang and Nambeesan, *submitted*). Ethylene downregulated jasmonate and auxin biosynthesis and upregulated ABA signaling. Further quantification of hormones indicated that ethylene decreased JA and increased ABA levels (Wang and Nambeesan, *submitted*). These results suggest a strong role for ethylene in promoting fruit developmental transition towards ripening. In typical climacteric fruit, ethylene accelerates fruit ripening by influencing multiple processes involved in ripening such as cell wall degradation, increasing sugar: acid ratio, and pigment biosynthesis (Osorio et al., 2013). In some non-climacteric fruit, however ethylene stimulates pigment synthesis without affecting fruit quality (Fan et al., 2022). Blueberry fruit have been classified as exhibiting atypical ripening (Wang et al., 2022).

Both ethephon and ACC increased fruit ethylene levels at 1-5 DAT. Although data for ethylene evolution were collected at 1 DAT only for Powderblue in 2020, they clearly show that ethephon application increased ethylene evolution almost immediately (5.8-fold at 1 DAT) followed by a decline, whereas the peak in ethylene production by ACC appears to be 1-3 d after application. Ethephon releases ethylene non-enzymatically when the pH is greater than 3.5, usually after absorption by plant cells (Aiken et al., 2015). Further, ethephon application is pH and temperature dependent, with higher pH and temperature resulting in greater ethylene evolution and ethylene-dependent effects (Lougheed and Franklin, 1972; Aiken et al., 2015). On the other hand, ACC conversion to ethylene is *via* the action of an enzyme, ACC oxidase, which is not rate-limiting (Wang et al., 2022) and may allow for more controlled rate of ethylene release compared to ethephon. The higher level of ethylene production observed immediately after applying ethephon may be attributed primarily to non-enzymatic ethylene conversion,

which could result in a more rapid effect compared to the enzymatic conversion. In this study, in general, ethephon exhibited an increased rate of ripening earlier than ACC, by 3 DAT, which may be linked to an immediate increase in ethylene evolution after ethephon application. The rate of ripening after ACC application, was similar to that induced by ethephon by 5 DAT in all trials except for 'Powderblue' in 2020, suggesting a slightly protracted but equally effective response in enhancing ripening. The effect of PGRs in enhancing ripening in 'Premier' in 2019 was not evident because of advanced maturity of fruit at the time of application, which did not allow for observing effects of enhanced ripening rates. Overall, these results with increase in the rate of ripening after application of ethylene-releasing compounds is consistent with that in previous studies (Eck, 1970; Wang et al., 2018). In addition, both ethephon and ACC increased respiration within the 3 DAT in 'Premier', further supporting the idea that ripening is promoted due to the treatment effect.

The major sugars that accumulate in ripe blueberry fruit include glucose, fructose, and sucrose (Chapter 2). Similarly, malate, citrate, and quinate constitute the major organic acids. The concentration of malate and quinate decrease during ripening, whereas citrate concentration is generally low and does not display a ripening-specific pattern. In this study, a transient increase in sucrose, fructose, and glucose concentrations was noted after ethephon and ACC applications in 'Premier'. Sucrose can be metabolized into UDP-glucose and fructose *via* the action of sucrose synthase (SuSy), and to glucose and fructose by three types of invertases based on its localization; cell wall invertases (cwINV), neutral invertases (nINV) vacuolar invertases (vINV). Among genes coding for these enzymes, the transcript abundance of *vINV* is notably high during fruit ripening, indicating significant breakdown of sucrose into glucose and fructose

for storage in vacuoles (Chapter 2). These sugars can be transported out the vacuole to cytosol if a demand arises or to maintain sugar homeostasis in various cellular compartments (Tang et al., 1999). Further, transcript abundance of *SuSy2* and *nINV* increased only in ripe fruit mainly in 'Powderblue' suggesting catabolism of sucrose in the cytoplasm to hexose sugars to be used for glycolysis (Chapter 2). Notably, *vINV* displayed increased expression at 2 DAT in 'Premier' and at 1 and 3 DAT in 'Powderblue', and that of *SuSy2* increased only in 'Powderblue' at 2 DAT. The transient increase in gene-expression in both cultivars is indicative of ethylene-induced stimulation of sugar metabolism related genes, especially that of *vINV*. These gene expression changes after ethephon application were correlated with increase in glucose and fructose especially in 'Premier'. Given the transient nature of metabolite alterations, it is plausible that in 'Powderblue', modifications in sugar concentrations occurred earlier, potentially prior to 3 DAT. The increase in sucrose in 'Premier' suggests increased translocation into the fruit or sucrose re-synthesis from hexose sugars. The transcript abundance of sugar transporter gene *BIDIRECTIONAL SUGAR TRANSPORTER* was induced by ethephon (in PB), whereas *SPS* (*SUCROSE PHOSPHATE SYNTHASE*) and *SPP* (*SUCROSE PHOSPHATE PHOSPHATASE*) were not affected (data not presented). Whether increase in transcript abundance of the sugar transporter gene is associated with enhanced sucrose import into the fruit requires further study. It is not clear if resulting increase in sugars leads to higher glycolytic flux. Ethephon application increased, in both cultivars, the transcript abundance of *PK*, an enzyme involved in glycolysis. However, transcript abundance of genes coding for some other rate limiting enzymes like *HEXOKINASE* (*HK*), *FRUCTOKINASE* (*FK*), and *PHOSPHOFRUCTOKINASE* (*PFK*) were not different between treatments. These data support results from a previous study that indicated that

the role of ethylene in promoting blueberry softening, pectin degradation, and sucrose metabolism (increased expression of *SuSY*, *vINV,* and decreased the expression of *SPS* and *nINV*) in PH stages (Wang et al., 2020). In climacteric fruits, ethylene increases the soluble solids content in peach and kiwifruit (Ampa et al., 2016; Mariño-González et al., 2019), suggesting its positive role in stimulating sugar metabolism. In apple, pre-harvest application of ethephon increased starch degradation, and the content of glucose, fructose, sucrose, soluble sugars, and reducing sugars during PH storage (Sun et al., 2021). Further, the transcript abundance of multiple genes and enzyme activity associated with carbohydrate metabolism including *SPS*, *SuSY*, *vINV*, *nINV*, *cwINV*, and *AMYLASE*, were enhanced, up to 120 d after cold storage (Sun et al., 2021). In fig, expression of genes related to cell wall modification (*POLYGALACTURONASE*, *PECTATE LYASE*) and sugar accumulation increased in response to ethephon treatment (Cui et al., 2021). In addition, in non-climacteric fruits like grape and strawberry, ethylene treatment increased the sugar content by increasing the expression of sugar metabolism related genes like *SUGAR TRANSPORTER*, *SuSY*, and *cwINV* (Chervin et al., 2006; Villarreal et al., 2010; Wang et al., 2022). In the current study, transient alterations of metabolites during fruit ripening after ethephon and ACC application suggests accelerated ripening. The transient increases in sugars may be reflective of fruit sugar status since blueberry fruit is continuously dependent on sucrose import from the source. The transient nature of the influence of ethylene on sugar metabolism is also supported by the fact that after ethephon treatment, the initial increase in ethylene evolution is also transient and not sustained. This is not surprising since negative regulators of ethylene signaling are increased after ethephon treatments thereby fine-tuning ethylene responses (Wang et al., 2022).

During fruit development and ripening in blueberry, malate concentration is greater during the earlier developmental stages (green fruit), and decreases during ripening. This is associated with an increase in respiration and transcript abundance of *PEPCK* (Chapter 2). The application of both PGRs, ethephon and ACC, decreased malate at 3 DAT in 'Premier', a stage when increased sugar concentration was noted. At this time-point there was also an increase in CO_2 concentration in 'Premier'. At 5 DAT, only ethephon treatment resulted in decreased malate concentration in both cultivars. However, in 'Powderblue', ethephon-induced malate reduction did not lead to changes in respiration. Since fruit were collected only at 3 and 5 DAT and consisted of a pool fruit of different developmental changes, transient alterations in metabolite concentrations are likely to have been missed. Thus, the effect of ethylene on malate concentration and how it relates to blueberry fruit respiration warrants further study.

Ethephon treatment reduced malate concentration in kiwifruits during ripening (Ampa et al., 2016). In this study, ethylene induced an increase in the transcript abundance of *PEPCK* at 3 DAT in 'Premier' and displayed an increasing trend at 1 DAT in 'Powderblue'. Further, multiple transcripts of *PEPCK* showed a 1.6-to1.7-fold increase after ethephon treatment in 'Powderblue' fruit (data not presented; Wang and Nambeesan, *submitted*). Similar to sugar metabolism, the reduction in malate levels and the downregulation of genes associated with acid metabolism following ethephon treatment is indicative of accelerating ripening.

During fruit ripening, citrate concentrations were relatively low in rabbiteye blueberry and did not show a distinctive ripening-related pattern in either cultivar (Chapter 2). These findings are supportive of lack of changes in citrate concentration, and transcript abundance of *CS*, upon ethephon and ACC treatments in both cultivars. The response of ethylene on citrate

concentration in other fruits is not consistent, with apples displaying no effect upon 1-MCP application, and kiwifruit showing reduction upon ethylene treatment (Liu et al., 2016; Choi et al., 2022).

Quinate was the major acid accumulating during fruit development and ripening in blueberry, with its concentration decreasing during ripening (Chapter 2). In contrast, the concentration of shikimate increased during ripening in blueberry. These two acids serve as precursors for the formation of aromatic amino acids, anthocyanins, and other secondary metabolites. During fruit development and ripening, individual anthocyanin concentrations are initially detectable in mature green fruit (around 25% pink coloration; S6 stage) and display increased accumulation in ripe berries (S8 stage) (Chapter 2). The increase in anthocyanin concentration during the ripening is associated with increase in transcript abundance of *BIFUNCTIONAL 3-DEHYDROQUINATE DEHYDRATASE/SHIKIMATE DEHYDROGENASE* and anthocyanin biosynthesis related genes, as evidenced by their strong correlation with anthocyanin concentrations (Chapter 2). In this study, ethylene did not induce changes in quinate concentration, however only ethephon treatment increased shikimate concentration at 3 DAT in both cultivars and at 5 DAT in ‘Premier’. It is very likely that changes in shikimate were not as evident with ACC treatment since ACC accelerated ripening at a slower rate as compared to ethephon. Also changes in shikimate after PGR treatments were not dramatically altered which is likely due to the flux directed towards anthocyanin production. In fact, in this study, both ethephon and ACC treatments increased all/multiple anthocyanin compounds and affected the expression of genes linked to anthocyanin metabolism. These findings indicate that ethylene stimulates the expression of anthocyanin metabolism related genes, which is reflected in the

changes observed in anthocyanin concentration during fruit ripening. A stimulation of anthocyanin production after ethylene treatment has been reported in other fruits such as strawberry and plum fruit peel (Villarreal et al., 2009; Cheng et al., 2016).

Interestingly at 10 DAT, when ripe fruit were harvested, no changes in metabolites related to sugars, acids and anthocyanins were observed. These results suggest that ethephon stimulates sugar, acid and anthocyanin metabolism, thus accelerating the fruit development transition to ripening. This is supported by previous work that indicated that ethephon accelerates ripening initiation by downregulation of photosynthesis-related genes and cross talk with other hormones (Wang and Nambeesan, in submission).

Finally, we determined the effect of ethylene releasing PGRs on fruit quality attributes during storage. Postharvest application of ethylene increased fruit softening by enhancing protein degradation in blueberry (Wang et al., 2020). Contrary to expectations, when ethylene perception was blocked by 1-MCP, reduction in fruit firmness, but no effects on other fruit quality attributes was observed in rabbiteye blueberry (MacLean and NeSmith, 2011). In addition, pre-harvest application of ethephon did not affect fruit quality attributes in rabbiteye and low bush blueberry (Ismail, 1974; Wang et al., 2018). In the current study, ethephon and ACC did not display consistent effects on fruit compression, puncture, TA, TSS, and visual quality. The lack of changes in TSS and TA may be reflective of unaltered sugar and acid concentrations in ripe fruit harvested at 10 d after PGR applications. This study did not determine the effect of ethylene on cell wall modification enzymes. Hence it is not clear if ethylene induces transient changes in cell wall loosening enzymes and cell wall modifications. However, overall ripe fruit did not exhibit changes in texture suggesting that ethylene related

PGR treatments do not affect ripe fruit firmness. Interestingly either a significant decline or a trend toward slight decrease in fruit weight was evident especially after ethephon treatments (with the exception of 'Premier' in 2019). It is very likely that a decrease in fruit weight is associated with increased rate of ripening observed, especially with ethephon application. An accelerated developmental transition into ripening may limit fruit expansion related changes that occur prior to ripening.

Since both ethephon and ACC accelerated ripening with minimal changes in fruit quality parameters, these PGRs could be tested as potential ripening aids to concentrate ripening. Especially with the industry moving towards mechanical harvesting, ripening aids would allow for fruit to be picked at more uniform maturity thereby lowering fruit losses due to picking of overripe and under ripe fruit. Thus future studies focused on the use of ethephon and ACC after the 1st pick (after harvesting 20% ripe fruit) will need to be performed to determine the viability of using these PGRS as ripening aids.

Conclusion

This study highlights the beneficial effect of ethephon and ACC on accelerating the fruit ripening in southern highbush and rabbiteye blueberry cultivars, without affecting the PH fruit quality attributes. In addition, during ripening there is a transient alteration in sugars, acids, and anthocyanin metabolism which is supported by changes in the concentration of metabolites and biosynthesis related genes. Future studies should focus on lower concentrations of these PGRs and their effect on fruit ripening, metabolism and fruit quality.

References

Aiken MG, Scoggins HL, Latimer JG (2015) Substrate pH impacts efficacy of ethephon drenches on growth of herbaceous perennials. HortScience **50:** 1187-1191.

Alexander L, Grierson D (2002) Ethylene biosynthesis and action in tomato: a model for climacteric fruit ripening. Journal of experimental botany **53:** 2039-2055.

Ampa K, Ikeura H, Saito T, Okawa K, Ohara H, Kondo S (2016) Effects of pre-harvest application of ethephon or abscisic acid on 'Kohi'kiwifruit (Actinidia chinensis) ripening on the vine. Scientia horticulturae **209:** 255-260.

Ampa K, Saito T, Okawa K, Ohara H, Kondo S (2017) Effects of ethephon and abscisic acid application on ripening-related genes in 'Kohi'kiwifruit (Actinidia chinensis) on the vine. Horticultural Plant Journal **3:** 29-33.

Andrews J (1995) The climacteric respiration rise in attached and detached tomato fruit. Postharvest Biology and Technology **6:** 287-292.

Ayaz F, Kadioglu A, Bertoft E, Acar C, Turna I (2001) Effect of fruit maturation on sugar and organic acid composition in two blueberries (Vaccinium arctostaphylos and V. myrtillus) native to Turkey.

Ban T, Kugishima M, Ogata T, Shiozaki S, Horiuchi S, Ueda H (2007) Effect of ethephon (2-chloroethylphosphonic acid) on the fruit ripening characters of rabbiteye blueberry. Scientia Horticulturae **112:** 278-281.

Bapat VA, Trivedi PK, Ghosh A, Sane VA, Ganapathi TR, Nath P (2010) Ripening of fleshy fruit: molecular insight and the role of ethylene. Biotechnology advances **28:** 94-107.

Basra A (2000) Plant growth regulators in agriculture and horticulture: their role and commercial uses. CRC Press.

Beshir WF, Mbong V, Hertog ML, Geeraerd AH, Van den Ende W, Nicolaï BM (2017) Dynamic labeling reveals temporal changes in carbon re-allocation within the central metabolism of developing apple fruit. Frontiers in plant science **8:** 1785.

Bleecker AB, Kende H (2000) Ethylene: a gaseous signal molecule in plants. Annual review of cell and developmental biology **16:** 1-18.

Bouzayen M, Latché A, Nath P, Pech J-C (2010) Mechanism of fruit ripening. *In* Plant developmental biology-Biotechnological perspectives. Springer, pp 319-339.

Chen J, Mao L, Lu W, Ying T, Luo Z (2016) Transcriptome profiling of postharvest strawberry fruit in response to exogenous auxin and abscisic acid. Planta **243:** 183-197.

Cheng Y, Liu L, Yuan C, Guan J (2016) Molecular characterization of ethylene-regulated anthocyanin biosynthesis in plums during fruit ripening. Plant Molecular Biology Reporter **34:** 777-785.

Chervin C, Terrier N, Ageorges A, Ribes F, Kuapunyakoon T (2006) Influence of ethylene on sucrose accumulation in grape berry. American Journal of Enology and Viticulture **57:** 511-513.

Choi HR, Baek MW, Cheol LH, Jeong CS, Tilahun S (2022) Changes in metabolites and antioxidant activities of green ‘Hayward’and gold ‘Haegeum’kiwifruits during ripening with ethylene treatment. Food Chemistry **384:** 132490.

Cui Y, Zhai Y, Flaishman M, Li J, Chen S, Zheng C, Ma H (2021) Ethephon induces coordinated ripening acceleration and divergent coloration responses in fig (Ficus carica L.) flowers and receptacles. Plant Molecular Biology **105:** 347-364.

Dekazos E (1979) Maturity and quality responses of'Tifblue'rabbiteye blueberries to SADH and ethephon [Growth regulators]. *In* Proceedings of the Florida State Horticultural Society.

Downey MO, Rochfort S (2008) Simultaneous separation by reversed-phase high-performance liquid chromatography and mass spectral identification of anthocyanins and flavonols in Shiraz grape skin. Journal of Chromatography A **1201:** 43-47.

Eck P (1970) Influence of Ethrel Upon Highbush Blueberry Fruit Ripening. HortScience **5:** 23-25.

El-Kereamy A, Chervin C, Roustan JP, Cheynier V, Souquet JM, Moutounet M, Raynal J, Ford C, Latché A, Pech JC (2003) Exogenous ethylene stimulates the long-term expression of genes related to anthocyanin biosynthesis in grape berries. Physiologia plantarum **119:** 175-182.

Fan D, Wang W, Hao Q, Jia W (2022) Do Non-climacteric Fruits Share a Common Ripening Mechanism of Hormonal Regulation? Frontiers in Plant Science **13:** 923484.

Giovannoni JJ (2004) Genetic regulation of fruit development and ripening. The plant cell **16:** S170-S180.

Hancock J, Callow P, Serçe S, Hanson E, Beaudry R (2008) Effect of cultivar, controlled atmosphere storage, and fruit ripeness on the long-term storage of highbush blueberries. HortTechnology **18:** 199-205.

Howard LR, Clark JR, Brownmiller C (2003) Antioxidant capacity and phenolic content in blueberries as affected by genotype and growing season. Journal of the Science of Food and Agriculture **83:** 1238-1247.

Ismail AA (1974) Preharvest Application of Ethephon and SADH on Ripening and Quality of Lowbush Blueberry Fruit. HortScience **9:** 205-206.

Kumar R, Khurana A, Sharma AK (2014) Role of plant hormones and their interplay in development and ripening of fleshy fruits. Journal of experimental botany **65:** 4561-4575.

Li L, Guo M, Wang X, Zhang X, Liu T (2017) Effects and Mechanism of 1-Methylcyclopropene and Ethephon on Softening in Ailsa Craig Tomato Fruit. Journal of Food Processing and Preservation **41:** e12883.

Li S, Chen K, Grierson D (2021) Molecular and hormonal mechanisms regulating fleshy fruit ripening. Cells **10:** 1136.

Liu M, Pirrello J, Chervin C, Roustan J-P, Bouzayen M (2015) Ethylene control of fruit ripening: revisiting the complex network of transcriptional regulation. Plant physiology **169:** 2380-2390.

Liu R, Wang Y, Qin G, Tian S (2016) Molecular basis of 1-methylcyclopropene regulating organic acid metabolism in apple fruit during storage. Postharvest Biology and Technology **117:** 57-63.

Lougheed E, Franklin E (1972) Effects of temperature on ethylene evolution from ethephon. Canadian Journal of Plant Science **52:** 769-773.

MacLean DD, NeSmith DS (2011) Rabbiteye blueberry postharvest fruit quality and stimulation of ethylene production by 1-methylcyclopropene. HortScience **46:** 1278-1281

Malladi A, Vashisth T, Johnson LK (2012) Ethephon and methyl jasmonate affect fruit detachment in rabbiteye and southern highbush blueberry. HortScience **47:** 1745-1749.

Malladi A, Vashisth T, NeSmith S (2013) Development and evaluation of a portable, handheld mechanical shaker to study fruit detachment in blueberry. HortScience **48:** 394-397.

Mariño-González LA, BUITRAGO C, BALAGUERA-LÓPEZ HE, Martínez-Quintero E (2019) Effect of 1-methylcyclopropene and ethylene on the physiology of peach fruits (Prunus persica L.) cv. Dorado during storage. Revista Colombiana de Ciencias Hortícolas **13:** 46-54.

Naczk M, Grant S, Zadernowski R, Barre E (2006) Protein precipitating capacity of phenolics of wild blueberry leaves and fruits. Food Chemistry **96:** 640-647.

Osorio S, Scossa F, Fernie AR (2013) Molecular regulation of fruit ripening. Frontiers in plant science **4:** 198.

Paul V, Pandey R, Srivastava GC (2012) The fading distinctions between classical patterns of ripening in climacteric and non-climacteric fruit and the ubiquity of ethylene—an overview. Journal of food science and technology **49:** 1-21.

Pilati S, Bagagli G, Sonego P, Moretto M, Brazzale D, Castorina G, Simoni L, Tonelli C, Guella G, Engelen K (2017) Abscisic acid is a major regulator of grape berry ripening onset: new insights into ABA signaling network. Frontiers in plant science **8:** 1093.

Protzman E (2021) Blueberries around the globe–past, present, and future. US Department of Agriculture International Agricultural Trade Report**:** 2021-2010.

Quinet M, Angosto T, Yuste-Lisbona FJ, Blanchard-Gros R, Bigot S, Martinez J-P, Lutts S (2019) Tomato fruit development and metabolism. Frontiers in plant science**:** 1554

Retamales JB, Hancock JF (2018) Blueberries, Vol 27. Cabi.

Rieu I, Powers SJ (2009) Real-time quantitative RT-PCR: design, calculations, and statistics. The Plant Cell **21:** 1031-1033.

Rudell D, Mattinson D, Fellman J, Mattheis J (2000) The Progression of Ethylene Production and Respiration in the Tissues of RipeningFuji'Apple Fruit. HortScience **35:** 1300-1303.

Ruijter J, Ramakers C, Hoogaars W, Karlen Y, Bakker O, Van den Hoff M, Moorman A (2009) Amplification efficiency: linking baseline and bias in the analysis of quantitative PCR data. Nucleic acids research **37:** e45-e45.

Seymour GB, Østergaard L, Chapman NH, Knapp S, Martin C (2013) Fruit development and ripening. Annual review of plant biology **64:** 219-241.

Silva S, Costa EM, Coelho MC, Morais RM, Pintado ME (2017) Variation of anthocyanins and other major phenolic compounds throughout the ripening of four Portuguese blueberry (Vaccinium corymbosum L) cultivars. Natural product research **31:** 93-98

Strik B (2004) Blueberry production and research trends in North America. *In* VIII International Symposium on Vaccinium Culture 715, pp 173-184.

Suehiro Y, Mochida K, Tsuma M, Yasuda Y, Itamura H, Esumi T (2019) Effects of abscisic acid/ethephon treatments on berry development and maturation in the yellow-green skinned ‘Shine Muscat’grape. The Horticulture Journal **88:** 189-201.

Sun Y, Shi Z, Jiang Y, Zhang X, Li X, Li F (2021) Effects of preharvest regulation of ethylene on carbohydrate metabolism of apple (Malus domestica Borkh cv. Starkrimson) fruit at harvest and during storage. Scientia Horticulturae **276:** 109748.

Tucker G, Yin X, Zhang A, Wang M, Zhu Q, Liu X, Xie X, Chen K, Grierson D (2017) Ethylene and fruit softening. Food Quality and Safety **1:** 253-267.

US-EPA (2010) Ethrel brand ethephon plant regulator. https://www3.epa.gov/pesticides/chem_search/ppls/000264-00267-20100629.pdf. *In*, United States Enviromental Protection Agence, Washington, D.C.

Vashisth T, Johnson LK, Malladi A (2011) An efficient RNA isolation procedure and identification of reference genes for normalization of gene expression in blueberry. Plant cell reports **30:** 2167-2176.

Villarreal NM, Bustamante CA, Civello PM, Martínez GA (2010) Effect of ethylene and 1-MCP treatments on strawberry fruit ripening. Journal of the Science of Food and Agriculture **90:** 683-689.

Villarreal NM, Martínez GA, Civello PM (2009) Influence of plant growth regulators on polygalacturonase expression in strawberry fruit. Plant Science **176:** 749-757.

Wang P, Yu A, Ji X, Mu Q, Haider MS, Wei R, Leng X, Fang J (2022) Transcriptome and metabolite integrated analysis reveals that exogenous ethylene controls berry ripening processes in grapevine. Food Research International **155:** 111084.

Wang S, Zhou Q, Zhou X, Zhang F, Ji S (2020) Ethylene plays an important role in the softening and sucrose metabolism of blueberries postharvest. Food chemistry **310:** 125965.

Wang Y-W, Acharya TP, Malladi A, Tsai H-J, NeSmith DS, Doyle JW, Nambeesan SU (2022) Atypical climacteric and functional ethylene metabolism and signaling during fruit ripening in blueberry (Vaccinium sp.). Frontiers in plant science **13.**

Wang Y-W, Malladi A, Doyle JW, Scherm H, Nambeesan SU (2018) The Effect of Ethephon, Abscisic Acid, and Methyl Jasmonate on Fruit Ripening in Rabbiteye Blueberry (Vaccinium virgatum). Horticulturae **4:** 24.

Wang Y-W, Nambeesan SU (2022) Full-length fruit transcriptomes of southern highbush (Vaccinium sp.) and rabbiteye (V. virgatum Ait.) blueberry. BMC genomics **23:** 1-15.

Wang YW, Acharya TP, Malladi A, Tsai H-J, NeSmith DS, Doyle JW, Nambeesan SU (2022) Atypical climacteric and functional ethylene metabolism and signaling during fruit ripening in blueberry (Vaccinium sp.). Frontiers in Plant Science **13:** 932642.

Yokotani N, Nakano R, Imanishi S, Nagata M, Inaba A, Kubo Y (2009) Ripening-associated ethylene biosynthesis in tomato fruit is autocatalytically and developmentally regulated. Journal of experimental botany **60:** 3433-3442.

Zhang P, Zhou Z (2019) Postharvest ethephon degreening improves fruit color, flavor quality and increases antioxidant capacity in 'Eureka'lemon (Citrus limon (L.) Burm. f.). Scientia Horticulturae **248:** 70-80.

Zhou Q, Ma C, Cheng S, Wei B, Liu X, Ji S (2014) Changes in antioxidative metabolism accompanying pitting development in stored blueberry fruit. Postharvest biology and technology **88:** 88-95.

Zifkin M, Jin A, Ozga JA, Zaharia LI, Schernthaner JP, Gesell A, Abrams SR, Kennedy JA, Constabel CP (2012) Gene expression and metabolite profiling of developing highbush blueberry fruit indicates transcriptional regulation of flavonoid metabolism and activation of abscisic acid metabolism. Plant Physiology **158:** 200-224.

Figures and Tables

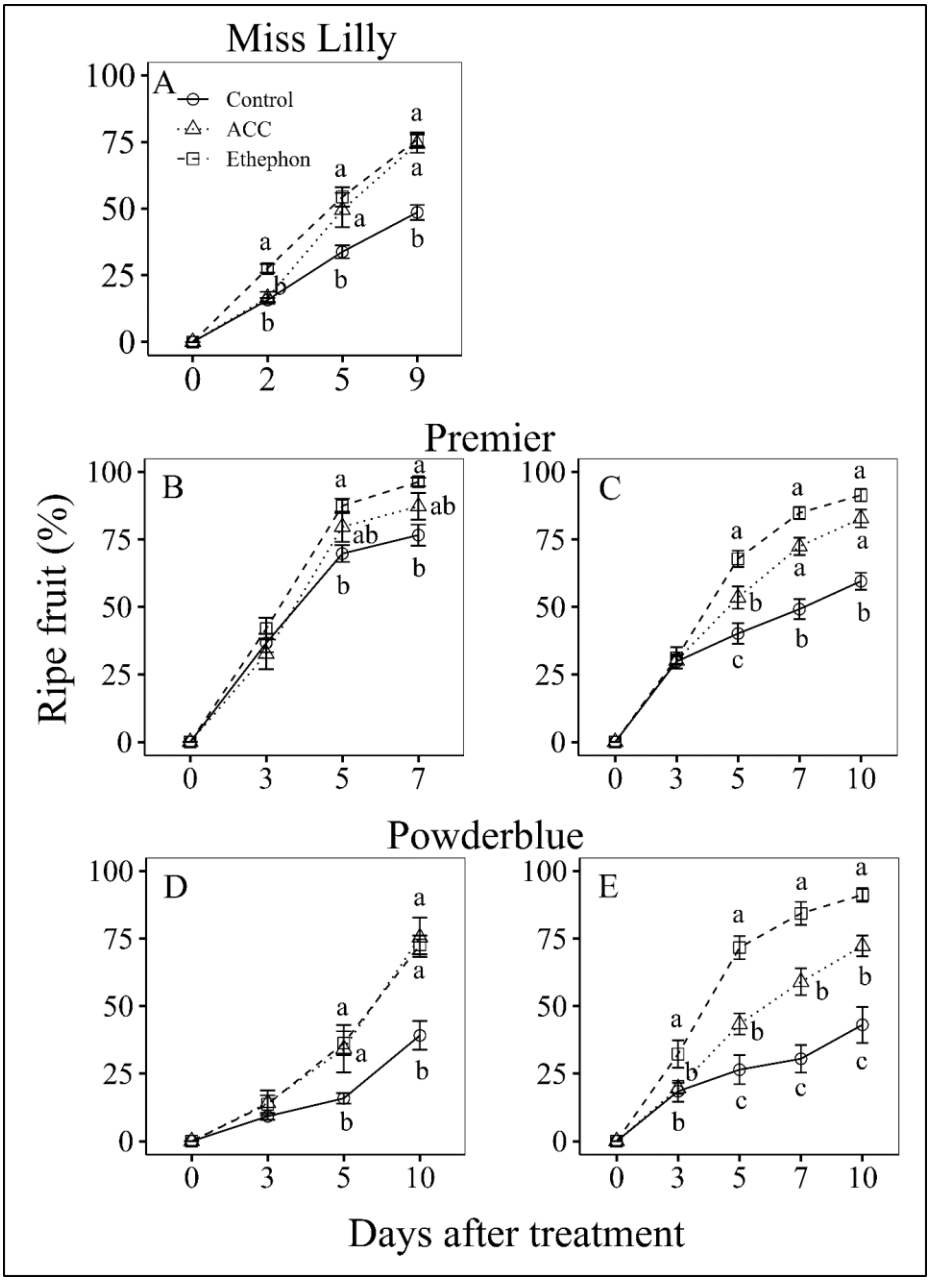

Figure 3.1: Percentage of ripe fruit after application of ethephon, ACC, and control. A: Miss Lilly 2019; B, C: Premier 2019, 2020; D, E: Powderblue 2019,2020. Different letters above symbols indicate that the means are significantly different between the treatment (within a day after treatment) according to ANOVA and Fischer's LSD (α=0.05).

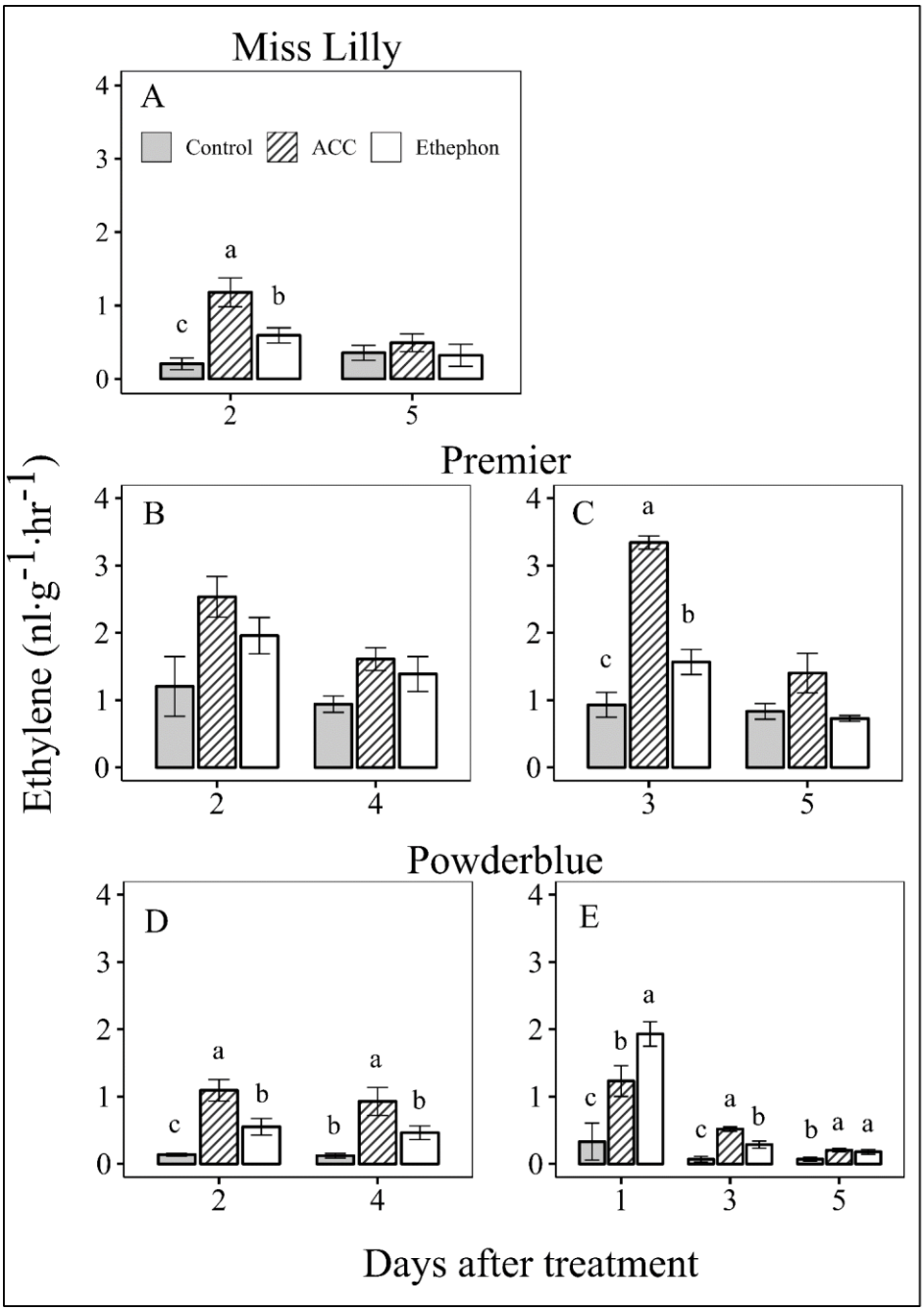

Figure 3.2: Ethylene production in fruits after application of ethephon, ACC, and control. A: Miss Lilly 2019; B, C: Premier 2019, 2020; D, E: Powderblue 2019,2020. Different letters above symbols indicate that the means are significantly different between the treatment (within a day after treatment) according to ANOVA and Fischer's LSD (α=0.05).

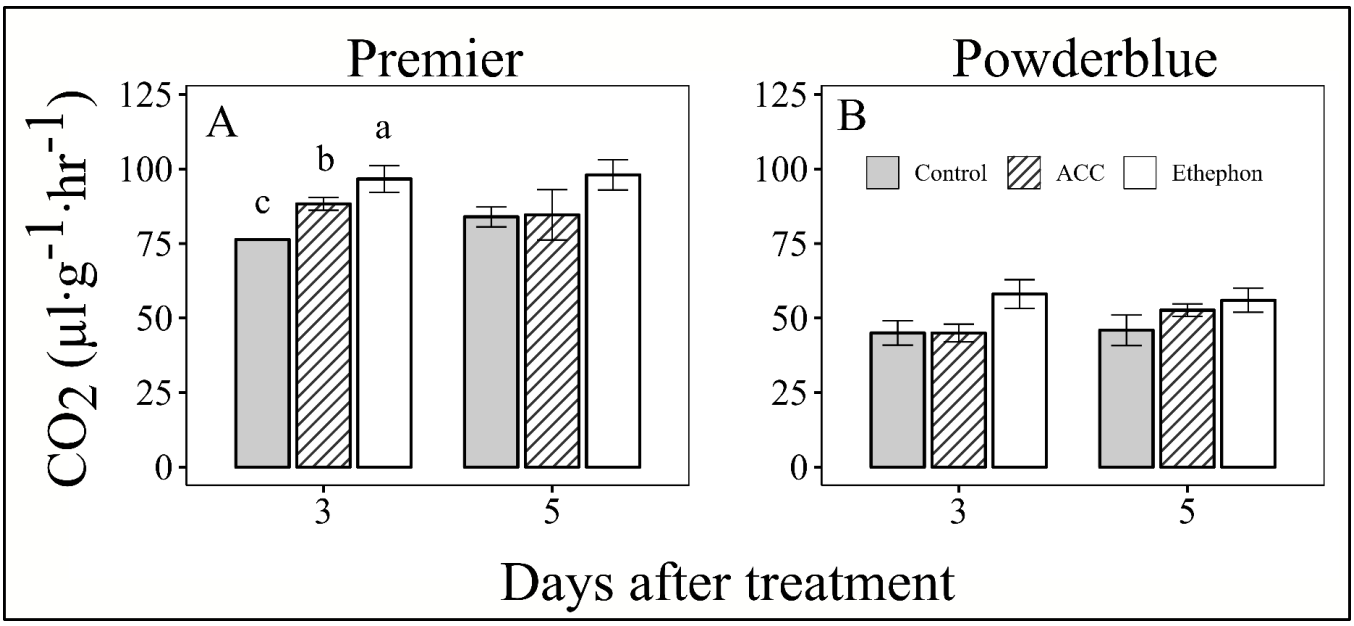

Figure 3.3: Carbondioxide production in fruits after application of ethephon, ACC, and control. A: A: Premier 2020; B: Powderblue 2020. Different letters above symbols indicate that the means are significantly different between the treatment (within a day after treatment) according to ANOVA and Fischer's LSD (α=0.05).

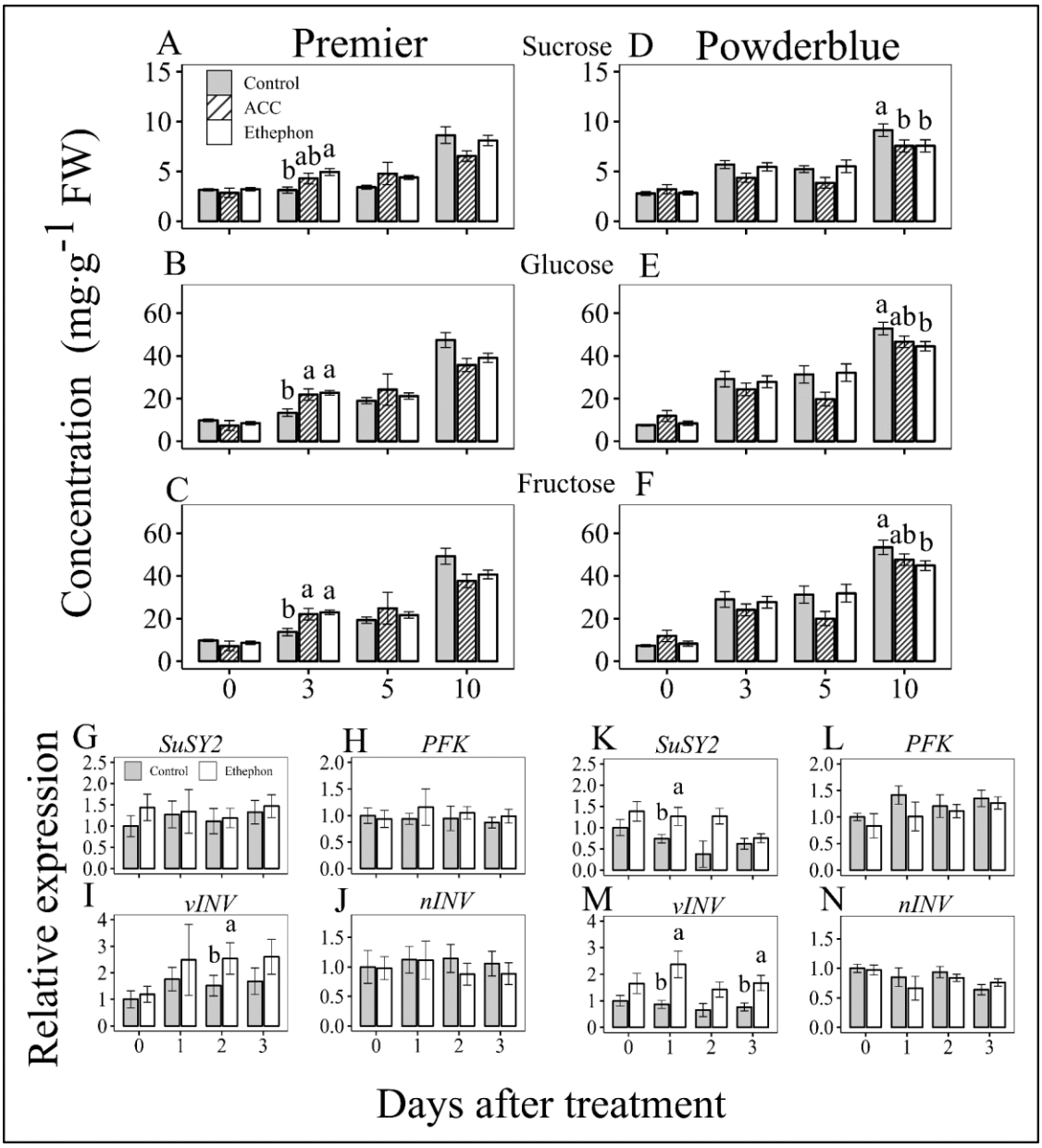

Figure 3.4: Concentration of sucrose (A, D), glucose (B, E), fructose (C, F), and transcript abundance of their metabolism related genes. Sugars measured from ethephon, ACC, and control. Transcript abundance measured from the ethephon and control. A, B, C, G, H, I, J: Premier 2020; D, E, F, K, L, M, N: Powderblue 2020. *SuSY2=SUCROSE SYNTHASE 2*, *PFK=PHOSPHORFUCTOKINASE*, *vINV= VACUOLAR INVERTASE*, *nINV= NEUTRAL INVERTASE.* Different letters above symbols indicate that the means are significantly different between the treatment (within a day after treatment) according to ANOVA and Fischer's LSD (α=0.05).

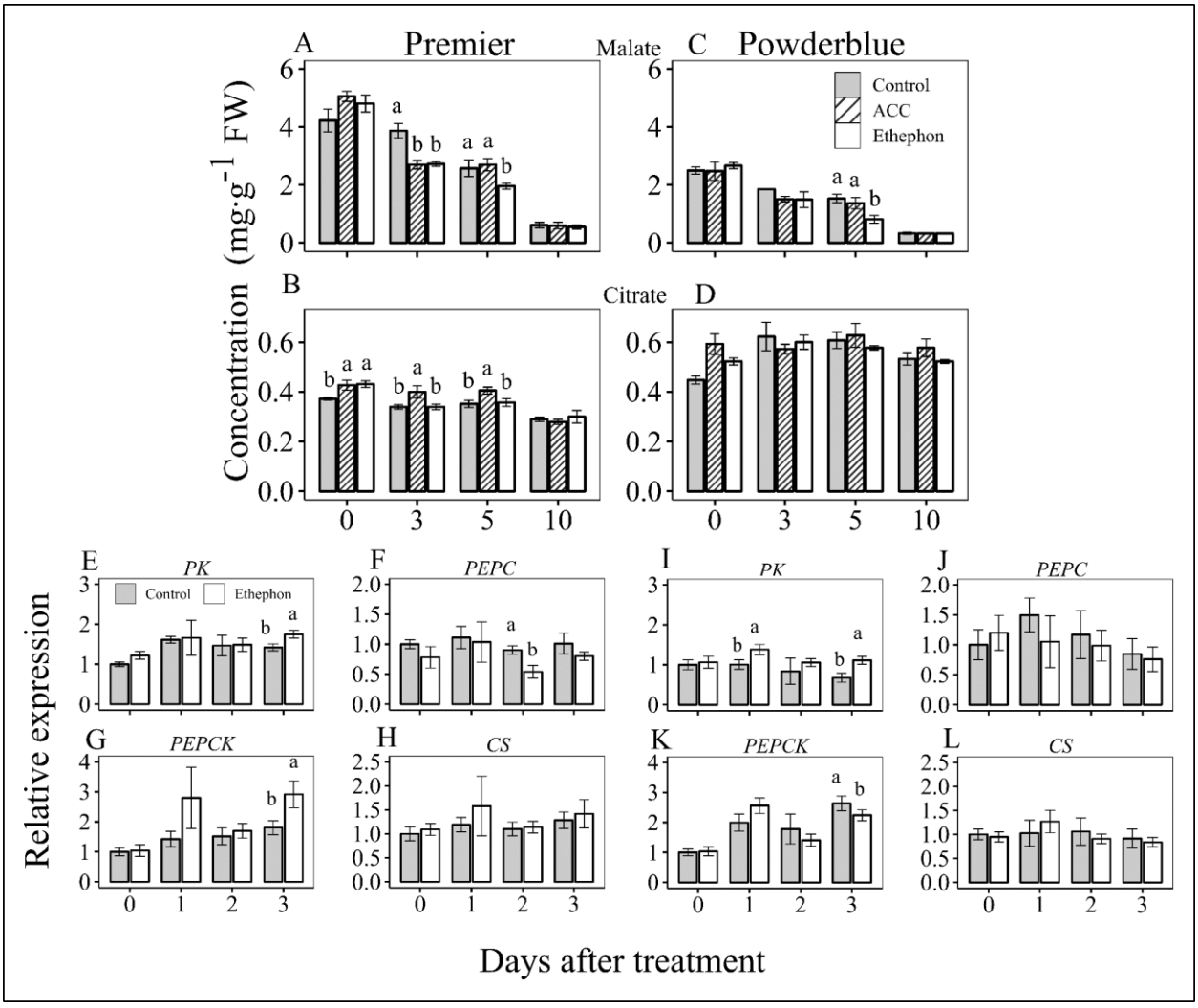

Figure 3.5: Concentration of malic acid (A, C), citric acid (B, D) and transcript abundance of their metabolism related genes. Acids measured from ethephon, ACC, and control. Transcript abundance measured from the ethephon and control. A, B, E, F, G, H: Premier 2020; C, D, I, J, K, L: Powderblue 2020. *PK=PYRUVATE KINASE*, *PEPC=PHOSPHOENOYL PYRUVATE CARBOXYLASE*, *PEPECK=PHOSPHOENOYL PYRUVATE CARBOXYKINASE*, *CS= CITRATE SYNTHASE*. Different letters above symbols indicate that the means are significantly different between the treatment (within a day after treatment) according to ANOVA and Fischer's LSD (α=0.05).

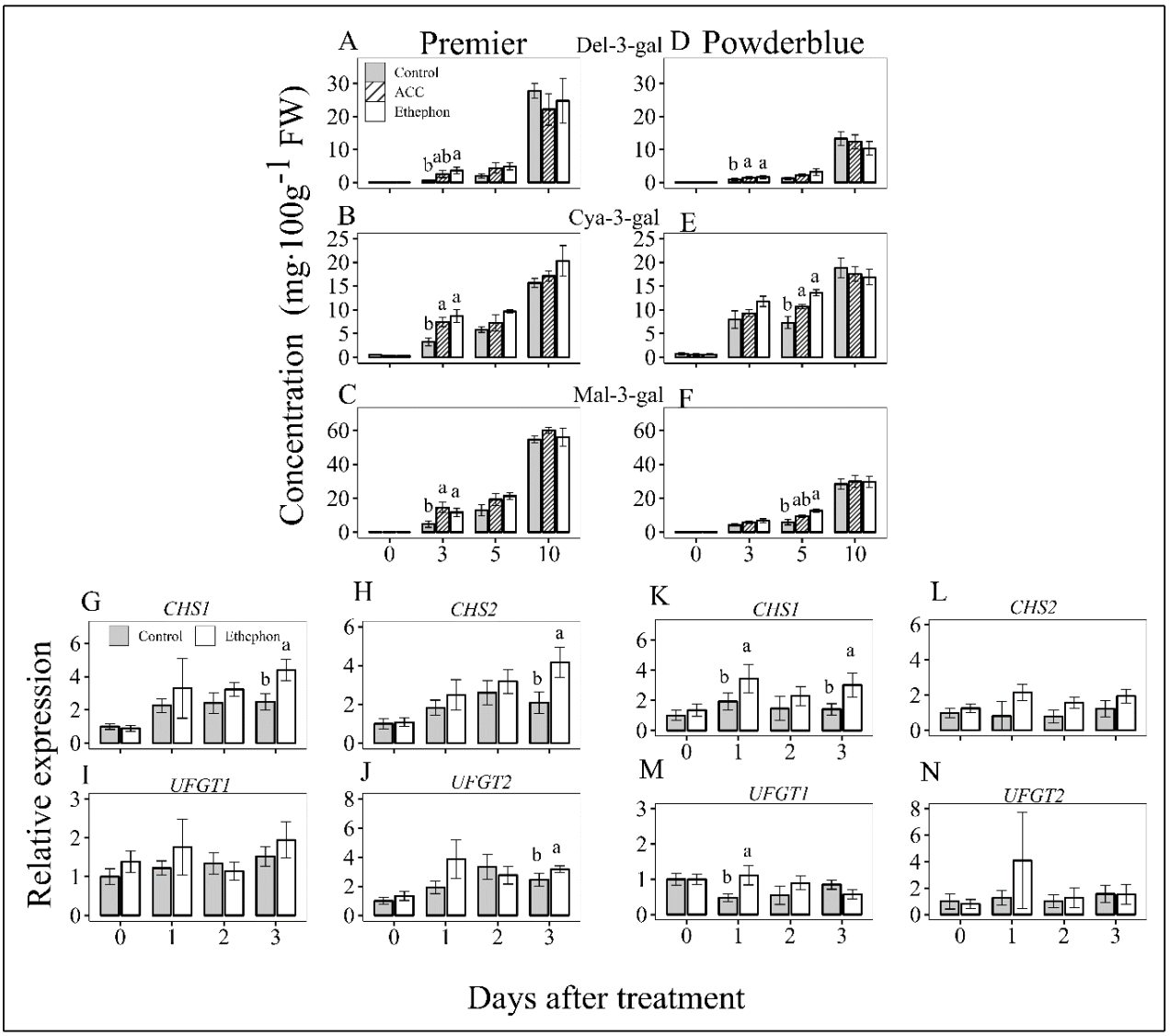

Figure 3.6: Concentration of Delphidin 3-galactoside (A, D), cyaniding 3-galactoside (B, E), malvidin 3-galactoside (C, F), and transcript abundance of their metabolism related genes. Anthocyanin measured from ethephon, ACC, and control. Transcript abundance measured from the ethephon and control. A, B, C, G, H, I, J: Premier 2020; D, E, F, K, L, M, N: Powderblue 2020. *CHS1=CHALCONE SYNTHASE 1*, *CHS2=CHALCONE SYNTHASE 2*, *UFGT1= ANTHOCYANIDIN 3-O-GLUCOSYLTRANSFERASE* 1, *UFGT2= ANTHOCYANIDIN 3-O-GLUCOSYLTRANSFERASE 2.* Different letters above symbols indicate that the means are significantly different between the treatment (within a day after treatment) according to ANOVA and Fischer's LSD (α=0.05).

Table 3.1: Effect of pre-harvest treatment of Latron (Control), ACC, Ethephon on compression, puncture and fruit weight in blueberry. 2019. 2020.

	Compression (kg)			Puncture (kg)			Fruit weight (g)		
Cultivar/Treatment	PH3	PH10	PH21	PH3	PH10	PH21	PH3	PH10	PH21
Miss Lilly 2019									
Control	0.263	0.256	0.228	0.168	0.169	0.162	1.31	1.34	1.32
Ethephon	0.273	0.279	0.245	0.177	0.175	0.178	1.20	1.21	1.24
ACC	0.432	0.265	0.233	0.163	0.167	0.154	1.18	1.22	1.13
P-value	ns	ns	ns	ns	ns	ns	ns	ns	ns
Premier 2019									
Control	0.213	0.210	0.180	0.136	0.139	0.128	1.19	1.22	1.19
Ethephon	0.214	0.185	0.181	0.129	0.124	0.118	1.36	1.17	1.22
ACC	0.192	0.174	0.161	0.126	0.131	0.115	1.31	1.31	1.16
P-value	ns	ns	ns	ns	ns	ns	ns	ns	ns
Powderblue 2019									
Control	0.209	0.194	0.161	0.153	0.144 b	0.137 b	1.16 a	1.21 a	1.19 a
Ethephon	0.213	0.199	0.190	0.162	0.156 a	0.160 a	0.99 b	1.08 b	0.99 b
ACC	0.218	0.215	0.189	0.163	0.156 a	0.157 a	0.99 b	0.94 c	0.96 b
P-value	ns	ns	ns	ns	ns	0.020	0.005	0.0004	0.0043
Premier 2020									
Control	0.24	0.25	0.20	0.19	0.22	0.21	1.87 a	1.66 a	1.74 a
Ethephon	0.26	0.27	0.25	0.22	0.24	0.22	1.41 b	1.33 b	1.31 b
ACC	0.24	0.25	0.22	0.19	0.19	0.20	1.74 a	1.63 a	1.63 a
P-value	ns	ns	ns	ns	ns	ns	0.0003	0.0496	0.008
Powderblue 2020									
Control	0.23	0.21	0.21 b	0.24 c	0.24	0.25	1.02 a	0.97	1.00
Ethephon	0.24	0.23	0.25 a	0.28 a	0.28	0.28	0.90 b	0.80	0.84
ACC	0.22	0.21	0.22 b	0.26 b	0.27	0.27	0.94 ab	0.85	0.90
P-value	ns	ns	0.0221	0.0050	ns	ns	0.0469	ns	ns

Means followed by the different letter within a column for a given time-point after storage within the cultivars are significantly different, according to ANOVA and Fischer's LSD (α=0.05).

Table 3.2: Effect of pre-harvest treatment of Latron (Control), ACC, Ethephon on titratable acidity (TA), total soluble solid (TSS) content and defect (%) in blueberry. 2019. 2020.

	TA (%)			TSS (%)			Defect (%)		
Cultivar/Treatment	PH3	PH10	PH21	PH3	PH10	PH21	PH3	PH10	PH21
Miss Lilly 2019									
Control	0.522	0.424	0.359	11.15	11.65	11.78	3.75	10.00	20.00
Ethephon	0.530	0.469	0.327	10.88	11.88	11.25	2.50	6.25	17.50
ACC	0.526	0.448	0.348	11.35	11.88	11.95	5.00	10.00	31.25
P-value	ns	ns	ns	ns	ns	ns	ns	ns	ns
Premier 2019									
Control	0.403	0.410 a	0.338	15.30 a	14.68 a	14.58	1.25	8.75	21.25
Ethephon	0.416	0.356 b	0.308	14.63 ab	14.35 a	14.38	1.25	6.25	13.75
ACC	0.385	0.346 b	0.317	13.38 b	13.15 b	13.05	2.50	11.25	20.20
P-value	ns	0.0325	ns	0.0195	0.0005	ns	ns	ns	ns
Powderblue 2019									
Control	0.433 b	0.426 b	0.421	16.65 a	16.55 a	15.95	1.25	0.00	6.25
Ethephon	0.520 a	0.444 b	0.468	14.35 b	14.08 b	14.15	1.25	0.00	6.25
ACC	0.513 a	0.501 a	0.493	14.75 b	14.33 b	14.45	2.50	1.25	3.75
P-value	0.0241	0.0258	ns	0.0023	0.00402	ns	ns	ns	ns
Premier 2020									
Control	0.48	0.43	0.35	13.48	12.70	12.30	5.00	6.25	20.00
Ethephon	0.51	0.47	0.39	12.28	12.15	11.88	3.75	7.50	13.75
ACC	0.48	0.40	0.34	12.95	12.63	12.15	3.75	13.75	18.75
P-value	ns	ns	ns	ns	ns	ns	ns	ns	ns
Powderblue 2020									
Control	0.51	0.49	0.48	17.18 a	16.25	16.73	0.00	3.75	12.50 a
Ethephon	0.58	0.59	0.55	15.75 b	15.10	14.95	1.25	0.00	3.75 b
ACC	0.55	0.53	0.53	15.15 b	15.93	15.05	2.50	1.25	8.75 a
P-value	ns	ns	ns	0.0054	ns	ns	ns	ns	0.012

Means followed by the different letter within a column for a given time-point after storage within the cultivars are significantly different, according to ANOVA and Fischer's LSD (α=0.05).

Appendix A: Supplementary figures

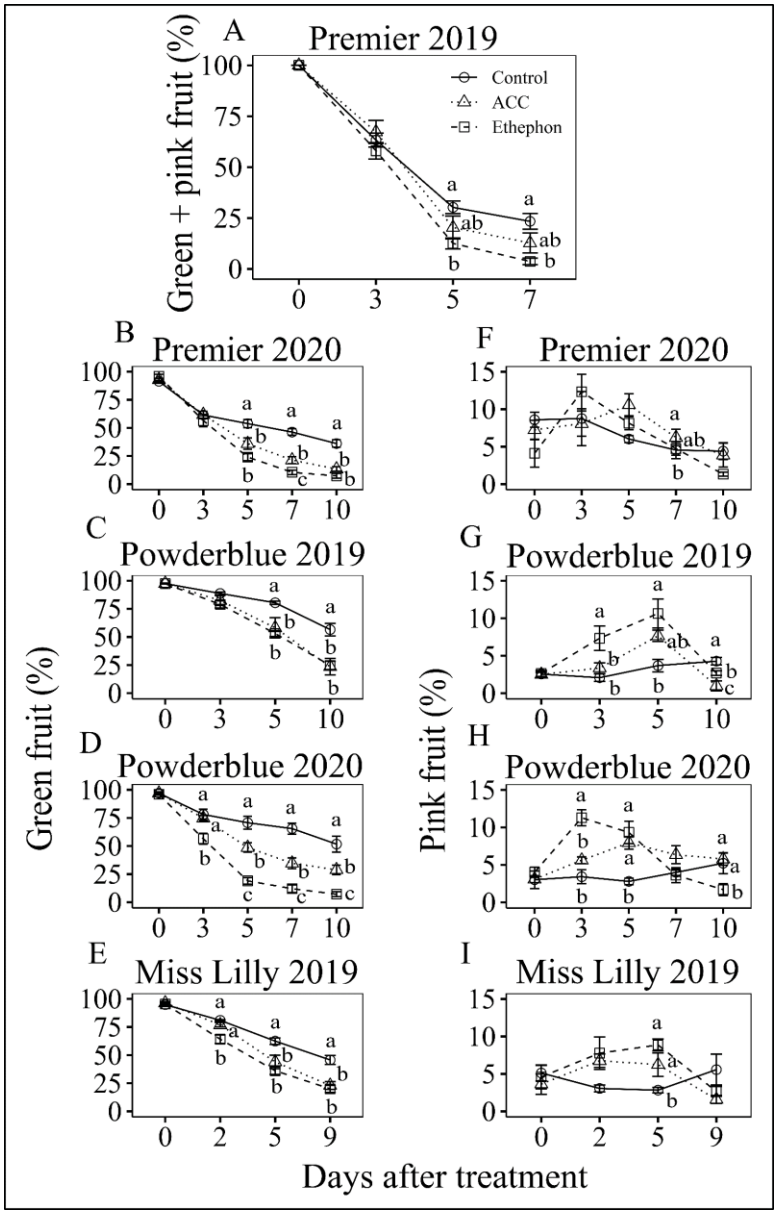

Figure 3. S1: Percentage of Unripe fruit (green and pink together, A), green (B, C, D, E) and pink (F, G, H, I) fruit after application of ethephon, ACC, and control. A=Premier 2019, B, F=Premier 2020, C, G=Powderblue 2019, D, H=Powderblue 2020, and E, I=Miss Lilly 2019. Different letters above symbols indicate that the means are significantly different between the treatment (within a day after treatment) according to ANOVA and Fischer's LSD (α=0.05).

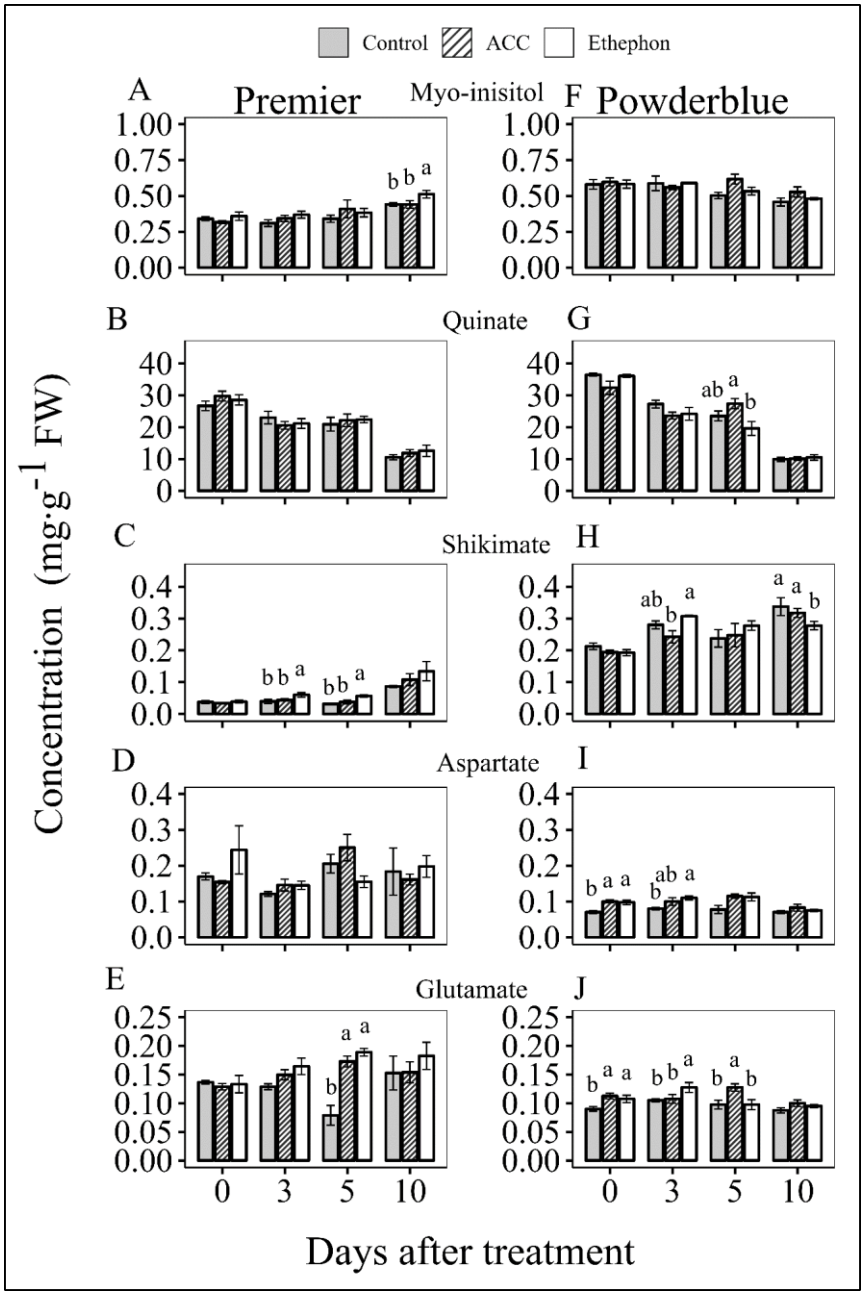

Figure 3. S2: Concentration of myo-inisitol (A, C), quinate (B, D), shikimate (C, H), aspartate (D, I), and glutamate (E, J) after application of ethephon, ACC, and control. A, B, C, D, E: Premier 2020; F, G, H, I, J: Powderblue 2020. Different letters above symbols indicate that the means are significantly different between the treatment (within a day after treatment) according to ANOVA and Fischer's LSD (α=0.05).

Table 3. S1: Ethylene releasing plant growth regulators (PGRs) application, sampling time for the rate of ripening, ethylene production, fruit harvest date, and postharvest measurement time.

	2019			2020	
Activities	Miss Lilly	Premier	Powderblue	Premier	Powderblue
Ethylene releasing					
Treatment application	1-May	14-Jun	21-Jun	7-Jun	26-Jun
Rate of ripening (DAT)	0,2,5,9	0,3,5,7	0,3,5,10	0,3,5,7,10	0,3,5,7,10
Ethylene measurement (DAT)	2,5	2,4	2,4	3,5	1,3,5
Fruit harvest for PH analysis (DAT)	9	7	10	10	10
Metabolite measurement (DAT)				0,3,5,10	0,3,5,10
Carbon dioxide measurement (DAT)					
PH analyses (PH)	3, 10,21	3, 10,21	3, 10,21	3, 10,21	3, 10,21

DAT: days after treatment application, PH: Postharvest time after fruit harvest

Table 3. S2: List of blueberry genes and primer sequences used for the quantitative PCR analyses

Gene	Accession number	Primer orientation	Primer sequences (5' to 3')
SuSY2	PB.576/2567/12940	Forward	5'- TCA GCG ATG GTC CCT TTG GC -3'
		Reverse	5'- ACA CCA GGC CTT GGA CGA AC -3'
vINV	PB.10450/10199/14249/5938	Forward	5'- TGC TAT GTT GGC TTG GCA GAG G -3'
		Reverse	5'- GGT GGT ACC ACC CCA AGT GAT AC -3'
nINV	PB.8898/1251/9014	Forward	5'- CTT CAT GGC TTT GAG ATG CGC GT -3'
		Reverse	5'- GTT CTA CAA ACT CCT TCC CCT CAG CA -3'
AGPase	PB.13245/14754/3497/4667	Forward	5'- CTC CCC TTA AGG ACA CTA GTC CTG C -3'
		Reverse	5'- GAA CTT TGG CAG CAT CCT CAG GG -3'
PFK	PB.7197/968	Forward	5'- GGA GGG GAT GGA ACT CAA AAA GGA G -3'
		Reverse	5'- AGC AAC TAC AAC TTT GAG GCC ACG -3'
PEPC	PB.4955/5134	Forward	5'- CAC ACC GAC GTG ATG GAT GCT -3'
		Reverse	5'- GGC GTT CTT CAG ACC ATT CTC GAT -3'
PEPCK	PB.14025/14026/12415/5724/1624	Forward	5'- GCA CTG CTG GAG TGA GAA TGG C -3'
		Reverse	5'- TCA GGC TCT TTC TCG CCA GAC AA -3'
PK	PB.11411/12220	Forward	5'- GTG GGA ATC TTG AAG GAA CTG CCC -3'
		Reverse	5'- CAA GCA TTG GCA CGC TTC GG -3'
CS	PB.14402/2236	Forward	5'- AGG TGT TTC GGC GCT TTC CAA -3'
		Reverse	5'- GCG CTC CTG TTG TTC GGG AA -3'
CHS1	PB.103	Forward	5'-TTG GGC AAA GAG GCT GCT GTG-3'
		Reverse	5'-CGG CAT GTC GAC TCC CGA-3'
CHS2	PB.6264	Forward	5'-TCA CTT GGT CTT CTG CAC CAC CAG-3'
		Reverse	5'-CCC GCG GAA AGT GAC AGC A-3'
UFGT1	PB.4659	Forward	5'-CCT AAT AAT GAAA AGG CCA AGG CCA-3'
		Reverse	5'-TTG GAT CTC CGC CGC TGC A-3'
UFGT2	PB.3506	Forward	5'-CAG CTA AGG TGT TGC CTT CTA GGG TAC-3'
		Reverse	5'-GTA GAT CGG CGG GAC CTT ATC GTC AC-3'

Table 3. S3: Concentration of anthocyanin measured from ethephon, ACC, and control treated fruits in 'Premier'.

Premier							
Treatment	**Concentration (mean ±SE) (mg/100 g FW)**						
	Del-3-gal	**Del 3-glu**	**Cya 3-gal**	**Del 3-ara**	**Cya 3-glu**	**Pet 3-gal/Cay 3-ara**	**Pet 3-glu**
0 day	***P*=0.422**	***P*=NA**	***P*=0.358**	***P*=NA**	***P*=NA**	***P*=0.629**	***P*=NA**
Control	0.00	0.00	0.53	0.00	0.0	0.23	0.00
ACC	0.00	0.00	0.28	0.00	0.0	0.12	0.00
Ethephon	0.03	0.00	0.28	0.00	0.0	0.17	0.00
3 day	***P*=0.048**	***P*=NA**	***P*=0.005**	***P*=0.210**	***P<0.0001***	***P*=0.012**	***P*=0.071**
Control	0.53 b	0.00	3.22 b	0.07	0.09 b	2.77 b	0.00
ACC	2.57 ab	0.00	7.46 a	0.72	0.34 a	8.23 a	0.04
Ethephon	3.63 a	0.00	8.69 a	1.03	0.34 a	9.44 a	0.04
5 day	***P*=0.263**	***P*=0.224**	***P*=0.102**	***P*=0.428**	***P*=0.049**	***P*=0.162**	***P*=0.082**
Control	1.93	0.00	5.84	0.57	0.18 b	6.35	0.01
ACC	4.36	0.00	7.29	1.33	0.23 ab	9.59	0.04
Ethephon	4.90	0.03	9.67	1.55	0.44 a	11.80	0.05
10 day	***P*=0.543**	***P*=0.998**	***P*=0.258**	***P*=0.381**	***P*=0.816**	***P*=0.601**	***P*=0.589**
Control	27.80	0.43	15.67	10.94	0.68	28.75	0.59
ACC	22.16	0.43	17.11	8.53	0.72	28.68	0.45
Ethephon	24.76	0.44	20.34	9.39	0.79	31.22	0.44
	Peo 3-gal	**Pet 3-ara**	**Peo 3-glu**	**Mal 3-gal**	**Peo 3-ara**	**Mal 3-glu**	**Mal 3-ara**
0 day	***P*=0.612**	***P*=NA**	***P*=NA**	***P*=0.225**	***P*=NA**	***P*=NA**	***P*=0.027**
Control	0.05	0.00	0.00	0.13	0.00	0.00	0.07 a
ACC	0.02	0.00	0.00	0.02	0.00	0.00	0.01 b
Ethephon	0.06	0.00	0.00	0.06	0.00	0.00	0.043 ab
3 day	***P*=0.007**	***P*=0.039**	***P*=0.0337**	***P*=0.023**	***P<0.0001***	***P*=0.012**	***P*=0.031**
Control	0.81 b	0.47 b	0.03 b	4.75 b	0.27 b	0.23 b	1.84 b
ACC	2.67 a	1.83 a	0.17 a	14.55 a	1.00 a	0.77 a	5.50 a

Ethephon	2.42 a	1.91 a	0.09 ab	11.64 a	0.94 a	0.66 a	4.42 a
5 day	***P*=0.258**	***P*=0.175**	***P*=0.084**	***P*=0.304**	***P*=0.803**	***P*=0.100**	***P*=0.016**
Control	2.26	1.36	0.19	13.05	1.19	0.55	4.39 b
ACC	2.95	2.36	0.37	19.29	1.14	0.83	7.90 a
Ethephon	3.59	2.81	0.57	21.28	1.51	1.11	8.62 a
10 day	***P*=0.172**	***P*=0.830**	***P*=0.071**	***P*=0.355**	***P*=0.611**	***P*=0.217**	***P*=0.316**
Control	7.63	7.98	0.83	54.66	5.17	2.76	23.73
ACC	8.59	7.95	0.70	60.07	5.58	2.97	27.68
Ethephon	9.02	8.30	0.38	55.94	5.42	2.69	24.53

Different letters above symbols indicate that the means are significantly different between the treatment (within a day after treatment) according to ANOVA and Fischer's LSD (α=0.05) for each anthocyanin.

Table 3. S4: Concentration of anthocyanin measured from ethephon, ACC, and control treated fruits in 'Powderblue'.

Powderblue							
Treatment	**Concentration (mean ±SE) (mg/100 g FW)**						
	Del-3-gal	**Del 3-glu**	**Cya 3-gal**	**Del 3-ara**	**Cya 3-glu**	**Pet 3-gal/Cay 3-ara**	**Pet 3-glu**
0 day	***P*=NA**	***P*=NA**	***P*=0.401**	***P*=NA**	***P*=0.103**	***P*=0.637**	***P*=NA**
Control	0.00	0.00	0.76	0.00	0.19	0.36	0.00
ACC	0.00	0.00	0.50	0.00	0.08	0.25	0.00
Ethephon	0.00	0.00	0.59	0.00	0.09	0.30	0.00
3 day	***P*= 0.042**	***P*=0.025**	***P*=0.074**	***P*=0.088**	***P*=0.035**	***P*=0.041**	***P*=0.116**
Control	0.87 b	0.37 b	7.96	0.28	3.82 b	5.40 b	1.46
ACC	1.49 a	0.67 a	9.29	0.73	4.78 ab	6.98 ab	2.11
Ethephon	1.61 a	0.77 a	11.77	0.71	6.12 a	8.50 a	2.53
5 day	***P*=0.155**	***P*=NA**	***P*=0.009**	***P*=0.245**	***P*=0.007**	***P*=0.021**	***P*=0.112**
Control	1.29	0.58	7.29 b	0.56	3.73 b	5.80 b	1.84
ACC	2.29	1.21	10.74 a	1.23	5.78 a	8.84 ab	3.24
Ethephon	3.18	1.57	13.63 a	1.67	7.56 a	11.53 a	4.03
10 day	***P*=0.322**	***P*=NA**	***P*=0.533**	***P*=0.329**	***P*=0.524**	***P*=0.501**	***P*=0.428**
Control	13.29	7.31	18.88	7.93	10.59	21.65	10.64
ACC	12.37	6.83	17.53	7.94	9.84	20.66	9.82
Ethephon	10.33	5.44	16.89	6.36	9.50	19.42	9.25
	Peo 3-gal	**Pet 3-ara**	**Peo 3-glu**	**Mal 3-gal**	**Peo 3-ara**	**Mal 3-glu**	**Mal 3-ara**
0 day	***P*=NA**	***P*=NA**	***P*=0.422**	***P*=0.422**	***P*=NA**	***P*=0.260**	***P*=0.352**
Control	0.00	0.00	0.04	0.00	0.00	0.07	0.04
ACC	0.00	0.00	0.00	0.05	0.00	0.04	0.04
Ethephon	0.00	0.00	0.00	0.00	0.00	0.00	0.01
3 day	***P*=0.399**	***P*=0.002**	***P*=0.034**	***P*=0.057**	***P*=0.017**	***P*=0.039**	***P*=0.045**
Control	1.33	0.69 b	2.39 b	4.09	0.26 b	4.36 b	2.05 b

ACC	1.52	1.18 a	3.16 ab	5.77	0.35 b	6.41 ab	3.16 ab
Ethephon	2.06	1.47 a	4.02 a	6.78	0.57 a	7.96 a	3.73 a
5 day	***P*=0.152**	***P*=0.064**	***P*=0.012**	***P*=0.023**	***P*=0.036**	***P*=0.008**	***P*=0.023**
Control	1.85	1.15	2.84 b	5.86 b	0.47 b	5.87 b	3.47 b
ACC	2.70	1.91	4.36 ab	9.28 ab	0.55 b	9.54 b	5.68 ab
Ethephon	3.25	2.44	5.99 a	12.63 a	0.83 a	13.42 a	7.76 a
10 day	***P*=0.736**	***P*=0.839**	***P*=NA**	***P*=0.878**	***P*=0.347**	***P*=0.904**	***P*=0.408**
Control	6.61	6.07	10.27	28.35	1.27	25.53	14.65
ACC	7.21	6.12	11.02	29.89	1.59	26.69	17.14
Ethephon	6.89	5.80	10.51	29.68	1.37	26.53	16.89

Different letters above symbols indicate that the means are significantly different between the treatment (within a day after treatment) according to ANOVA and Fischer's LSD (α=0.05) for each anthocyanin.

CHAPTER 4

ROLE OF RIPENING-RELATED TRANSCRIPTION FACTORS IN BLUEBERRY RIPENING

[3] Tej P. Acharya, and Savithri U. Nambeesan. To be submitted to BMC Plant Biology.

Abstract

Transcription factors (TFs) are proteins that bind to the promoters or enhancer regions of DNA and regulate transcription. TFs play an important role in many plant growth and developmental processes including ripening. Blueberry (*Vaccinium spp*.) fruit is in high demand because of its flavor and nutrition. During fruit ripening, accumulation of sugars, acids and anthocyanins contribute to blueberry flavor and nutrition. The role of TFs in regulating blueberry ripening is not well characterized. The objective of this study was to identify key ripening-related TFs and their regulation by ethylene. This study was performed using fruit from various developmental stages including ripening from cultivars, Premier and Powderblue. TFs belonging to the MADS, NAC, and SPL family have shown to regulate ripening in tomato and strawberry. The homologs of these TFs were identified from the 'Powderblue' transcriptome by using blasttx in NCBI and specific primers were designed. This analysis led to the identification of 8 MADS, 14 NAC and 4 SPL transcripts. Expression analysis was performed using qRT-PCR. The transcript abundance of *VvMADS7, VvNAC1, VvNAC2*, and *VvNAC8* increased during the ripening, suggesting they may positively regulate ripening. In addition, we found that *VvMADS7, VvNAC1*, and *VvNAC2* were induced by ethylene, however *VvNAC8* regulation was independent from ethylene. In conclusion, this study identified four TFs that may be important regulators of fruit ripening in blueberry.

Key words: *VvMADS, VvNAC, VvSPB,* ethylene, fruit development and ripening

Introduction

Ripening of fleshy fruit is complex, and a series of physiological and biochemical changes occur during ripening that include alterations in texture, color, flavor and aroma (White, 2002). Generally, the ripening behavior of fruits are categorized as climacteric and non-climacteric based on ethylene production and respiratory patterns during ripening. Fruits like tomatoes, bananas, and apples produce elevated ethylene levels with increased respiration rates at the onset of ripening and are classified as climacteric fruits (Alexander and Grierson, 2002; Paul et al., 2012; Seymour et al., 2013). In these fruits, ethylene regulation is autocatalytic, and ethylene positively regulates ripening-related changes (Yokotani et al., 2009; Liu et al., 2015). However, non-climacteric fruits such as citrus and strawberries do not display a respiratory burst during ripening, and the role of ethylene in ripening is not clear (Lelièvre et al., 1997; Paul et al., 2012; Seymour et al., 2013). In these fruits, abscisic acid (ABA) has shown to play a larger role to facilitate ripening (Kumar et al., 2014; Chen et al., 2016; Pilati et al., 2017). Similar to climacteric fruit, blueberries (*Vaccinium spp*.) display an increase in respiration and ethylene production during ripening (Wang et al., 2022). However, their ethylene regulation is not autocatalytic. Further ethylene metabolism is functional indicating that blueberry fruit display an atypical climacteric ripening physiology (Wang et al., 2022).

Transcription factors (TFs) belonging to the gene families such as, MADS, NAC, and SPL play an important role in the ripening of climacteric and non-climacteric fruits. The acronym ‘MADS’ stands for MINICHROMOSOME MAINTENANCE FACTOR 1 (*Saccharomyces cerevisiae*), AGAMOUS (*Arabidopsis thaliana*), DEFICIENS (*Antirrhinum*

majus) and SERUM RESPONSE FACTOR (*Homo sapiens*); while NAC includes NO APICAL MERISTEM, (Petunia), *ARABIDOPSIS THALIANA* ACTIVATING FACTOR 1-2, and *C*UP-SHAPED COTYLEDON 2 (Arabidopsis); and finally SPL denotes SQUAMOSA PROMOTER BINDING PROTEIN-LIKE (*A. majus*). These three TFs are regarded as the primary regulators of the ripening process, as the original mutant exhibit deficiencies in both ethylene production and ripening characteristics (Li et al., 2023). Further, the *rin* and *nor* mutants have been used in the modern day breeding program to extend the shelf-life of tomato (Adaskaveg et al., 2021).

The MADS domain TFs are associated with floral development, fruit development, and ripening process (Shore and Sharrocks, 1995; Ito et al., 2008; Díaz-Riquelme et al., 2009; Gramzow and Theissen, 2010; Ireland et al., 2013). Approximately 56-60 amino acids in the N-terminal contain the DNA-binding domain, whereas the C-terminal domains are involved in protein dimerization (Smaczniak et al., 2012). The MADS-domain TFs involved in the ripening of tomato include the RIPENING INHIBITOR (RIN), FRUITFUL (FUL1/TDR4 and FUL2/MBP7), and TOMATO AGAMOUS-LIKE1 (TAGL1) (Karlova et al., 2014). In tomato, RIN (SEPALLATA subfamily MADS-domain) is the master regulator of fruit ripening and interacts with the promoter of genes and other TFs like NON-RIPENING (NOR), COLORLESS NONRIPENING (CNR), FRUITFULL (FUL), and HOMEOBOX 1 (HB1), and can influence the overall ripening phenomena (Martel et al., 2011). The original *rin* mutation results in impaired ripening, which cannot be rescued by exogenous ethylene application (Vrebalov et al., 2002; Manning et al., 2006). However, the role of RIN has recently been reconsidered as *rin* was shown to be negative gain of function mutation (Ito et al., 2020). Further, the generation of RIN-CRISPR-Cas9 (RIN-CR-KO) lines indicated that RIN TFs may not be as crucial for the ripening

initiation but is still important for ripening completion (Ito et al., 2017). In addition, other members of the MADS-box gene family, including TOMATO AGAMOUS-LIKE1 (TAGL1) as well as FRUITFUL homologs FUL1 and FUL2, have been demonstrated to positively regulate ripening by forming higher-order complexes with RIN (Itkin et al., 2009; Shima et al., 2013; Fujisawa et al., 2014). The MADS domain TFs also regulate ripening in non-climacteric fruits (Seymour et al., 2011; Lu et al., 2018). Silencing of the SEPALLATA *(SEP) 1/2-like* (*FaMADS9*) TFs resulted in the inhibition of ripening-related characteristics in strawberry (Seymour et al., 2011).

NAC is the largest family of TFs having a conserved N-terminal DNA binding and a variable C-terminal domain (Olsen et al., 2005). The member of NAC TFs positively regulate fruit ripening and their cross talk with ethylene has been identified in banana, apple, and tomato (Shan et al., 2012; Wang and Xu, 2012; Gao et al., 2021). Similarly, other members of the NAC TF family, such as NOR influence fruit ripening. The silencing of *NOR-like1* through virus-induced gene silencing and *NAC-NOR* using CRISPR-Cas9 led to a reduction in fruit ripening initiation by lowering the accumulation of carotenoids, reducing chlorophyll metabolism, and decreasing the expression of genes involved in ethylene biosynthesis (Gao et al., 2018; Wang et al., 2019). Consistently, a transcriptomic analysis revealed that *NOR* had a positive regulatory effect on the expression of genes responsible for ethylene and carotenoid biosynthesis, as well as enzymes involved in cell wall modification (Gao et al., 2019). The NOR-CR-KO fruits delayed color break by 3 days compared to the wild type and produced an orange phenotype, thus partially inhibiting the ripening process but not completely retarding (Gao et al., 2020). Furthermore, other members of the NAC gene family, including *SlNAC4*, were discovered to

positively impact fruit ripening. Reduced expression of *SlNAC4* by RNAi reduced chlorophyll breakdown and suppressed the expression of genes involved in ethylene and carotenoid biosynthesis (Zhu et al., 2014). It remains unclear whether NAC TFs form higher-order complexes to jointly regulate the ripening process (Gao et al., 2019). In strawberry, the NAC TF member, *FaNAC035* has been shown to induce ABA biosynthesis, and ABA, in turn, transcriptionally induce *FaNAC035,* hence positively influence ripening (Martín-Pizarro et al., 2021). Similarly, the cis-elements responsive to ABA and auxin were found in the promoter of *FcNAC1* in wild strawberry (Carrasco-Orellana et al., 2018). In addition, the SPL-CNR is another TFs involved in fruit ripening. The *cnr* mutant in tomato resulted in the reduction of lycopene, total soluble solid content, ripening-related genes, and cell wall-degrading enzymes, leading to the formation of mature fruits with a colorless pericarp (Eriksson et al., 2004; Zhou et al., 2022). However, new studies with CNR-CR-KO lines indicates only a delayed ripening phenotype by 2 to 3 days, after which full coloration is obtained similar to the wild-type (Gao et al., 2019).

The ripening-related processes can also be influenced by cross-talk between hormonal pathways and TFs. In tomato, RIN-CR-KO and NOR-CR-KO lines significantly reduced ethylene levels compared to the control (Ito et al., 2017; Gao et al., 2020). Furthermore, Chip-Seq analysis suggested that RIN binds to the promoter regions of genes related to ethylene biosynthesis (Fujisawa et al., 2011; Martel et al., 2011). Additionally, the application of ethrel, a plant growth regulator (PGR) that releases ethylene, increased the transcript abundance of *NOR*, while the use of 1-methylcyclopropene (1-MCP), an ethylene perception inhibitor, reversed this effect (Gao et al., 2020). Other NAC-family TFs, such as *NOR-like 1*, *NAC4*, and *NAC9*, have

been shown to positively regulate genes involved in ethylene biosynthesis in tomato (Gao et al., 2018; Kou et al., 2018). However, treatment with ethylene did not enhance the transcript abundance of *SlNAC4* and *NOR-like 1* (Zhu et al., 2014; Gao et al., 2018), suggesting a potential role upstream of the regulation influenced by ethylene.

This study aims to identify ripening-related TFs belonging to MADs, NAC and SPL gene families in blueberry. Initially TFs that are abundantly and/or differentially expressed during ripening were identified from a fruit transcriptome previously generated in the laboratory (Wang et al., 2023, submitted), and expression was validated using qRT-PCR analyses. Further, the role of ethylene in transcriptional regulation of key ripening related TFs were investigated.

Material and Methods

Plant Material: Fruit samples were collected at five developmental stages in rabbiteye cultivars Premier and Powderblue from the Horticulture Farm in Athens, GA, in 2020 and categorized into S4, S5, S6, S7, and S8 stages based on (Zifkin et al., 2012). Stages 4 and 5 were collected based on fruit size (S4 < 9 mm, and S5 >9-<13 mm in diameter), and stages 6, 7, and 8 were based on the fruit color (S6: 25-50% light pink skin, S7: predominately light to dark pink skin with some blue, and S8: blue skin). All samples were frozen in liquid nitrogen and stored at -80°C until analysis. Each stage of ripening had four replicates per cultivar.

Treatment with plant growth regulators: The experimental design was a randomized complete block design with four replications. Before the PGRs application, very small (S1, S2 and S3; Zifkin et al., 2012) and fully ripe fruits were removed from the plants. Then, ethephon was

applied at 250 mg·L^{-1} using 0.15% Latron-1956 as a surfactant. Also, 0.15% Latron-1956 was sprayed as a control. Treatment with 1-methylcyclopropene (1-MCP; AgroFresh, Collegeville, PA) was applied with deionized water in one cultivar Powderblue at 6.6 g·L^{-1} in 2022. Treatments with water were control for the 1-MCP treatments. Fruits were randomly collected at 0, 1, 2, and 3 days after PGR applications from one of the branches and stored at -80°C until analysis. There were four replications per treatment for each cultivar.

Identification of transcription factors: Transcription factor families belonging to MADS, NAC, and SPL were identified from tomato and strawberry using a literature search. Tomato and strawberry were chosen since they are model plants for climacteric and non-climacteric ripening behavior, respectively. Sequences for tomato and strawberry TFs genes were retrieved from Sol Genomics Network (https://solgenomics.net/) and NCBI (https://www.ncbi.nlm.nih.gov/), respectively. The MADS box gene in tomato included: *RIN* (Solyc05g012020), *MADS1* (Solyc03g114840), *FUL1* (Solyc06g069430), *FUL2* (Solyc03g114830), *TAGL1* (Solyc07g055920), and in strawberry, *MADS-RIN* (AF484683.1). Similarly, TFs belonging to the NAC family include *NAC4* (Solyc11g017470) and *NOR* (Solyc10g006880) from tomato, and *FcNAC1* (MH577996.1) from the strawberry. The tomato SPL (*SPL-CNR*: Solyc02g077920) was used as a candidate gene from the SPL gene family. Next nucleotide sequences encoded by these genes were retrieved and blasted using tblastx against the 'Powderblue' transcriptome (Wang and Nambeesan, 2022), using a code in Command Prompt in Windows. The top hit from the 'Powderblue' transcriptome for every gene was retrieved. Using this top hit gene, a second blast analysis was performed by doing another blast analysis to the 'Powderblue' transcriptome. This

resulted in the identification of all transcripts for a given family present in the 'Powderblue' transcriptome. All TFs were categorized as *VvMADS, VvNAC,* or *VvSPL*. Finally, blueberry homologs were reciprocally blasted against tomato and grape in the NCBI database using blastx function, to validate their identity and identify the closest homologs. In this case, we selected grape since it provides the closest identity with blueberry protein sequences (Gupta et al., 2015). This led to the identification of 19 *MADS*, 37 *NAC* and 6 *SPL* transcripts. Of all the blueberry TFs identified from the 'Powderblue' transcriptome, a subset of transcripts was selected based on the criteria of (a) differentially expressed during the ripening (cutoff of < 0.01 false discovery rate and ≥ 2-fold change; Wang and Nambeesan, *submitted*), (b) not differentially expressed but had higher transcript abundance (>50) in at least one developmental stage, and (c) not differentially expressed but displayed increasing or decreasing trend during fruit development and ripening. Based on our criteria we identified a total of 13 *MADS*, 28 *NAC*, and 6 *SPL* transcripts. Next, transcripts belonging to each gene family were aligned using ClustalW alignment in Mega 11 software to identify unique transcripts (Tamura et al., 2021). Sequences within each family were aligned resulting in the identification of unique transcripts, which included 8 for *MADS* (only 7 used for qRTPCR, primers designed for transcript PB.8760/PB.1429 could not be used due to multiple peaks observed), 14 for *NAC* and 4 for the *SPL* families. Primers for the transcripts were designed using the Integrated DNA Technologies (IDT) software (https://www.idtdna.com/calc/analyzer).

***RNA extraction and RT-PCR*:** Transcript abundance of TFs was measured by quantitative real-time polymerase chain reaction (qRT-PCR) as described below. Total RNA was extracted using

the modified cetyltrimethylammonium bromide (CTAB) method followed by cDNA synthesis and qRT-PCR analyses as described previously (Vashisth et al., 2011). Three reference genes were used for the normalization of target genes: *UBIQUITIN-CONJUGATING ENZYME* (*UBC28*), *RNA HELICASE-LIKE* (*RH8*), and *CLATHRIN ADAPTER COMPLEXES MEDIUM SUBUNIT FAMILY PROTEIN* (*CACSa*). The list of genes and primers used for this study are presented in the Table 4. S1. Expression of genes during fruit development are presented as fold change with respect to the transcript abundance of 'Powderblue' at S4 developmental stage. For treatment with PGRs 'Powderblue' control day 0 was used to normalize fold change with the remaining samples.

Statistical analysis: Data were analyzed and visualized using the R-studio 2023 (R core 2023, Vienna, Austria). Analysis of variance (ANOVA) was performed to evaluate the significance of the treatment effect. In addition, multiple comparisons were made by Fisher's least significant difference (LSD), and t-test at the 0.05 significance level.

Results

***Transcript abundance of MADS TFs during fruit development and ripening*:** Of the seven MADS TFs investigated, *VvMADS7* showed an increase expression pattern during ripening (Fig. 4.1A, Fig. 4.4A). The transcript abundance of *VvMADS7* increased by 2.3-fold from S4 to S5, 1.6-fold from S5 to S7, and then remained similar between S7 to S8 stages in 'Premier (Fig. 4.4A). In 'Powderblue', the transcript abundance of *VvMADS7* increased gradually from S4 to S6 stage, with 5.5-fold increase between these two stages, remained similar at the S6 and S7, and

subsequently decreased by 1.9-fold from S7 to S8 stage (Fig. 4.4A). Of the remaining genes, *VvMADS6* showed a downregulation of transcript abundance in both cultivars between S4-S6 stages (Fig. 4. S1F). *VvMADS2* displayed a downregulation of transcript abundance between S5 and S6 stages in 'Premier' and between S5 and S7 in 'Powderblue' (Fig. 4. S1B). The transcript abundance of *VvMADS1* decreased between S6 and S7 stages in only 'Powderblue' with a relatively constant pattern in 'Premier' (Fig. 4. S1A). Overall *VvMADS3*, *VvMADS4*, and *VvMADS5* did not show any consistent trends in gene expression patterns in both cultivars during fruit ripening (Fig. 4. S1C-E). Among the *VvMADS* gene analyzed, *VvMADS1* displayed highest abundance followed by *VvMADS3*, *VvMADS5*, and *VvMADS2*; whereas *VvMADS4* and *VvMADS6* displayed a relatively lower transcript abundance (based on Ct values) (Fig. 4.1B).

***Transcript abundance of NAC TFs during fruit development and ripening*:** Among the 14 NAC TFs, *VvNAC1*, *VvNAC2*, and *VvNAC8* were upregulated during the ripening in both cultivars (Fig. 4.2A, Fig. 4.4B-D). The expression pattern of *VvNAC1* was similar in both cultivars (Fig. 4.4B). The transcript abundance of *VvNAC1* was 1.7-fold greater in S5 than S4, remained similar up to S7 stage, and declined by 1.8-fold from S7 to S8 stage in 'Premier' (Fig. 4.4B). In 'Powderblue', it increased by 3.4- and 1.6- fold between S4 to S5 and S5 to S6 stage, respectively, then remained similar at S6 and S7; after that, it decreased by 3.9-fold from S7 to S8 (Fig. 4.4B). The expression pattern of *VvNAC2* increased by 6.2- and 2.9- fold between S4 to S5 and S5 to S6 stage, respectively and remained similar thereafter during ripening in 'Premier' (Fig. 4.4C). In 'Powderblue', it increased dramatically by almost 10.8- and 2.8-fold from S4 to S5, and S5 to S6 stages, respectively, remained similar between S6 and S7 stages, and declined

by 2.8-fold between S7 and S8 stage. The transcript abundance of *VvNAC8*, increased between S4 and S6 by 6.1- and 5.5-fold in 'Premier' and 'Powderblue', respectively and thereafter remained similar at S7 and S8 stages (Fig. 4.4D).

In both cultivars, the transcript abundance of *VvNAC10* decreased during ripening, in 'Premier' it decreased between S4 and S5 by 5.6-fold and in 'Powderblue' between S5 and S6 by 3.2-fold and remained similar thereafter during ripening (Fig. 4.2A, Fig. 4. S3A). In general transcript abundance of *VvNAC4* and *VvNAC9* decreased from S6 to S8 stages in both cultivars (Fig. 4. S2B, F). *VvNAC6*, *VvNAC11*, and *VvNAC13* did not exhibit any difference in expression pattern during fruit ripening in both cultivars (Fig. 4. S2D, Fig. 4. S3B, D). The remaining NAC transcripts showed expression patterns during ripening only in one cultivar. *VvNAC5* exhibited higher transcript abundance throughout ripening only in 'Premier' (Fig. 4. S2C). In general, *VvNAC7* and *VvNAC12* showed high transcript abundance from S6 to S8 stages in only 'Powderblue' (Fig. 4. S2E, Fig. 4. S3C). The transcript abundance of *VvNAC3* decreased between S4 to S5 and *VvNAC14* between S5 and S7 only in 'Premier' (Fig. 4. S2A, Fig. 4. S3E).

Comparison of transcript abundance among genes, showed separation into two groups. One set of 12 genes displaying higher transcript abundance compared to two genes, *VvNAC14* and *VvNAC11* with relatively lower abundance during fruit development (Fig. 4.2B). Of highly abundant transcripts, *VvNAC1* displayed the greatest transcript abundance (Fig. 4.2B).

***Transcript abundance of SPL* TFs *during fruit development and ripening*:** Of the four SPL genes investigated, only *VvSPL2* exhibited a decrease in transcript abundance between S5-S6 stages in both cultivars (Fig. 4.3A, Fig. 4. S4A-D). Overall *VvSPL1* displayed highest and

VvSPL3 and *VvSPL4* showed low transcript abundance (Fig. 4.3B), without any consistent trends in gene expression patterns during fruit ripening in both cultivars (Fig. 4.3A, Fig. 4. S4A-D).

Effect of ethephon on transcript abundance of MADS TFs: Ethephon treatment enhanced the transcript abundance of *VvMADS7* (upregulated during ripening) at 2 DAT by 2.0-fold in 'Powderblue' and by 1.5- and 1.4-fold at 3 DAT in 'Premier' and 'Powderblue' compared to the control, respectively (Fig. 4.4E). Ethephon treatment reduced the transcript abundance of *VvMADS6* (downregulated during ripening) at 1 and 3 DAT by 2.7-and 1.4-fold compared to the control, respectively, in 'Premier' and by 2.3-fold at 2 DAT in 'Powderblue' (Fig. 4. S1L). The transcript abundance of *VvMADS5* (no change during ripening) decreased by 1.5- and 1.6-fold in ethephon treatment compared to the control at 2 DAT in 'Premier' and 'Powderblue', respectively (Fig. 4. S1K). Two transcripts, *VvMADS3* and *VvMADS4* did not exhibit any changes in transcript abundance after ethephon treatment compared to the control (Fig. 4. S1I, J). Others MADS genes did not display any consistent patterns in both cultivars after ethephon application. Ethephon treatment compared to the control reduced the transcript abundance of *VvMADS1* and *VvMADS2* by 1.3- and 1.2-fold at 1 DAT, respectively, in 'Premier'; whereas in 'Powderblue', ethephon treatment slightly increased the transcript abundance of *VvMADS1* at 3 DAT by 1.2-fold (Fig. 4. S1G, H).

Effect of ethephon on transcript abundance of NAC TFs: Ethephon treatment compared to the control increased the transcript abundance of *VvNAC1* (upregulated during ripening) at 3 DAT in 'Premier' by 1.4-fold, and at 1, 2 and 3 DAT in 'Powderblue' by 1.3-, 1.7- and 1.4-fold,

respectively (Fig. 4.4F). Similarly, ethephon treatment increased the transcript abundance of *VvNAC2* (upregulated during ripening) at 2 DAT in 'Premier' by 1.6-fold, and 2 and 3 DAT in 'Powderblue' by 2.3- and 1.7-fold, respectively (Fig. 4.4G). In contrast, ethephon treatment decreased the transcript abundance of *VvNAC3* in both 'Premier' and 'Powderblue' (Fig. 4. S2G). Ethephon treatment did not influence the transcript abundance of *VvNAC4*, *VvNAC6*, *VvNAC7*, *VvNAC9*, *VvNAC10*, *VvNAC11*, and *VvNAC12* (Fig. 4. S2H, J-L and Fig. 4. S3F-H). Other NAC genes did not show consistent patterns between both cultivars in response to ethephon. The transcript abundance of *VvNAC5* increased by 1.5- and 2.0-fold at 2 and 3 DAT, respectively only in 'Premier' (Fig. 4. S2I), and that of *VvNAC13* increased by 1.3-fold at 3 DAT only in 'Powderblue' (Fig. 4. S3I). Ethephon treatment decreased the transcript abundance of *VvNAC14* by 3.0-and 3.2-fold at 1 and 2 DAT, respectively in 'Powderblue' (Fig. 4. S3J). In case of *VvNAC8* (upregulated during ripening), transcript abundance increased at 2 DAT in 'Premier' and decreased at 1 and 3 DAT in 'Powderblue' (Fig. 4.4H).

Effect of ethephon on transcript abundance of SPL TFs: Ethephon treatment reduced the transcript abundance of *VvSPL2* by 1.4-fold in 'Premier' and 1.5-fold in 'Powderblue' at 1 DAT (Fig. 4. S4F). Overall transcript abundance of *VvSPL3* and *VvSPL4* were not different after ethephon treatment in both cultivars (Fig. 4. S4G, H). The transcript abundance of *VvSPL1* increased by 1.3-fold at 3 DAT only in 'Powderblue following ethephon treatment compared to the control (Fig. 4. S4E).

Effect of 1-MCP on key transcription factors: In response to 1-MCP, transcript abundance of only the TFs differentially regulated after ethephon treatment, *VvMADS5-7, VvNAC1-3,* and *VvSPL2* were investigated. None of the TFs showed any significant difference between control and 1-MCP treatments (Fig. 4. S5).

Discussion

In this paper we characterized the three major classes of TFs, MADS, NAC and SPL, and their transcriptional regulation during fruit development and ripening. Genome-wide approaches have identified the following numbers of TFs genes, *MADS*: 131 in tomato (Wang et al., 2019), 54 in grape (Wang et al., 2015), and 85 in strawberry (Zhou et al., 2018); *NAC*: 101 in tomato (Tweneboah and Oh, 2017), 74 in grape (Wang et al., 2013), and 112 in strawberry (Moyano et al., 2018); and *SPL*: 15 in tomato (Salinas et al., 2012), 18 in grape (Hou et al., 2013), and 14 in strawberry (Xiong et al., 2018). In southern highbush blueberry, genome wide analysis identified 249 putative *MADS* genes (Wang et al., 2023). The higher number of MADS genes in blueberry is due to multiple genome wide duplication resulting in the multiple transcripts with the similar sequences (Wang et al., 2023). There is no information available on the characterization of NAC and SPL TFs in blueberry. In our study using the Powderblue transcriptome, we specifically focused on three families of TFs related to mid-to-late fruit development. This resulted in the identification of a total of 19 transcripts belonging to the MADS family, 37 transcripts to the NAC family, and six to the SPL family. Of these 7, 14, and 4 unique transcripts were identified for MADS, NAC and SPL family of TFs, respectively. These were subsequently used for qRT-PCR analyses. It is possible that multiple transcripts having

similar sequences were found due to bioinformatics limitations that classified them as unique transcripts or due to the hexaploid nature of rabbiteye blueberry resulting in almost identical genes. In this study, five developmental stages categorized as S4-S8 are of specific interest in relation to ripening. Of these stages, ripening initiation is evident at the pedicel-end of the fruit at S6 developmental stage. Therefore, changes in transcript abundance between mid-stages of fruit development and ripening, S4 to S5/S6 is reflective of ripening initiation and that from subsequent stages, S6 to S7/S8 of ripening progression.

Based on the transcript abundance and an increasing pattern during the ripening, we postulated that one MADS TF and three NAC TFs may positively regulate fruit ripening in blueberry. Overall, the transcripts abundance of *VvMADS7, VvNAC1, VvNAC2*, and *VvNAC8* increased between the S4 and S5 stages, and further increased between the S5 and S6 stages. These results indicated transcriptional regulation of these four TFs during fruit maturation leading into ripening initiation. It is possible that these TFs play a role in a developmental switch between fruit growth/maturation and ripening initiation. Similar to our study, ripening related TFs like *SIRIN, SIFUL1, SINAC4,* and *SINAM1* expression level increased later during the fruit maturation (between immature green/mature green and breaker stages) leading into to fruit ripening in tomato (Wang et al., 2014; Zhu et al., 2014; Gao et al., 2021). Additionally, in strawberry's receptacle and achene, gene expression of *FaMADS9* increased between the mature green and white stages, suggesting it may be associated with positive regulation of fruit ripening (Seymour et al., 2011). Surprisingly, the six MADS genes showing high expression during ripening (*VcMADS6, VcMADS44, VcMADS45, VcMADS180, VcMADS188, VcMADS212*) in southern highbush blueberry (Wang et al., 2023) were not the closest ortholog to *VvMADS7*

identified in this study. The sequence similarities between the TFs identified in Wang et al. (2023) and in our study are as follows: *VcMADS6* to *VvMADS5*, *VcMADS44* to *VvMADS3*, *VcMADS45* and *VcMADS212* to *VvMADS2*, and *VcMADS180* and *VcMADS188* to *VvMADS1*. In southern highbush blueberry, *VcMADS188* (ortholog to *VvMADS1* in our study) transcript abundance was relatively higher in S4, S5, and S8 stages, without distinct ripening-related pattern (Wang et al., 2023).

In this study, transcript abundance of *VvMADS6* and *VvNAC10* decreased during the ripening initiation in both cultivars suggesting the role of these genes in negatively regulating fruit ripening in blueberry. In tomato, *MADS1*, *MBP8*, and *FYFL* (*FOREVER YOUNG FLOWER like*), expression level decreased during ripening, and are indicated as negative regulators of fruit ripening (Dong et al., 2013; Xie et al., 2014; Yin et al., 2017). MBP8 and FYFL, are both MADS TFs, and can interact with RIN, thus inhibiting the ripening process (Li et al., 2019). Similarly, in the strawberry, *FaMADS1a* expression level decreased during ripening, and overexpression of it resulted in the reduction of the anthocyanin biosynthesis gene and a delay in fruit coloration during ripening. This suggest that *FaMADS1a* negatively regulate fruit ripening (Lu et al., 2018). Additionally, in this study, *VvMADS1*, *VvNAC3*, and *VvNAC4* transcripts abundance were high during fruit development and ripening with minimal/no change during ripening progression suggesting these genes may be regulating fruit development rather than ripening-specific TFs. In case of *VvNAC5*, it was upregulated during ripening initiation only in 'Premier. Further studies will be needed to determine if the transcript abundance of this TF is positively associated with ripening in a cultivar-specific manner.

None of the SPL genes expressed in the fruit showed an up-regulation during ripening, suggesting that, in this study SPL TFs that positively regulate ripening were not identified. Originally, it was indicated in tomato that *cnr* mutation had reduction in expression of *SPL-CNR* gene due to the hypermethylation of the promoter region (Manning et al., 2006). However, subsequent studies revealed that *cnr* fruit underwent a more general DNA hypermethylation across the entire genome (Zhong et al., 2013). Therefore, the functions of multiple genes including *CNR* were also affected, contributing to the non-ripening phenotype observed in the original mutant. Furthermore, even before the ripening initiation, the original *cnr* mutant exhibits earlier chlorophyll degradation and distinct gene expression patterns during fruit growth and development. These findings suggest that *cnr* mutants are more related to fruit development rather than primarily related to the ripening (Wang et al., 2020; Adaskaveg et al., 2021). In CNR-CR-KO lines, the delay in ripening phenotype only occurred by 2 to 3 days, after which full coloration occurs similar to wild-type (Gao et al., 2019). The role of *CNR/SPL* gene in early fruit developmental processes leading up to ripening is being considered (Adaskaveg et al., 2021). In this study, *VvSPL2* downregulation between S5 and S6 stages is not dramatic and not consistent between both cultivars. However, both *VvSPL1* and *VvSPL2* displayed high transcript abundance suggesting that these genes may be important in regulating fruit development rather than specifically regulating ripening.

To determine the ethylene inducibility of the TFs, we studied the transcriptional regulation of TFs in response to ethephon treatments. In tomato, the *RIN*/*MADS* act upstream of ethylene biosynthesis and signaling genes and increases the transcript abundance of *ACS2* and *ACS4* (Ito et al., 2008; Fujisawa et al., 2011; Martel et al., 2011). Similarly, the *FUL1* and *FUL2*

suppressed line via RNAi resulted in decreased ethylene production and transcripts abundance of *ACS2* and *ACS4* (Shima et al., 2014). In this study, the transcript abundance of the four ripening-related TFs increases between stages S4 and S5 whereas ethylene levels increase between S5 and S6 (and not S4 and S5, data not shown) suggesting that the upregulation of TF precedes ethylene evolution. Whether these four TFs regulate ethylene biosynthesis will need future studies aimed at functional validation.

Further, ethylene signaling can lead to positive or negative regulation of TFs thus creating positive or negative feedback loops, especially in climacteric fruits (Li et al., 2022). The application of 1-MCP decreased the transcript abundance of *RIN*, *FUL1* and *NOR*, but did not affect *CNR* and this process was carried out by the decrease in transcript abundance of *ACS2* and *AP2a* (Fujisawa et al., 2013). Similarly, the expression level of *RIN* and *FUL1* increased with ethephon treatments compared to control, suggesting that they are ethylene inducible (Ampa et al., 2017). Additionally, ethylene increased the gene expression of *NOR* in tomato, while 1-MCP reduced its expression (Gao et al., 2020). In this study, we ascertained that the expression of three of the ripening-related TFs, *VvMADS7*, *VvNAC1* and *VvNAC2* are positively regulated by ethephon application, suggesting they are ethylene inducible. The transcript abundance of *VvNAC8* remained unaffected by ethylene application, suggesting that the expression of this gene during ripening is independent from ethylene-mediated signaling. Similar to our study, the transcripts abundance of tomato *NAC4* and *NOR like-1* did not increase after ethylene application (Zhu et al., 2014; Gao et al., 2018). In addition, ethylene downregulated the expression of *VvMADS5, VvMADS6,* and *VvNAC3*. Ethylene induced downregulation of *VvMADS6*, a negative regulator of ripening indicates a consistent role of ethylene in accelerating ripening initiation

(Wang and Nambeesan, manuscript s*ubmitted*). However, in case of transcripts, *VvMADS5* and *VvNAC3* that are associated with fruit development, their downregulation by ethylene may be independent of ripening-related processes.

The transcript abundance of none of the selected TFs is affected by the 1-MCP treatments. Blueberry exhibits an atypical climacteric behavior, as it increases ethylene and carbon dioxide production during ripening, but the transcript abundance of ACS genes and ACC concentration did not increase with exogenous ethylene production (Wang et al., 2022). Another study in our laboratory has indicated that 1-MCP application increases ethylene production during ripening (data not shown). Consequently, it is possible that 1-MCP does not block ethylene perception completely due to formation of new receptors, thus diluting its effect on regulation of TFs. However, further research on the role of 1-MCP in ethylene biosynthesis and its impact on genes related to ethylene signaling is essential to conclude its influence on TFs regulation.

Conclusion

From this study, we characterized MADS, NAC, and SPL TFs involved in blueberry fruit ripening. Among them, expression patterns of *VvMADS7*, *VvNAC1*, *VvNAC2*, and *VvNAC8* suggested a positive involvement in fruit ripening. Further *VvMADS7*, *VvNAC1*, and *VvNAC2* exhibiting increased transcript abundance in response to ethylene application, while *VvNAC8* remained unaffected. Future studies with functional validation will provide a better understanding of the roles of these TFs in fruit ripening.

References

Adaskaveg JA, Silva CJ, Huang P, Blanco-Ulate B (2021) Single and double mutations in tomato ripening transcription factors have distinct effects on fruit development and quality traits. Frontiers in Plant Science **12:** 647035.

Alexander L, Grierson D (2002) Ethylene biosynthesis and action in tomato: a model for climacteric fruit ripening. Journal of experimental botany **53:** 2039-2055.

Ampa K, Saito T, Okawa K, Ohara H, Kondo S (2017) Effects of ethephon and abscisic acid application on ripening-related genes in 'Kohi'kiwifruit (Actinidia chinensis) on the vine. Horticultural Plant Journal **3:** 29-33.

Carrasco-Orellana C, Stappung Y, Mendez-Yañez A, Allan A, Espley R, Plunkett B, Moya-Leon M, Herrera R (2018) Characterization of a ripening-related transcription factor FcNAC1 from Fragaria chiloensis fruit. Scientific reports **8:** 10524.

Chen J, Mao L, Lu W, Ying T, Luo Z (2016) Transcriptome profiling of postharvest strawberry fruit in response to exogenous auxin and abscisic acid. Planta **243:** 183-197.

Díaz-Riquelme J, Lijavetzky D, Martínez-Zapater JM, Carmona MJ (2009) Genome-wide analysis of MIKCC-type MADS box genes in grapevine. Plant physiology **149:** 354-369.

Dong T, Hu Z, Deng L, Wang Y, Zhu M, Zhang J, Chen G (2013) A tomato MADS-box transcription factor, SlMADS1, acts as a negative regulator of fruit ripening. Plant physiology **163:** 1026-1036.

Eriksson EM, Bovy A, Manning K, Harrison L, Andrews J, De Silva J, Tucker GA, Seymour GB (2004) Effect of the Colorless non-ripening mutation on cell wall

biochemistry and gene expression during tomato fruit development and ripening. Plant Physiology **136:** 4184-4197.

Fujisawa M, Nakano T, Ito Y (2011) Identification of potential target genes for the tomato fruit-ripening regulator RIN by chromatin immunoprecipitation. BMC plant biology **11:** 1-14.

Fujisawa M, Nakano T, Shima Y, Ito Y (2013) A large-scale identification of direct targets of the tomato MADS box transcription factor RIPENING INHIBITOR reveals the regulation of fruit ripening. The Plant Cell **25:** 371-386.

Fujisawa M, Shima Y, Nakagawa H, Kitagawa M, Kimbara J, Nakano T, Kasumi T, Ito Y (2014) Transcriptional regulation of fruit ripening by tomato FRUITFULL homologs and associated MADS box proteins. The Plant Cell **26:** 89-101.

Gao Y, Fan ZQ, Zhang Q, Li HL, Liu GS, Jing Y, Zhang YP, Zhu BZ, Zhu HL, Chen JY (2021) A tomato NAC transcription factor, SlNAM1, positively regulates ethylene biosynthesis and the onset of tomato fruit ripening. The Plant Journal **108:** 1317-1331.

Gao Y, Wei W, Fan Z, Zhao X, Zhang Y, Jing Y, Zhu B, Zhu H, Shan W, Chen J (2020) Re-evaluation of the nor mutation and the role of the NAC-NOR transcription factor in tomato fruit ripening. Journal of Experimental Botany **71:** 3560-3574.

Gao Y, Wei W, Zhao X, Tan X, Fan Z, Zhang Y, Jing Y, Meng L, Zhu B, Zhu H (2018) A NAC transcription factor, NOR-like1, is a new positive regulator of tomato fruit ripening. Horticulture research **5.**

Gao Y, Zhu N, Zhu X, Wu M, Jiang C-Z, Grierson D, Luo Y, Shen W, Zhong S, Fu D-Q (2019) Diversity and redundancy of the ripening regulatory networks revealed by the

fruitENCODE and the new CRISPR/Cas9 CNR and NOR mutants. Horticulture Research **6.**

Gramzow L, Theissen G (2010) A hitchhiker's guide to the MADS world of plants. Genome biology **11:** 214.

Gupta V, Estrada AD, Blakley I, Reid R, Patel K, Meyer MD, Andersen SU, Brown AF, Lila MA, Loraine AE (2015) RNA-Seq analysis and annotation of a draft blueberry genome assembly identifies candidate genes involved in fruit ripening, biosynthesis of bioactive compounds, and stage-specific alternative splicing. Gigascience **4:** s13742-13015-10046-13749.

Hou H, Li J, Gao M, Singer SD, Wang H, Mao L, Fei Z, Wang X (2013) Genomic organization, phylogenetic comparison and differential expression of the SBP-box family genes in grape. PLoS One **8:** e59358.

Ireland HS, Yao JL, Tomes S, Sutherland PW, Nieuwenhuizen N, Gunaseelan K, Winz RA, David KM, Schaffer RJ (2013) Apple SEPALLATA1/2-like genes control fruit flesh development and ripening. The Plant Journal **73:** 1044-1056.

Itkin M, Seybold H, Breitel D, Rogachev I, Meir S, Aharoni A (2009) TOMATO AGAMOUS-LIKE 1 is a component of the fruit ripening regulatory network. The Plant Journal **60:** 1081-1095.

Ito Y, Kitagawa M, Ihashi N, Yabe K, Kimbara J, Yasuda J, Ito H, Inakuma T, Hiroi S, Kasumi T (2008) DNA-binding specificity, transcriptional activation potential, and the rin mutation effect for the tomato fruit-ripening regulator RIN. The Plant Journal **55:** 212-223.

Ito Y, Nishizawa-Yokoi A, Endo M, Mikami M, Shima Y, Nakamura N, Kotake-Nara E, Kawasaki S, Toki S (2017) Re-evaluation of the rin mutation and the role of RIN in the induction of tomato ripening. Nature plants **3:** 866-874.

Ito Y, Sekiyama Y, Nakayama H, Nishizawa-Yokoi A, Endo M, Shima Y, Nakamura N, Kotake-Nara E, Kawasaki S, Hirose S (2020) Allelic mutations in the ripening-inhibitor locus generate extensive variation in tomato ripening. Plant physiology **183:** 80-95.

Karlova R, Chapman N, David K, Angenent GC, Seymour GB, De Maagd RA (2014) Transcriptional control of fleshy fruit development and ripening. Journal of Experimental Botany **65:** 4527-4541.

Kou X, Zhao Y, Wu C, Jiang B, Zhang Z, Rathbun JR, He Y, Xue Z (2018) SNAC4 and SNAC9 transcription factors show contrasting effects on tomato carotenoids biosynthesis and softening. Postharvest Biology and Technology **144:** 9-19.

Kumar R, Khurana A, Sharma AK (2014) Role of plant hormones and their interplay in development and ripening of fleshy fruits. Journal of experimental botany **65:** 4561-4575.

Lelièvre JM, Latchè A, Jones B, Bouzayen M, Pech JC (1997) Ethylene and fruit ripening. Physiologia plantarum **101:** 727-739.

Li C, Lu X, Xu J, Liu Y (2023) Regulation of fruit ripening by MADS-box transcription factors. Scientia Horticulturae **314:** 111950.

Li S, Chen K, Grierson D (2019) A critical evaluation of the role of ethylene and MADS transcription factors in the network controlling fleshy fruit ripening. New Phytologist **221:** 1724-1741.

Li X, Wang X, Zhang Y, Zhang A, You C-X (2022) Regulation of fleshy fruit ripening: From transcription factors to epigenetic modifications. Horticulture Research **9.**

Liu M, Pirrello J, Chervin C, Roustan J-P, Bouzayen M (2015) Ethylene control of fruit ripening: revisiting the complex network of transcriptional regulation. Plant physiology **169:** 2380-2390.

Lu W, Chen J, Ren X, Yuan J, Han X, Mao L, Ying T, Luo Z (2018) One novel strawberry MADS-box transcription factor FaMADS1a acts as a negative regulator in fruit ripening. Scientia Horticulturae **227:** 124-131.

Manning K, Tör M, Poole M, Hong Y, Thompson AJ, King GJ, Giovannoni JJ, Seymour GB (2006) A naturally occurring epigenetic mutation in a gene encoding an SBP-box transcription factor inhibits tomato fruit ripening. Nature genetics **38:** 948-952.

Martel C, Vrebalov J, Tafelmeyer P, Giovannoni JJ (2011) The tomato MADS-box transcription factor RIPENING INHIBITOR interacts with promoters involved in numerous ripening processes in a COLORLESS NONRIPENING-dependent manner. Plant physiology **157:** 1568-1579.

Martín-Pizarro C, Vallarino JG, Osorio S, Meco V, Urrutia M, Pillet J, Casanal A, Merchante C, Amaya I, Willmitzer L (2021) The NAC transcription factor FaRIF controls fruit ripening in strawberry. The Plant Cell **33:** 1574-1593.

Moyano E, Martínez-Rivas FJ, Blanco-Portales R, Molina-Hidalgo FJ, Ric-Varas P, Matas-Arroyo AJ, Caballero JL, Muñoz-Blanco J, Rodríguez-Franco A (2018) Genome-wide analysis of the NAC transcription factor family and their expression during the development and ripening of the Fragaria× ananassa fruits. PLoS One **13:** e0196953.

Olsen AN, Ernst HA, Leggio LL, Skriver K (2005) NAC transcription factors: structurally distinct, functionally diverse. Trends in plant science **10:** 79-87.

Paul V, Pandey R, Srivastava GC (2012) The fading distinctions between classical patterns of ripening in climacteric and non-climacteric fruit and the ubiquity of ethylene—an overview. Journal of food science and technology **49:** 1-21.

Pilati S, Bagagli G, Sonego P, Moretto M, Brazzale D, Castorina G, Simoni L, Tonelli C, Guella G, Engelen K (2017) Abscisic acid is a major regulator of grape berry ripening onset: new insights into ABA signaling network. Frontiers in plant science **8:** 1093.

Salinas M, Xing S, Höhmann S, Berndtgen R, Huijser P (2012) Genomic organization, phylogenetic comparison and differential expression of the SBP-box family of transcription factors in tomato. Planta **235:** 1171-1184.

Seymour GB, Østergaard L, Chapman NH, Knapp S, Martin C (2013) Fruit development and ripening. Annual review of plant biology **64:** 219-241.

Seymour GB, Ryder CD, Cevik V, Hammond JP, Popovich A, King GJ, Vrebalov J, Giovannoni JJ, Manning K (2011) A SEPALLATA gene is involved in the development and ripening of strawberry (Fragaria× ananassa Duch.) fruit, a non-climacteric tissue. Journal of experimental botany **62:** 1179-1188.

Shan W, Kuang J-f, Chen L, Xie H, Peng H-h, Xiao Y-y, Li X-p, Chen W-x, He Q-g, Chen J-y (2012) Molecular characterization of banana NAC transcription factors and their interactions with ethylene signalling component EIL during fruit ripening. Journal of Experimental Botany **63:** 5171-5187.

Shima Y, Fujisawa M, Kitagawa M, Nakano T, Kimbara J, Nakamura N, Shiina T, Sugiyama J, Nakamura T, Kasumi T (2014) Tomato FRUITFULL homologs regulate fruit ripening via ethylene biosynthesis. Bioscience, biotechnology, and biochemistry **78:** 231-237.

Shima Y, Kitagawa M, Fujisawa M, Nakano T, Kato H, Kimbara J, Kasumi T, Ito Y (2013) Tomato FRUITFULL homologues act in fruit ripening via forming MADS-box transcription factor complexes with RIN. Plant Molecular Biology **82:** 427-438.

Shore P, Sharrocks AD (1995) The MADS-box family of transcription factors. European Journal of Biochemistry **229:** 1-13.

Smaczniak C, Immink RG, Angenent GC, Kaufmann K (2012) Developmental and evolutionary diversity of plant MADS-domain factors: insights from recent studies. Development **139:** 3081-3098.

Tamura K, Stecher G, Kumar S (2021) MEGA11: molecular evolutionary genetics analysis version 11. Molecular biology and evolution **38:** 3022-3027.

Tweneboah S, Oh S-K (2017) Biological roles of NAC transcription factors in the regulation of biotic and abiotic stress responses in solanaceous crops. Journal of Plant Biotechnology **44:** 1-11.

Vashisth T, Johnson LK, Malladi A (2011) An efficient RNA isolation procedure and identification of reference genes for normalization of gene expression in blueberry. Plant cell reports **30:** 2167-2176.

Vrebalov J, Ruezinsky D, Padmanabhan V, White R, Medrano D, Drake R, Schuch W, Giovannoni J (2002) A MADS-box gene necessary for fruit ripening at the tomato ripening-inhibitor (rin) locus. Science **296:** 343-346.

Wang A, Xu K (2012) Characterization of two orthologs of REVERSION-TO-ETHYLENE SENSITIVITY1 in apple. Journal of Molecular Biology Research **2:** 24.

Wang L, Yin X, Cheng C, Wang H, Guo R, Xu X, Zhao J, Zheng Y, Wang X (2015) Evolutionary and expression analysis of a MADS-box gene superfamily involved in ovule development of seeded and seedless grapevines. Molecular Genetics and Genomics **290:** 825-846.

Wang N, Zheng Y, Xin H, Fang L, Li S (2013) Comprehensive analysis of NAC domain transcription factor gene family in Vitis vinifera. Plant cell reports **32:** 61-75.

Wang R, da Rocha Tavano EC, Lammers M, Martinelli AP, Angenent GC, de Maagd RA (2019) Re-evaluation of transcription factor function in tomato fruit development and ripening with CRISPR/Cas9-mutagenesis. Scientific reports **9:** 1-10.

Wang R, Lammers M, Tikunov Y, Bovy AG, Angenent GC, de Maagd RA (2020) The rin, nor and Cnr spontaneous mutations inhibit tomato fruit ripening in additive and epistatic manners. Plant Science **294:** 110436.

Wang S, Lu G, Hou Z, Luo Z, Wang T, Li H, Zhang J, Ye Z (2014) Members of the tomato FRUITFULL MADS-box family regulate style abscission and fruit ripening. Journal of experimental botany **65:** 3005-3014.

Wang X, Huang Q, Shen Z, Baron GC, Li X, Lu X, Li Y, Chen W, Xu L, Lv J (2023) Genome-Wide Identification and Analysis of the MADS-Box Transcription Factor Genes

in Blueberry (Vaccinium spp.) and Their Expression Pattern during Fruit Ripening. Plants **12:** 1424.

Wang Y-W, Acharya TP, Malladi A, Tsai H-J, NeSmith DS, Doyle JW, Nambeesan SU (2022) Atypical climacteric and functional ethylene metabolism and signaling during fruit ripening in blueberry (Vaccinium sp.). Frontiers in Plant Science **13.**

Wang Y-W, Nambeesan SU (2022) Full-length fruit transcriptomes of southern highbush (Vaccinium sp.) and rabbiteye (V. virgatum Ait.) blueberry. BMC genomics **23:** 1-15.

Wang Y, Zhang J, Hu Z, Guo X, Tian S, Chen G (2019) Genome-wide analysis of the MADS-box transcription factor family in Solanum lycopersicum. International journal of molecular sciences **20:** 2961.

White PJ (2002) Recent advances in fruit development and ripening: an overview. Journal of Experimental Botany **53:** 1995-2000.

Xie Q, Hu Z, Zhu Z, Dong T, Zhao Z, Cui B, Chen G (2014) Overexpression of a novel MADS-box gene SlFYFL delays senescence, fruit ripening and abscission in tomato. Scientific reports **4:** 4367.

Xiong J-S, Zheng D, Zhu H-Y, Chen J-Q, Na R, Cheng Z-M (2018) Genome-wide identification and expression analysis of the SPL gene family in woodland strawberry Fragaria vesca. Genome **61:** 675-683.

Yin W, Hu Z, Cui B, Guo X, Hu J, Zhu Z, Chen G (2017) Suppression of the MADS-box gene SlMBP8 accelerates fruit ripening of tomato (Solanum lycopersicum). Plant Physiology and Biochemistry **118:** 235-244.

Yokotani N, Nakano R, Imanishi S, Nagata M, Inaba A, Kubo Y (2009) Ripening-associated ethylene biosynthesis in tomato fruit is autocatalytically and developmentally regulated. Journal of experimental botany **60:** 3433-3442.

Zhong S, Fei Z, Chen Y-R, Zheng Y, Huang M, Vrebalov J, McQuinn R, Gapper N, Liu B, Xiang J (2013) Single-base resolution methylomes of tomato fruit development reveal epigenome modifications associated with ripening. Nature biotechnology **31:** 154-159.

Zhou M, Wang Y, Tang H-R, Chen Q (2018) Genome-wide Investigation of MADS-box Members and Validation of a New Member MADS8 in Fragaria Vesca. *In* 2017 2nd International Conference on Biological Sciences and Technology (BST 2017). Atlantis Press, pp 122-127.

Zhou T, Li R, Yu Q, Wang J, Pan J, Lai T (2022) Proteomic Changes in Response to Colorless nonripening Mutation during Tomato Fruit Ripening. Plants **11:** 3570.

Zhu M, Chen G, Zhou S, Tu Y, Wang Y, Dong T, Hu Z (2014) A new tomato NAC (N AM/A TAF1/2/C UC2) transcription factor, SlNAC4, functions as a positive regulator of fruit ripening and carotenoid accumulation. Plant and Cell Physiology **55:** 119-135.

Zifkin M, Jin A, Ozga JA, Zaharia LI, Schernthaner JP, Gesell A, Abrams SR, Kennedy JA, Constabel CP (2012) Gene expression and metabolite profiling of developing highbush blueberry fruit indicates transcriptional regulation of flavonoid metabolism and activation of abscisic acid metabolism. Plant Physiology **158:** 200-224.

Figures

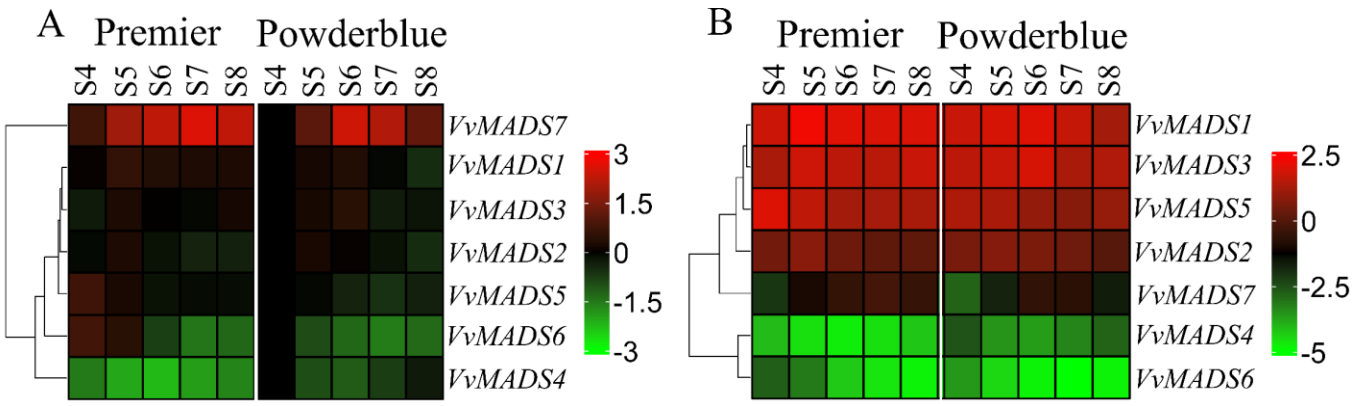

Figure 4.1: MADS transcription factors during fruit development and ripening. A: Comparing each gene during fruit development and ripening. Fold change of each gene was normalized to its expression pattern of 'Powderblue' at S4 developmental stages, and expression is presented in the Log2 scale. B: Comparing transcript abundance of different genes during fruit development and ripening. Expression is presented in the Log2 scale. Color scale from green to red indicates lower and higher transcript abundance, respectively.

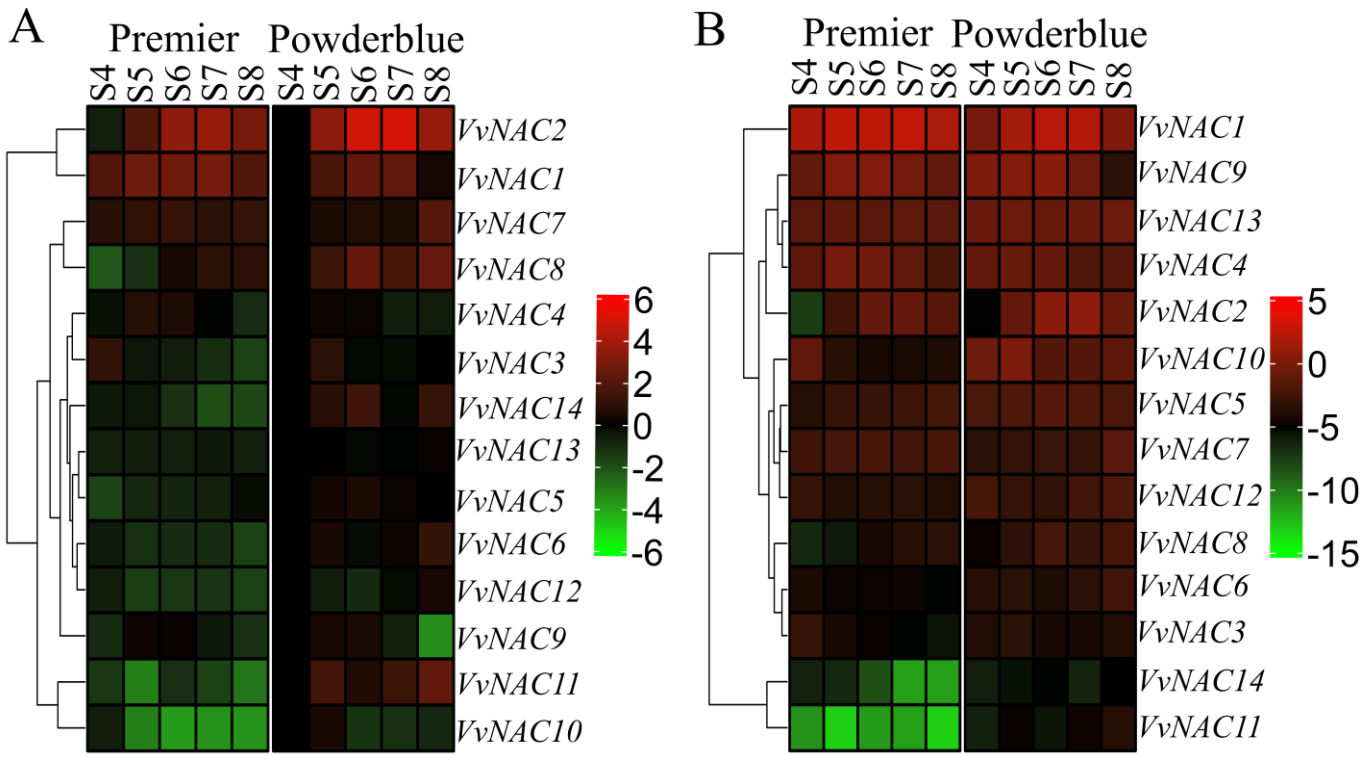

Figure 4.2: NAC transcription factors during fruit development and ripening. A: Comparing each gene during fruit development and ripening. Fold change of each gene was normalized to its expression pattern of 'Powderblue' at S4 developmental stages, and expression is presented in the Log2 scale. B: Comparing transcript abundance of different *NAC* genes during fruit development and ripening. Expression is presented in the Log2 scale. Color scale from green to red indicates lower and higher transcript abundance, respectively.

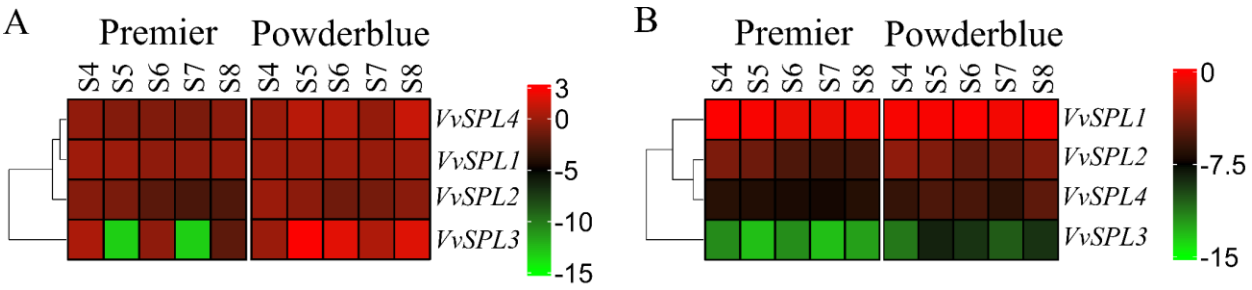

Figure 4.3: SPL transcription factors during fruit development and ripening. A: Comparing each gene during fruit development and ripening. Fold change of each gene was normalized to its expression pattern of 'Powderblue' at S4 developmental stages, and expression is presented in the Log2 scale. B: Comparing transcript abundance of different genes during fruit development and ripening. Expression is presented in the Log2 scale. Color scale from green to red indicates lower and higher transcript abundance, respectively.

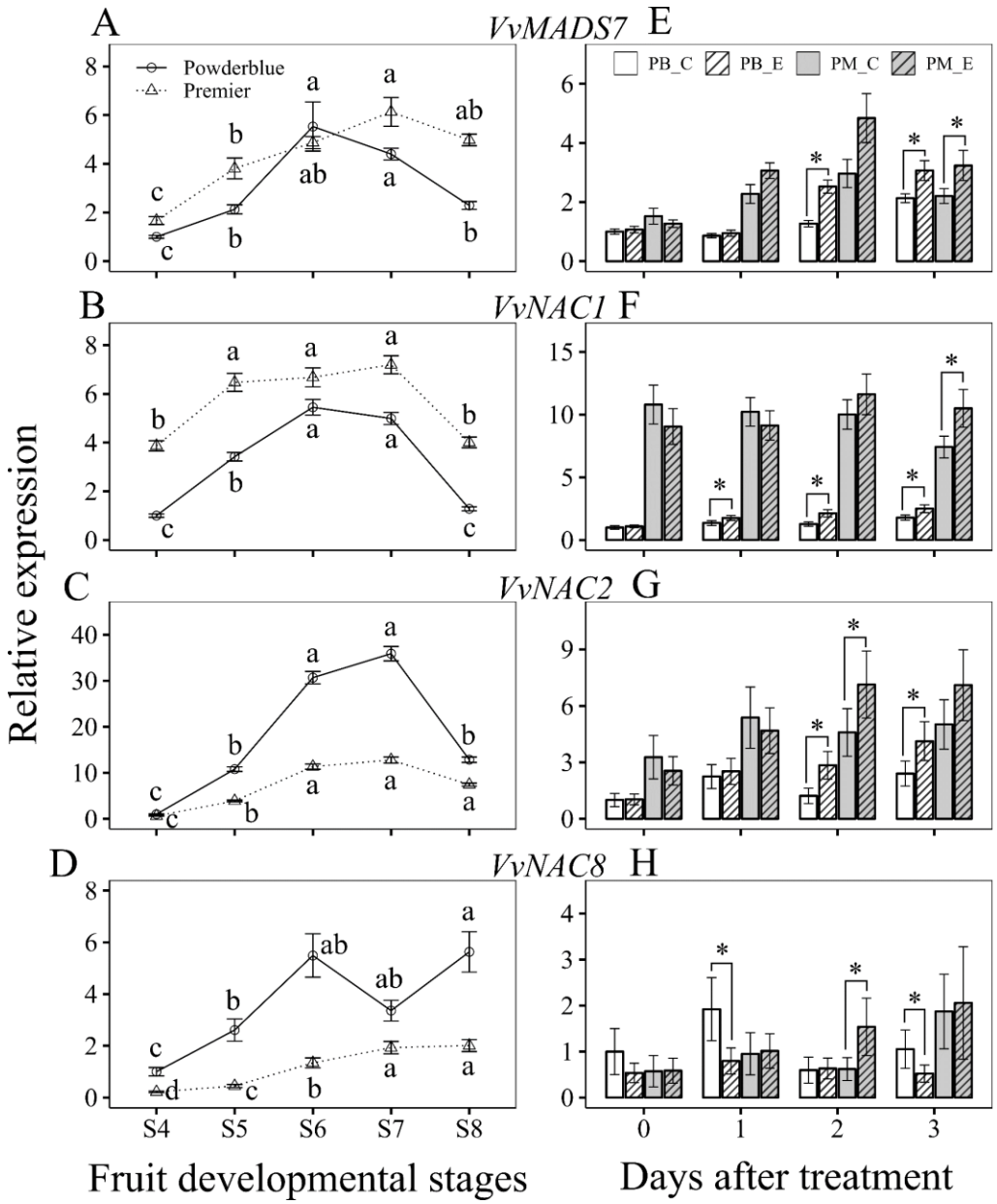

Figure 4.4: Transcript abundance of transcription factors: *VvMADS7* [A, E], *VvNAC1* [B, F], *VvNAC2* [C, G], and *VvNAC8* [D, H] during ripening (left panels) and treatments with 0.15% Latron-1956 (control) and 250 ppm ethephon (right panels). PB_C, Powderblue control; PB_E, Powderblue ethephon; PM_C, Premier control; and PM_E, Premier ethephon. Different letters above symbols indicate that the means are significantly different across fruit developmental stages (within a cultivar) according to ANOVA and Fischer's LSD ($\alpha = 0.05$). Asterisk indicates the means are significantly different between treatments (control and ethephon), within a cultivar and given date, according to t-test ($\alpha = 0.05$).

Appendix A: Supplementary figures

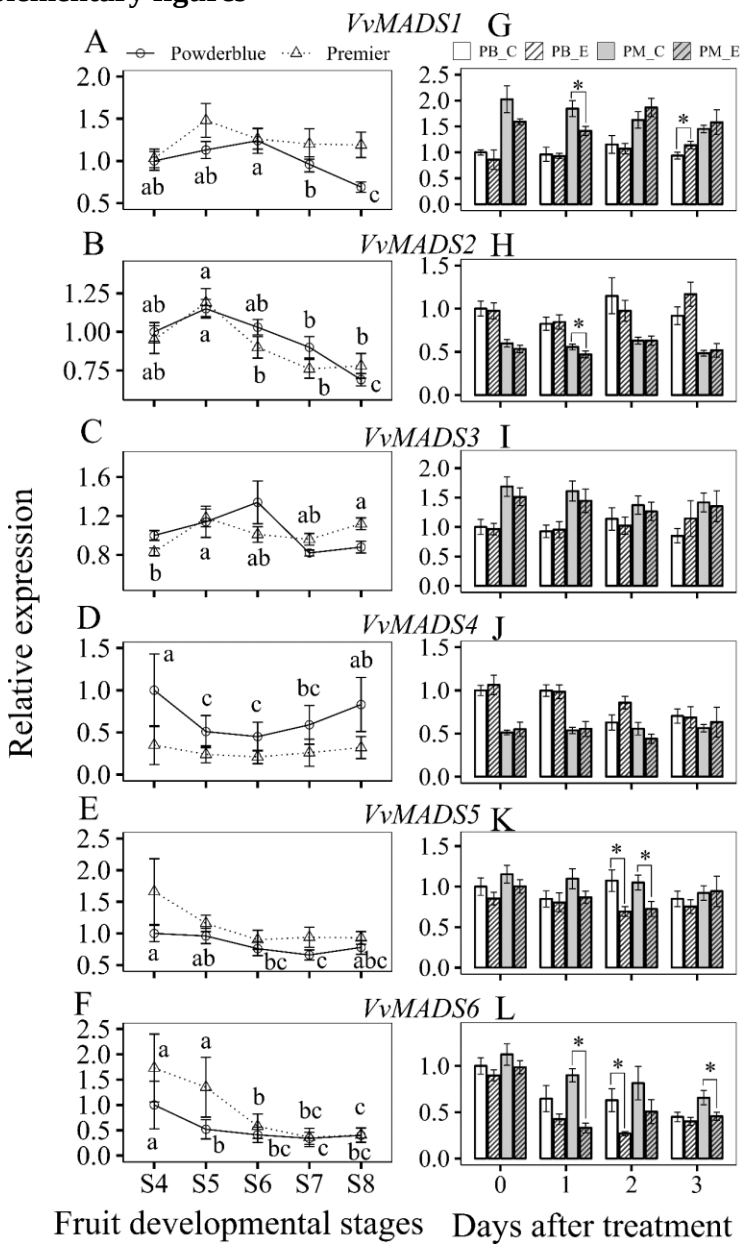

Figure 4. S1: Transcript abundance of MADS box transcription factors during ripening (left panels) and treatments with 0.15% Latron-1956 (control) and 250 ppm ethephon (right panels). PB_C, Powderblue control; PB_E, Powderblue ethephon; PM_C, Premier control; and PM_E, Premier ethephon. Different letters above symbols indicate that the means are significantly different across fruit developmental stages (within a cultivar) according to ANOVA and Fischer's LSD ($\alpha = 0.05$). Asterisk indicates the means are significantly different between treatments (control and ethephon), within a cultivar and given date, according to t-test ($\alpha = 0.05$).

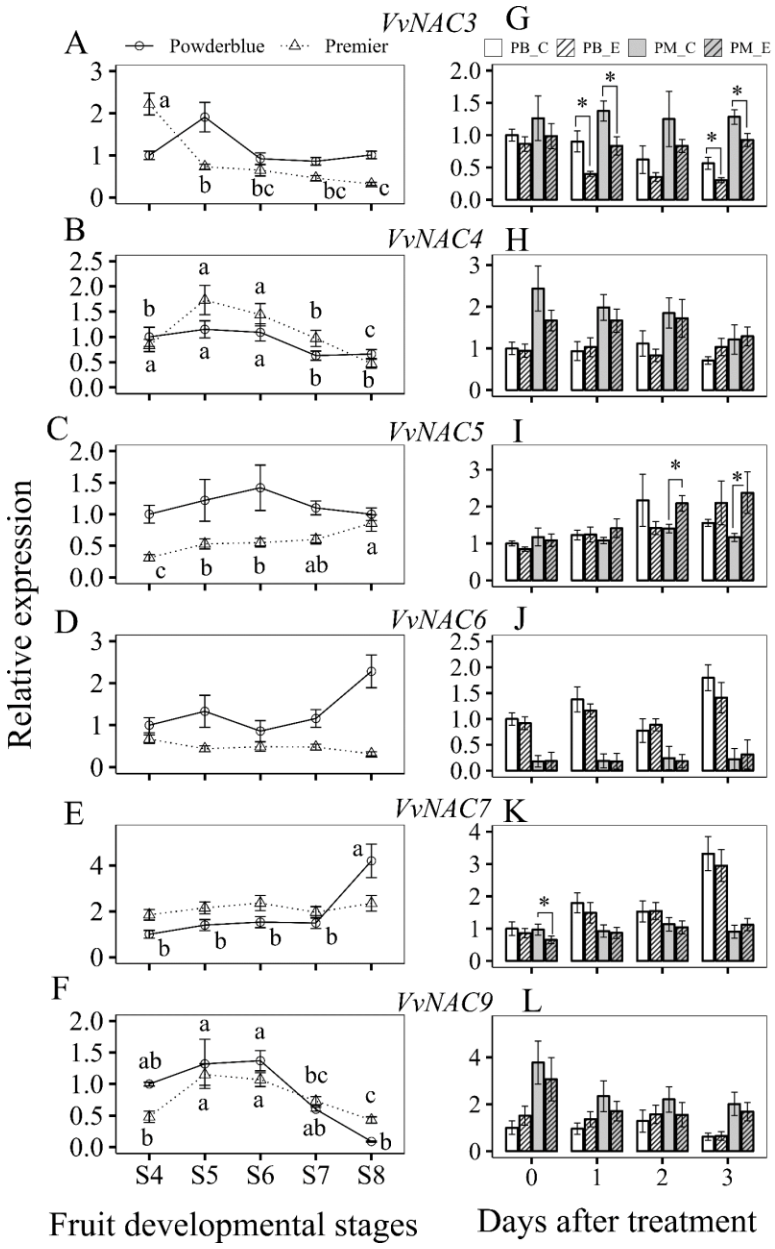

Figure 4. S2: Transcript abundance of NAC transcription factors during ripening (left panels) and treatments with 0.15% Latron-1956 (control) and 250 ppm ethephon (right panels). PB_C, Powderblue control; PB_E, Powderblue ethephon; PM_C, Premier control; and PM_E, Premier ethephon. Different letters above symbols indicate that the means are significantly different across fruit developmental stages (within a cultivar) according to ANOVA and Fischer's LSD ($\alpha = 0.05$). Asterisk indicates the means are significantly different between treatments (control and ethephon), within a cultivar and given date, according to t-test ($\alpha = 0.05$).

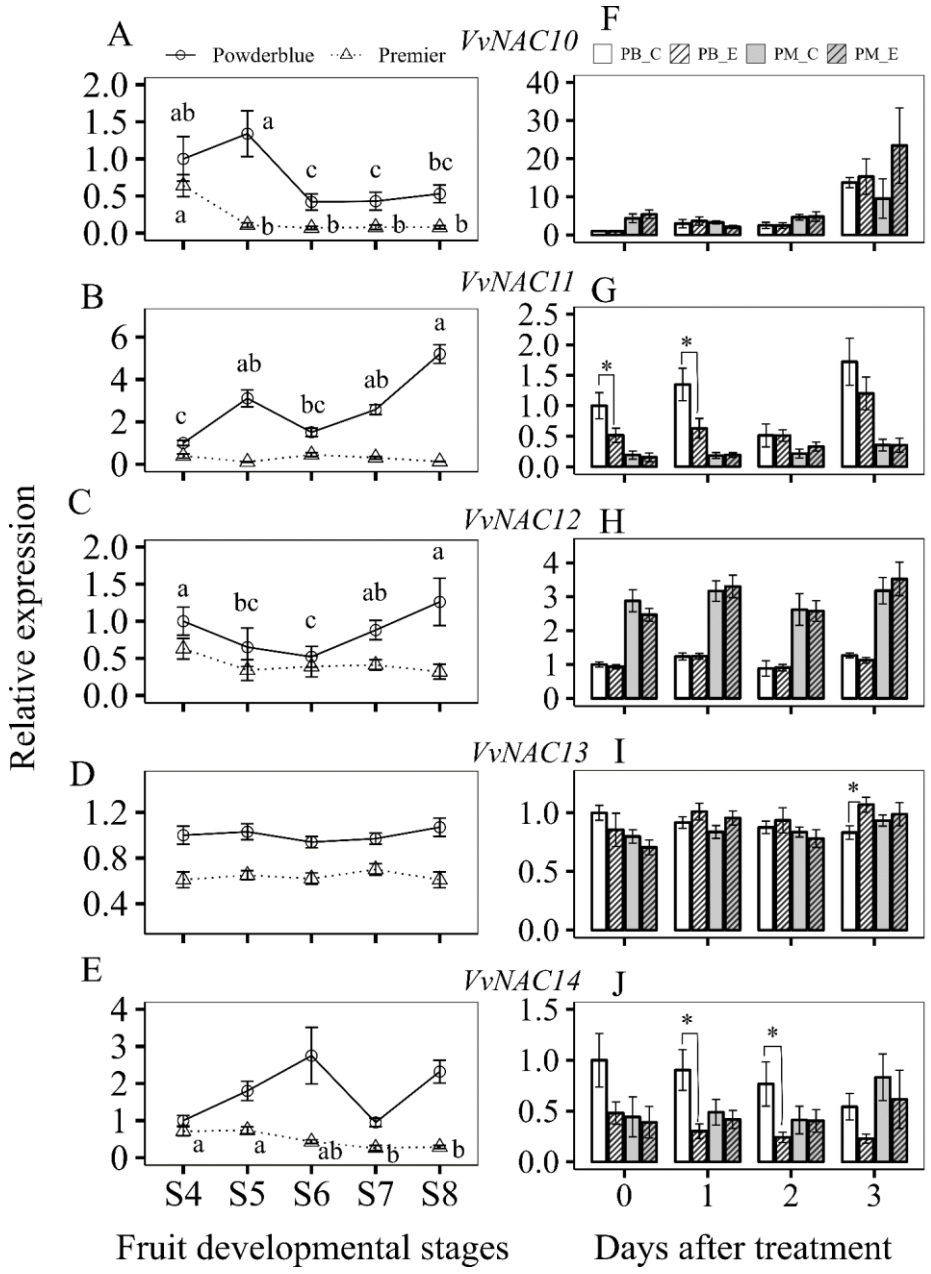

Figure 4. S3: Transcript abundance of NAC transcription factors during ripening (left panels) and treatments with 0.15% Latron-1956 (control) and 250 ppm ethephon (right panels). PB_C, Powderblue control; PB_E, Powderblue ethephon; PM_C, Premier control; and PM_E, Premier ethephon. Different letters above symbols indicate that the means are significantly different across fruit developmental stages (within a cultivar) according to ANOVA and Fischer's LSD ($\alpha = 0.05$). Asterisk indicates the means are significantly different between treatments (control and ethephon), within a cultivar and given date, according to t-test ($\alpha = 0.05$).

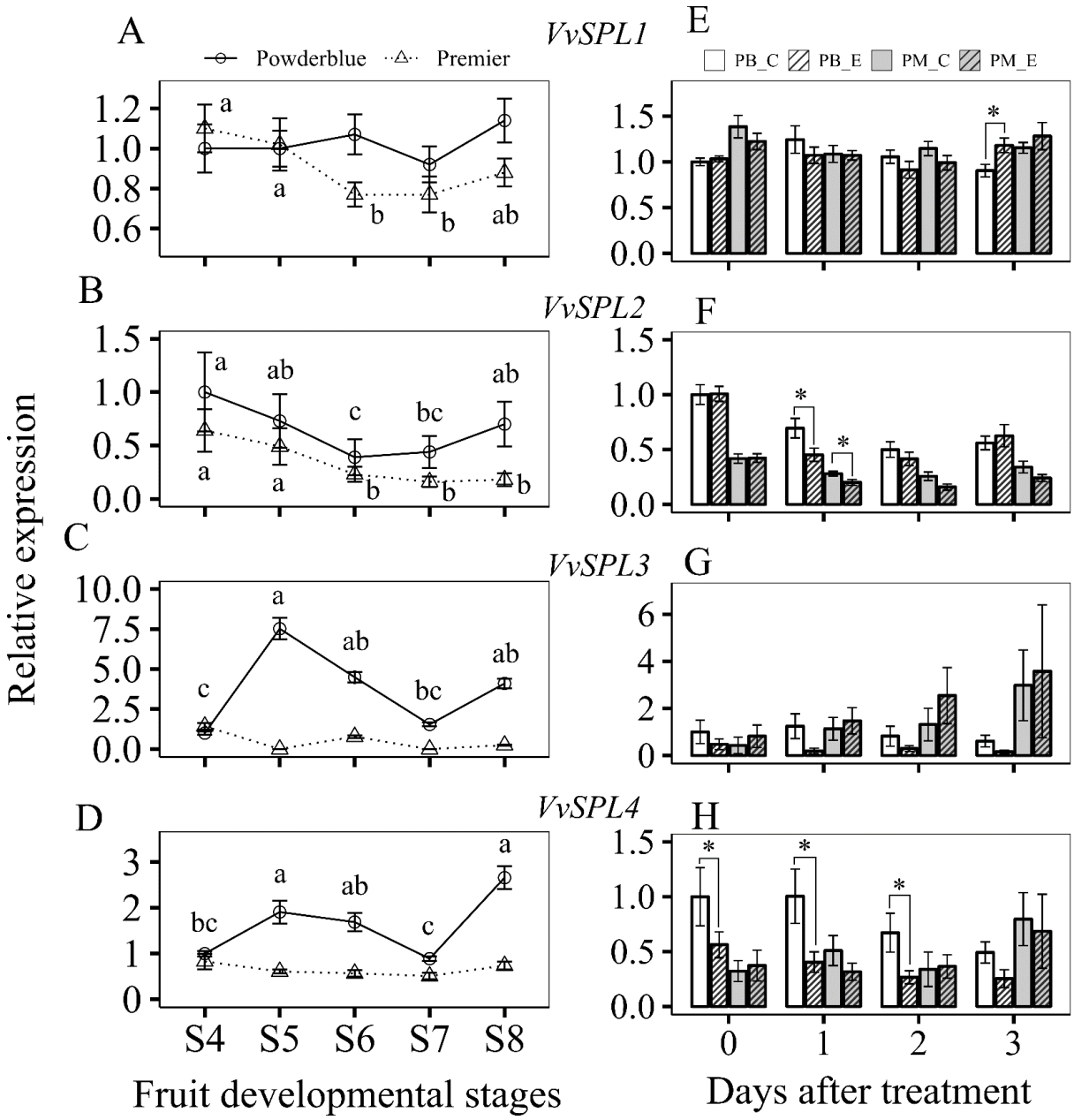

Figure 4. S4: Transcript abundance of SBP transcription factors during ripening (left panels) and treatments with 0.15% Latron-1956 (control) and 250 ppm ethephon (right panels). PB_C, Powderblue control; PB_E, Powderblue ethephon; PM_C, Premier control; and PM_E, Premier ethephon. Different letters above symbols indicate that the means are significantly different across fruit developmental stages (within a cultivar) according to ANOVA and Fischer's LSD ($\alpha = 0.05$). Asterisk indicates the means are significantly different between treatments (control and ethephon), within a cultivar and given date, according to t-test ($\alpha = 0.05$).

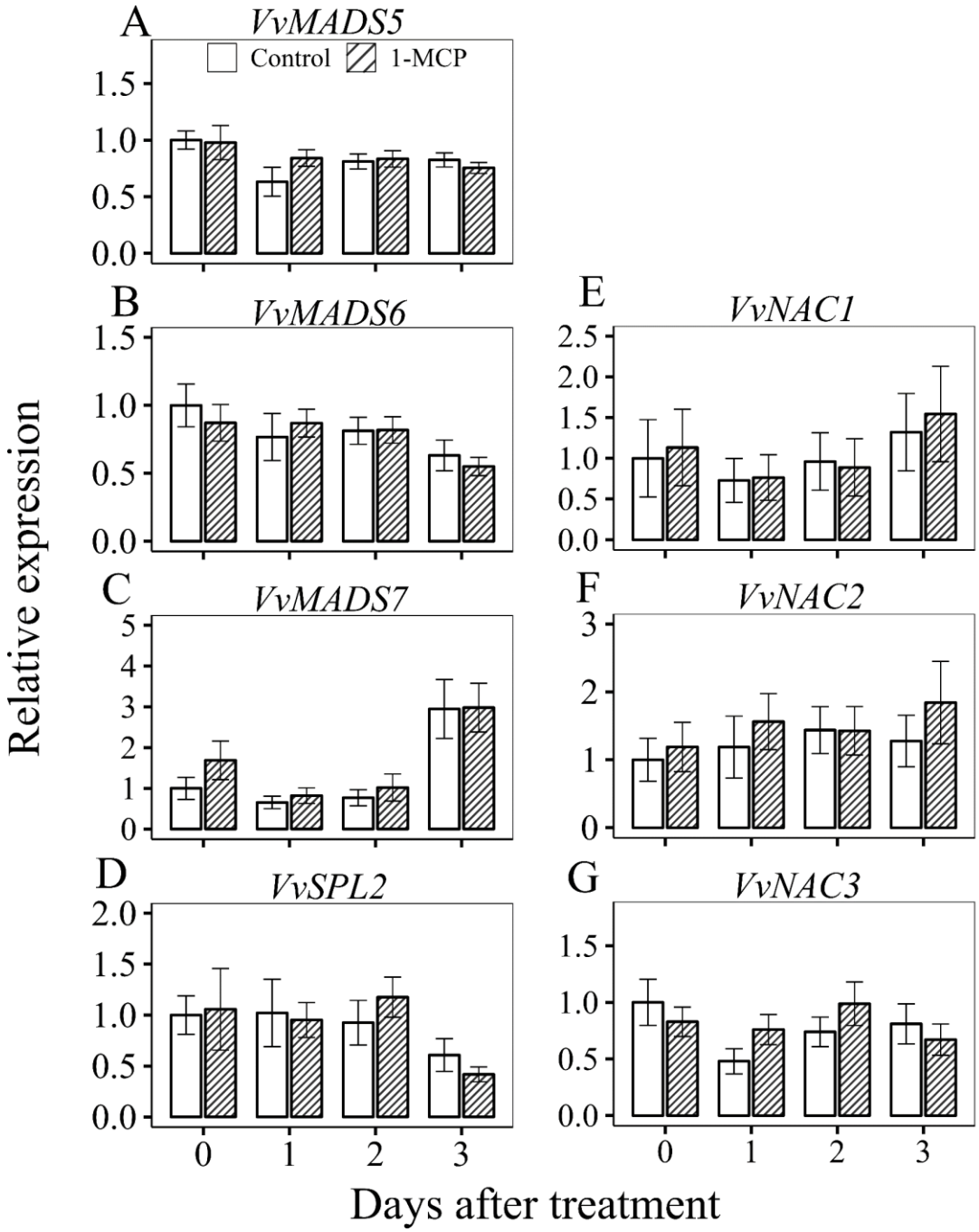

Figure 4. S5: Transcript abundance of transcription factors after treatments with water (control) and 6.6 g/L 1-MCP in 'Powderblue'.

Appendix B: Supplementary table

Table 4. S1: List of blueberry genes and primer sequences used for the quantitative RTPCR analysis.

SN	Accession number	gene	Primer orientation	Primer sequences (5' to 3')
1	PB.9095/PB.8757	*VvMADS1*	Forward	5'- GCT ATG GGT TGA GGC TAA CAA GGG T -3'
			Reverse	5'- CTT GGG TTG TCG CAG CAG TTA TCT G -3'
2	PB.15126/PB.302/PB.7873	*VvMADS2*	Forward	5'- GAG CAC AAA GGA GCT CGA GCA G -3'
			Reverse	5'- GAA TTG CAT GCT CTC CGG CCT C -3'
3	PB.14372/PB.8144	*VvMADS3*	Forward	5'- GGA ACC CAG GTG AAC ATG ATG TGG -3'
			Reverse	5'- ATC ATG TTG CCT ACC ACG ACA CG -3'
4	PB.14373	*VvMADS4*	Forward	5'- AAG CAC TTG CAA GTG GGT CAG G -3'
			Reverse	5'- TGC TAG CTA CCG TGA CAC TGC TAC -3'
5	PB.6532	*VvMADS5*	Forward	5'- GCA GCA AGG AGC TCG AGT CG -3'
			Reverse	5'- GAG TGA TAT TTG GTC TCC TCC CCA CAG -3'
6	PB.8860	*VvMADS6*	Forward	5'- GAC AAG GCA TTG CAG GAG CAG A -3'
			Reverse	5'- CTT CTC CTC TCT CTC CTT CTC CTC C -3'
7	PB.9093	*VvMADS7*	Forward	5'- CGG ATG AAG ACG AAG GCA ACA AGA -3'
			Reverse	5'- GGA GAG CGG TGT GTT CCC AT -3'
8	PB.4452	*VvSPL1*	Forward	5'- GGT GGG AGT TGA AGC TTG GAT GA -3'
			Reverse	5'- AGA GTA GTG TCC CCG CAA TCG A -3'
9	PB.306	*VvSPL2*	Forward	5'- ATG ACC CAG ATC ATT GGA GTG GC -3'
			Reverse	5'- GTC CAT TTG CGG TGG GCA TTG -3'
10	PB.3678/PB.4793	*VvSPL3*	Forward	5'-CTC CTC TGA CTG AAC CCG GTC -3'
			Reverse	5'-TAA TTG GGG CAA GTC AAC CTG GG -3'
11	PB.13418/PB.3306	*VvSPL4*	Forward	5'- GAC ATT CAT TCC AAG GCC GGT AGA G -3'

			Reverse	5'- CCT GCT ACA CTG CTG ACA GAA CC -3'
12	PB.10040/PB.9452	*VvNAC1*	Forward	5'- AAC CTT CCA CCA GGA TTC CGA -3'
			Reverse	5'- GTG GAA GGG TAA GAG AGC GGC -3'
13	PB.5254	*VvNAC2*	Forward	5'- CGG TTT TGG GCT TAA CGG TAA TGG G -3'
			Reverse	5'- AAA TGG AGA AGC ACC GGA TGC C -3'
14	PB.11364	*VvNAC3*	Forward	5'- CGT CAC CTA TCC TCT TCT CTC CCT -3'
			Reverse	5'- CGA CCA ATC CGT GCT CTC CAT G -3'
15	PB.3589	*VvNAC4*	Forward	5'- CGA CGT ACT GGG CCG TTG AC -3'
			Reverse	5'- CAA GCC ATG GTG TTG ATA CGG TTG TC -3'
16	PB.6957/PB.6283	*VvNAC5*	Forward	5'-AGA CCT GGA ACG TCT GTG AGA GTG-3'
			Reverse	5'-CAT TTC CAT CGC TGG ACC CCA AT-3'
17	PB.2804/PB.5873/ PB.10154/PB.10403	*VvNAC6*	Forward	5'-CTC TCC TAG CAG TGA GAG TTG TCT CG-3'
			Reverse	5'-GCC ATT CAG TAG CCA AAG GAG CAT C-3'
18	PB.1154	*VvNAC7*	Forward	5'- CCC GTG GTG GCT TCA GAA CTC -3'
			Reverse	5'- AGT AGG AGG ACT AGT GAT CTC CCT CG -3'
19	PB.11367/PB.4867	*VvNAC8*	Forward	5'-CCC GAC TGA TGA AGA GCT CCT TG -3'
			Reverse	5'-TGC AAG GAG AAA TGG TGC CCT G -3'
20	PB.621	*VvNAC9*	Forward	5'- GGG AGA ATT TGG CGG TCT ATG GTC -3'
			Reverse	5'- GAG AAA CAC CGC AAC GGC AAC -3'
21	PB.15164/PB.11133	*VvNAC10*	Forward	5'- CAT GGA CAC GAC GCT ATG CCA -3'
			Reverse	5'- TTC CCA CTC CCA CAG AGG GT -3'
22	PB.2969/PB.1799	*VvNAC11*	Forward	5'- TCG AGG AGA GCT GAT GGC TGT -3'
			Reverse	5'- GCG ACA TAG CAG GCA AAT CCC AG -3'
23	PB.1890/PB.3070	*VvNAC12*	Forward	5'- CCA CCC GAC TGA TGA GGA ATT GG -3'
			Reverse	5'- CCA GGG CTC AGA TTT GTA CAC ATC G -3'
24	PB.2717/PB.10507/	*VvNAC13*	Forward	5'- CAT GCT GGA AAG CAT TGC TGC TC -3'

	PB.6024/PB.10261		Reverse	5'- CCA TTG CCA CCA GAG GTC GTA -3'
25	PB.3073/PB.1893/ PB.13472	*VvNAC14*	Forward	5'- CCG CTT CGA CGC TAT CTC TGA TG -3'
			Reverse	5'- CTG GTC TTC AGC TTC GAC CTA CC -3'

CHAPTER 5

PREDICTION OF FRUIT FIRMNESS DURING POSTHARVEST STORAGE USING FRUIT PHYSICAL TRAITS AND TARGETED METABOLOMICS IN SOUTHERN HIGHBUSH AND RABBITEYE BLUEBERRY

[4] Tej P. Acharya, Yi-Wen Wang, Anish Malladi, Lynne Seymour, and Savithri U. Nambeesan. To be submitted to Scientia Horticulturae.

Abstract

Blueberries (*Vaccinium spp*.) have a shelf-life of between 1 to 7 weeks depending on cultivar, harvesting, handling, and storage method. The aim of this study is to identify relationships between metabolites, fruit quality attributes, and fruit firmness. Fruit samples were collected during the multiple time of storage from southern highbush and rabbiteye cultivars in 2015-2018. In addition, fruits samples from southern highbush cultivars, Suziblue, and Rebel in 2015 and seven other cultivars (Suziblue, Rebel, Farthing, Miss Jackie, Miss Alice Mae, Miss Lilly, and Emerald) in 2017 were collected for the metabolites analysis. Fruit quality attributes such as fruit firmness, total soluble solids content (TSS), titratable acidity (TA), fruit weight, pH, and visual quality were determined during the various postharvest stages. In 2015, 'Suziblue' displayed higher firmness (compression and puncture), whereas 'Rebel' had lower firmness during postharvest storage. In 2017, cultivars were separated according to their firmness values as follows: high ('Suziblue', 'Farthing'), medium ('Miss Jackie', 'Miss Alice Mae', 'Miss Lilly'), and low ('Rebel', 'Emerald'). Other fruit quality attributes such as TA, pH, and TSS also differed among the cultivars and at different postharvest stages. For example, 'Emerald' and 'Miss Jackie' displayed higher TA, whereas 'Rebel' and 'Miss Alice Mae' had low TA in 2017. Analysis of metabolites suggested that glucose, fructose, and sucrose comprise the major sugars, whereas quinate, malate, and citrate are the major acids in blueberry fruit. The multiple linear regression and LASSO regression model indicated that TA, mainly quinate and citrate were positively associated and major sugars were negatively associated with the fruit firmness.

Keyword: metabolites, firmness, LASSO, linear regression, postharvest

Introduction

Blueberries (*Vaccinium spp.*) are a perishable commodity and deteriorate quickly after harvest due to water loss, increase in fruit softening, and decay caused by postharvest (PH) pathogens (Li et al., 2011; Mehra et al., 2013; Paniagua et al., 2013). Therefore, the shelf-life of blueberries is relatively short, typically ranging from 1 to 7 weeks depending on factors such as the cultivar, harvesting methods, handling, and storage conditions (Connor et al., 2002; Hancock et al., 2008). Fruit firmness is generally used to determine fruit maturity and is one of the important economic traits in blueberry (Cappai et al., 2018). Further, it is associated with modifications of the major cell wall components such as a cellulose, hemicellulose, and pectin (Chen et al., 2015). These changes can cause the fruit to be susceptible to physical damage and pathogens, which ultimately results in decline of fruit quality. Inhibition of cell wall degradation enzymes, polygalacturonase, cellulase, β-galactosidase, and α-mannosidase can increase the blueberry PH shelf life (Chen et al., 2015). Similarly, certain metabolites have been associated with changes in fruit firmness and PH shelf life. For example, galactinol, raffinose, myo-inositol, and trehalose can increase PH storage life by withstanding the stress condition in plums (Farcuh et al., 2018). It is speculated that these metabolites play a role in osmoprotection and prevent water loss (Iturriaga et al., 2009). Studies in tomatoes have shown that metabolites such as citramalic, gluconic, and keto-l-gulonic acids positively associated with the PH shelf-life (Oms-Oliu et al., 2011). Also, membrane-bound fatty acids can have a significant impact on increasing fruit firmness. Studies in peaches have revealed that saturated fatty acids and oleic acids exhibit a

positive correlation with fruit firmness, while linolenic acid displays a negative correlation (Duan et al., 2013).

When comparing the shelf-life of fruits based on at least 50% healthy fruits during storage, it was observed that northern highbush cultivars like Brigitta, Legacy, and Bluegold could be stored for up to 4 to 7 weeks at 0 °C with ambient oxygen, carbon dioxide, and 90% relative humidity (Hancock et al., 2008). However, cultivars like Nelson, Little Giant, and Jersey only remained viable for 1 to 2 weeks under similar storage conditions, suggesting variation in shelf-life among cultivars within northern highbush blueberry (Hancock et al., 2008). Two other types of blueberries, the southern highbush (*V. corymbosum*) and rabbiteye (*V. virgatum*) are commonly grown blueberries in southeastern U.S. The southern highbush (SHB) was developed by crossing northern highbush cultivars with *Vaccinium spp.* found in Florida and southeastern U.S. (Williamson et al., 2019). Rabbiteye (RE) blueberry are native in the southeastern U. S. (Strik et al., 2014). These types of cultivars require low-chilling temperatures, and readily grown in areas with long and hot summers. SHB fruit ripen early and therefore growers get a premium price. However, RE blueberries make up a significant portion of the blueberry industry in the southeastern region. Previous studies found that SHB cultivars had higher fruit firmness at harvest and 30 days after storage, compared to RE cultivars (Mooneyham et al., 2020). However, limited information available on the total soluble solids (TSS), titratable acidity (TA) and other metabolites (individual sugars and acids) that predict fruit quality in blueberries. Identifying the physical or metabolic traits that are key determinants of fruit firmness would be invaluable for enhancing breeding programs aimed at selecting cultivars with improved fruit quality attributes. This is particularly important because both wholesale buyers and consumers place great

importance on the appearance and firmness of fruits, as these factors are closely associated with overall fruit quality (Boyette et al., 1993; MacLean and NeSmith, 2011). Therefore, our interest lies in identifying candidate metabolite markers to enhance blueberry fruit firmness by analyzing both the physical and chemical traits of the fruit during PH storage.

Material and Methods:

Plant Material: Fruit were collected over four years from 2015-2018, from two farms, a research farm in Alapaha, GA and a commercial farm in Manor GA (Table 1). In 2015, blueberry fruits were collected from 2 southern highbush cultivars, Suziblue and Rebel, and 4 rabbiteye cultivars, Premier, Powderblue, Titan, and Vernon, at UGA Blueberry Research Farm in Alapaha, GA. Similarly, in 2016, fruits were harvested from 5 southern highbush blueberry cultivars: Suziblue, Rebel, Miss Lilly, Miss Jackie, and Miss Alice Mae, and 3 rabbiteye blueberry cultivars: Premier, Krewer, and Titan, at UGA Blueberry Research Farm in Alapaha, GA. In 2017, fruits were harvested from 7 southern highbush blueberry cultivars: Suziblue, Rebel, Miss Lilly, Miss Jackie, Miss Alice Mae, Emerald, and Farthing, and 4 rabbiteye blueberry cultivars: Krewer, Titan, Alapaha, and Brightwell, at Cornelius Farms in Manor, GA. In 2018, fruits from 3 southern highbush blueberry cultivars, Rebel, Miss Alice Mae, and Emerald, were collected at Cornelius Farms in Manor, GA. Additionally, three more southern highbush blueberry cultivars, Suziblue, Miss Lilly, Miss Jackie, and 4 rabbiteye blueberry cultivars, Alapaha, Brightwell, Krewer, and Titan, were collected at UGA Blueberry Research Farm in Alapaha, GA (Table 1). All fruits were harvested at the fully ripe stage.

Sampling of fruit during postharvest storage: Fruit harvested from farms were brought back to Athens, GA and stored in a walk-in cooler maintained at 4 °C and ~95% relative humidity. The following day fruit were sorted to remove any damaged fruit that were harvested and distributed in clamshells, such that fruit for a given time-point and from a single replicate was stored in one clamshell. All clamshells were placed back into the walk-in cooler. Subsequently, multiple PH fruit quality attributes (see next section) were measured at following times during storage. Fruit quality attributes were measured in 2015 for SHB at PH3, 8, 12, 21, and for RE at PH3, 8, 12, 21, 28; in 2016 for SHB at PH3, 10, 17, 24, 32, 38, 45 and RE at PH3, 10, 17, 26, 33. In 2017 for SHB, 'Suziblue', 'Miss Lilly', 'Miss Jackie' at PH5, 12, 21, 35, 47, for 'Miss Alice Mae' at PH5, 12, 21, 35, and for 'Rebel', 'Emerald', and 'Farthing' at PH4, 12, 21, 32, 47. For the RE cultivars, measurements were done for Krewer and Titan at PH4, 12, 21, 32, and for Alapaha and Brightwell at PH4, 12, 21, 32, 47 . Moreover, in 2018, 'Suziblue', 'Miss Lilly', and 'Miss Jackie' fruit quality measurements were done at PH2, 12, 20, 'Rebel' and 'Emerald' at PH3, 11, 21, 32, 44; and 'Miss Alice Mae' at PH3, 11, 21, 32. Additionally, PH quality measurements for RE cultivars Krewer and Titan at PH4, 12, 21; and for Alapaha and Brightwell at PH4, 12, 21, 32 were conducted in 2018. Prior to the measurements for fruit quality attributes, the samples were allowed to equilibrate at room temperature for one hour, after which the measurements were conducted. If cultivars displayed deterioration beyond a certain point in given year due to shriveling, dent, and mold symptoms, it resulted in discontinuation of fruit quality measurements for those cultivars during the later PH storage.

Measurement of fruit quality attributes: Fruit quality attributes including the percentage of healthy fruit, TSS, TA, ratio between TSS and TA, pH, fruit weight, compression, and puncture were measured at the various PH storage. A visual assessment was performed with 30 fruit for symptoms of shriveling, cracking, bruising, or mold, and percent healthy fruit was calculated. For determination of TSS, TA and pH, 40 g of fruit were pureed using a blender (Magic Bullet, China) and subjected to centrifugation at 4000 x *g* for 10 min. The supernatant was used to determine TSS, TA, and pH. TSS was measured using a digital handheld refractometer (Atago, USA). The TA and pH were measured using an automated mini titrator (Hanna Instruments, USA). The pH electrode associated with the titrator displays an initial pH measurement of the supernatant before the titration process commences, and this initial value was recorded for the pH measurement. The TA was measured using a citric acid standard. Fruit weight of 20 fruits were measured using a precision balance (Quintix® Precision Balance, Sartorius, Bohemia, NY, USA). The fruit firmness, compression and skin puncture measurements were performed using a Fruit Texture Analyzer [Model GS-15, Güss Manufacturing (Pty) Ltd., Strand, South Africa]. Twelve fruits from each replication were used for this textural analysis.

Metabolite determination using gas chromatography: Fruits samples were collected at the three developmental time-points: green, pink, ripe in 2015 and 2017; and during PH storage PH3, PH13, and PH21 in 2015 and PH4/5, PH12, and PH21 in 2017. For the developmental time-points, green fruits were collected based on the size and color (<13 mm and <30% pink), the pink stage was characterized as predominately pink in color, and ripe as a fully ripe fruits. The PH samples were stored in a walk-in cooler as described above and 6-8 fruit were randomly

selected from a clamshell for metabolite analysis on respective days. All samples were collected in four replicates and frozen in liquid nitrogen, then stored at -80°C until further analysis.

The key sugars, acids, and amino acids were extracted according to Beshir et al. (2017), with some modifications. First, frozen fruit tissues were ground into fine powder using a mortar and pestle in liquid nitrogen. Then, 125-150 mg of fruit powder was extracted into 1.5 ml methanol containing 0. l25 mg/ml of phenyl-β-D-glucoside as an internal standard. After that, methanol extracted samples were centrifuged at 22,000 x *g* for 30 minutes at 4 ℃. Next, 100 µl of supernatant was transferred into a 300 µl of glass insert in a 2 ml GC vial. The solvent was evaporated using nitrogen gas at 45 ℃. Subsequently, samples were derivatized by methoxymation followed by the silylation. First, 50 µl of methoxamine (20 mg methoxamine in 1 ml pyridine) was added to each sample and heated at 50 ℃ for 30 minutes. Then, 100 µl of N-Methyl-N-(trimethylsilyl) trifluoroacetamide (MSTFA) + 1% TMCS (trimethylchlorosilane) was added to each sample and heated at 50 °C for 30 minutes. Finally, these derivatized samples were utilized to analyze the metabolites using GC.

Metabolites were quantified using the Gas Chromatography-Fame Ionization Detector (GC-FID) (GC-2014; Shimadzu, Japan). A HP-5 fused capillary column (J&W Scientific, Fulsom, CA, USA) was used. Helium was used as a carrier gas. The 20:1 split ratio was used for this study. The initial temperature of the oven was set up at 120 °C for 1 minute, then 4 °C per minute ramped to 180 ℃, 0.5 min at 180 °C, 0.5 ℃ per minute ramped to 185 ℃, 0.5 min at 185 ℃, 1 ℃ per minute ramped to 210 ℃, 0.5 minutes at 210 ℃, 10 °C per minute ramped to 260 °C, and finally held for 12 minutes at 260 °C. A standard solution was prepared for each of the

identified metabolites. The standards were extracted and derivatized as described for the fruit samples. Standard curves were generated individually for each metabolite and used for the quantification.

Anthocyanin determination: Anthocyanin measurements were conducted on the same samples used for metabolite measurements. Total anthocyanins were extracted according to Karppinen et al. (2018), with some modifications. Approximately, 100 mg of fine powder was extracted using 2 ml of 100% methanol containing 0.1% HCl. The samples were thoroughly vortexed and then sonicated in the dark for 10 minutes using a sonicator (Branson Ultrasonics Corp., Danbury, CT). Subsequently, the tubes were mixed in the dark for 1 hour at 300 x *g* using an Environ-shaker (Lab-Line Instruments Inc., Melrose Park, IL). Finally, the samples were centrifuged at 2000 x *g* at 20°C for 25 minutes, and the supernatant was transferred to new 1.5 ml tubes.

The determination of anthocyanin content was carried out using the differential pH method. Initially, buffer solutions were prepared: one with 0.025 M potassium chloride at pH 1.0 and another with 0.6 M sodium acetate at pH 4.5. Subsequently, 160 µl of each buffer solution was added individually to each well of a 96-well plate (Becton Dickinson, Franklin Lakes, NJ), and 40 µl of the extracted supernatant was added to each well. Blank samples were prepared by adding 40 µl of the extraction buffer (100% methanol + 0.1% HCl) to each potassium chloride and sodium acetate solution. The samples were thoroughly mixed using a multi-channel pipette, and absorbance readings were taken at 520 and 700 nm using a microplate reader (BioTek, Winooski, VT). Finally, anthocyanin concentrations were calculated as cyanidin-3-glucoside equivalents using a previously described equation (Lee et al., 2005; Lee et al., 2008).

Statistical analysis: The data were analyzed and visualized using R-studio 2023 (R core 2023, Vienna, Austria). To assess the significance of treatment effects, an analysis of variance (ANOVA) was conducted. Additionally, multiple comparisons were performed using Fisher's Least Significant Difference (LSD). Principal component analysis (PCA) was carried out using the FactoMiner and Factoextra packages in R. The results of PCA, including contributions of the first two principal components, loading plots, and scree plots, are presented in this study. In addition, stepwise linear regression (SLR) and LASSO (least absolute shrinkage and selection operator) were performed as described below.

Stepwise linear regression: The SLR model was used for prediction of fruit compression or puncture as a dependent variable and fruit physical traits as an independent variable. The fruit quality attributes at different PH storage from 2015-2018 were pooled together and fitted together to obtain meaningful information. The model for MLR is: $Y = \beta0 + \beta1*X1 + \beta2*X2 + ... + \beta n*Xn + \varepsilon$, where Y is the dependent variable; X1, X2, Xn are the independent variables; $\beta0, \beta1, \beta2, ..., \beta n$ are the coefficients to be estimated; and ε is the error term. In this model, we utilized a backward elimination procedure. In other words, we started a model with all predictors as a variable and removed the least significant predictor one at a time until all predictors were significant at $\alpha=0.05$ level.

LASSO regression: The LASSO regression model was used to predict compression or puncture as a dependent variable and fruit metabolite as an independent variable. Fruit

metabolite measurements during the PH storage in 2015 and 2017 and their respective compression and puncture at the same time points were taken for the analysis. LASSO finds the optimal regression coefficients by minimizing the function given as below (James et al., 2013).

$$J = \text{RSS} + \lambda \sum_{j=1}^{p} |\beta_j|, \text{ and } RSS = \sum_{i=1}^{n} \left(Y_i - \beta_0 - \sum_{j=1}^{p} \beta_j x_{ij}\right)$$

Where, J is the objective function to be minimized, RSS is the residual sum of squared, $\lambda \sum_{j=1}^{p} |\beta_j|$ is the regularization component and λ is the penalty term, p is the number of predictor variable, Y_i is the target variable for the i^{th} data, β_0 is the intercept, β_j is the coefficient for the j^{th} variable, and x_{ij} is the value for the j^{th} predicted variable for the i^{th} data.

We used the R package 'glmnet' to fit the linear regression with LASSO. The train and test data sets were divided into 80% and 20%, respectively, and the parameter was optimized using 10-fold cross-validation. The optimal λ values were selected based on the minimum mean squared error (MSE) via cross-validation. Finally, the coefficients of the most important variables, variable importance, and predicted vs. observed values were identified and presented in this study.

Results and Discussion:

Fruit quality attributes: The percentage of healthy fruits decreased as PH stages progressed in all cultivars and years (Fig. 5.1-5.2A and Fig. 5. S1-S6A). Visual assessment was based on presence of dents, shriveling, bruising and appearance of mold. Other studies support that reduction in the percentage of healthy fruits during storage could be attributed to factors such as

softening, pathogen infestations, denting, and shriveling (Li et al., 2011; Mehra et al., 2013; Paniagua et al., 2013). In 2015, ‘Suziblue’ exhibited a consistently higher percentage of healthy fruit throughout the storage period compared to ‘Rebel’ (Fig. 5. S1A). In 2016, ‘Miss Alice Mae’, ‘Miss Jackie’, and ‘Miss Lilly’ demonstrated relatively better storage performance compared to ‘Suziblue’ and ‘Rebel’ (Fig. 5. S3A). In 2017, ‘Suziblue’, ‘Miss Lilly’, and ‘Rebel’ showed good storage characteristics, while ‘Emerald’, ‘Miss Jackie’, and ‘Miss Alice Mae’ had a lower percentage of healthy fruits. In 2018, the percentage of healthy fruit declined rapidly in ‘Suziblue’, ‘Miss Lilly’, ‘Miss Jackie’, and ‘Miss Alice Mae’, while ‘Rebel’ and ‘Emerald’ maintained relatively higher visual quality. Overall, the percentage of healthy fruits in SHB cultivars exhibited some inconsistencies across different years of the study. This variability was mostly attributed to differences in environmental conditions, for example in 2018, a lot of rain resulted some cultivars such as Suziblue displaying lower fruit quality compared to previous years. The management practices in commercial farms were geared towards achieving optimal fruit quality and therefore may have better fruit quality compared to the research farms. Since fruit were picked when available the harvesting time points may have varied across years, and previous studies have indicated that timing of picking may influence fruit quality (Cvetković et al., 2022).

In case of RE cultivars in 2015, we observed that the percentage of healthy fruits was greater in ‘Vernon’ compared to ‘Powderblue’, ‘Premier’, and ‘Titan’ (Fig. 5. S2A). In 2016, no significant differences in visual quality were observed among all three cultivars used for this study (Fig. 5. S4A). In 2017 and 2018, ‘Alapaha’ and ‘Brightwell’ had higher percentage of

healthy fruits than other cultivars (Fig, 5.2A and Fig. 5. S6A), leading us to conclude that these two cultivars exhibited better visual PH shelf life when compared to other RE cultivars. Conversely, the percentage of healthy fruits in ‘Krewer’ and ‘Titan’ was consistently lower across all the studied years, suggesting that these two cultivars had relatively poorer visual PH shelf life.

Comparison between SHB and RE cultivars, showed that, except in 2015, where no significant differences were found, in 2016, 2017, and 2018, SHB cultivars increased the percentage of healthy fruits by 21%, 18%, and 7% respectively, compared to RE cultivars (Fig. 5.3A). Overall within the cultivars surveyed in this study, SHB cultivars exhibited better visual storage performance compared to RE cultivars.

Fruit firmness, measured through compression and puncture, generally did not decrease over time (Fig. 5.1, 5.2G, H; Fig.5.S1-S6G). However, certain cultivars, such as ‘Rebel’ from 2016 to 2018, displayed a softening of fruit and a decrease in skin toughness over time. In fact, in many cultivars, a common trend was observed, where firmness increased initially during storage, only to decline and return to the initial compression value for the remaining storage period, as exemplified by ‘Miss Jackie’ in 2016. These result aligns with a previous study which found that a small loss of fruit weight (≤1.34%) during cold storage resulted in firmer blueberry fruits due to localized dehydration of the outer cell layers of blueberries (Paniagua et al., 2013).

Fruit texture varied among cultivars in both SHB and RE blueberries. Among SHB cultivars, Suziblue and Farthing exhibited higher compression and puncture values, while Rebel

and Miss Lilly had relatively lower values (Fig. 5.1G, H, Fig. 5. S1, S3, S5G, H). Among RE cultivars, Titan and Brightwell had higher compression and puncture values, while Premier and Powderblue had lower values (Fig. 5.2G, H, Fig. 5. S2, S4, S6G, H). The cultivars, with differences in fruit texture, offers future opportunities to investigate how variations in texture lead to the maintenance of visual PH fruit quality attributes.

When comparing SHB and RE cultivars, compression values were higher in SHB in the 2018 study, while puncture values were consistently higher across all years. The puncture test represents a composite of skin toughness and fruit firmness, whereas compression values mostly measure fruit firmness. Therefore, our data suggests that SHB cultivars generally had firmer skin toughness compared to RE cultivars (Figure 5.3H). This is consistent with the previous study where they found greater fruit firmness in SHB cultivars compared to RE (Mooneyham et al., 2020).

We also assessed several other fruit quality attributes, including TSS, TA, TSS/TA ratio, and pH. Overall, we did not observe consistent variations within a given cultivar during the PH storage over the years (Fig. 5.1-5.2B-E; Fig. 5. S1-S6B-E). The only consistent trend observed was in the two SHB cultivars, Rebel and Emerald, where TSS and TA consistently decreased, while the TSS: TA ratio and pH increased during post-harvest storage, except for TA and TSS/TA ratio in ‘Rebel’ 2016 and TSS in ‘Emerald’ 2018. Specifically, in the third week of storage compared to the first week, these two cultivars exhibited decreases of 0.5 to 1.4 level °Brix in TSS and 0.07-0.25% in TA, while TSS/TA and pH increased by 5.8-47 in ratio and 0.30-0.45 in pH, respectively. In the other cultivars, the trends for these four fruit quality

attributes were inconsistent across different years during PH storage. ‘Miss Alice Mae’ showed a consistent decrease in TSS during storage in all years, however, TA levels decreased and TSS: TA ratios and pH increased in 2016 and 2018, with no significant change in 2017. ‘Miss Lilly’ displayed no change in TSS at all sampling dates, with TA decreasing only in 2016. The decrease in TA resulted in an increase in TSS/TA that year during storage. In the RE cultivars, we observed a decrease in TSS and TA content in ‘Premier’ and ‘Powderblue’, while all other RE cultivars exhibited inconsistent responses in TSS, TA, TSS/TA ratio, and pH during PH storage (Fig. 5.2, Fig. 5. S2, Fig. 5. S4, and Fig. 5. S6).

We also compared TSS content between the cultivars. In 2015 and 2018, ‘Suziblue’ had higher TSS and TA content and lower TSS/TA ratio and pH content than ‘Rebel’. In 2016, both cultivars exhibited similar TSS and TA content. In 2017, ‘Rebel’, ‘Emerald’, and ‘Miss Alice Mae’ had higher TSS than ‘Suziblue’, ‘Miss Lilly’, and ‘Miss Jackie’. In 2018, ‘Suziblue’, ‘Rebel’, and ‘Miss Jackie’ had higher TSS. Therefore, the TSS contents in the cultivars varied inconsistently, depending on the year, environmental conditions, and cultivation practices. The TA was higher in ‘Miss Jackie’ in 2016, 2017 and ‘Emerald’ in 2017. Overall, this study allows us to conclude that ‘Miss Jackie’ and ‘Emerald’ had higher TA compared to other SHB cultivars. The TSS/TA ratio and pH were higher in ‘Rebel’ and ‘Miss Alice Mae’ compared to other SHB cultivars throughout the growing season.

In the RE cultivars in 2015, TSS was higher in ‘Powderblue’, followed by ‘Premier’, with ‘Titan’ and ‘Vernon’ having lower TSS (Fig. 5. S2B). The higher TSS, along with lower TA, resulted in a higher TSS/TA ratio and pH in ‘Premier’ compared to other RE cultivars in

2015 (Fig. 5. S2C-E). In 2016, TSS, TSS/TA ratio, and pH were higher in ‘Krewer’ and ‘Premier’ compared to ‘Titan’, whereas TA was greater in 'Titan’, (Fig. 5. S4). In 2017 and 2018, TSS was lower in ‘Titan’ compared to 'Alapaha’, ‘Brightwell’, and ‘Krewer’, while TA was higher in ‘Titan’ in 2018 (Fig. 5.2B and Fig. 5. S6B). In 2017, inconsistent results were found for the TSS: TA ratio and pH content. The TSS/TA ratio and pH were greater in ‘Krewer’ and ‘Titan’ in 2017 but shifted to ‘Alapaha’ and ‘Brightwell’ in 2018 (Fig. 5.2 D, E, and Fig. 5.2 S6 D, E). Overall, inconsistent results were observed for the TSS, TA, TSS/TA ratio, and pH content in RE cultivars. Previous study found that higher rainfall decreased the fruit firmness, TSS and TA content in the fruits (Sater et al., 2021). Similarly, TSS and TA content in fruits is affected by the year and harvest date in blueberry (Kalt and McDonald, 1996; Redpath et al., 2021).

In the case of SHB vs. RE cultivars, the average TSS was higher in RE blueberries compared to SHB blueberries (Figure 5.3B). In SHB, the TA was higher in 2017, pH in 2018, whereas the TSS/TA ratio was lower in 2018 compared to RE cultivars (Fig. 5.3C-E).

Fruit weight remained relatively stable throughout the PH storage in both SHB and RE cultivars, with a few exceptions noted in ‘Premier’ and ‘Titan’ in 2016, ‘Emerald’ and ‘Krewer’ in 2017, and ‘Suziblue’ and ‘Rebel’ in 2018, where a slight decline in fruit weight was observed during PH storage (Fig. 5.1F, Fig. 5.2F, and Fig. 5.1S1-S6F). Fruit storage at 4 °C and 95% relative humidity likely contributed to this minimal variation in weight, as these conditions are conducive to reduced respiration and water loss.

In our study, we found variation in fruit weight among both SHB and RE cultivars. Among SHB cultivars, Miss Lilly exhibited higher fruit weight compared to other SHB cultivars studied in this research (Fig. 5.1F, Fig. 5. S1F, Fig. 5. S3F, and Fig. 5. S5F). In the case of RE cultivars, fruit weight was higher in 'Titan' and 'Krewer' compared to all other RE cultivars included in the study (Fig. 5.2F, Fig. 5. S2F, Fig. 5. S4F, and Fig. 5. S6F). When comparing SHB and RE cultivars, RE cultivars had higher fruit weight only in 2016, while in other years, the two groups exhibited similar fruit weights (Fig. 5.3F).

Fruit firmness prediction using quality attributes: In our study, we employed SLR model to predict fruit firmness. The coefficients and *P*-values are presented in Table 5.2. These coefficients provide insights on the direction and magnitude of the relationship between the dependent and independent variables. A positive coefficient suggests that when the independent variable increases, the dependent variable typically follows suit, while a negative coefficient indicates the opposite relationship, where an increase in the independent variable is associated with a decrease in the dependent variable.

When compression was used as an independent variable, six fruit quality parameters displayed significant differences, with the exception of TSS, which did not exhibit variation (Table 5.2A). The coefficient value for puncture was 0.76 and significant, indicating that for each unit increase in puncture, the compression value increases by 0.76, assuming all other parameters remain constant. Given that puncture and compression are both related fruit firmness, a high association between the two parameters is expected. Additionally, the percentage of healthy berries had a positive association with compression, suggesting that healthy berries tend

to exhibit less shriveling and damage, resulting in firmer fruit. Fruit weight showed a positive association, indicating that increasing fruit size could increase fruit compression. However, other factors like TA, TSS/TA, and pH should also be considered, as they exhibit negative associations with fruit compression.

Also, we predicted puncture, another significant variable related to fruit firmness, and found that it was positively related to compression. Other quality attributes, such as TA and TSS, showed positive and negative associations with puncture, respectively (Table 5.2B). This implies that cultivars with higher TA tend to have higher puncture values, while those with more TSS content tend to have lower puncture values. It's intriguing to note that TA was negatively associated with compression and positively associated with puncture. The measurement of TA results in a composite value for all the acids present in fruits, making it important to assess the contribution of each acid in the regression model. Lastly, we evaluated the accuracy of the prediction versus the observed values, which yielded R-squared (R^2) values of 0.51 for compression and 0.55 for puncture (Fig. 4.4A-B), reflecting the model's performance and explanatory power.

Metabolites analysis: To determine the variation among metabolites during fruit development and ripening in both cultivars, a PCA was conducted (Fig. 5.5). Overall, 59.1% of the variation in data was explained by the first two dimensions (Fig. 5.5A). The first dimension captured the variation among the ripening and PH stages, where green to PH21 separated on the X-axis. Malate, citrate and quinate were mainly associated with green stages. In contrast, the major sugars were associated with the ripe and PH stages. Dimension 2 depicted the variation among

the cultivars separated on the Y-axis (Fig. 5.5A). Analysis of the loading plot explained the contribution of each metabolite in the first two PCs (Fig. 5.5B). Most of the metabolites accounted for over 7% of the variance in the first two PCA, with the exception of quinate, succinate, myo-inisitol, glutamine, malate, xylose, glutamate, and shikimate, which contributed less than 7%.

Furthermore, we determined major metabolites changes during the ripening and PH stages. Overall, sugars increased and acid decreased during the ripening stages which included green, pink and ripe (Fig. 5.6, Fig. 5. S7). The concentration of glucose, fructose, and sucrose at ripe fruits compared to green fruits increased by 2.5-, 2.6-, and 2.0-fold, respectively in 2015 (Fig. 5. S7A-C). Whereas in 2017, glucose, fructose and sucrose at ripe compared to green stage increased by 2.1-, 2.1-, and 1.8-fold, respectively (Fig. 5.6A-C). These results are consistent with our previous study that found increase in major sugars during the ripening in rabbiteye blueberries (Chapter 2). The increase in sucrose was due to the continuous translocation from the source organs and associated with increased in transcript abundance of sucrose catabolism enzymes like *SUCROSE SYNTHASE* and *VACUOLAR INVERTASE* (Chapter 2). Ripening-related increases in sucrose was also observed in other fruits such as apple (Li et al., 2012), strawberry (Liu et al., 2020), and grape (Zhu et al., 2017). In addition, the concentration of glucose and fructose increased steadily or remained relatively stable during earlier to mid-developmental stages, while at later developmental stages, rapid sugar accumulation was observed in grapes, strawberries, and bilberries (Zhu et al., 2017; Liu et al., 2020; Samkumar et al., 2022).

In contrast, the concentration of malate, citrate and quinate in ripe fruits decreased by 4.9-, 4.0-, and 3.6-fold, respectively compared to green fruits in 2015 (Fig. 5. S7D-F). In 2017, the overall concentration of malate, citrate and quinate at ripe compared to green stages decreased by 7.2-, 3.4-, and 3.2-fold, respectively (Fig. 5.6D-F). This trend observed during ripening is consistent with a decrease in concentration of major acids during ripening in rabbiteye blueberries, with the exception of citrate which did not decrease during the ripening in rabbiteye cultivars. Also, in the rabbiteye cultivars, quinate was the primary acid to accumulate during ripening (Chapter 2). However, in this study citrate was the primary acid in southern highbush cultivars, consistent with a previous study (Zhang et al., 2020). Blueberry fruits increased respiration during the onset of ripening (Wang et al., 2022). Organic acid accumulation, which occurs earlier during fruit development is an important substrate needed for the respiratory burst during the onset of ripening in fruits (Seymour et al., 2013).

The concentration of aspartate and glutamate, two major amino acids detected in this study also increased at the ripe fruit stage compared to green fruits in majority of the cultivars tested in this study (Fig. 5.6 G, H; Fig. 5. S7G, H). The increase in these two amino acids could be due to an increase in their biosynthesis during the ripening using oxaloacetate as a precursor for the formation to these compounds. We also determined other compounds like shikimate, myo-inisitol, glycerate, serine, threonine, xylose, and glutamine; however, their concentration was low during ripening.

In majority of cultivars, malate, citrate and quinate concentrations did not change during PH storage. In case of sugars, only sucrose exhibited slightly decreased in pattern from the ripe to various PH storage in majority of cultivars. Overall, after two weeks of storage sucrose

concentration decreased by 1.9- and 1.2-fold in 2015 and 2017, respectively. During the metabolic processes, the breakdown of sucrose can occur in various cellular compartments, including the apoplastic space, cytosol, and vacuoles. Importantly, after harvest, there is no translocation of sucrose from the source organs to other parts of the plant. As a result, the observed decrease in sucrose concentration in this study may be attributed to providing a carbon source for various metabolic processes during the PH stages. Overall, storage at 4 C may have led to relatively minor changes in metabolite concentration during PH storage. The concentration of shikimate, myo-inisitol, glycerate, serine, threonine, xylose, and glutamine were low during PH storage.

Fruit firmness prediction using metabolites: In the metabolite data, we encountered issues of multicollinearity, particularly concerning fructose, glucose, and sucrose, which had variance inflation factors of 247, 277, and 25, respectively (Table 5. S1). In such a scenario, the SLR model does not perform well due to the collinearity issues, that can lead to overfitting and a loss of robustness in the models (Saranwong et al., 2001; Næs et al., 2002; Nicolai et al., 2007). Hence, we employed the LASSO regression model to predict fruit firmness using the metabolite data. The LASSO regression model reduces the coefficients of less important variables in the dataset to zero, retaining only the most important variables for model prediction (Ljubobratović et al., 2022). This approach helps address the issue of multicollinearity and enhances the model's performance and interpretability.

In this study, we identified several metabolites that were either positively or negatively associated with fruit compression and puncture predictions, as presented in Table 5.3. Notably,

serine, quinate, citrate, and myo-inositol exhibited positive associations with fruit compression. Conversely, sucrose, fructose, xylose, shikimate, succinate, glutamate, threonine, aspartate, anthocyanin, and malate were negatively associated with fruit compression. Similarly, for puncture prediction, sugars like fructose and xylose showed negative associations, while acids like quinate and citrate were positively associated (Table 5.3). These findings suggest that cultivars with higher citrate and quinate concentration along with a reduction in malate levels, are associated with higher fruit firmness. In this study, RE cultivars displayed a lower fruit firmness compared to SHB cultivars. Interestingly RE cultivars had higher levels of malate compared to citrate during fruit development and ripening (Chapter 1, Figure 5.6D, E). If the reduction in fruit firmness in RE cultivars is associated with higher malate content and lower citrate content during fruit ripening requires further investigation. Contrary to our study, positive association between malate content and fruit firmness of found in tomato (López et al., 2015). In blueberries, a higher concentration of citrate and phenylalanine in ripe fruits is positively correlated with fruit firmness, while xylose, leucine, and shikimate show a negative correlation (Montecchiarini et al., 2018).

Additionally, decrease in sugar concentration may enhance fruit firmness. An increase in sugar import in the fruit from source tissue increases water influx during fruit ripening (Chapter 2). If an increase in water uptake can increase cell turgor and associated decline in fruit firmness due to pressure exerted on the cell wall will warrant further investigation. However, it is essential to consider that high sugars and low acids in ripe fruit play a significant role in contributing to the flavor of the fruits

The variable importance plot provides insights into the contribution of each variable to the model's prediction. In the compression prediction, serine made the most significant contribution, followed by quinate, shikimate, sucrose, and succinate (Figure 5.7A). On the other hand, aspartate, citrate, and malate made relatively lesser contributions in this context. Similarly, for the puncture prediction, fructose was the most influential variable, followed by glutamine, quinate, and myo-inositol. In contrast, citrate, glycerate, and glutamate were among the variables that made the least contribution (Figure 5.7B). Lastly, the prediction versus observed plot demonstrated the model's accuracy, yielding an R^2 value of 0.70 for the compression prediction and 0.60 for the puncture prediction (Fig. 4.4A-B), showing the model's effectiveness in explaining the observed data.

Conclusion: In this study, we comprehensively compared fruit quality attributes during the PH stages in RE and SHB blueberry cultivars. We revealed significant variability and differences among cultivars within SHB and RE groups, shedding light on the detailed dynamics of fruit quality attributes during storage. Furthermore, we successfully predicted fruit firmness using a combination of fruit quality attributes and metabolites. Notably, TA, specifically quinate and citrate, exhibited positive associations with fruit firmness. Conversely, sugars and amino acids displayed negative associations with fruit firmness. This valuable information can inform and guide future breeding programs to enhance fruit firmness in blueberries.

References

Beshir WF, Mbong VB, Hertog ML, Geeraerd AH, Van den Ende W, Nicolaï BM (2017) Dynamic labeling reveals temporal changes in carbon re-allocation within the central metabolism of developing apple fruit. Frontiers in Plant Science **8:** 1785.

Boyette M, Estes E, Mainland C, Cline W (1993) Postharvest cooling and handling of blueberries. AG (USA) .

Cappai F, Benevenuto J, Ferrão LFV, Munoz P (2018) Molecular and genetic bases of fruit firmness variation in blueberry—A review. Agronomy **8:** 174.

Chen H, Cao S, Fang X, Mu H, Yang H, Wang X, Xu Q, Gao H (2015) Changes in fruit firmness, cell wall composition and cell wall degrading enzymes in postharvest blueberries during storage. Scientia Horticulturae **188:** 44-48.

Connor AM, Luby JJ, Hancock JF, Berkheimer S, Hanson EJ (2002) Changes in fruit antioxidant activity among blueberry cultivars during cold-temperature storage. Journal of agricultural and food chemistry **50:** 893-898.

Cvetković M, Kočić M, Dabić Zagorac D, Ćirić I, Natić M, Hajder Đ, Životić A, Fotirić Akšić M (2022) When Is the Right Moment to Pick Blueberries? Variation in Agronomic and Chemical Properties of Blueberry (Vaccinium corymbosum) Cultivars at Different Harvest Times. Metabolites **12:** 798.

Duan Y, Dong X, Liu B, Li P (2013) Relationship of changes in the fatty acid compositions and fruit softening in peach (Prunus persica L. Batsch). Acta physiologiae plantarum **35:** 707-713.

Farcuh M, Rivero RM, Sadka A, Blumwald E (2018) Ethylene regulation of sugar metabolism in climacteric and non-climacteric plums. Postharvest Biology and Technology **139:** 20-30.

Hancock J, Callow P, Serçe S, Hanson E, Beaudry R (2008) Effect of cultivar, controlled atmosphere storage, and fruit ripeness on the long-term storage of highbush blueberries. HortTechnology **18:** 199-205.

Iturriaga G, Suárez R, Nova-Franco B (2009) Trehalose metabolism: from osmoprotection to signaling. International journal of molecular sciences **10:** 3793-3810.

James G, Witten D, Hastie T, Tibshirani R (2013) An introduction to statistical learning, Vol 112. Springer.

Kalt W, McDonald JE (1996) Chemical composition of lowbush blueberry cultivars. Journal of the American Society for Horticultural Science **121:** 142-146.

Karppinen K, Tegelberg P, Häggman H, Jaakola L (2018) Abscisic acid regulates anthocyanin biosynthesis and gene expression associated with cell wall modification in ripening bilberry (Vaccinium myrtillus L.) fruits. Frontiers in plant science **9:** 1259.

Lee J, Durst RW, Wrolstad RE, Kupina CETGMHJHHKSKD, JD SMSMBMTPFRASGTUW (2005) Determination of total monomeric anthocyanin pigment content of fruit juices, beverages, natural colorants, and wines by the pH differential method: collaborative study. Journal of AOAC international **88:** 1269-1278.

Lee J, Rennaker C, Wrolstad RE (2008) Correlation of two anthocyanin quantification methods: HPLC and spectrophotometric methods. Food chemistry **110:** 782-786.

Li C, Luo J, MacLean D (2011) A novel instrument to delineate varietal and harvest effects on blueberry fruit texture during storage. Journal of the Science of Food and Agriculture **91:** 1653-1658.

Li M, Feng F, Cheng L (2012) Expression patterns of genes involved in sugar metabolism and accumulation during apple fruit development. PloS one **7:** e33055.

Liu H-T, Ji Y, Liu Y, Tian S-H, Gao Q-H, Zou X-H, Yang J, Dong C, Tan J-H, Ni D-A (2020) The sugar transporter system of strawberry: genome-wide identification and expression correlation with fruit soluble sugar-related traits in a Fragaria× ananassa germplasm collection. Horticulture research **7.**

Ljubobratović D, Vuković M, Brkić Bakarić M, Jemrić T, Matetić M (2022) Assessment of various machine learning models for peach maturity prediction using non-destructive sensor data. Sensors **22:** 5791.

López MG, Zanor MI, Pratta GR, Stegmayer G, Boggio SB, Conte M, Bermúdez L, Leskow CC, Rodríguez GR, Picardi LA (2015) Metabolic analyses of interspecific tomato recombinant inbred lines for fruit quality improvement. Metabolomics **11:** 1416-1431.

MacLean DD, NeSmith DS (2011) Rabbiteye blueberry postharvest fruit quality and stimulation of ethylene production by 1-methylcyclopropene. HortScience **46:** 1278-1281.

Mehra L, MacLean D, Savelle A, Scherm H (2013) Postharvest disease development on southern highbush blueberry fruit in relation to berry flesh type and harvest method. Plant disease **97:** 213-221.

Montecchiarini ML, Bello F, Rivadeneira MF, Vazquez D, Podesta FE, Tripodi KEJ (2018) Metabolic and physiologic profile during the fruit ripening of three blueberries highbush (Vaccinium corymbosum) cultivars. Journal of Berry Research **8:** 177-192.

Mooneyham RT, Nambeesan SU, Itle RA (2020) Postharvest keeping quality of Southern Highbush, Rabbiteye, and Northern Highbush blueberry cultivars in cold storage. *In* A Sial, ed, UGA Blueberry Blog, Vol 2023. University of Georgia, Postharvest, pp https://site.caes.uga.edu/blueberry/2020/2007/postharvest-keeping-quality-of-southern-highbush-rabbiteye-and-northern-highbush-blueberry-cultivars-in-cold-storage/.

Næs T, Isaksson T, Fearn T, Davies T (2002) A user-friendly guide to multivariate calibration and classification, Vol 6. NIR Chichester.

Nicolai BM, Beullens K, Bobelyn E, Peirs A, Saeys W, Theron KI, Lammertyn J (2007) Nondestructive measurement of fruit and vegetable quality by means of NIR spectroscopy: A review. Postharvest biology and technology **46:** 99-118.

Oms-Oliu G, Hertog M, Van de Poel B, Ampofo-Asiama J, Geeraerd A, Nicolai B (2011) Metabolic characterization of tomato fruit during preharvest development, ripening, and postharvest shelf-life. Postharvest Biology and Technology **62:** 7-16.

Paniagua A, East A, Hindmarsh J, Heyes J (2013) Moisture loss is the major cause of firmness change during postharvest storage of blueberry. Postharvest Biology and Technology **79:** 13-19.

Redpath LE, Gumpertz M, Ballington JR, Bassil N, Ashrafi H (2021) Genotype, environment, year, and harvest effects on fruit quality traits of five blueberry (Vaccinium corymbosum L.) cultivars. Agronomy **11:** 1788.

Samkumar A, Karppinen K, Dhakal B, Martinussen I, Jaakola L (2022) Insights into sugar metabolism during bilberry (Vaccinium myrtillus L.) fruit development. Physiologia Plantarum **174:** e13657.

Saranwong I, Sornsrivichai J, Kawano S (2001) Improvement of PLS calibration for Brix value and dry matter of mango using information from MLR calibration. Journal of Near Infrared Spectroscopy **9:** 287-295.

Sater H, Ferrao LFV, Olmstead J, Munoz PR, Bai J, Hopf A, Plotto A (2021) Exploring environmental and storage factors affecting sensory, physical and chemical attributes of six southern highbush blueberry cultivars. Scientia Horticulturae **289:** 110468.

Seymour GB, Østergaard L, Chapman NH, Knapp S, Martin C (2013) Fruit development and ripening. Annual review of plant biology **64:** 219-241.

Strik BC, Finn CE, Moore PP (2014) Blueberry Cultivars for the Pacific Northwest. A Pacific Northwest Extension Publication. Oregon State University-University of Idaho-Washington State University. Access 23 Jan. 2020. https://catalog.extension.oregonstate.edu/.

Wang Y-W, Acharya TP, Malladi A, Tsai H-J, NeSmith DS, Doyle JW, Nambeesan SU (2022) Atypical climacteric and functional ethylene metabolism and signaling during fruit ripening in blueberry (Vaccinium sp.). Frontiers in plant science **13.**

Williamson JG, Phillips DA, Lyrene P, Munoz PR (2019) Southern Highbush Blueberry Cultivars from the University of Florida: HS1245, rev. 2/2019. Edis **2019.**

Zhang J, Nie J-y, Jing L, Zhang H, Ye L, Farooq S, Bacha SAS, Jie W (2020) Evaluation of sugar and organic acid composition and their levels in highbush blueberries from two regions of China. Journal of Integrative Agriculture **19:** 2352-2361.

Zhu X, Zhang C, Wu W, Li X, Zhang C, Fang J (2017) Enzyme activities and gene expression of starch metabolism provide insights into grape berry development. Horticulture research **4.**

Tables and Figures

Table 5.1. Blueberry samples were collected at UGA Blueberry Research Farm in Alapaha, GA (A) or Cornelius Farms in Manor, GA (M)

	Year			
Type/Cultivars	2015	2016	2017	2018
Southern highbush				
Suziblue	A	A	M	A
Rebel	A	A	M	M
Miss Lilly		A	M	A
Miss Jackie		A	M	A
Miss Alice Mae		A	M	M
Emerald			M	M
Farthing			M	
Rabbiteye				
Premier	A	A		
Powderblue	A			
Krewer		A	M	A
Titan	A	A	M	A
Alapaha			M	A
Brightwell			M	A
Vernon	A			

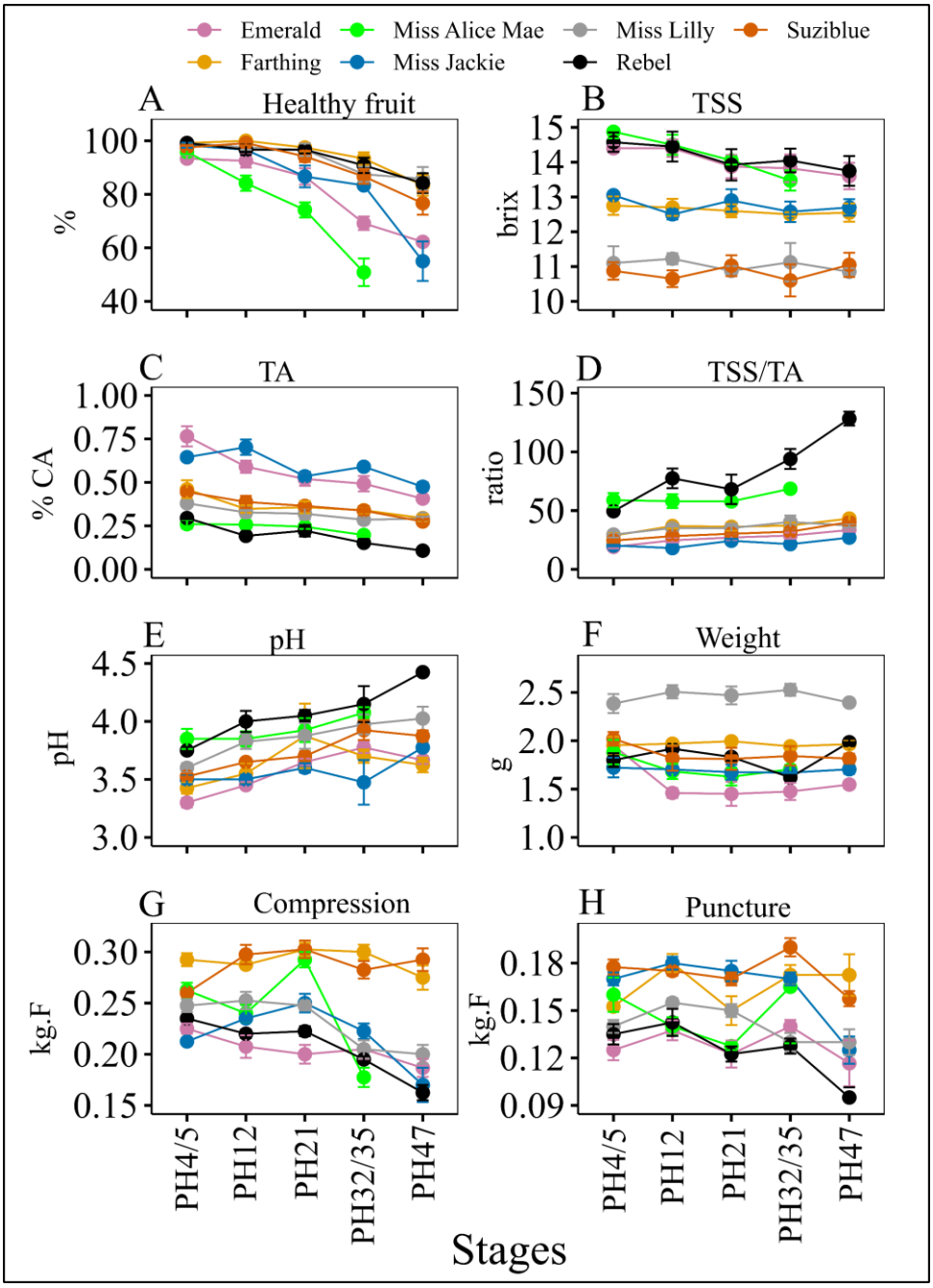

Figure 5.1: Postharvest (PH) fruit quality attributes of southern highbush blueberries in 2017. Error bars represent standard error. TSS: total soluble solid, TA: titratable acidity, CA: citric acid.

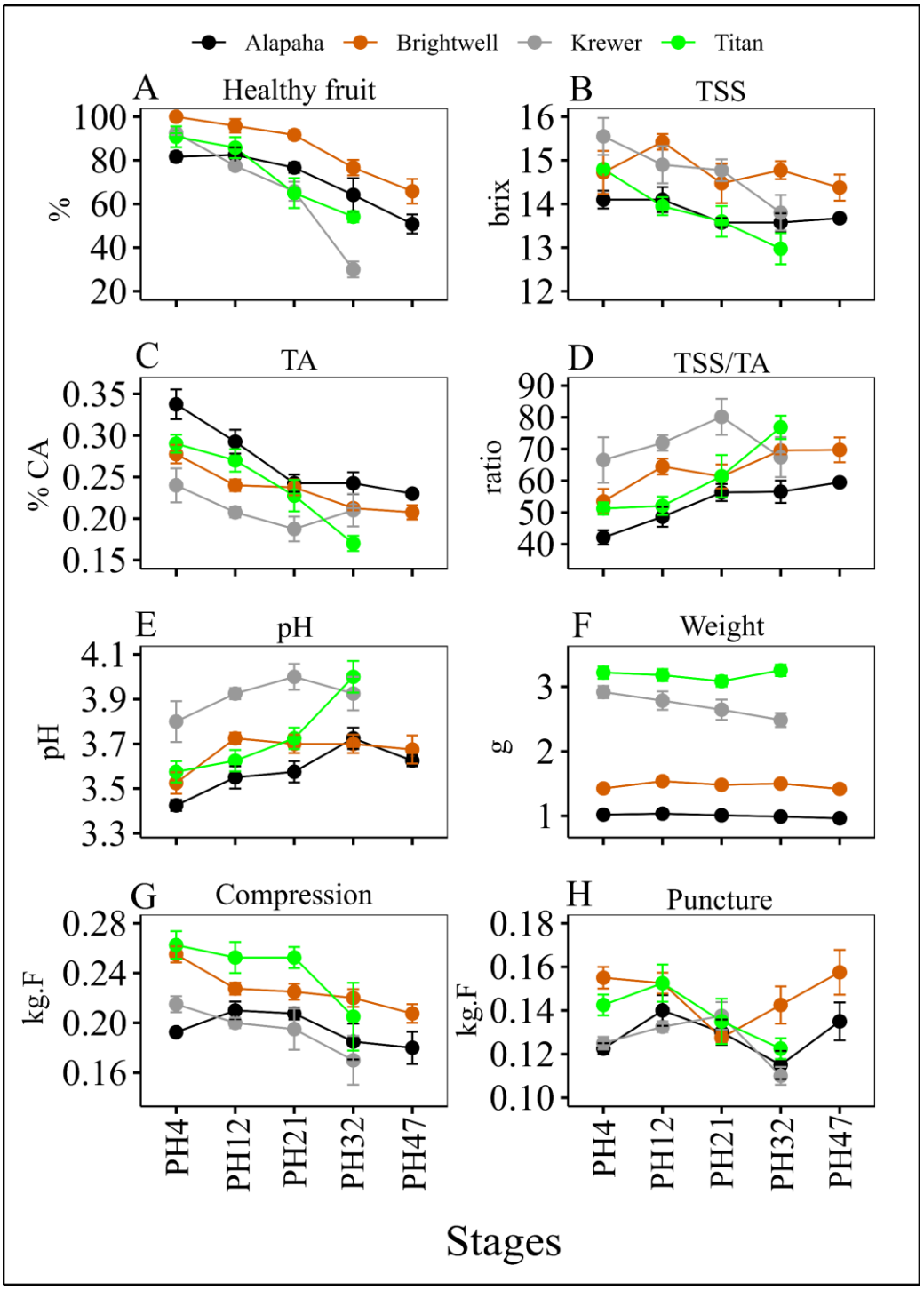

Figure 5.2 Postharvest (PH) fruit quality attributes of rabbiteye blueberries in 2017. Error bars represent standard error. TSS: total soluble solid, TA: titratable acidity, CA: citric acid.

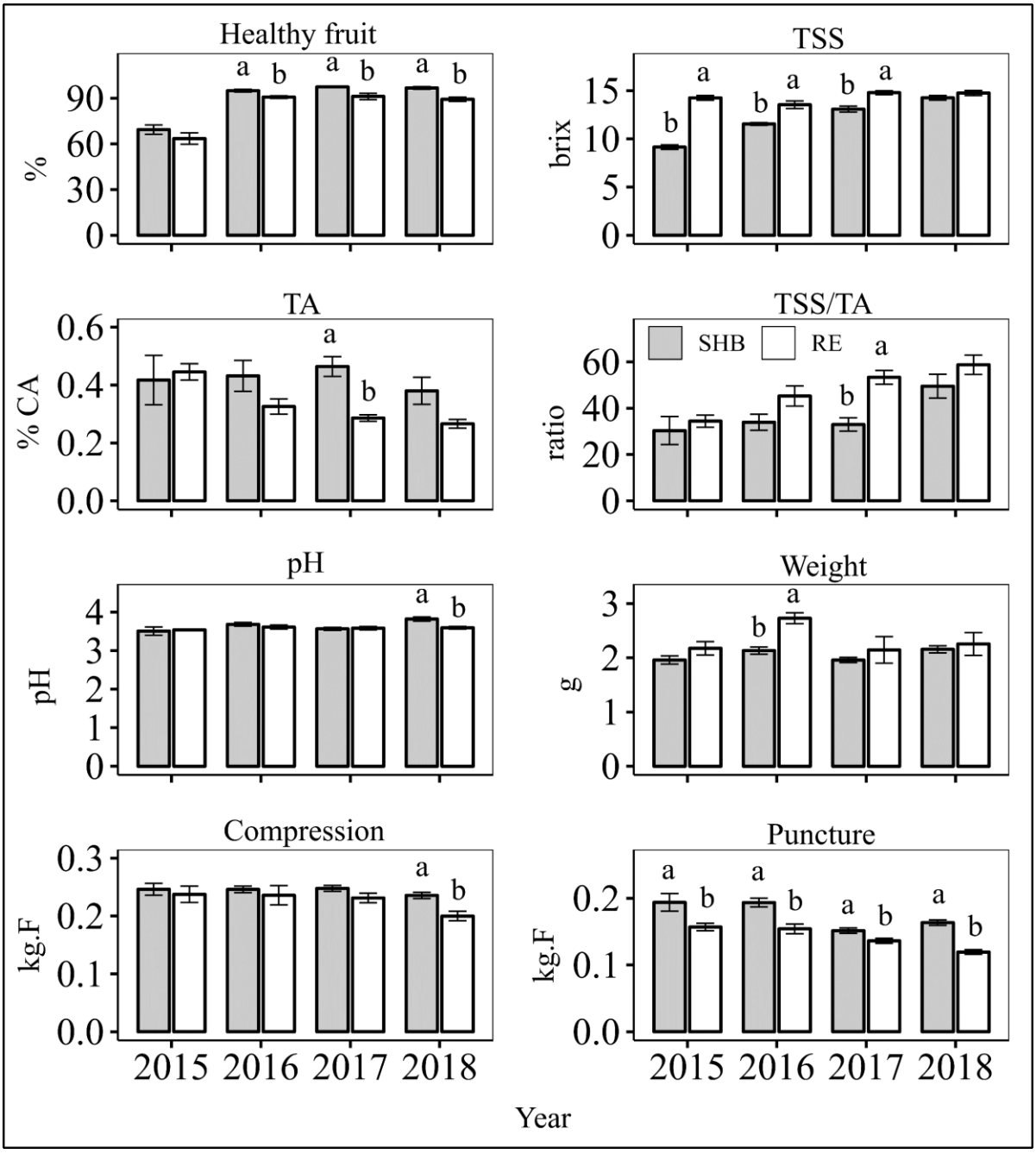

Figure 5.3: Fruit quality attributes between the southern highbush (SHB) and rabbiteye (RE) cultivars at 2-5 days after postharvest (PH) storage. 2015 & 16 at PH3; 2017 at PH4 & PH5; and 2018 at PH2-PH4. Different letters above symbols indicate that the means are significantly different between the cultivar type (within a year) according to ANOVA (α=0.05). TSS: total soluble solid, TA: titratable acidity, CA: citric acid.

Table 5.2: Prediction of Fruit Firmness (Compression & Puncture) using Stepwise Multiple Linear Regression Model with fruit quality attributes. The table displays coefficients and *P*-Values of Significant Variables for Compression (A) and Puncture (B).

Fruit compression prediction (A)			Fruit puncture prediction (B)		
Fruit quality traits	Estimate	*P*-value	Fruit quality traits	Estimate	P-value
(Intercept)	0.1522	<0.0001	(Intercept)	0.0652	<0.0001
Puncture	0.7612	<0.0001	Compression	0.3809	<0.0001
Healthy berry (%)	0.0005	<0.0001	TA	0.0651	<0.0001
TA	-0.0737	0.0115	TSS	-0.0012	0.0339
Fruit weight	0.0127	<0.0001	Healthy berry (%)	-0.0001	0.002
TSS/TA	-0.0005	<0.0001	Type (SHB)	0.0142	<0.0001
pH	-0.0152	0.00587			
R^2	0.51		R^2	0.55	

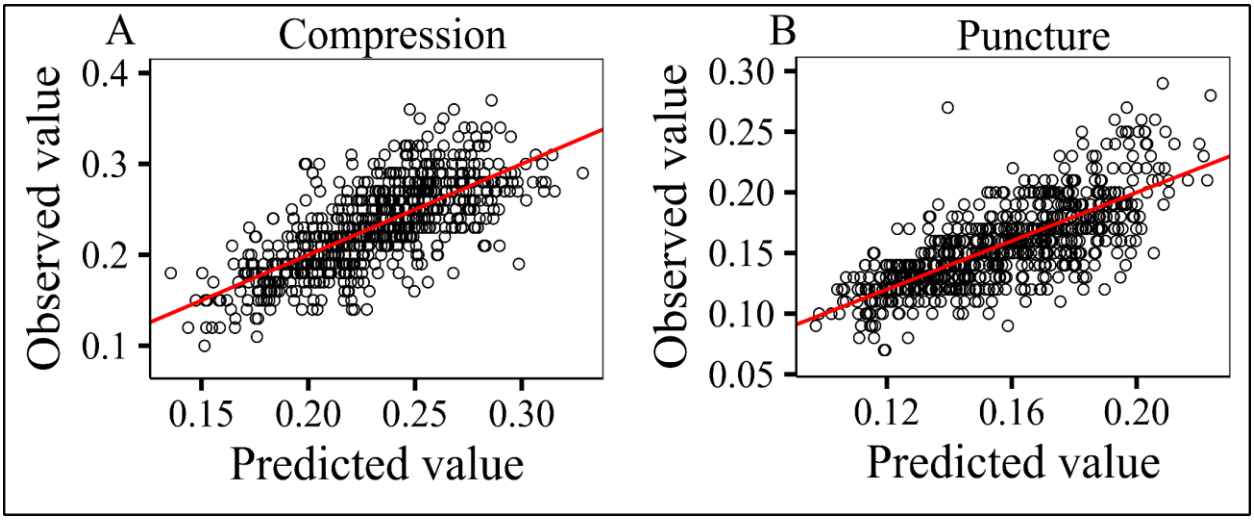

Figure 5.4: Comparison between predicted and observed values for fruit compression (A) and puncture (B). The x-axis represents the predicted values, while the y-axis represents the observed values.

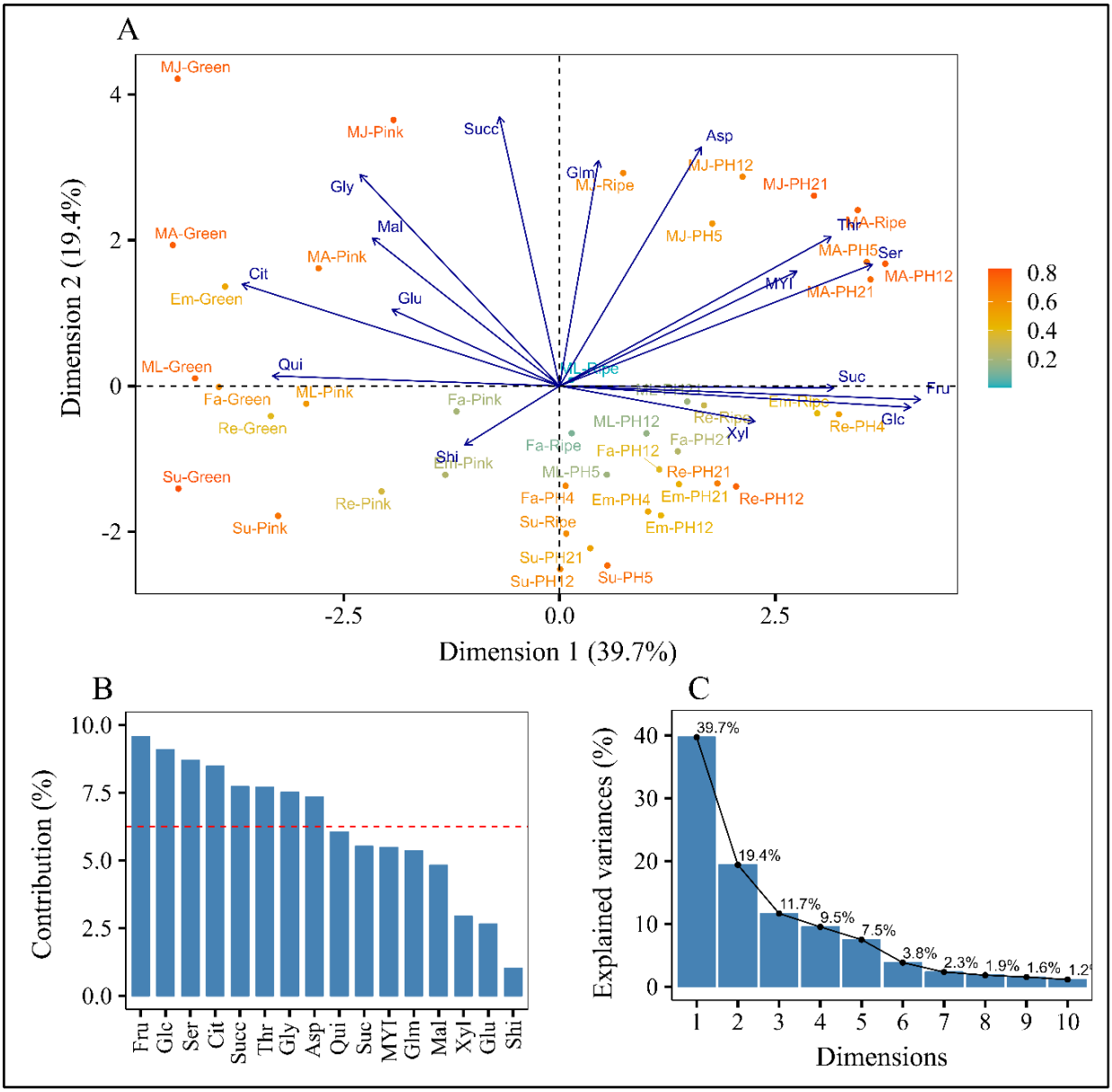

Figure 5.5: PCA analysis of metabolites composition of southern highbush cultivars during fruit development, ripening, and various postharvest storage. 2017. A: PCA bi-plot showing variation in metabolites during ripening and postharvest stages and between the cultivars in first two components. B: Contribution of each metabolite in first two principal components (PCs). C: Scree plots showing dimensions and percentage of variability explained by each dimension in principal component analysis. Glc: glucose, Fru: fructose, Suc: sucrose, Mal: malate, Asp: aspartate, Glu: glutamate, Cit: citrate, Qui: quinate, MYI: myo-inisitol, Succ: succinate, Gly: glycerate, Ser: serine, Thr: threonine, Xyl: xylose, Shi: shikimate, and Glm: glutamine.

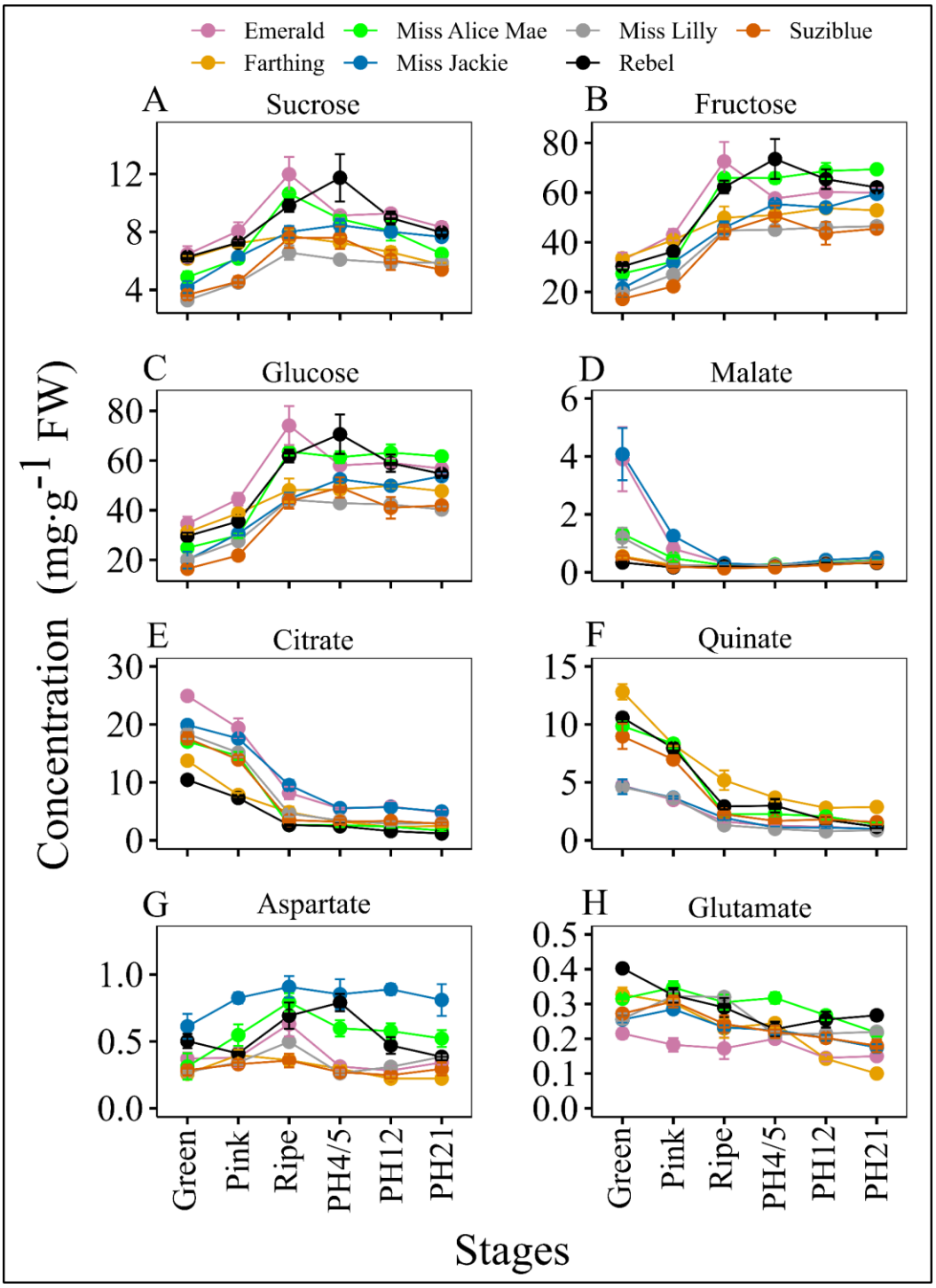

Figure 5.6: Concentration of major metabolites during fruit development, ripening, and postharvest stages in southern highbush cultivars 2017. Error bars represent standard error.

Table 5.3: Prediction of Fruit Firmness (Compression & Puncture) using LASSO Regression Model with metabolites during postharvest storage. We conducted a study to predict fruit firmness, both in terms of compression and puncture, utilizing a LASSO regression model. The model incorporated various primary and secondary metabolites as predictor variables.

Fruit compression Prediction		Fruit puncture Prediction	
Fruit chemical traits	Estimate	Fruit chemical traits	Estimate
(Intercept)	0.2501	(Intercept)	0.1569
Serine	0.0244	Fructose	-0.0091
Quinate	0.0209	Glutamine	0.006
Shikimate	-0.0176	Quinate	0.0054
Sucrose	-0.0143	Myo-inisitol	-0.0052
Succinate	-0.0115	Shikimate	-0.0035
Xylose	-0.0076	Xylose	-0.0031
Glutamate	-0.0072	Malate	-0.0028
Threonine	-0.0066	Glutamate	-0.0009
Fructose	-0.005	Glycerate	0.0009
Anthocyanin	-0.0046	Citrate	0.0006
Myo-inisitol	0.0034	R^2	0.60
Malate	-0.0008	RMSE	0.0719
Citrate	0.0007		
Aspartate	-0.0001		
R^2	0.70		
RMSE	0.0212		

R^2= coefficient of determination and RMSE=root mean square error determines from the respective test samples of compression and puncture.

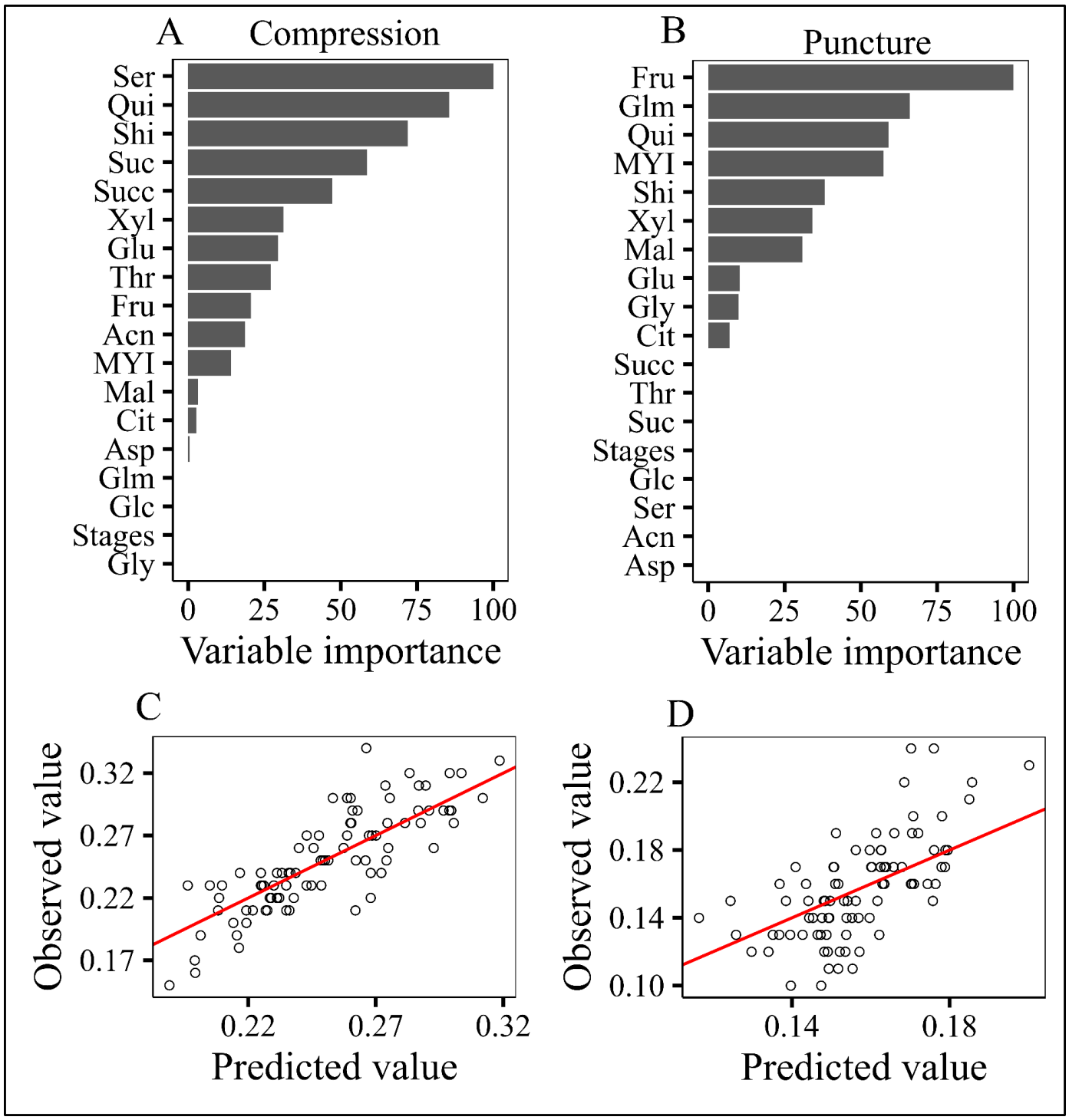

Figure 5.7: Variable importance (A, B) and Predicted Vs Observed (C, D) plot during the prediction of compression (A, C) and puncture (B, D).

Appendix A: Supplementary figures

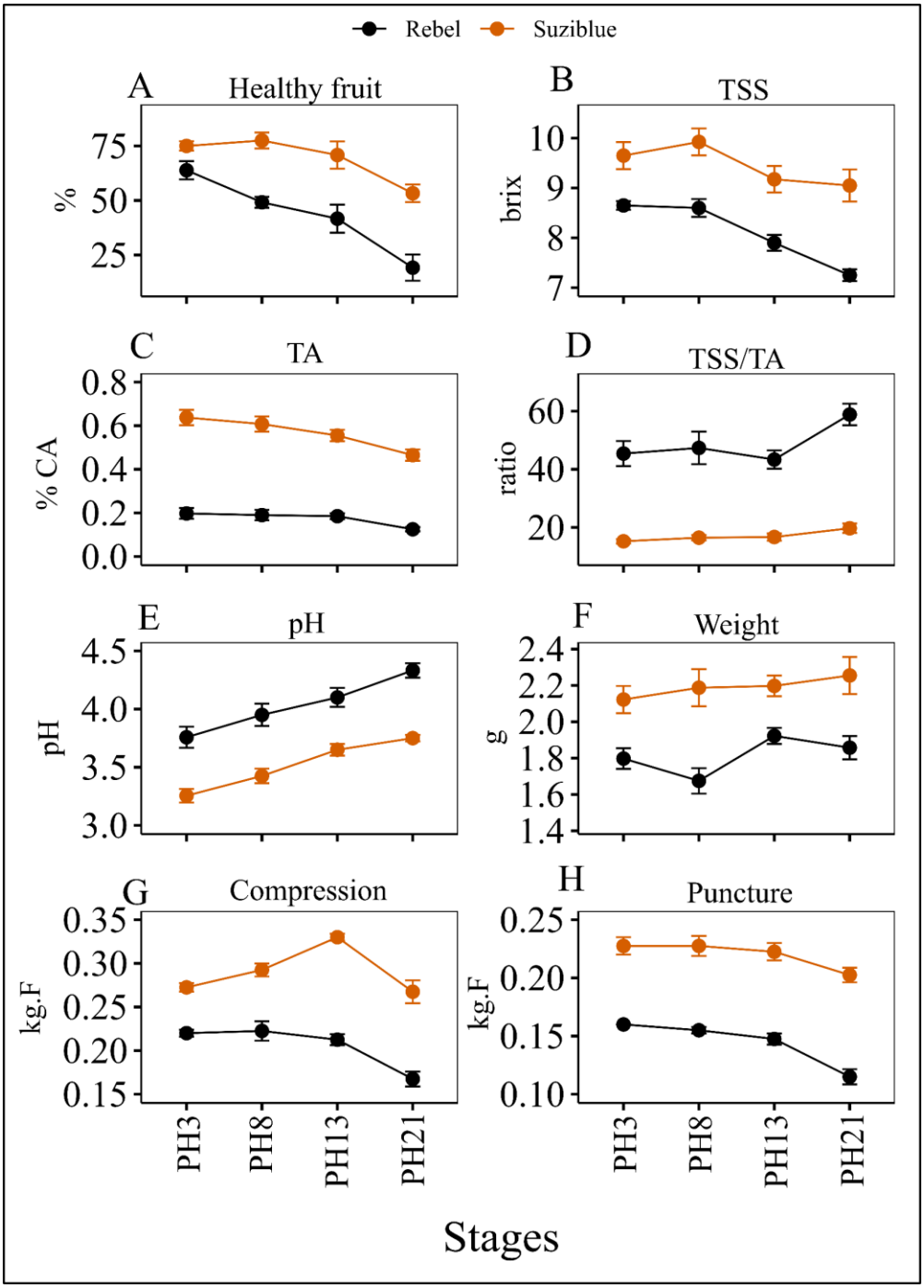

Figure 5. S1: Postharvest (PH) fruit quality attributes of southern highbush blueberries in 2015. Error bars represent standard error. TSS: total soluble solid, TA: titratable acidity, CA: citric acid.

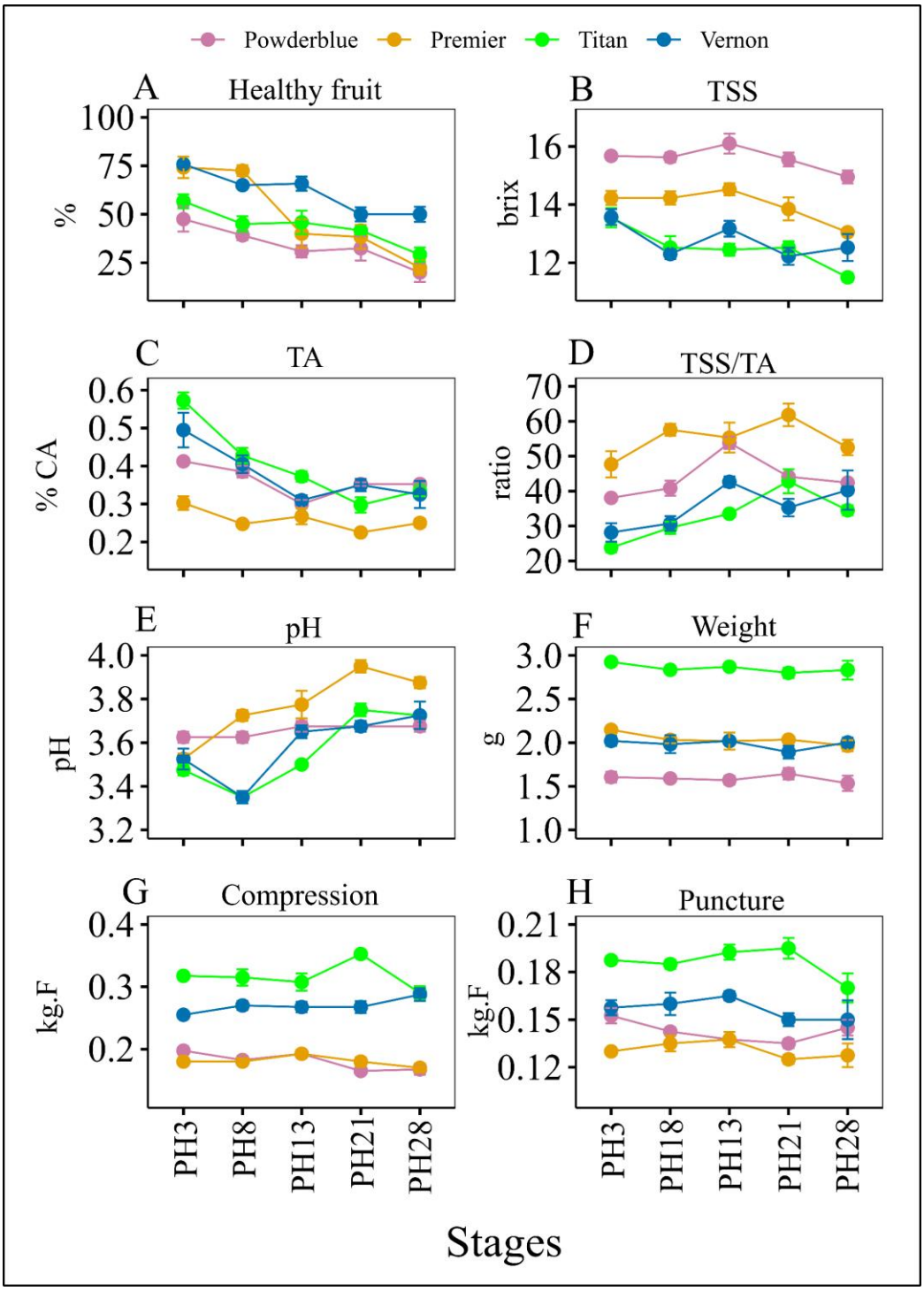

Figure 5. S2: Postharvest (PH) fruit quality attributes of rabbiteye blueberries in 2015. Error bars represent standard error. TSS: total soluble solid, TA: titratable acidity, CA: citric acid.

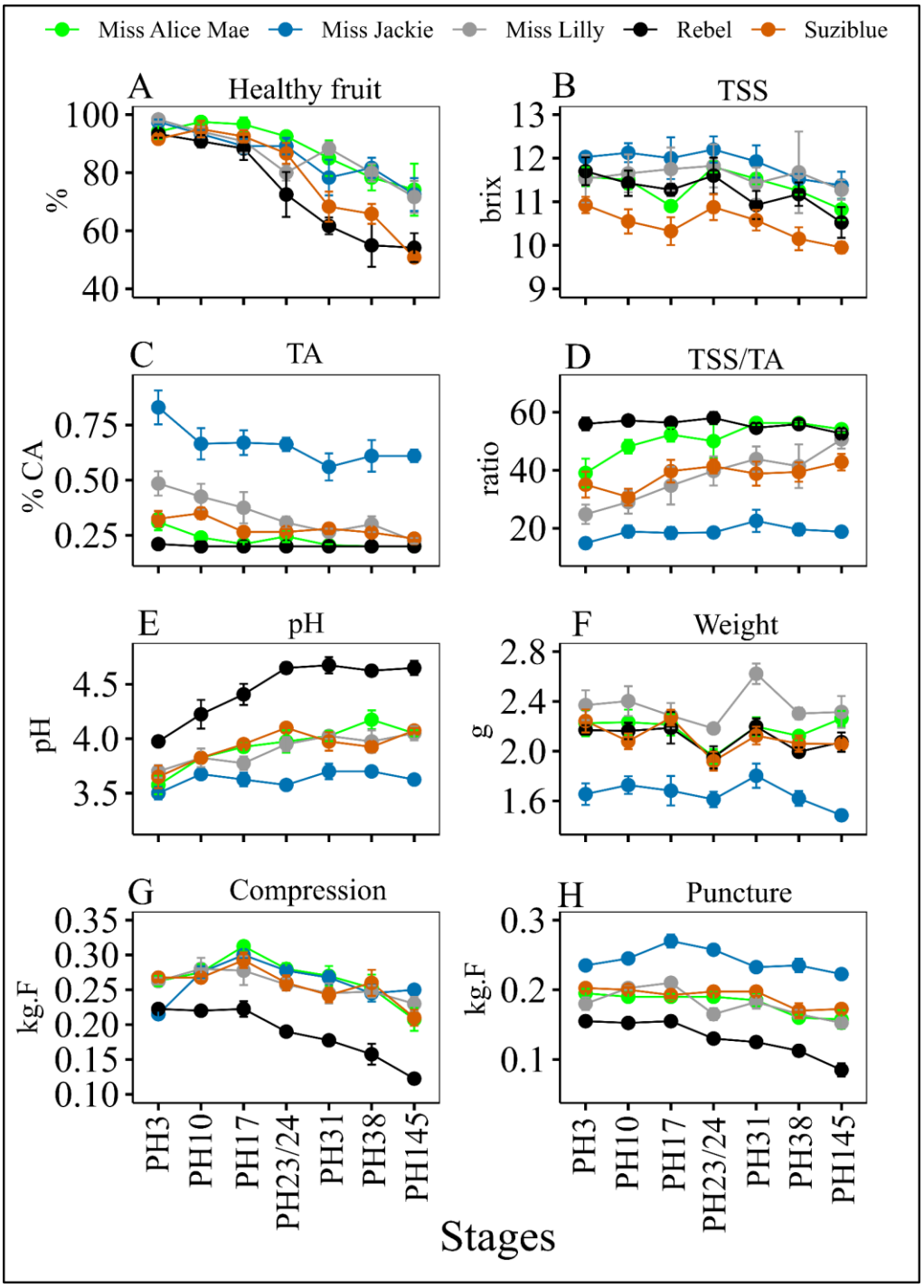

Figure 5. S3: Postharvest (PH) fruit quality attributes of southern highbush blueberries in 2016. Error bars represent standard error. TSS: total soluble solid, TA: titratable acidity, CA: citric acid.

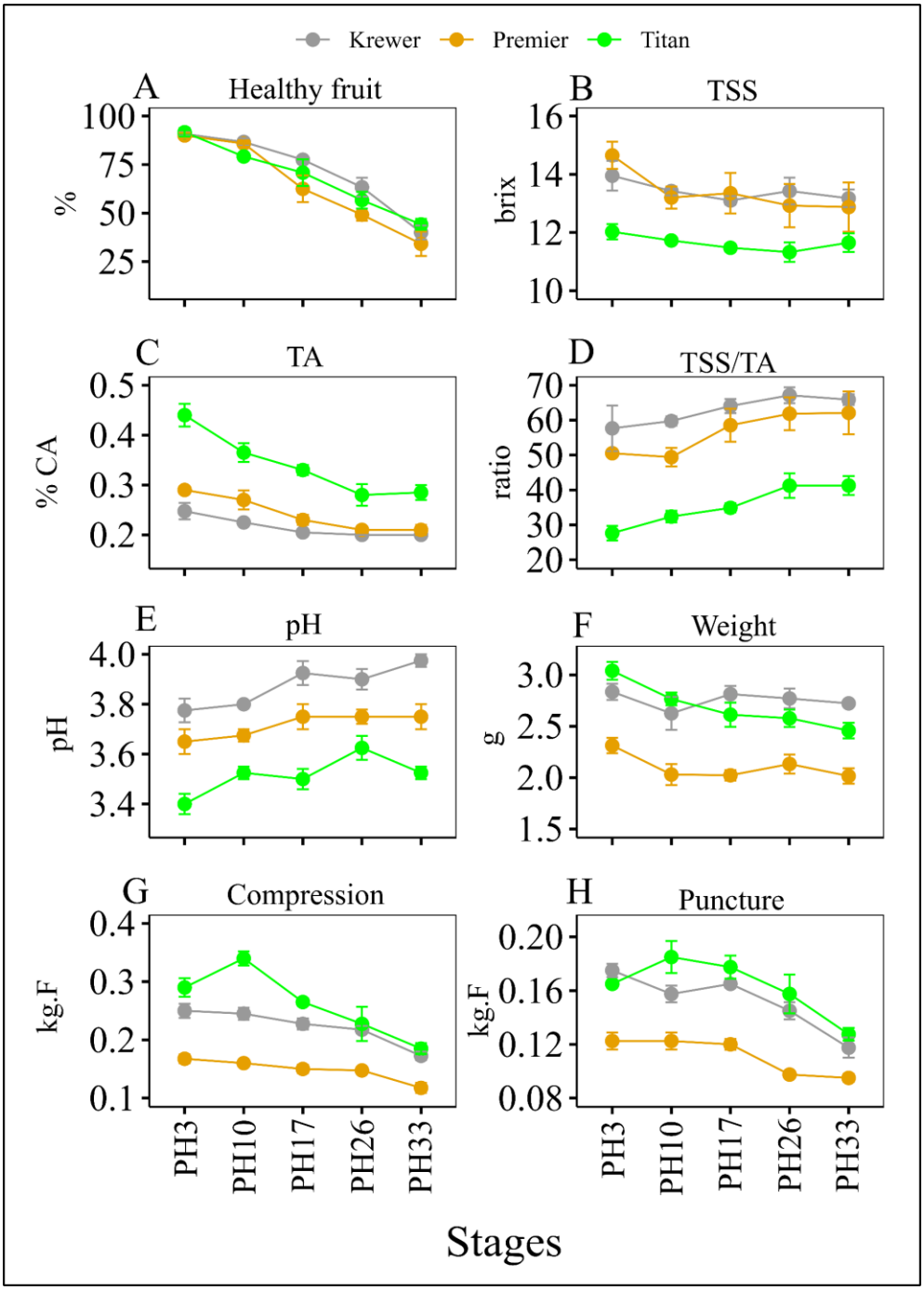

Figure 5. S4: Postharvest (PH) fruit quality attributes of rabbiteye blueberries in 2016. Error bars represent standard error. TSS: total soluble solid, TA: titratable acidity, CA: citric acid.

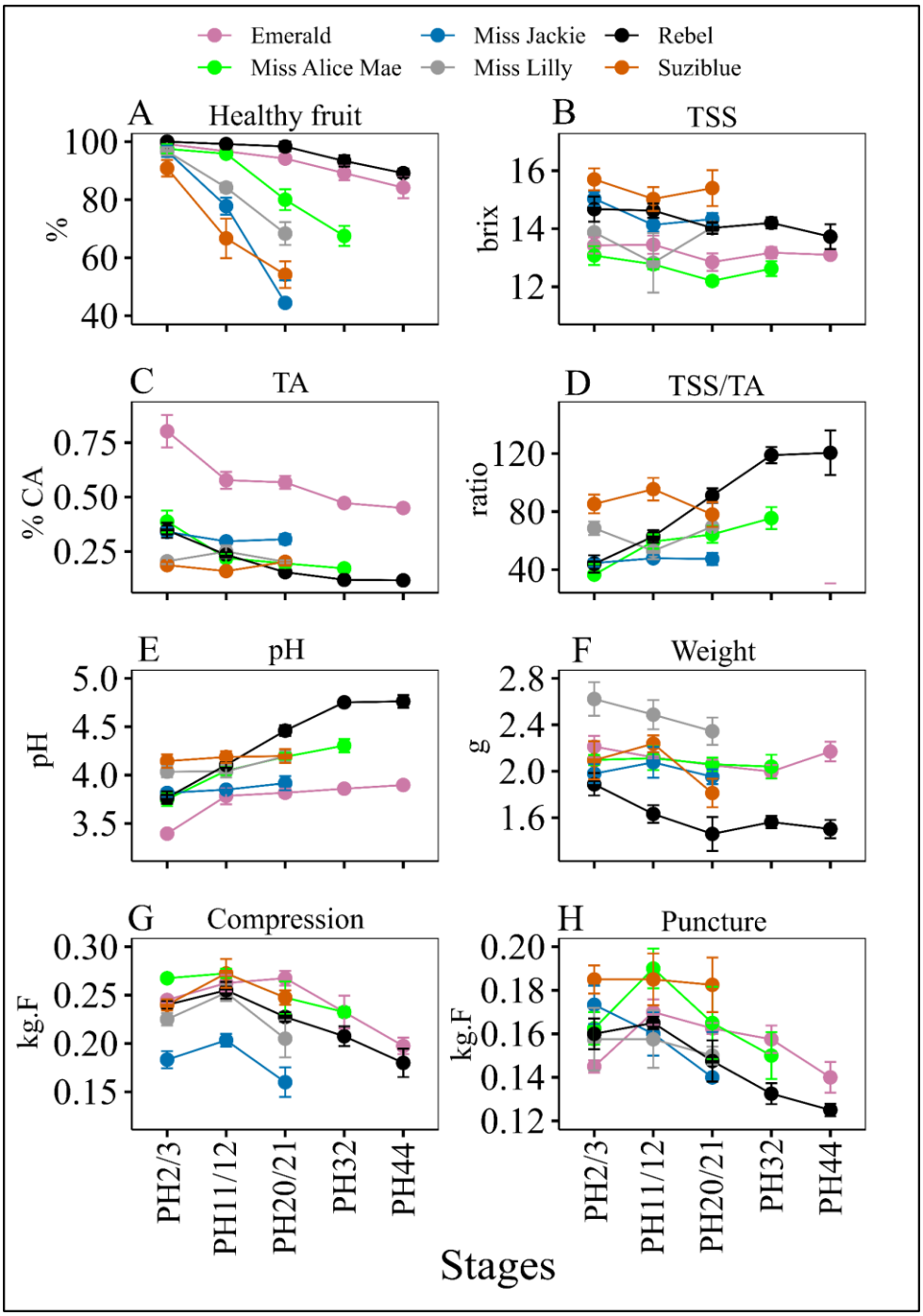

Figure 5. S5: Postharvest (PH) fruit quality attributes of southern highbush blueberries in 2018. Error bars represent standard error. TSS: total soluble solid, TA: titratable acidity, CA: citric acid.

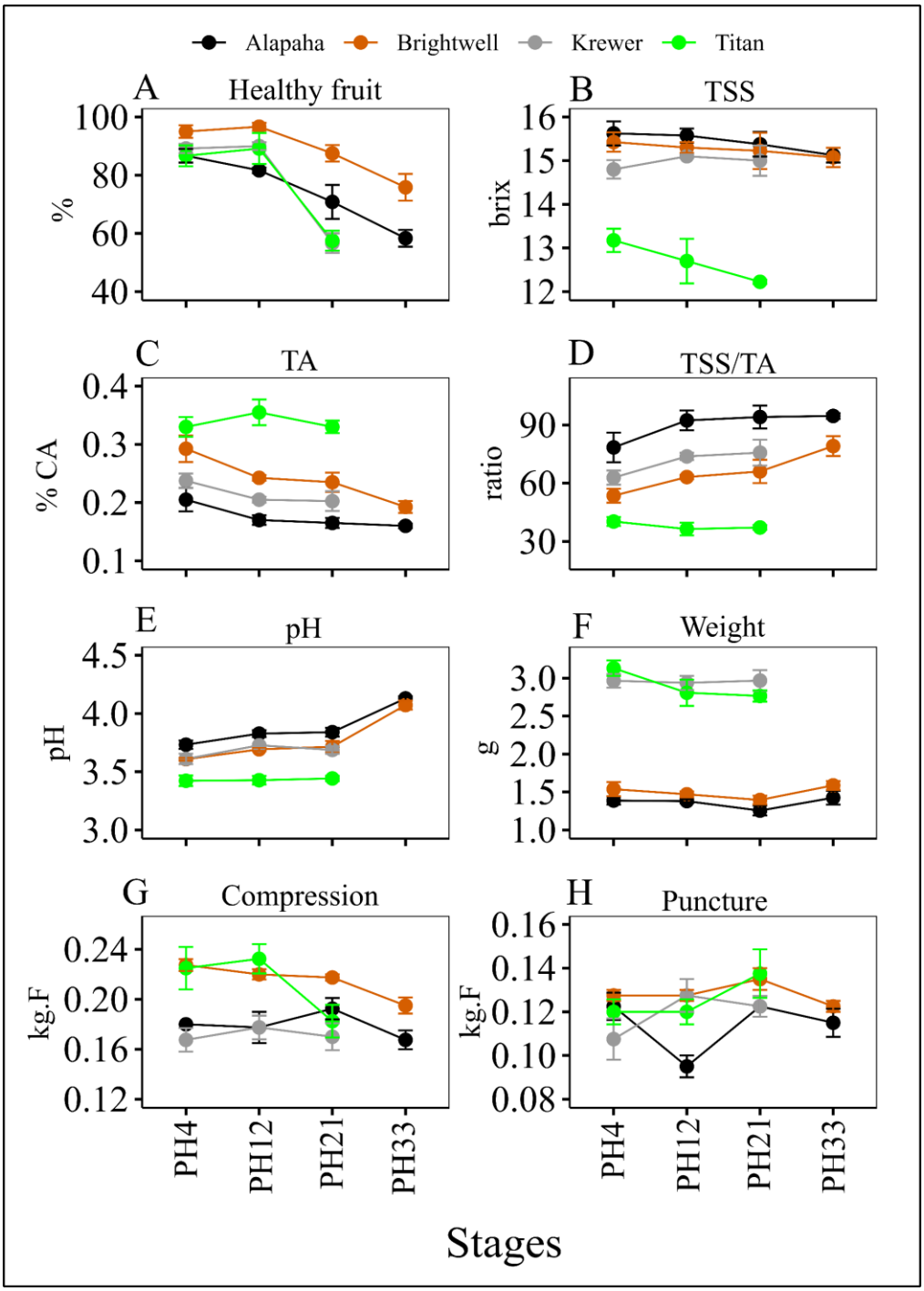

Figure 5. S6: Postharvest (PH) fruit quality attributes of rabbiteye blueberries in 2018. Error bars represent standard error. TSS: total soluble solid, TA: titratable acidity, CA: citric acid.

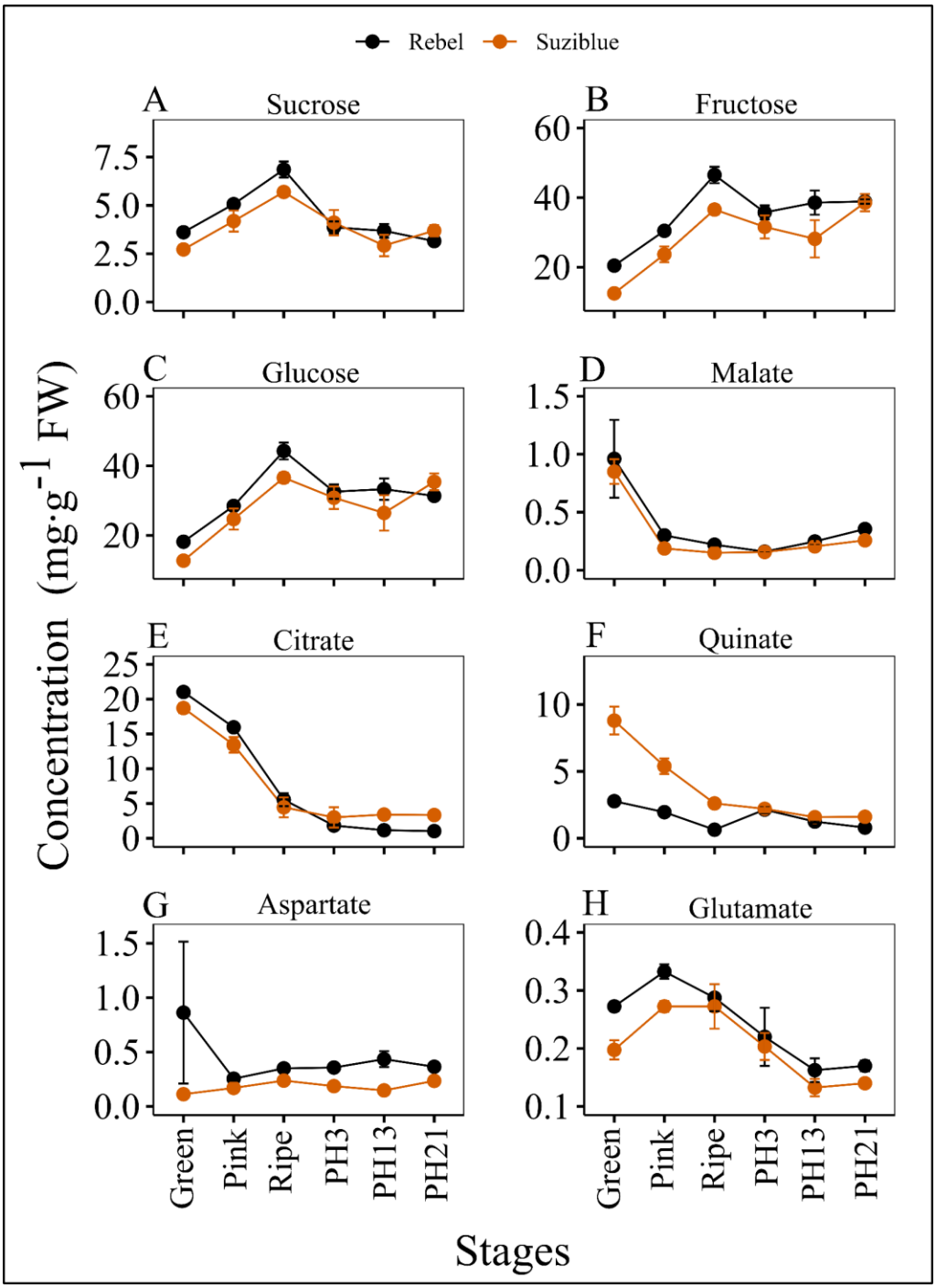

Figure 5. S7: Concentration of major metabolites during fruit development, ripening, and postharvest stages in southern highbush cultivars 2017. Error bars represent standard error.

Appendix B: Supplementary Table

Table 5. S1: Variance inflation factors (VIF) of depended variables

Dependent variables	VIF
Stages	6.5
Succinate	4.3
Glycerate	3.7
Serine	8.1
Threonine	7.6
Malate	7.2
Aspartate	8.8
Glutamate	2.6
Xylose	2.1
Glutamine	7.3
Shikimate	2.6
Citrate	4.4
Quinate	2.5
Fructose	246.9
Glucose	277
Myo-inisitol	6
Sucrose	25.2
Anthocyanin	3.6

CHAPTER 6

SUMMARY AND FUTURE DIRECTION

This study investigated the molecular and metabolomics mechanisms regulating fruit development and ripening in blueberries, revealing increased sucrose uptake, stimulated glycolysis, TCA, and anthocyanin-related metabolites during ripening. Follow-up gene expression analyses revealed important genes associated with sugar, acid, and anthocyanin metabolism. The major sugars: glucose, fructose, and sucrose, continuously increased during the fruit development and ripening in blueberries. The transcript abundance of vacuolar *INVERTASE* (*vINV*) and *BIFUNCTIONAL SUGAR TRANSPORTER* was high during the ripening suggesting that these two enzymes are mainly responsible for the catabolism and translocation of sucrose in the fruits. In addition, malate decreased during the ripening due to the increase in respiration and transcripts abundance of *PHOSPHOENOLPYRUVATE CARBOXYKINASE* (*PEPCK*). The majority of carbon during the ripening is also diverted toward the formation of anthocyanin compounds, as evidenced by the higher anthocyanin concentration and increased transcript abundance of the *BIFUNCTIONAL 3-DEHYDROQUINATE DEHYDRATASE/SHIKIMATE DH* (*DD/SDH*), and anthocyanin biosynthesis genes. Future studies should focus on the molecular and metabolomics basis in the formation of volatiles and other flavonoid compounds in rabbiteye cultivars.

Furthermore, we studied the effect of preharvest application of ethylene-releasing plant growth regulators (PGRs) such as ethephon and ACC on the rate of ripening, sugar, acid, anthocyanin metabolism, and postharvest fruit quality attributes. Both ethephon and ACC transiently stimulated sugar, acid, and anthocyanin metabolism, increasing the rate of ripening with minimal impact on fruit quality attributes. Future studies should focus on the lower concentration of these PGRs on fruit ripening, metabolism, and postharvest fruit quality attributes.

Characterization of ripening-related transcription factors (TFs) during fruit development and ripening identified four important TFs, potentially involved in fruit ripening. Among them, the transcript abundance of *VvMADS7*, *VvNAC1*, and *VvNAC2* increased after the application of ethephon, suggesting that they are ethylene inducible. The transcript abundance of *VvNAC8* remained unaffected by ethylene application, suggesting that the expression of this gene during ripening is independent of ethylene-mediated signaling. Future studies should focus on the functional validation of these TFs, which will provide a better understanding of the roles of these TFs in fruit ripening.

Finally, we identified physical and metabolic markers associated with blueberry fruit firmness using linear and LASSO regression models. Notably, titratable acidity (TA), specifically quinate and citrate, exhibited positive associations with fruit firmness. Conversely, sugars and amino acids displayed negative associations with fruit firmness. This information can be valuable for future breeding programs aimed at enhancing fruit firmness in blueberries. Future studies should focus on investigating the molecular mechanisms responsible for changes in

firmness due to changes in metabolite concentration. In summary, our research has shed light on both the applied and basic aspects of ripening and postharvest physiology mechanisms in blueberries, which can be utilized to improve ripening characteristics, fruit quality, and postharvest shelf life.